SYNTHETIC AND THEORETICAL INVESTIGATIONS OF BENZO-13-p-TOLYL PHENALENE

by

JELENA T. ZIVKOVIC

A dissertation submitted to the Graduate Faculty in Chemistry in partial fulfillment of the requirements for the degree of Doctor of Philosophy, The City University of New York

2003

This manuscript has been read and accepted for the Graduate Faculty in Chemistry in satisfaction of the dissertation requirements for the degree of Doctor of Philosophy.

7-15-03

Date

Prof. Klaus Grohmann

Chairman of the Examining Committee

9-17-2003

Date

Prof. Gerald Koeppl

Executive Officer

Prof. Richard Franck

Supervisory Committee

Prof. David Baker

Supervisory Committee

The City University of New York

Abstract

Synthetic and Theoretical Investigation of Benzo-13-p-tolylphenalene (11c-p-Tolyl-11cH-benzo[de]anthracene)

by

Jelena T. Zivkovic

Mentor: Klaus G. Grohmann

13-methylphenalene, a long sought after molecule, has been a synthetic objective in many research groups because of its suitability for the study of effects associated with antiaromatic,[4n]annulenes. This [12]annulene would have a rigid, nearly planar structure. Its high symmetry is predicted to minimize the pseudo Jahn -Taller effect, allowing the maximum paratropicity. The internal methyl group serves as a very sensitive NMR probe for the investigation of expected ring current effects. Previous experimental results in our group suggest the weakness of the methyl-central carbon bond: the attempts to introduce the last double bond into the system always led to the loss of the methyl group.

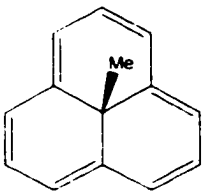

13-methylphenalene

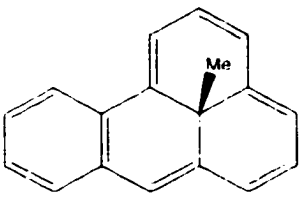

Benzo-13-methylphenalene

Based on the fact that the fusion of benzene rings onto annulene perimeter stabilizes the molecule, while lowering the paratropicity, the synthesis of Benzo-13-methylphenalene has been attempted, but the same facile methyl loss has been observed.

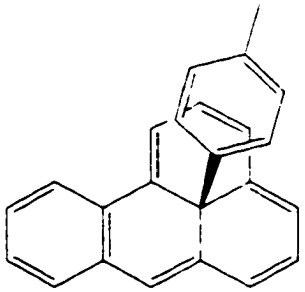

Benzo-13-p-tolylphenalene

In order to strengthen the central carbon-carbon bond, changing the substituent from an alkyl (sp^3) group to an aryl (sp^2) group has been investigated.

This investigation is comprised of two parts:

1. Theoretical study of the effects of benzannulation and substituent at the central position on bond dissociation energies (BDE's). Furthermore, two processes, namely the 1,5 shift and dissociation of the substituent group, are investigated as well.
2. The investigation of the very flexible synthetic methodology based on the

intramolecular Diels-Alder reaction (IMDA) for the synthesis of a variety of benzo-13-substituted phenalenes, including our synthetic target - Benzo-13-p-tolylphenalene, a molecule that, we believe, offers a perfect balance between paratropicity and isolabilty.

To Pavle and Luka

ACKNOWLEDGEMENTS

I am greatly indebted to my mentor, Professor Klaus G. Grohmann, for his encouragement, guidance and friendship, throughout the course of my studies. I would also like to express my gratitude to the members of my doctoral committee, Professors Richard Franck and David Baker, for their interest in my project and the help they provided. I thank Professor Joseph J. Dannenberg for his assistance with the AM1 calculations.

My thanks go to Dr. M. Blumenstein for helping me with the temperature dependent NMRs, Dr. Louis Todaro for providing the X-ray spectra, and Dr. C. Soll for supplying the Gas Chromatography/ Mass spectra.

I am grateful to a number of colleagues for their friendship and backing: Milos Miljkovic, Kai Fan Cheng, Junyi Wang, Dr. Shu-ya Hsu, Dr. Ghislain Mandouma, Dr. Guangwu Chen, Ajit Parhi, Jun Pu, Dr. Darrin Dabideen, Fatoumata Camara, Dr. Paolo Passeto, Dr. Tatjana Milic, Tomoko Hagane, Sharon Abrams-Perez, John Zambrano ...

I am indebted to mother, Ljubinka Zivkovic, for her support and generous help, and my father, Tomislav Zivkovic, for always believing in me. I thank my sisters, Ksenija Kolacek and Aleksandra Tisma, and their families, for all the love and caring.

My greatest thanks go to Pavle Levi and Luka Levi, for being by my side every step of the way.

TABLE OF CONTENTS

LIST OF FIGURES

CHAPTER 1. INTRODUCTION

1.1 Definition of aromaticity/antiaromaticity

Ever since Faraday[1], in 1825, isolated the prototype of the aromatic molecule-benzene- chemists have been trying to qualitatively, and later on, quantitatively describe aromaticity. However, despite numerous attempts, throughout the history of chemistry[2], to this date there still is no precise and generally accepted definition of it.

Kekule was the first to use the term aromatic, for compounds containing a benzene ring[3].Soon after, Erlenmeyer observed a reactivity pattern, noticing that aromatic molecules react similarly to benzene[4]. The first one to use the term "aromatic sextet" and to propose the circle inside the benzene ring to symbolize this sextet was Robinson in 1925[5]. Hückel's rule offered a general guide for recognizing aromaticity in a molecule: a molecule was aromatic if it was reasonably planar and contained (4n+2) π electrons[6]. Other properties of aromatic molecules, usually benzene, served as a basis for determining and explaining aromaticity, such as bond equalization[7] and ^{1}H NMR shifts[8]. More recently, the advancement in the field of semi-empirical and *ab initio* calculations, sophisticated theoretical calculations came as the new means for quantifications and prediction of aromaticity[9].

The above mentioned are only a few examples of chemists' constant striving to solve the problem of what aromaticity is.

Generally, aromatic molecules are thought to be planar, cyclic systems with delocalized π-electrons, which exhibit equalization of bond lengths and increased stability compared to their olefinic analogs.

The term antiaromaticity is even more elusive. Until 1965, when Breslow for the first time used the term antiaromatic[10], cyclic conjugated systems with 4n π-electrons were classed as pseudoaromatic molecules. Opposite to aromatic molecules, antiaromatic molecules are cyclic conjugated systems that show destabilization in comparison to their cyclic, non-conjugated analogs.

In order to make a clear distinction between aromatic, antiaromatic and non aromatic molecules certain criteria have been established. The three main groups of these criteria are: energetic, structural and magnetic criteria. All will be discussed in detail in the following section.

1.2. Criteria for aromaticity/antiaromaticity

1.2.1. Energetic criteria

Aromatic molecules are always associated with stabilization, whereas antiaromatic molecules involve destabilization of the system relative to their olefinic counterparts. Stabilization/destabilization as an effect of the cyclic bond delocalization is called resonance energy. There are different methods for estimating resonance energies and some will be discussed here. In order to better understand the concept of resonance energies we have to be familiar with Hückel's molecular orbital theory[6,11,12].

1.2.1.1 Hückel MO theory

To derive the energies of the system one has to solve secular equation (equation 1.1) obtained by applying variation method to Schrödinger's equation.

$$\begin{vmatrix} H_{11} - ES_{11} & \cdot & \cdot & H_{1n} - ES_{1n} \\ \cdot & \cdot & \cdot & \cdot \\ \cdot & \cdot & \cdot & \cdot \\ H_{1n} - ES_{1n} & \cdot & \cdot & H_{nn} - ES_{nn} \end{vmatrix} = 0 \qquad (1.1)$$

where H_{ii} is the Coulumb intergral , H_{ij} is resonance integral, S_{ij} is the overlap integral and E is the energy.

Calculating the energies of molecular orbitals for benzene, using the same equation, would involve solving a 42 by 42 matrix with many unknowns. To simplify the equation, Hückel made certain approximations, and developed a method that was very successful in explaining the observed high stability of benzene, as well as the importance of the aromatic sextet.

In his method, Hückel treated σ electrons and π electrons separately, based on the assumption that σ electrons are localized and that the only ones responsible for the behavior of benzene are π electrons. Hückel, also, considered only electronic interactions between neighboring atoms to be of importance in calculating energies of a given system. Using these approximations the equation (1.1) is given a new, much simpler form:

$$\begin{vmatrix} x & 1 & 0 & 0 & 0 & 1 \\ 1 & x & 1 & 0 & 0 & 0 \\ 0 & 1 & x & 1 & 0 & 0 \\ 0 & 0 & 1 & x & 1 & 0 \\ 0 & 0 & 0 & 1 & x & 1 \\ 1 & 0 & 0 & 0 & 1 & x \end{vmatrix} = 0 \qquad (1.2)$$

where $X= (\alpha-E)/\beta$ $\alpha = H_{ii}$; $\beta = H_{ij}$

Six energy levels corresponding to six molecular orbitals in benzene are obtained solving this equation and are represented here following the method of Frost and Musulin.

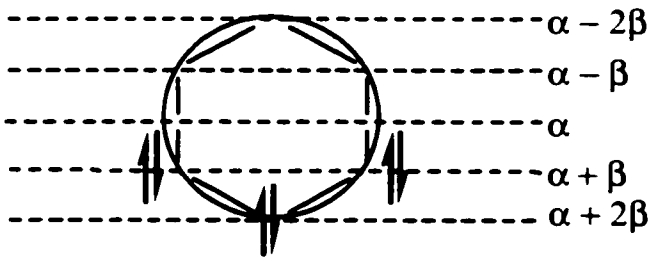

Figure 1. Hückel's molecular orbitals of benzene represented using Frost and Musulin method

Hückel's molecular orbital theory served as a basis for the formulation of what is known as "Hückel's rule" or "4n+2 rule", stating that the monocyclic conjugated molecules with (4n+2) π electrons are exceptionally stable.

1.2.1.2. Resonance energies

The oldest theoretical parameter used for the quantitative characterization of aromaticity is the resonance energy[13]. In order to calculate resonance energies one has to find a suitable reference molecule. Depending on the reference molecules and the method used, different resonance energies are obtained.

Hückel's resonance energies or delocalization energies (DE) are calculated relative to the energies of analogous molecule with isolated double bonds (equation 1.3).

$$DE = - (E_{\pi} - n_{c=c}(2\alpha + 2\beta) \qquad (1.3)$$

As it can be seen from the figure 2, Hückel's delocalization energies show positive stabilization energies for all annulenes, except for cyclobutadiene. For this reason, Hückel's method for calculating stabilization energies can not be used for differentiating between aromatic, non aromatic and antiaromatic molecules.

The method that can be successfully applied to a wide range of molecules and that gives values which better agree with the observed properties of the molecules, is Dewar's method[14]. ***Dewar resonance energies*** are defined as difference in heat of atomization between the cyclic conjugated system and its linear acyclic analog with the same number of carbon carbon single and carbon carbon double bonds(equation 1.4). Using SCF-LCAO-MO method, Dewar has found that the heat of atomization of nonconjugated polyene can be calculated by summing bond energies (ΔH_a^{add}).

$$DRE = \Delta H_a^{M} - \Delta H_a^{add} \qquad (1.4)$$

When Dewar's method is applied, aromatic systems show positive resonance energies, while antiaromatic systems give negative stabilization energies. Dewar's resonance energies agree well with other criteria for aromaticity.

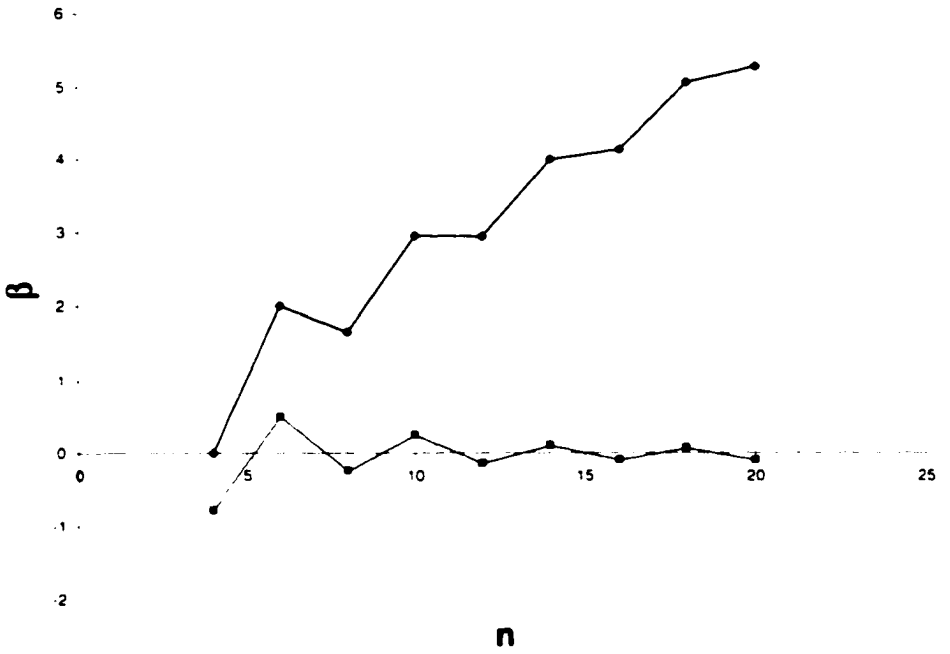

Figure 2. Hückel's delocalization energies (circle) and Dewar resonance energies (square)

For calculating resonance energies of conjugated systems for which a linear reference model is not suitable, Hess and Schaad have offered a method that takes into account branching of the molecule. Using Hückel's MO method as a framework, they have classified the bonds in acyclic polyene into eight different types and calculated their corresponding energies[15]. ***Hess and Schaad resonance energies*** (HSRE) are obtained by subtracting the sum of energy of all types of bonds existing in a reference molecule from the energy of the given cyclic conjugated molecule.

Two other resonance energies- TRE-***topological resonance energy***[16] and CCMRE- ***conjugated circuits method resonance energies***[17] are not

derived using quantum chemical calculations. In the former, stabilization energies are obtained with the use of graph theory and in the latter they are calculated by applying conjugated circuits method on cyclic conjugated molecules.
The advantage of using graph theory lies in its applicability to radicals and ions. Furthermore, without the introduction of any new parameters, graph theory can be used for the calculation of resonance energies in systems containing heteroatoms.

The conjugated circuits method does not provide as accurate resonance energies as other methods do. Its importance is apparent from the broadness of its application for deduction of the relative order of aromaticity among related structures.

For the purpose of comparing resonance energies of structures with different ring sizes, resonance energies are usually reported in the form of REPE - resonance energy per electron. REPE calculated by methods discussed above is given in Table 1.

Compound	DRE (β)	HSRE (β)	TRE (β)
benzene	0.120	0.065	0.046
naphthalene	0.930	0.055	0.039
cyclobutadiene	-0.136	-0.268	-0.307
cyclooctatetraene	-0.054	-0.060	-0.074

Table1. Resonance energies per electron calculated by different methods

Resonance energies derived from ***homodesmotic reactions*** (HRE) give reliable results and are now most widely used[18]. Homodesmotic reactions are reactions in which reactants and products have the same number of carbon atoms with the corresponding hybridization. In addition, the number of hydrogen atoms bonded to the individual carbon atoms remains the same. An example of the use of homodesmotic reaction in calculation of RE of benzene is given below:

$$C_6H_6 + 3\ CH_2{=}CH_2 \rightarrow 3\ CH_2{=}CH\text{-}CH{=}CH_2 \quad (s\text{-}trans) \qquad (1.5)$$

$$\Delta H^{o}_{calc}\ (MP2/6\text{-}31G^{**}) = 23.9\ kcal/mol\ (100.0\ kJ/mol)$$

Homodesmotic stabilizations energies (HSE) can be calculated experimentally, from the heats of formations, if those are known, or by using semiempirical and *ab initio* calculations. Since stabilization energies calculated by semiempirical and *ab initio* methods agree very well with experimentally obtained data and due to the high sophistication and development of *ab initio* methods, theoretical calculations have found a broad use for calculation of homodesmotic resonance energies for systems for which experimental data do not exist.

As can be seen, there are many types of resonance energies obtained using different methods[19]. Accuracy of the results depends on the sophistication of the method used and on the chosen reference molecule. However, between all of the above mentioned resonance energies (except DE) there is a qualitative

relationship and in some cases even a quantitative one, which indicates the significance and relevance of the energy criterion in determining aromaticity/antiaromaticity of the system[20].

1.2.2. Structural criteria

Three geometric features of the benzene molecule serve as structural criteria for aromaticity/antiaromaticity: planarity, equalization of the carbon-carbon bonds in the ring and high symmetry.

1.2.2.1. Planarity.

Stabilization of aromatic molecules is usually associated with the π electron delocalization. For the maximum overlap of p-orbitals that ensures π electron delocalization, the system has to have a planar structure. That is why aromatic molecules are likely to have planar structures while antiaromatic molecules, in order to avoid destabilization involved with their 4n electron systems, tend to have nonplanar structures.

Theoretical studies done on paracyclophanes have shown that there is, indeed, a relationship between the stabilization energies (HSE) and the ring bending angle, φ[20].

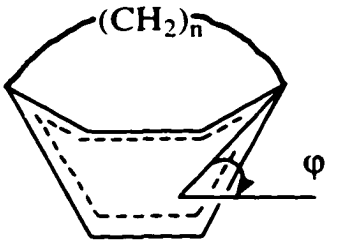

n=5 φ=23.7° HSE = -50.1 kcal/mol

n = 6 φ =18.6° HSE = -26.3 kcal/mol

Figure 3. The effect of nonplanarity on the resonance energy of [5] and [6]paracyclophanes

The more the benzene ring in paracyclophanes is bent out of planarity, the greater destabilization of the molecule. However, in the same study, the authors have also pointed out that even though there is an evident loss of aromaticity in terms of resonance energy, if magnetic criteria of aromaticity were used, namely NMR shifts, [5]paracyclophanes would still be classified as aromatic molecules.

There are examples of antiaromatic molecules with planar structures (cyclobutadiene) as well as examples of aromatic molecules possessing nonplanar structures ([10] annulene). What this shows is that planarity by itself can't be used as a criterion for aromaticity, and that other effects, like strain or steric crowding, play an important role in determining the geometry of the molecule.

1.2.2.2. Symmetry

As it is seen from figure 4, benzene's symmetrical structure has minimal energy on a potential energy surface (PES), while in the case of cyclobutadiene, a high symmetry structure corresponds to the energy maximum on PES. In general, aromatic molecules are expected to be stable toward distortions from highly symmetrical structures, whereas antiaromatic molecules are predicted to be distorted from the high symmetry form.

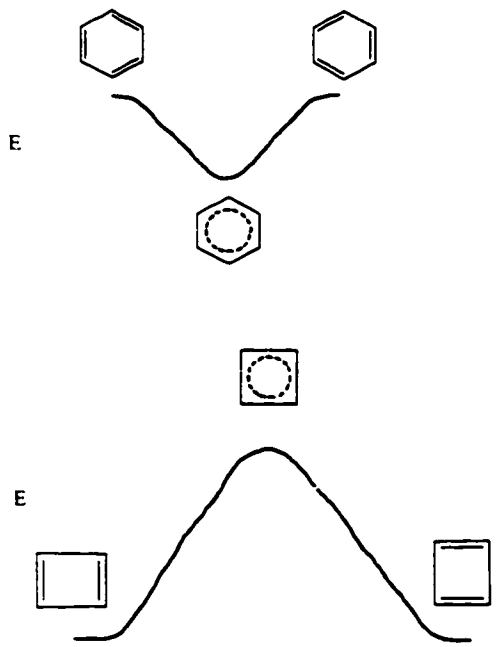

Figure 4. Potentional energy curves for benzene and cyclobutadiene

Distortion observed in antiaromatic molecules is explained by the pseudo Jahn-Teller effect, stating that cyclic $C_{4n}H_{4n}$ molecules having doubly degenerate orbitals in the ground state in Hückel's picture would be unstable toward distortions which remove the symmetry of the molecule[21]. In other words, there is a gain in stability in antiaromatic molecules when the degeneracy of the two HOMOs is removed by distortion from the symmetrical structure.

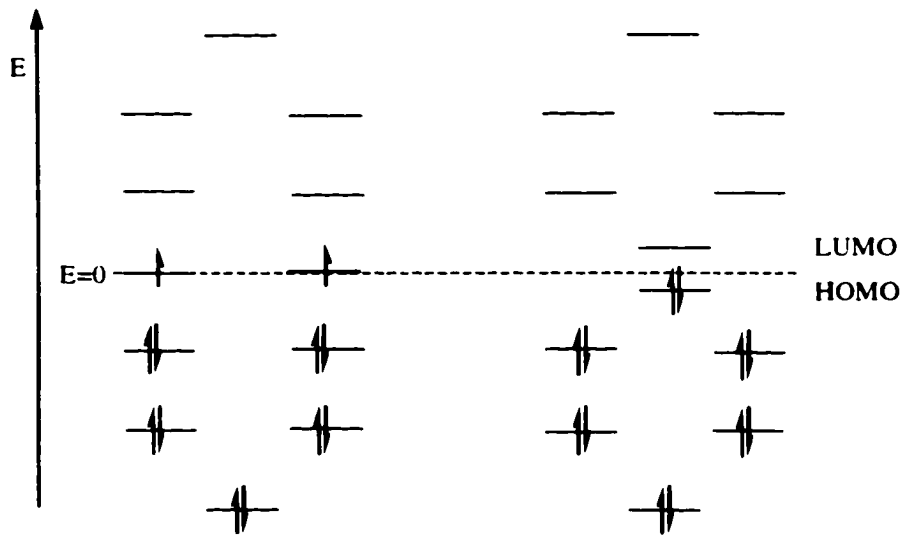

Figure 5. Jahn-Teller effect in a basic 12 π system

In the case of cyclobutadiene, the pseudo Jahn Teller effect is expressed in the form of bond alternation, which is why its ground state has a rectangular structure rather than a square one.

It is interesting to note that large $C_{4n+2}H_{4n+2}$ annulenes are predicted to have structures with alternating carbon-carbon bonds, due to the mixing of HOMO with a low lying LUMO of the molecule.

1.2.2.3. Bond equalization vs. bond alternation

Structurally, aromatic and antiaromatic molecules differ, above all, in bond lengths. As is very well known, carbon-carbon bond lengths in benzene are all equal: 1.3983 Å, a value that lies between the values for the bond length of a carbon-carbon single bond, and a carbon-carbon double bond in sp^2 hybridization. On the other hand, as we have seen, antiaromatic molecules trying to avoid high symmetry form have structures with alternating carbon-carbon bonds.

The first mathematical description of the effect of bond alternation on the aromaticity of a molecule was given by Julg and Francois as an aromaticity index[22]:

$$A = 1 - 225/n\sum (1 - R_r/R)^2 \qquad (1.6)$$

where n is the number of peripheral bonds with the bond length R_r, and R is a median bond length. However, since the aromaticity index takes into account only peripheral carbon carbon bonds, its use is limited to monocyclic, all carbon systems, only.

Krygowski has introduced a method that overcomes the drawbacks of aromaticity index. His approach consists of proposing an optimal bond length, R_{opt}, as a reference for calculating HOMA (harmonic oscillator model of aromaticity) index[23].

$$HOMA = 1 - \alpha/n \sum (R_{opt} - R_i) \qquad (1.7)$$

where n is the number of bonds, R_i is the individual bond length and α is a constant ensuring that HOMA is equal to 1 when the bond lengths are equal to optimal bond length and that HOMA is equal to 0 for systems with bond lengths as in acyclic polyene.

With further elaboration of the equation, HOMA can be expressed in terms of two effects contributing to the diminishing of aromaticity: 1. bond elongation-EN term; 2. bond alternation –GEO term.

$$HOMA=1 - [f\alpha (R_{opt}-R_{av}) + \alpha/n\sum(R_{av}-R_i)^2]= 1 - EN-GEO \qquad (1.8)$$

$f = 1$ when $R_{av} < R_{opt}$;

$f= -1$ when $R_{av} > R_{opt}$

where, R_{av} is an averaged bond length.

HOMA has been applied on a wide range of various types of molecules.

Different in nature, but still providing a description of aromaticity in terms of bond lengths, is HOSE (harmonic oscillator stabilization) index[24]. It is defined as a negative value of the energy needed for a real molecule to distort into its resonance structure. In other words, HOSE index offers estimation of stabilization energies based on bond lengths. In addition, HOSE model can be used for calculating the contribution of a particular resonance structure to the description of the given molecule.

1.2.3. Magnetic criteria

The explanation of magnetic properties of aromatic/antiaromatic molecules is based on the concept of interatomic ring currents, induced by an external magnetic fields[25]. Pople's ring current model[26], pictured in figure 6, has been used to describe the effect of those ring currents (be it diatropic or paratropic) on NMR chemical shifts[26,27].*

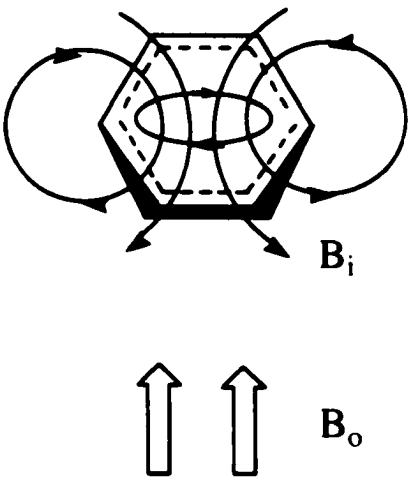

Figure 6. Pople's ring current model

---

* The most recent publication by Schleyer [28] suggests the incorrectness of Pople's model and offers a completely new picture of shielding/deshielding effects. Consequently, a theoretical connection between chemical shifts and aromaticity is undermined.

When a magnetic field is applied perpendicular to the plane of an aromatic molecule, cyclic delocalization of π-electrons causes a diamagnetic ring current which induces an additional magnetic field. The induced magnetic field is in the opposite direction to the applied field, above and under the plane of the ring and in the same direction in the plane of the ring. For antiaromatic molecules the model of the induced paratropic ring current predicts an opposite effect: the external magnetic field is reinforced in the center of the ring and diminished outside the ring.

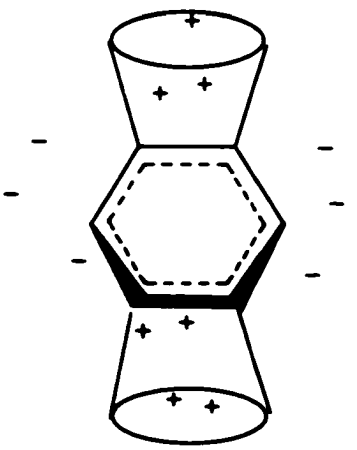

Figure 7. Areas of shielding and deshielding in benzene

Diatropic and paratropic ring currents are experimentally most easily detected by ^{1}H NMR chemical shifts. A good example of the effect of a diatropic ring current on the proton chemical shifts, is found in the ^{1}H NMR spectrum of [18] annulene

measured at – 60 °C. Here, the six internal protons appear at -2.99 ppm, while twelve external ones show a chemical shift of 9.28 ppm[29].

On the other hand, proton chemical shifts in [16] annulene indicate a paratropic ring current[29,30]. The ^{1}HNMR spectrum measured at -120 °C shows two signals: one at 10.4 ppm corresponding to the internal protons, and another one at 5.4 ppm, coming from the external protons.

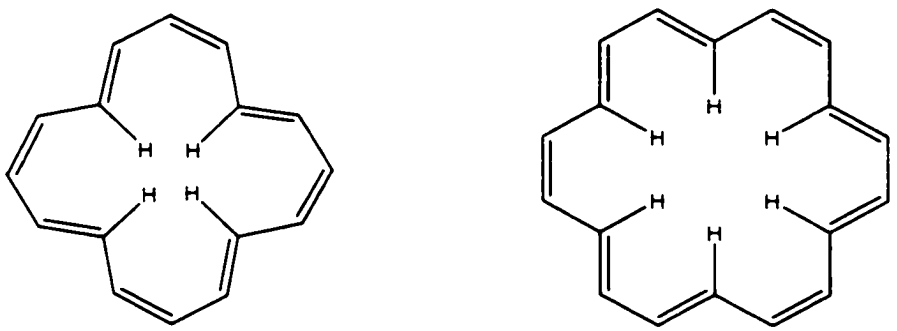

Figure 8. [16] and [18] annulene

Chemical shifts in the ^{1}H NMR can be used not only for qualitative, but also a quantitative estimation of aromaticity. To do so, correlations between chemical shifts and other properties (theoretical as well as experimental) of aromatic systems have to be established. The first such correlation was given by Hess, Schaad and Nakagawa, who showed that for the set of molecules shown in figure 9,the ring current-calculated as a difference between inner (H_i) and outer

protons (H_o)- is directly proportional to the resonance energy per electron (REPE)[31].

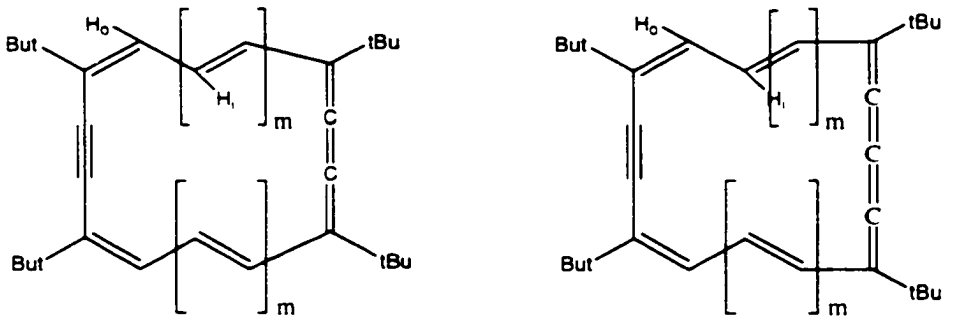

Figure 9. Tetra-*tert*-butyldehydro[n]annulenes

Later on, for the same group of compounds, Verbrugen has shown that the relationship is as follows[32] :

$$\Delta\delta/A = k' \text{ REPE} \qquad (1.9)$$

where A is the ring area, and is equal to 1 for benzene, and k' is a constant.

For the class of benzo-[n] annulenes (figure 10), Günther has proposed Q value, defined as a ratio of neighboring bond orders $P_{2,3}/ P_{3,4}$, as a useful tool for differentiating between aromatic and antiaromatic molecules.

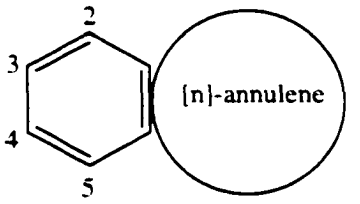

Figure 10. Generalized benzo[n]annulene

It is based on the observation of unequal bond lengths whenever two annulenes are fused together. Unequal bond lengths cause unequal vicinal coupling constants. Günther has formulated the relationship between bond orders and coupling constants $J_{a,b}$[32] :

$$P_{a,b}= 0.104\ {}^3J_{a,b} - 0.12 \qquad (1.10)$$

Using these easily obtainable values, annulenes can be categorized as aromatic, antiaromatic or non aromatic, based on the Q values. If Q is larger then 1.14 than the annulene is aromatic; if Q is smaller than 1.03 annulene is antiaromatic; annulenes with the Q values between 1.10 and 1.04 are classified as non aromatic.

For the set of various benzannelated [14] annulenes, Mitchell has formulated a correlation between chemical shifts of the internal methyl protons and the average deviation of the bond orders from that of the parent [14] annulene, Δp (equation 1.11 and 1.12). That is the basis of the estimation of the aromaticity which uses bridged annulenes as NMR probes[34].

Using two fairly simple equations :

$$\Delta\delta = 0.97 - \delta\,(Me) \qquad (1.11)$$

$$\Delta\delta = 5.533\text{-}27.52\ \Delta p \qquad (1.12)$$

one is able to predict chemical shifts in the series of molecules that, as it can be seen, show an excellent agreement with experimental results.

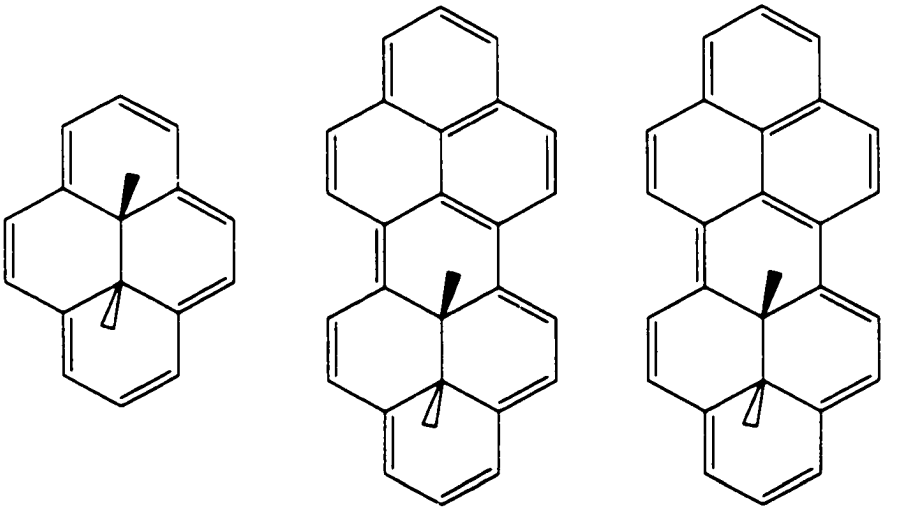

$\delta_{(CH3)}$			
calculated		-2.75	-3.97
found	-4.25	-2.78	-4.19
			-4.28

Figure 11. Comparison of calculated and experimental chemical shifts of internal methyl groups for [14]annulene and its benzo- derivatives

Recently introduced NICS (nucleus independent chemical shifts) values established by Schleyer, are attracting a lot of attention due to simplicity of calculation and good correlation with other criteria of aromaticity, especially stabilization energies[35].

NICS are defined as the absolute magnetic shielding computed at the ring center. In order to correlate with the NMR chemical shifts signs, large negative NICS values (magnetic shielding) indicate presence of diatropic ring current. Antiaromatic systems have large positive NICS values, indicating paratropic ring current (magnetic deshielding). The advantage of NICS values over other aromaticity indexes, is in that its evaluation does not require reference models, or calibration of homodesmotic equations.

Since NICS values are effected by local shielding effects in smaller systems, Schleyer has introduced NICS(1) values, calculated 1 Å above the ring center-- where the local contributions are diminished-- as a better measure of aromaticity[36].

1.3. Aromaticity/antiaromaticity as a multidimensional or one-dimensional phenomenon?

As we have seen, categorization of the molecules as aromatic, non-aromatic and antiaromatic is based on the use of various types of criteria. For the proper understanding of the concept of aromaticity, it is important to know if quantitative indices of aromaticity can be correlated with each other. By one group of authors[37], aromaticity is understood as a multidimensional phenomenon, meaning that at least two factors are necessary for the description of aromaticity. In 1995, Schleyer has offered a completely opposite view of aromaticity, as a one-dimensional property[38].

Extensive analysis of 105 different systems in the recent study[3], has shown that all indices (energetic, magnetic and geometric) allow a rough characterization of conjugated cyclic systems as aromatic, non-aromatic and antiaromatic. In that sense, aromaticity can be regarded as a one-dimensional phenomenon. However, within any one of these three main groups of molecules, indices could not be correlated implying multidimensional character of aromaticity.

From everything presented above, an inevitable conclusion suggests itself: aromaticity still presents one of the most intriguing phenomena, and study of it is therefore one of the most challenging and fascinating fields in chemistry.

1.4. Selected [12]Annulenes

The term annulene was for the first time used by Sondheimer and Wolovsky for monocyclic conjugated molecules with the general formula $(CH)_n$, where n is an even number and denotes the number of carbon atoms in the ring[40].

The smallest antiaromatic (4n) annulene that could accommodate internal hydrogens without severe distortions from planarity is [12] annulene **1**. However, there is considerable van der Waals repulsion between the inner hydrogens, and the molecule is distorted from planarity with the estimated torsional angle of 50 – 60 °. The molecule appears to be only slightly paratropic: the ^{1}H-NMR spectrum at –170 °C shows a 3H peak at δ 7.93 ppm (internal protons) and a 9H peak at δ 5.88 ppm (external protons). At higher temperature (-60 °C) there is a fast conformational interconversion (1a→1b) and the ^{1}H-NMR spectrum shows two peaks of equal intensities at δ 6.88 ppm (cis protons) and δ 5.97 ppm (trans protons)[11].

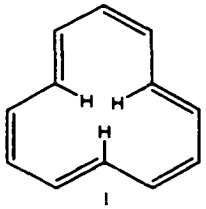

I

Ia Ib

In order to remove the destabilizing van der Waals repulsion of the inner hydrogens, to form a more rigid system and to force the system into planarity, bridging of annulenes with carbon and heteroatoms was investigated.

1.4.1 Bicyclic bridged [12]annulenes

Vogel et.al have synthesized bridged [12] annulenes with methano groups above the plane of the ring – 1,7 -methano[12]annulene (**2**)[41] and 1,6-methano[12]annulene (**4**)[42]. Both were found to be paratropic.

The importance of 1,7-methano[12]annulene for the study of paratropicity lies, besides the obvious structural advantage over [12] annulene, in its similarity to 1,6-methano[10]annulene (**3**). Comparison of the chemical shifts of bridged

protons in 1,7-methano[12]annulene (**2**) and in 1,6-methano[10]annulene (**3**) verifies an existence of a paramagnetic ring current in 4n π systems.

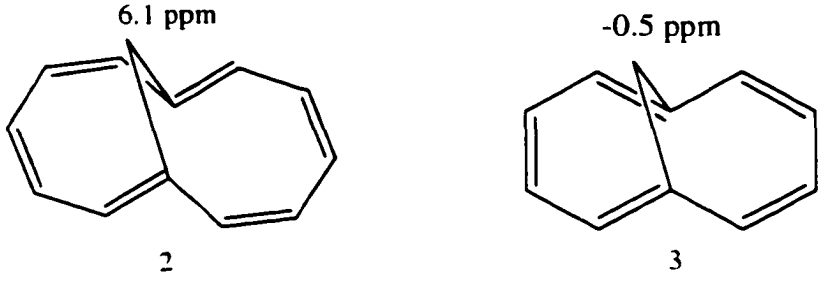

Figure 12. 1,7-methano[12]annulene (**2**) and 1,6-methano[10]annulene (**3**)

The ^{1}H NMR spectrum of 1,7-methano[12]annulene is temperature dependent indicating the equilibrium between two valence tautomers, **3** and **3a** :

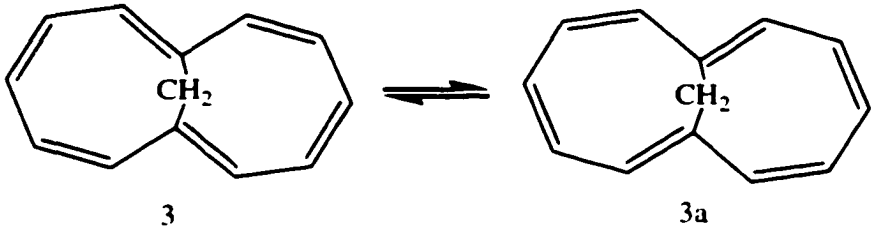

Figure 13. Valence tautomerism in 1,7-methano[12]annulene

On the other hand, the ^{1}H NMR spectrum of less symmetrical 1,6-methano[12]annulene (**4**) is temperature independent, suggesting preference for

only one of the two possible valence tautomers. Molecular models as well as NMR analysis point to valence tautomer shown below to be a preferred structure.

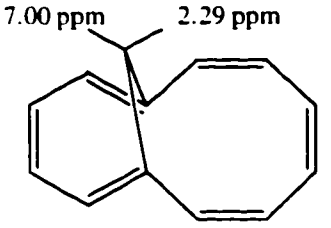

4

Figure 14. 1,6-methano[12]annulene

The two bridge protons in 1,6-methano[12]annulene have quite different chemical shifts which implies the conformation of the molecule as shown in figure 15.

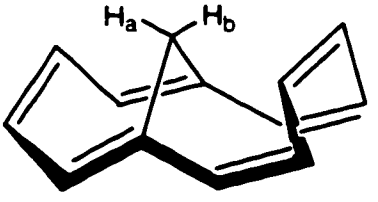

Figure 15. Conformation of 1,6-methano[12]annulene

Although paratropicity is somewhat lowered, and less obvious due to the deformation from planarity, comparison with its nonconjugated analog **5** clearly shows the existence of a paramagnetic ring current.

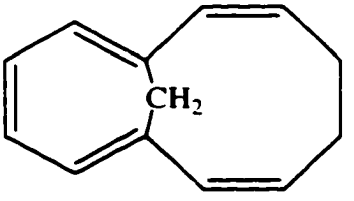

5

Figure 16. 9,10-dihydro-1,6-methano[12]annulene

1.4.2 Tricyclic bridged [12]annulenes

The nitrogen bridged [12] annulene ,cycl[3.3.3]azine,**6**, has been synthesized by Leaver[43] and its ^{1}HNMR spectrum shows two signals : one at 3.65 ppm corresponding to protons at 2,5 and 8 positions and the other at 2.07 ppm corresponding to the remaining six protons. As comparison, exocyclic protons in its 10 π analog, cycl[3.2.2]azine, resonate at δ 7.6 ppm, indicating presence of a diamagnetic ring current. Although NMR data show clear paratropicity for **6** and diatropicity for **7** , having nitrogen as a bridge imposes a problem of interaction between the nitrogen lone pair of electrons and the π-system of the ring[44].

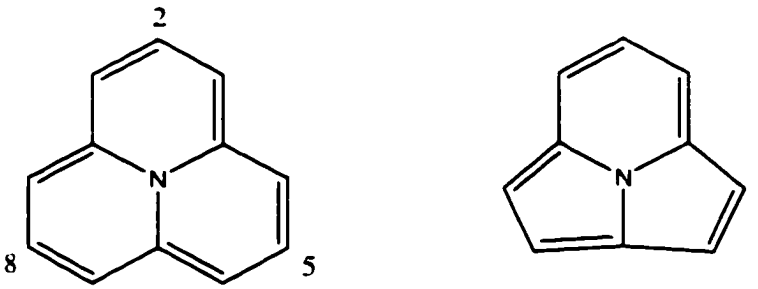

6 7

Figure 17. Cycl[3.3.3]azine (**6**) and cycl[3.2.2]azine (**7**)

Attempts to synthesize methine bridged [12] annulene (**8**) have failed, and only its more stable isomer **9**, formed by a thermally allowed [1,5] sigmatropic shift, was obtained[45].

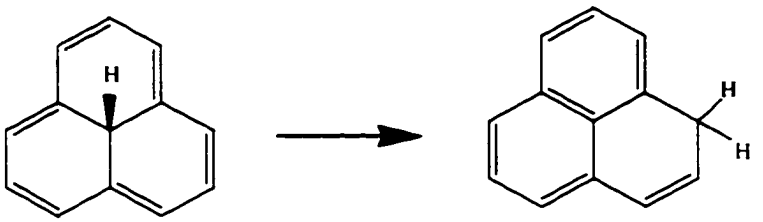

8 9

Figure 18. 1,5 shift in methane bridged [12]annulene

Bridging with a carbon bearing a methyl group could avoid problems such as the interference of the lone pair of electrons on heteroatoms and the lability of the methine group. 9b-methyl-9b*H*-benzo[cd]azulene(**10**) was synthesized by Hafner and its ^{1}H NMR shows a signal for the internal methyl group at 4.75 ppm, while protons outside the ring resonate at 3.88-4.69 ppm[46]. Hafner's molecule is stable in the solution up to 80 °. At higher temperatures, sigmatropic 1,5 shift occurs, giving 9a-methyl-9aH-benz[cd]azulene (**10a**).

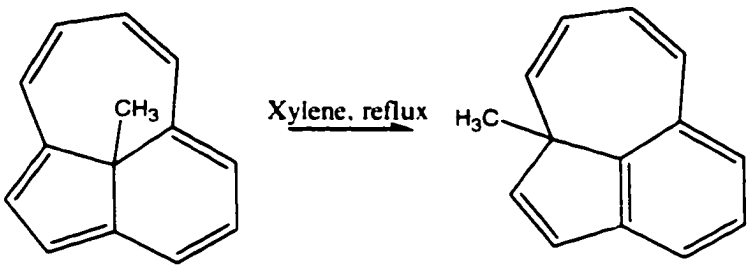

10 10a

Figure 19. 1,5 shift observed for 9b-methyl-9b*H*-benzo[cd]azulene

One system that would serve as a very good model for investigating paratropicity would be 13-methylphenalene (11). It is rigid, symmetrical, and nearly planar. Its highly symmetrical structure ensures minimum pseudo Jahn Teller distortion. For that reason, maximum paratropicity is expected in the system. In addition, the methyl group at central carbon would serve as an excellent NMR probe for studying paratropic effects.

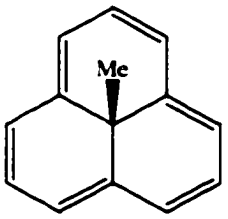

11

Figure 20. 13-methylphenalene

Previous studies directed toward the synthesis of **11** in our group, have shown that introduction of the last double bond in the final step always leads to the loss of the methyl group[47]. This suggested that the bond between the methyl group and the central carbon is very weak, as was later confirmed by AM1 calculations[48,49].

1.4.3. Benzannelated Annulenes

The effects of benzannulation of aromatic annulenes have been studied most intensely by Mitchell[50]. Series of benzannulated [4n+2] annulenes have been prepared and comparison of chemical shifts with their parent, nonbenzannelated system has shown that benzannulation causes bond alternation , decreases ring current and destabilizes the molecule.

The data available for the study of the fusion of the benzene ring onto antiaromatic molecules is less abundant due to the instability of molecules. Effects of benzannelations in 4n systems were studied by Sondheimer, Mitchell, Scott and in our group[34,50,52,53]. The difference in chemical shifts of the bridging hydrogens in the parent annulene and its benzannelated derivatives indicated that, just like in the case of aromatic systems, benzannulation reduces the ring current. Consequently, benzannulation has a stabilizing effect on 4n π systems. Scott has synthesized benz[b]homoheptalene (**12**), a benzo derivative of 1,7-methano[12]annulene (**3**)[52]. Coupling constants in the 1H NMR as well as the temperature independence of the spectrum indicate that there is no π bond shift,

observed in parent molecule (**3**), and that the highly favored structure is the one shown below. Furthermore, comparison of the chemical shifts of bridge protons in benzannulated derivative and in the parent compound indicates that the paratropicity is lowered with benzannulation.

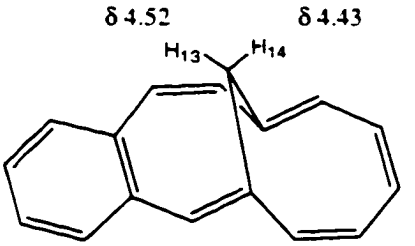

12

Figure 21. Benz[b]homoheptalene (**12**)

However, bridge protons still resonate at significantly lower field in comparison to the atropic molecule. Based on the NMR data Scott has estimated that benz[b]homoheptalene maintains 50-60% of the paramagnetic ring current present in 1,7-methano[12]annulene.

CHAPTER 2. THEORETICAL INVESTIGATIONS

2.1. Theoretical calculations

As mentioned earlier, we wanted to introduce extra stability into the system by fusing a benzene ring onto the parent system and changing the methyl group at the central carbon position for the phenyl group. The main aim of the first part of the theoretical studies, done on our target molecule and the similar systems, was to give us insight into the gain in stability of the systems as these features are changed. In addition, comparison of the values calculated for our system with already synthesized molecules of a similar type would predict the feasibility of preparation of our compound. Previous AM1 calculations in Grohmann's group, prompted by the observation of the loss of the central methyl group even under the mildest conditions, showed a very weak central carbon-carbon bond[49]. Calculations have also shown that benzannelation stabilizes the systems. In order to ensure consistency with the results obtained earlier in our group, we've performed the calculations on both 13-substituted phenalenes(**13 a,b,c**) and their mono-(**14 a,b,c**) and dibenzannelated-(**15 a,b,c**; **16 a,b,c**; **17 a,b,c**) derivatives (figure 22).

The second part of theoretical investigations deals with the possible pathways for the loss of the substituent group from its central position, namely, the 1,5 shift and dissociation of the substituent group.).

For the purpose of comparison, calculations for already synthesized 10π (**18 a,b,c**) and 12 π (**9 a,b,c**) systems have also been carried out.

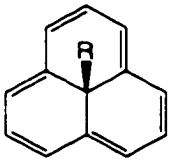

13 a. R= methyl
b. R= phenyl
c. R= ethynyl

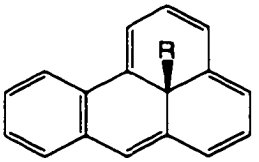

14 a. R= methyl
b. R= phenyl
c. R= ethynyl

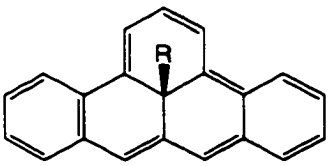

15 a. R= methyl
b. R= phenyl
c. R= ethynyl

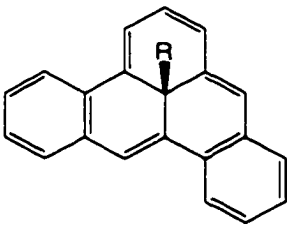

16 a. R= methyl
b. R= phenyl
c.R= ethynyl

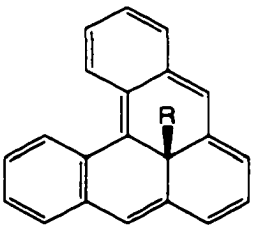

17 a. R= methyl
b. R= phenyl
c. R= ethynyl

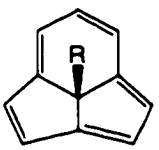

18 a.R= methyl
b.R= phenyl
c.R= ethynyl

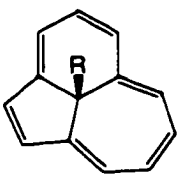

9 a. R= methyl
b. R= phenyl
c. R= ethynyl

Figure 22. Compounds investigated using AM1 calculations

Molecular orbital calculations were performed using AMPAC 6.0[54] at the semi-empirical theory level. Structures were drawn in AMPAC format and were used directly in AM1 calculations. All calculations were done with RHF constraints.

2.1.1. Calculation of Bond Dissociation Energies (BDE's)

First to be determined were bond dissociation energies-BDE's. The enthalpies of the formation of the ground states and the corresponding radicals were calculated first. BDE's were then computed as follows:

$$BDE=\Delta H_{rad} + \Delta H_R - \Delta H_f \qquad (2.1)$$

where ΔH_{rad} is the enthalpy of formation of the radical species, ΔH_R is the enthalpy of formation of substituent radical -methyl, ethynyl or phenyl, and ΔH_f is the enthalpy of formation of the compound in question.

The enthalpies of the formation for the methyl, the ethynyl, and the phenyl radical, are calculated to be 31.62 kcal/mol,148.75 kcal/mol and 79.41 kcal/mol, respectively. Literature reported values for heats of formation for methyl and phenyl radical are 35 kcal/mol and 79 kcal/mol, respectively. The value for the enthalpy of formation of the ethynyl radical could not be found in the literature.

Molecule	H_f (kcal/mol)	Bond length (Å)	BDE (kcal/mol)
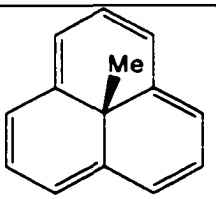	89.78	1.5451	11.43
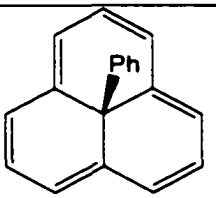	128.76	1.5273	20.62
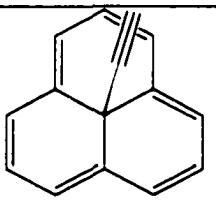	155.34	1.4610	63.38
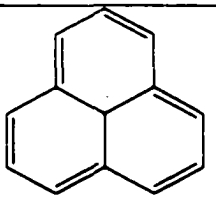	69.96		

Table 2. Calculated BDE's for 13-substituted phenalenes (13 a,b,c)

Molecule	H_f (kcal/mol)	Bond length (Å)	BDE (kcal/mol)
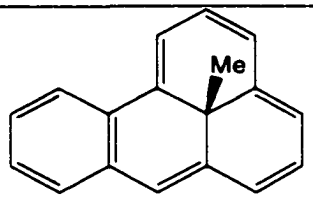	100.96	1.5436	18.83
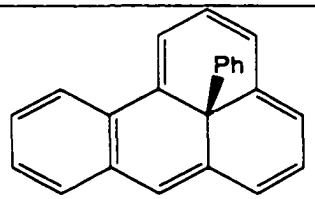	139.95	1.5262	28.04
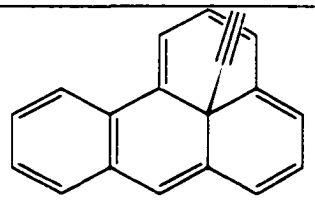	166.51	1.4600	71.02
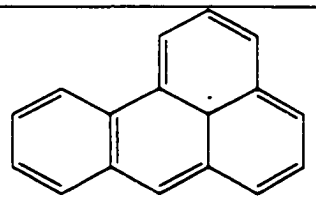	88.53		

Table 3. Calculated BDE's for benzo-13-substituted phenalenes (14 a,b,c)

Molecule	H_f (kcal/mol)	Bond length (Å)	BDE (kcal/mol)
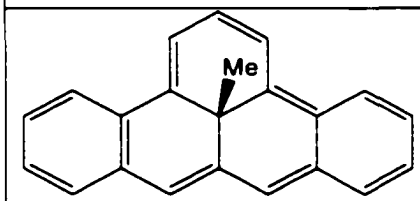	129.79	1.5457	7.01
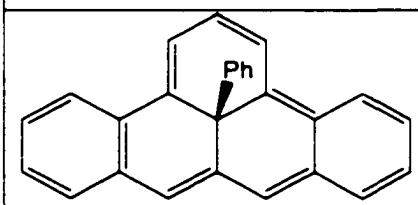	169.14	1.5279	15.9
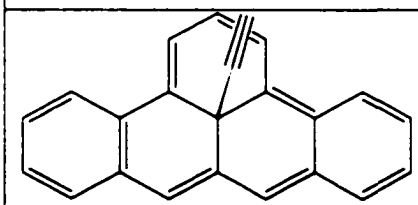	195.57	1.4610	58.99
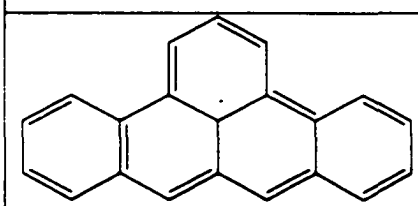	106.24		

Table 4. Calculated BDE's for 1,2,6,7-dibenzo-13-substituted phenalenes (15 a,b,c)

Molecule	H_f (kcal/mol)	Bond length (Å)	BDE (kcal/mol)
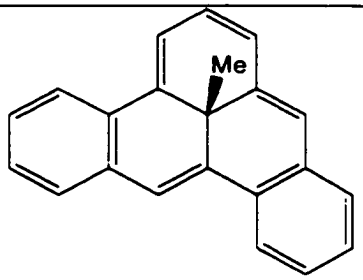	112.31	1.5411	26.08
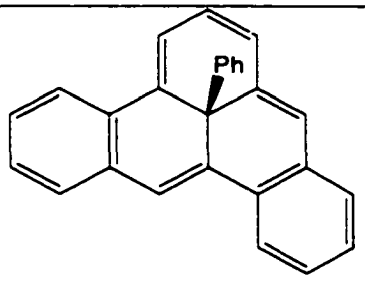	151.17	1.5245	35.44
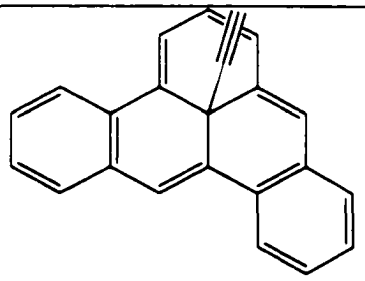	177.87	1.4599	78.28
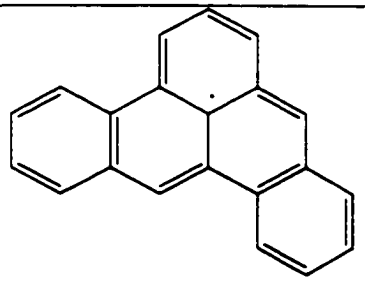	107.13		

Table 5. Calculated BDE's for 1,2,5,6-dibenzo-13-substituted phenalenes (16 a,b,c)

Molecule	H_f (kcal/mol)	Bond length (Å)	BDE (kcal/mol)
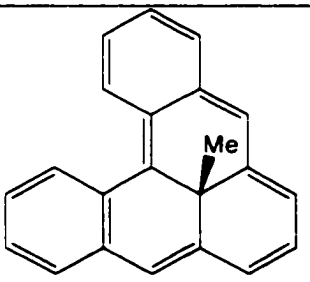	132.44	1.5422	13.64
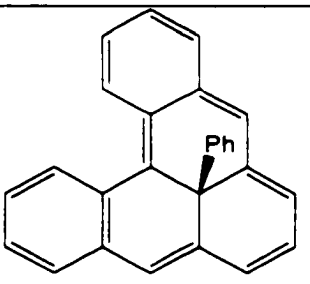	171.06	1.5243	22.85
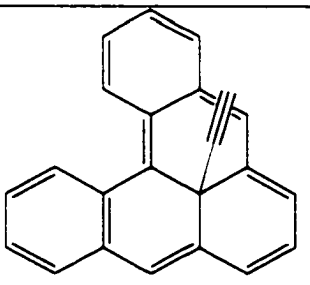	198.02	1.4591	65.91
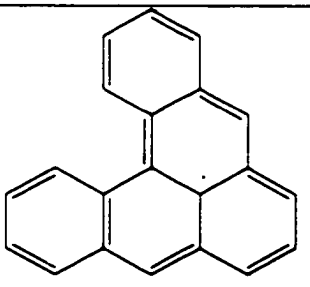	114.93		

Table 6. Calculated BDE's for 1,2,10,11-dibenz-13-substituted phenalenes (17 a,b,c,)

Molecule	H_f (kcal/mol)	Bond length (Å)	BDE (kcal/mol)
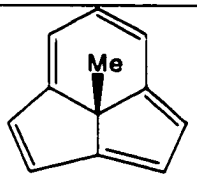	114.35	1.5131	53.92
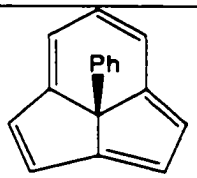	151.37	1.4960	65.11
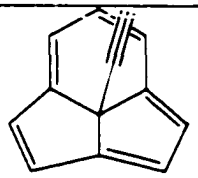	179.14	1.4348	106.88
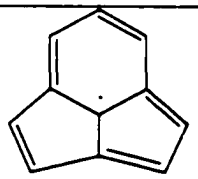	137.02		

Table 7. Calculated BDE's for 10 π system (18 a,b,c)

Molecule	H_f (kcal/mol)	Bond length (Å)	BDE (kcal/mol)
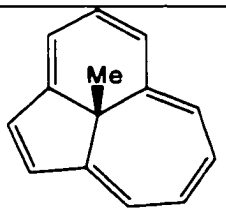	101.91	1.5313	29.98
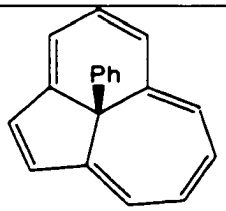	140.17	1.5126	39.93
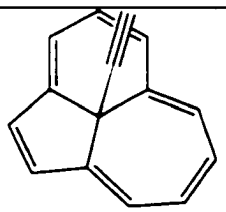	166.78	1.4490	82.86
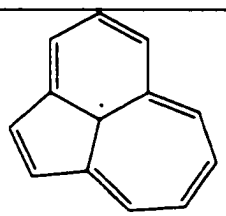	100.64		

Table 8. Calculated BDE's for 9b-substituted-9b*H*-benz[c,d]azullene (10 a,b,c)

2.1.2. Calculation of activation energies (E_{act}) for the dissociation of substituent group

To calculate the activation energy for the loss of the central group (methyl, ethynyl, phenyl), transition states needed to be located. Approximate transition states were calculated using the reaction path method. Reaction path calculations involve calculations of the enthalpies of formation of a series of geometries obtained by lengthening the bond between the central carbon and substituent group by 0.1 Ångstroms. Keywords used for obtaining approximate transition states for homolytic bond cleavage were PATH and BIRADICAL. Approximate transition states are located at the highest point of the reaction path curve. For refinement of found approximate transition states, the gradient norm had to be minimized. Gradient norm is the derivative of energy with respect to all atomic coordinates and as such should have the value close to zero for the transition state, which means that with infinitesimal changes in geometry, the change in energy of a transition state is very small. The gradient norm was minimized by the use of the keyword POWELL. For all structures calculated, the gradient norm was smaller than 0.2. After refinement of the gradient norm, all transition states were finally checked by performing frequency calculations using the keyword FORCE. Frequency calculations involve calculation of the second derivative of the energy of all pairs of atoms. Transition states must have only one negative frequency as the result of FORCE calculations.

The energy of activation was calculated by subtracting the enthalpy of the formation from the energy of the transition states.

$$E_{act.} = \Delta H_{f\,T.S} - \Delta H_f \qquad (2.2)$$

Molecule	H_f (kcal/mol)	$H_{f\,T.S.}$ (kcal/mol)	E_{act} (kcal/mol)
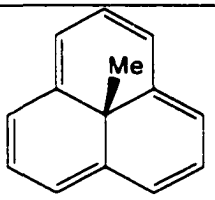	89.78	123.37	33.58
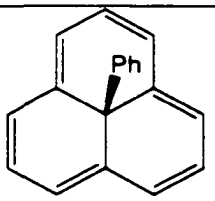	128.76	168.26	39.50
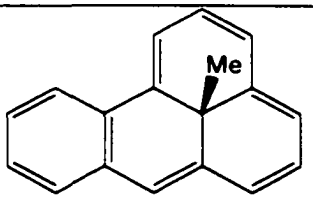	100.96	138.54	37.58
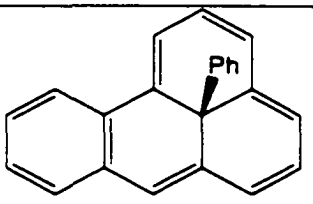	139.95	183.47	43.52

Table 9. Calculated dissociation E_{act} for **13 a,b** and **14 a,b**

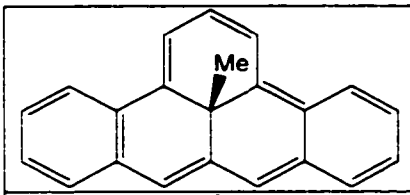	130.49	163.26	32.77
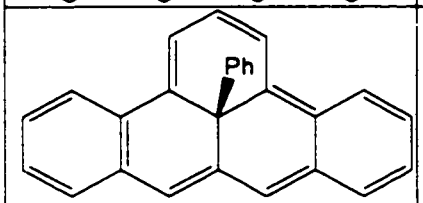	169.80	210.17	40.27
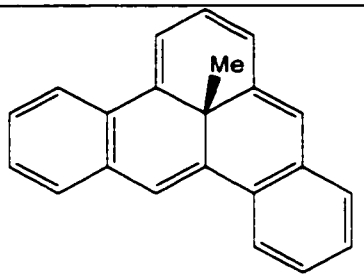	112.31	154.18	41.72
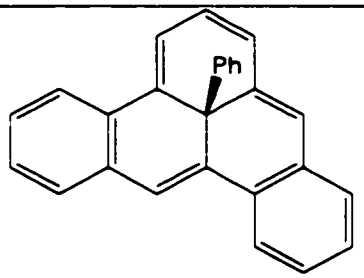	151.17	200.16	48.85
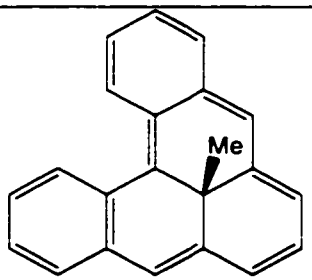	132.91	170.52	37.61
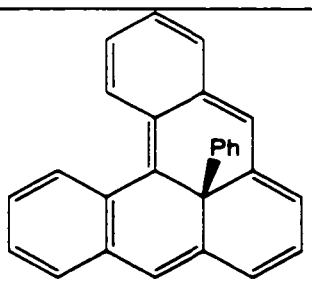	171.54	215.10	43.56

Molecule	H_f (kcal/mol)	$H_{f\ T.S.}$ (kcal/mol)	E_{act} (kcal/mol)
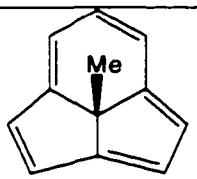	114.35	/	/
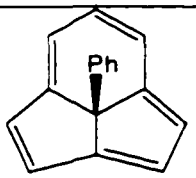	151.37	/	/
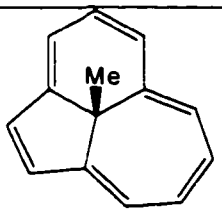	101.9	155.34	53.43
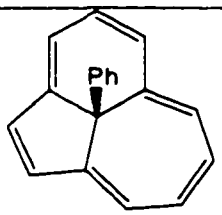	140.36	1.5126	41.28

Table 11. Calculated dissociation $E_{act.}$ for 18 a,b and 10 a,b.

2.1.3. Calculation of activation energy ($E_{act.}$) for the 1,5 shift

Calculations of approximate transition states for the 1,5 shift were performed by using chain method, with the use of the keyword CHAIN. In the input file were entered structures of the left and right minima, and approximate transition state, drawn as the structure of the molecule in question having substituent group (methyl, phenyl and ethynyl) at the middle point, between position 1 and position 5 (figure23). The output file gives energy minimized structure of approximate transition state, which is further optimized as described earlier for the calculation of transition states for dissociation of the substituent group. First, gradient norm was minimized, and the optimized structure finally checked by performing a frequency calculation.

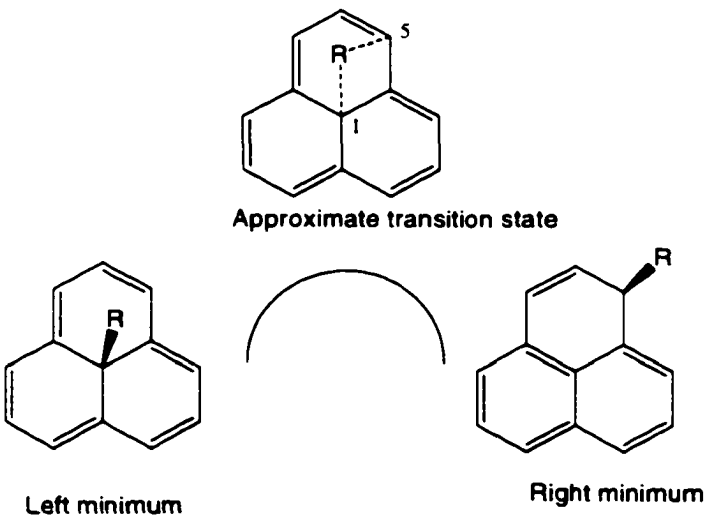

Figure 23. Structures entered in the input file for the chain method

Energy of the activation for 1,5 shift is calculated as a difference between the enthalpy of formation and enthalpy of transition state (equation 2.2).

There are three possible 1,5 shifts in the case of monobenzannelated systems:

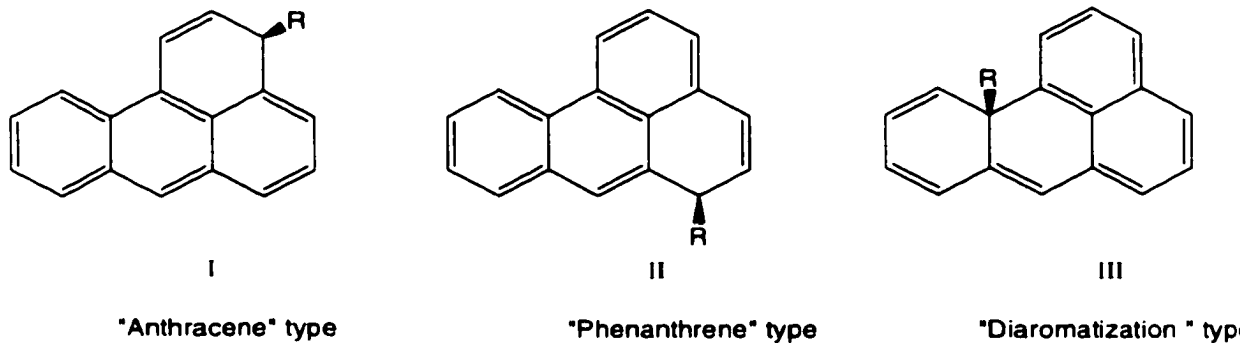

Figure 24. Three possible 1,5 shifts in monobenzannelated phenalenes

As it can be seen, pathway leading to the product "III" is the least probable since it involves the loss of aromaticity in the benzene ring, and therefore it was not further investigated.

Molecule	H_f (kcal/mol)	$H_{f\ T.S.}$ (kcal/mol)	E_{act} (kcal/mol)
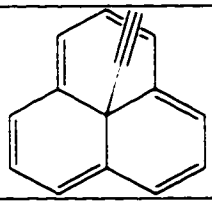	155.34	222.11	66.78
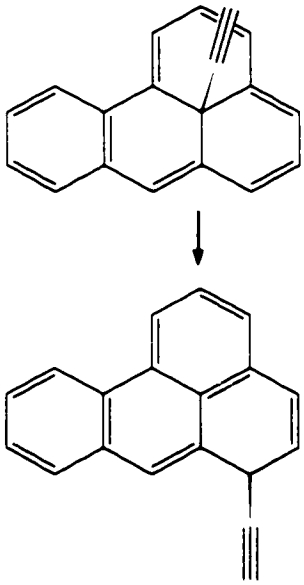	166.51	236.25	69.74
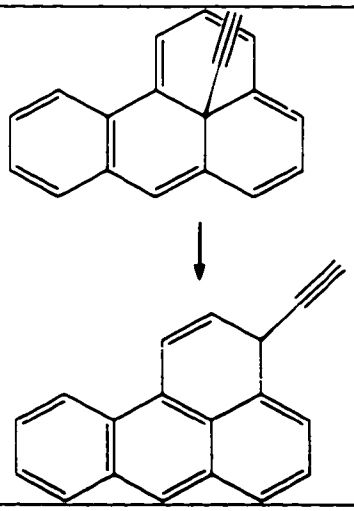	166.51	238.21	71.70

Molecule	H_f (kcal/mol)	$H_{f\ T.S.}$ (kcal/mol)	E_{act} (kcal/mol)
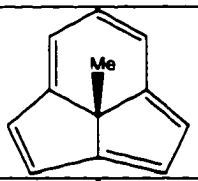	114.35	166.75	52.40
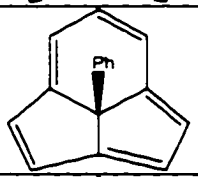	151.37	202.93	51.56
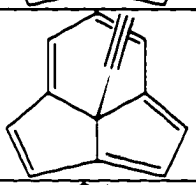	179.14	226.02	46.88
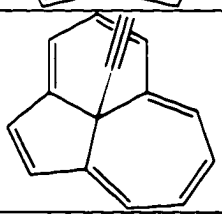	166.78	244.37	77.59

Table 12. Calculated $E_{act.}$ for the 1,5 shift

2.2. Discussion of AM1 calculations

2.2.1. The effect of benzannelation

Fusion of one or more benzene rings onto the conjugated π perimeter of an annulene causes bond localization to occur in both benzene ring(s) and annulene[33]. It is also known, that the size of the ring current is partially reduced if bond localization occurs[50b]. By reducing the paramagnetic ring current in antiaromatic annulenes, benzannelation has a stabilizing effect. The same reduction of the ring current caused by benzannelation, leads to destabilization of aromatic annulenes.

2.2.1.1. Monobenzannelation

As it can be seen, our results show the expected gain in stability for the benzannelated derivatives. Bond dissociation energies of benzo-13-methylphenalene (**14 a**), benzo-13-phenylphenalene(**14 b**) and benzo-13-ethynylphenalene(**14 c**), show increase by 7.4 kcal/mol, 7.42 kcal/mol and 7.64 kcal/mol, respectively, in comparison to the corresponding nonbenzannelated systems(**13 a,b,c**).

2.2.1.2. Dibenzannelation

Depending on the position of the second benzene ring, dibenzannelation can have either stabilizing or destabilizing effect.

In the case of "anthracene type" dibenzannelation (**15 a,b,c**), only one of the two benzene rings fused to the annulene can be aromatic. Thus, the destabilization of the molecule – calculated BDE's are 7.01 kcal/mol, 15.9 kcal/mol and 58.99 kcal/mol for the corresponding methyl, phenyl and ethynyl dibenzannelated phenalenes.

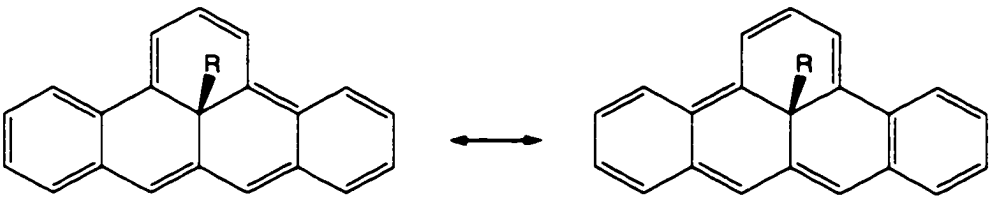

Figure 25. Resonance structures for anthracene type dibenzannelation

For "phenanthrene type" dibenzannelation (**16**), resonance structure with both benzene rings being aromatic can be written, which explains the increased stability of the system. Compared to nonbenzannelated molecules, BDE's for

dibenzannelated systems increased by: 14.65 kcal/mol for methyl, 14.82 kcal/mol for phenyl and 14.9 kcal/mol for ethynylphenalene.

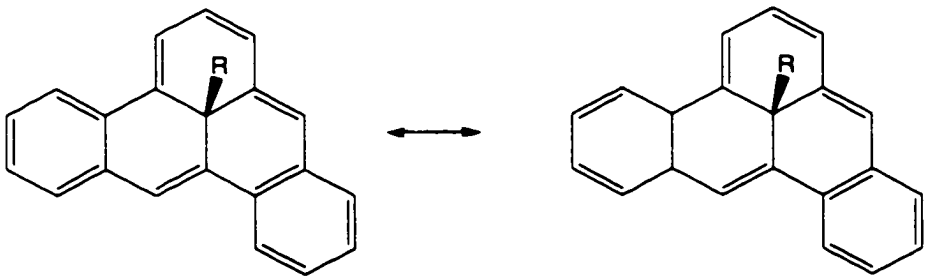

Figure 26. Resonance structures for phenanthrene type dibenzannelation

Due to the steric hindrance of the two hydrogens in **17 a,b** and **c** system is twisted out of planarity and we observe only small increase in BDE's . For methyl and phenyl phenalene that increase is of 2.2 kcal/mol, while dibenzoethynylphenalene -**17 c** BDE shows increase of 2.5 kcal/mol.

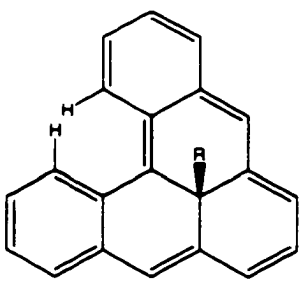

Figure 27. Steric hindrance in **17 a,b,c**

The results obtained concerning the effect of the benzannelation on the stability of the systems studied, were consistent with the results previously obtained in our group by Levinson[49] and Alva[48].

2.2.2. The effect of substituent at C13

As we have expected the central carbon-carbon bond is strengthened as we change the substituent from sp3 hybridized (methyl group), to a sp2 hybridized (phenyl group) to a sp hybridized (ethynyl group). That is apparent from the increase in BDE's. The average increase in BDE for having ethynyl group is 52.12 kcal/mol, while for the phenyl group that increase is 9.17 kcal/mol.

It is important to note here, that BDE is comprised of two energies: intrinsic bond energy – BE and the total (geometrical and electronic) reorganization energy- R[55].

$$BDE = BE + R \qquad (2.3)$$

Reorganization energy, R, is an evaluation of the stabilization of the corresponding radicals. If dissociation leads to stabilized radicals ($R < 0$), due to the gain in stabilization energy bond dissociation is facilitated. On the other hand, bond dissociation is impeded if dissociation leads to the formation of destabilized radicals.

Reorganization energies for methyl, phenyl and ethynyl radicals were calculated by Schleyer[55] as a difference between CH bond energies and heats of formation. While methyl radical shows stabilization of ~ 3kcal/mol, significant destabilization of about 5 kcal/mol for phenyl, and a large destabilization for the ethynyl radical has been predicted (~21 kcal/mol).

In the view of these values, increase in BDE's calculated for phenyl and ethynyl phenalenes can not be explained only by increase in intrinsic bond strength, but by geometric and electronic reorganizations during bond dissociation as well.

2.2.3. Comparison of BDE's of our target molecule with Hafner's molecule

The feasibility of preparation of benzo-13-phenylphenalene is apparent from a very close value of its bond dissociation energy with the value calculated for the already synthesized 12 π molecule.

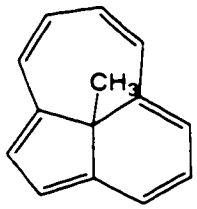

BDE 29.98 kcal/mol

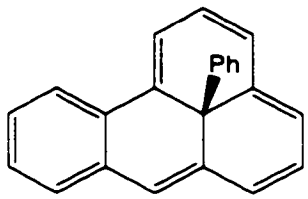

BDE 28.04 kcal/mol

Figure 28. Comparison of BDE's of benzo-13-phenylphenalene with Hafner's molecule

2.2.4. Dissociation vs. 1,5 shift

The loss of the methyl group in the attempt to introduce last double bond into the system was observed for both 13-methylphenalene and benzo-13-methylphenalene. That observation prompted the first AM1 calculations of bond dissociation energies in Grohmann's group. To get a better insight of the pathways leading to the removal of the methyl group from it's central position we have done AM1 calculations of energies of activation for the two possible reaction paths : 1,5 shift and a complete dissociation of the substituent group. Presumably 1,5 shifts have been observed for both 10π (7b-Methyl-7b*H*-cyclopenta[cd]indene) and 12π (9b-Methyl-9b*H*-benzo[cd]azulene) systems (figure 29).

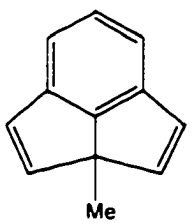

2a-Methyl-2a*H*-cyclopenta[*cd*]indene

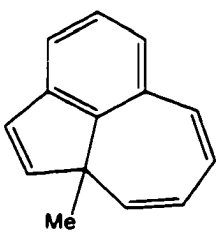

9a-Methyl-9a*H*-benzo[*cd*]azulene

Figure 29. Products of the 1,5 shift observed in Rees's and Hafner's molecule

The results in tables 9,10,11 and 12 show a clear trend. For 13-methylphenalene and 13-phenylphenalene as well as for their mono and dibenzo derivatives only transition states for dissociation of the substituent group were found. The attempt of calculating transition state for a 1,5 shift by the already described chain method (figure 23) as a result always gave approximate transition state for dissociation, indicating that transition state for dissociation is much lower in energy than the one for the 1,5 shift. That also means that for methyl and phenylphenalenes the preferred pathway for the loss of the substituent group from its central position would be dissociation. On the other hand, for ethynylphenalenes only the transition state for the 1,5 shift was obtained, meaning that the dissociation of the ethynyl group is hampered due to the stronger bond and destabilization associated with the ethynyl radical (section 2.2.2).

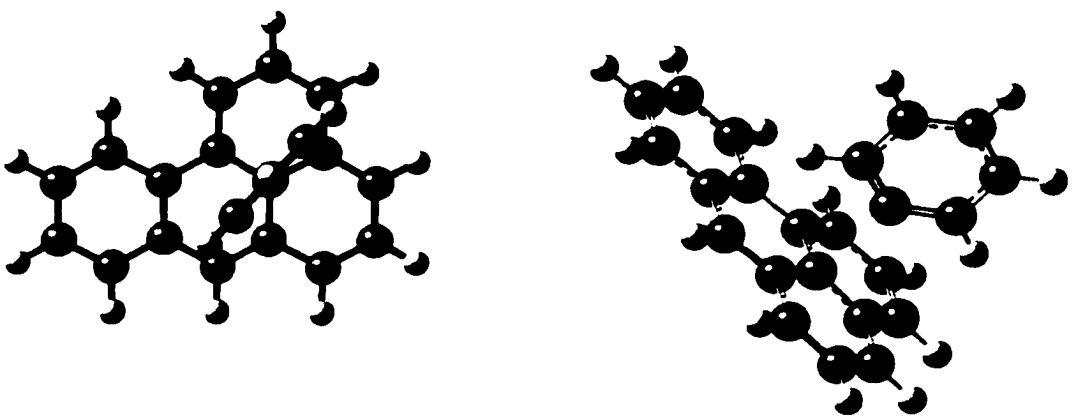

Figure 30. Calculated dissociation transition states for benzo-13-phenylpehnalene- top and side view

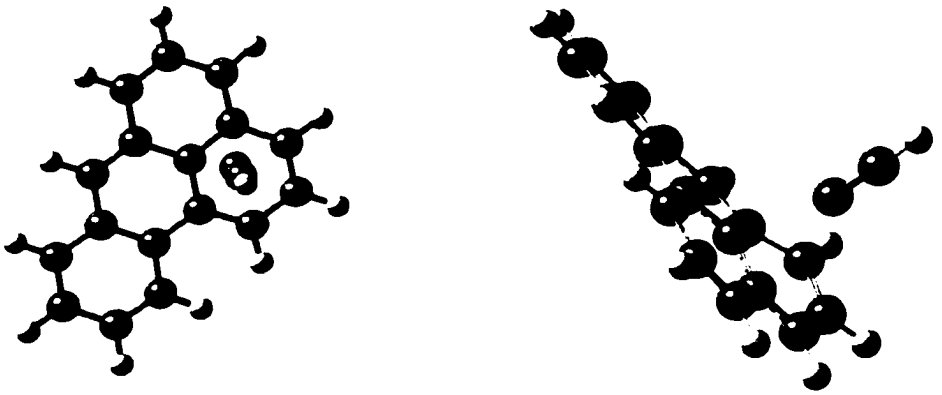

Figure 31. Calculated 1,5 shift transition state(anthracene type) for benzo-13-ethynylphenalene –top and side view

2.2.5. Anthracene vs. phenanthrene type 1,5 shift

The difference in stability of the product in the anthracene type 1,5 shift and the product in the phenanthrene type 1,5 shift (figure 24) reflects the difference in heats of formation between anthracene and phenanthrene .The barrier for phenanthrene type 1,5 shift is lower by 1.96 kcal/mol than the barrier for anthracene (respective energies of activation are 238.21 kcal/mol and 236.25 kcal/mol).

2.2.5. Energy of activation ($E_{act.}$) for the recombination of the radicals

In their theoretical studies of radical recombination, Huang and Dannenberg[56] have found a linear relationship between bond dissociation energy and activation energy for radical recombination:

$$\Delta H_{act} = 24.51 - 0.52BDE \qquad (2.4)$$

This equation implies that for all systems having BDE's equal or larger than 48 kcal/mol the activation energies for radical-radical recombination reaction will be insignificant. Our results agree very well with this finding. For methyl and phenylphenalenes that have BDE's lower than 48 kcal/mol, significant energies of activation for the recombination of radicals are found. That energy is calculated as difference between the enthalpy of the formation for the transition state and the sum of the two corresponding radicals:

$$E_{\text{act. for recombination}} = \Delta H_{f\ \text{discs. T.S}} - (\Delta H_{rad} + \Delta H_R) \qquad (2.5)$$

Molecule	$E_{a\ recombination}$ (kcal/mol)	$E_{a\ recombination}$ based on the equation (2.5) (kcal/mol)
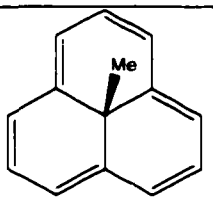	21.79	18.56
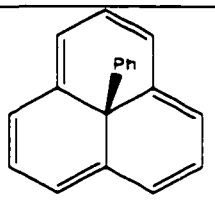	18.89	13.78
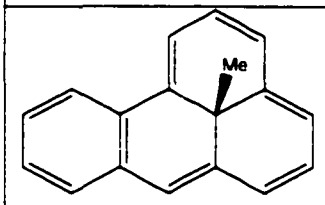	18.09	14.71
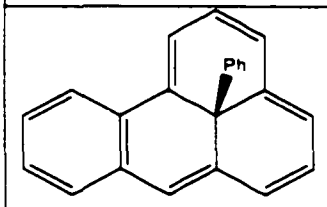	15.53	9.92

Table 13. Energies of activation for the radical recombination

Calculated activation energies of radical recombination are 3-5 kcal/mol higher than the ones obtained by using equation (2.5).

CHAPTER 3. SYNTHETIC INVESTIGATIONS

3.1 Intramolecular Diels-Alder reaction (IMDA) as the key step for the construction of the tetracyclic system

Our approach to benzo-13-p-tolyl-phenalene is based on the intramolecular Diels-Alder reaction (IMDA)[57] of o-quinodimethane **20** generated through thermolysis of benzocyclobutene derivative **19**.

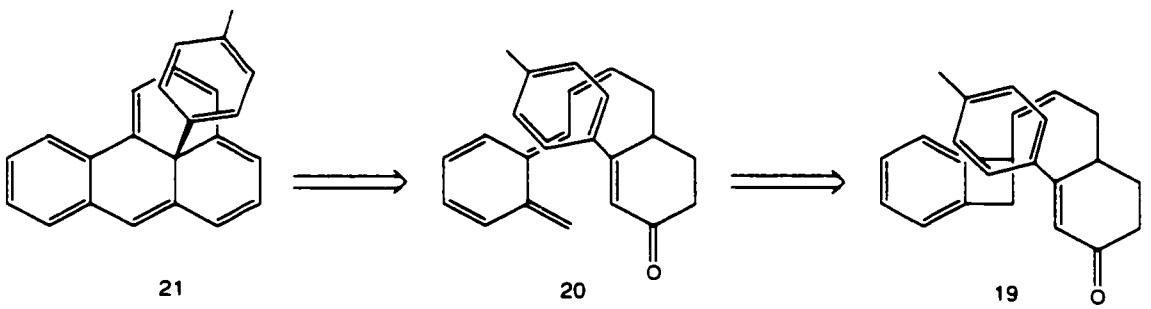

Figure 32. Intramolecular Diels Alder (IMDA) reaction employed for the construction of the tetracyclic system.

We have also investigated the synthesis of benzo-13-phenylphenalene, based on the same methodology.

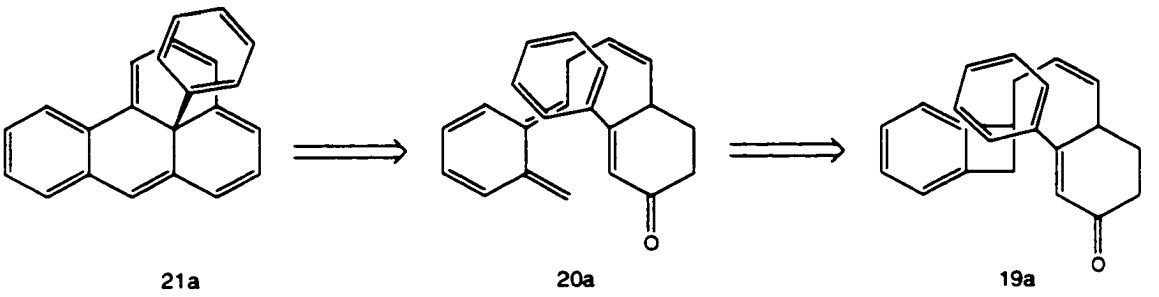

Figure 33. The IMDA methodology for the synthesis of benzo-13-phenylphenalene

Thermal opening of benzcyclobutenes and subsequent IMDA reaction have been studied among others[58] by Kametani[59] et. al. They have implemented this type of reaction in the synthesis of various natural products. Shown below is the application of this sequence for the synthesis of O-methyl-D-homoestrone **24**[60], that has been correlated to estrone **25**[61], an important precursor in the synthesis of 19-norsteroid used as an oral contraceptive.

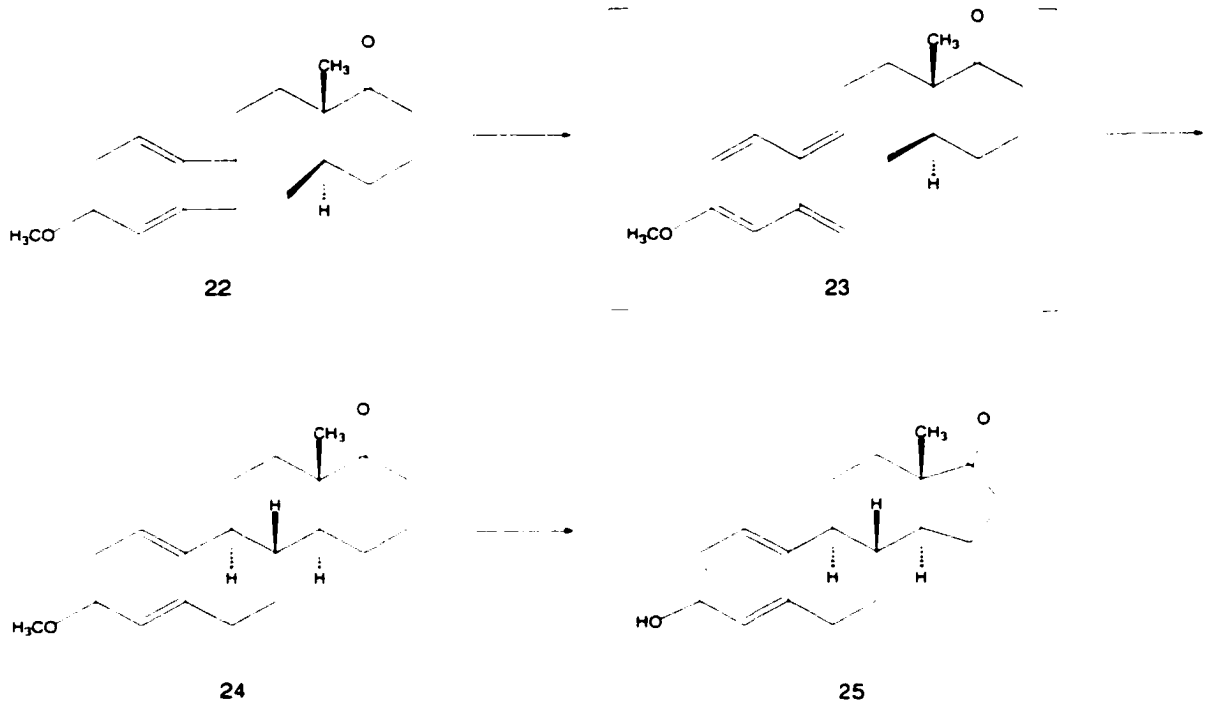

Figure 34. Thermolysis of benzocyclobutene derivative **22** followed by IMDA

The advantages of this synthetic methodology and the use of intramolecular Diels – Alder reaction for the construction of the tetracyclic carbon skeletons are summarized below:

1. Substituted benzcyclobutenes are readily available building blocks[62]

2. Benzocyclobutenes readily undergo thermal rearrangement to o-quinodimethanes[58,59].

3. o-Quinodimethanes are known to be highly reactive as dienes. There are numerous examples of the use of o-quinodimethanes in intramolecular Diels- Alder reaction for the construction of a wide range of hydrophenanthrene derivatives (steroids, alkaloids, diterpenes..)[63].

4. Compared to intermolecular reaction, the IMDA shows higher regioselectivity which ensures the right arrangement of the peripheral carbon skeleton.

5. This methodology offers flexibility : by the use of 3-substituted-cyclohex-2-enone derivatives as dienophiles, any group (alkyl, aryl, ethynyl) can be placed at the central position of the 12[annulene], perpendicular to the paramagnetic ring, thus allowing the maximum effect of the paramagnetic ring current on the chemical shifts of the group in question.

Problems that could be anticipated with this synthetic tactic are side reactions competing with intramolecular Diels-Alder reaction such as [1,7] sigmatropic hydrogen shift and Cope rearrangement.

3.2. Wittig approach to benzcyclobutene derivatives

For the synthesis of benzcyclobutene derivatives **19** and **19a**, different pathways have been considered, all making use of the Wittig reaction. The alkylation approach to benzcyclobutene derivative (figure 35), investigated by Alva, led to the successful preparation of **28**, but subsequent IMDA reaction did not provide the desired ketone **29**, due to the interference of the cyano group in the reaction[48, 64].

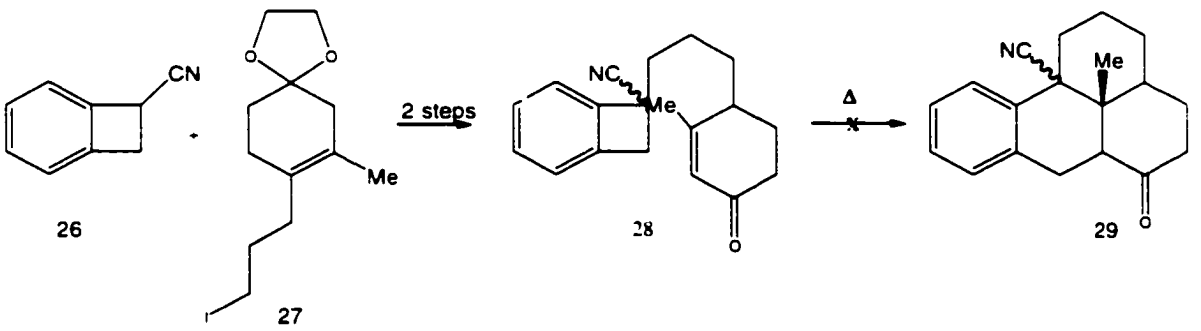

Figure 35. Alkylation approach toward benzcyclobutene derivative **28**

For that reason, cyano group had to be removed from the alkylation product **28** in order for the IMDA reaction to proceed.

Another advantage of the use of the Wittig reaction in the construction of the system suitable for intramolecular Diels-Alder reaction, lies in the introduction of the double bond into the upper ring of the polycyclic chain. Alkylation approach

is lacking the double bond functionality in the top ring, which also, led to difficulties in introducing it.

Shown below are routes we have investigated for the synthesis of benzcyclobutene derivative **19** and **19 a**.

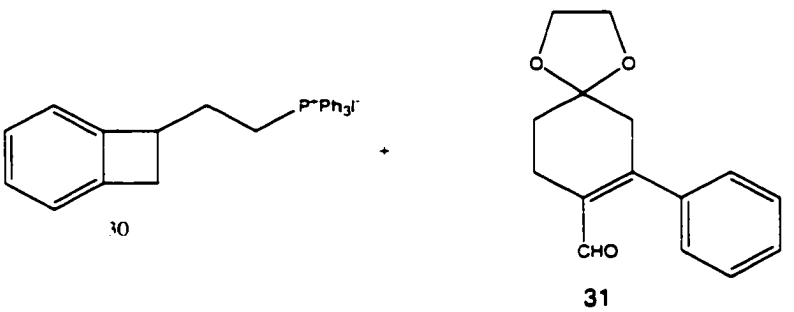

30 31

Figure 36. Route toward benzcyclobutene derivative **19a**

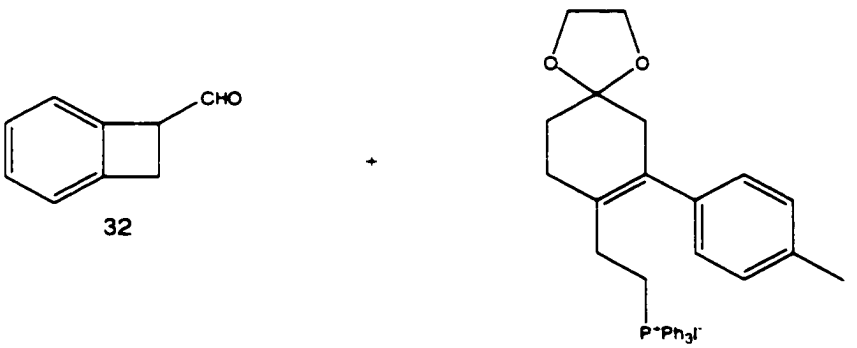

32 33

Figure 37. Route 1 to benzocyclobutene derivative **19**

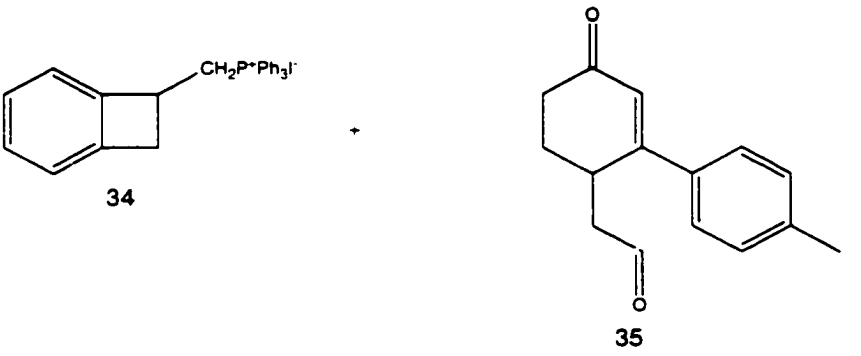

Figure 38. Route 2 to benzcyclobutene derivative **19**

3.3. An approach toward benzo-13-phenylphenalene (21a)

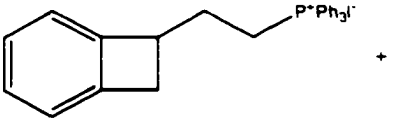

30

+

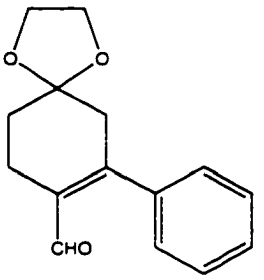

31

The first route to be investigated required the synthesis of triphenylphosphonium 1-ethyl benzcyclobutene salt **30** and aldehyde **31**.

3.3.1. Synthesis of aldehyde 31

The synthesis of aldehyde **31** was modeled after its methyl analog[48], and therefore required the preparation of the phenyl analog of Hagemann's ester. The phenyl analog of Hagemann's ester was prepared by Robinson annulation. Of the two methods investigated, we used the method that gives lower yield but by means of which, pure product can be obtained[66]. The other method that uses catalytic amounts of sodium hydride for the Michael addition step and piperidinium acetate for the aldol condensation step[67], gave a product mixture that was difficult to separate. The subsequent reactions are analogous to the ones used for the Hagemann's ester approach to benzo-13-methylphenalene[48].

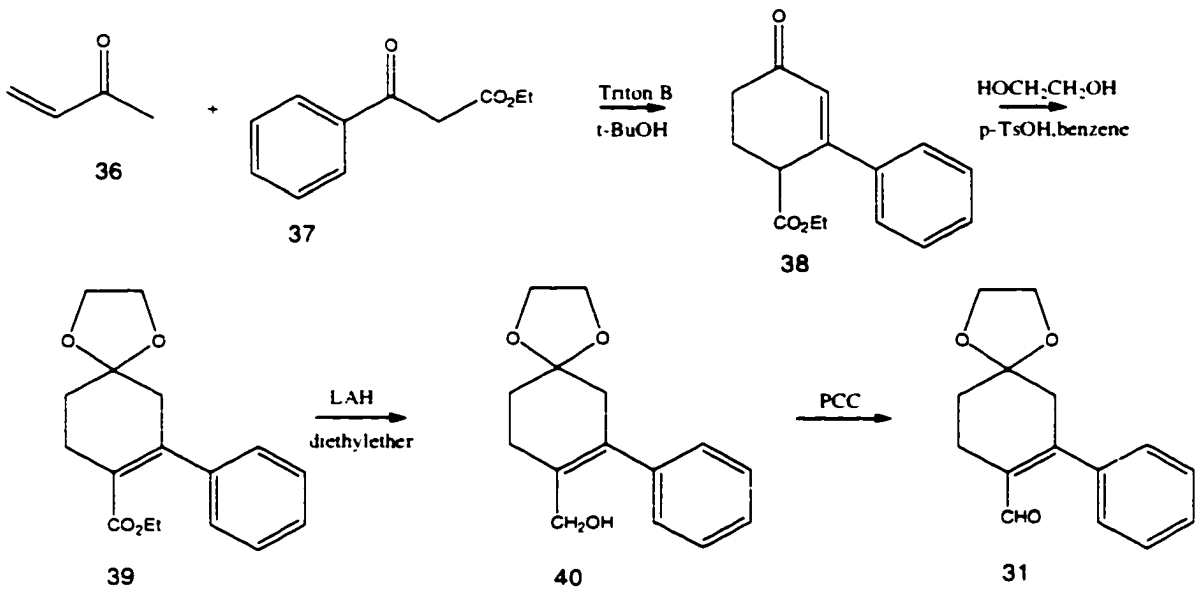

Figure 39. Synthesis of aldehyde **31**

Protection of phenyl Hagemann's ester **38** with ethylene glycol in refluxing benzene afforded protected ester **39** in 85.9 % yield. As in the case of the methyl analog, the double bond isomerization in the protected ester is observed, due to the conjugation with the ester group. Reduction of the ketal ester **39** with lithium aluminum hydride gave alcohol **40** in 81 % yield, which upon treatment with PCC provided aldehyde **31** in 74.7 % yield.

3.3.2. Attempted synthesis of phosphonium salt 30

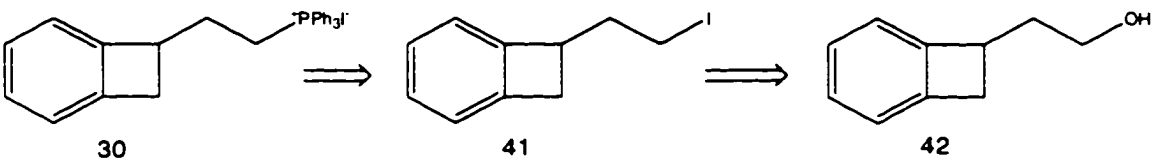

30 41 42

Figure 40. Retrosynthetic approach to phosphonium salt **30**

Preparation of phosphonium salt **30** required the synthesis of alcohol **42**. We have investigated two approaches for the preparation of this compound. Route one involved the intramolecular photochemical [2+2] cycloaddition reaction of 3-butenyl phenyl ether **47**, while the route two was based on the Grignard reaction between ethylene oxide and the benzcyclobutene Grignard reagent **45**.

3.3.2.1. Photochemical approach

Hoffmann et al. have investigated the intramolecular [2+2] photochemical cycloaddition towards benzcyclobutene derivatives[68]. They have obtained alcohols **44** and **45** in 54% yield with 89% conversion.

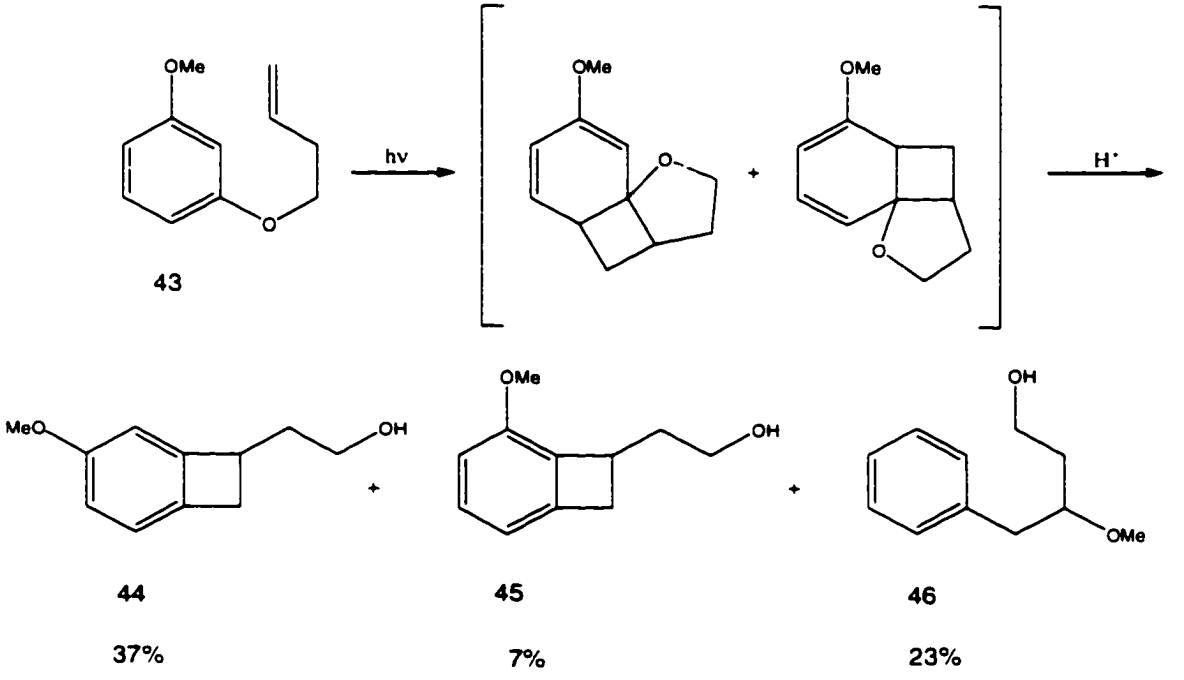

Figure 41. Hoffmann's approach toward benzcyclobutene derivatives

Although the yields reported are modest, the enormous advantage of this approach is that the benzcyclobutene alcohol **42** could be synthesized in one step.

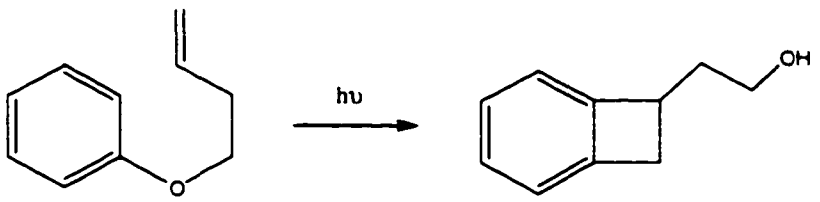

47 42

Figure 42. Attempted intramolecular [2+2] photochemical cycloaddition

A solution of 3-butenyl phenyl ether **47** in methanol was acidified with sulfuric acid and irradiated. The reaction was followed by GC/MS, which showed the disappearance of the starting material in only one hour after the irradiation. Based on the GC/MS and NMR data, the complex product mixture did not appear to contain desired alcohol **42**.

3.3.2.2. Attempted synthesis of alcohol 42 via Grignard reaction

The second method involved flash vacuum pyrolisis of α,α'-dichloro-o-xylene to provide 1-chlorobenzcyclobutene, reported by Schiess et. al in 1978[69]. Flash vacuum pyrolisis[70] (FVP) entails distillation of the substrate under vacuum through the hot quartz tube packed with clay filling, and collecting the products of the intramolecular processes in the gas phase in the receiving flask cooled with dry ice. That is a simple and rapid method to a variety of highly reactive structures.

When the heating of α,α'-dichloro-o-xylene was done fast with the Bunsen burner, only the starting material was recovered, while the slow distillation (over 4 hours for 0.5 moles) provided desired 1-chloro benzcyclobutene **49** in 28 % yield together with the unreacted starting material.

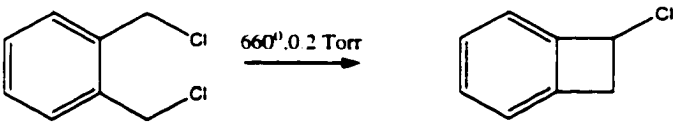

48 49

Figure 43. Flash vacuum pyrolisis of α,α'-dichloro-o-xylene

In order to get experience in handling ethylene oxide, we have done a Grignard reaction with ethylene oxide on a model molecule, chlorobenzene.

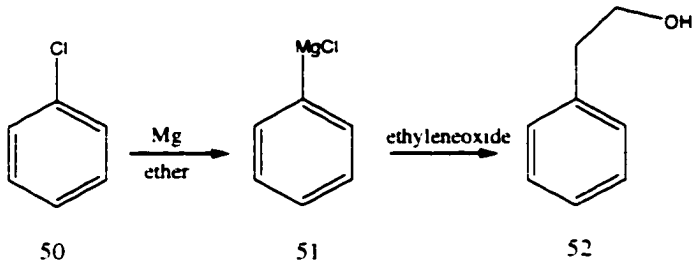

Figure 44. Grignard reaction between phenylmagnesium chloride and ethylene oxide

The reaction of phenylmagnesium bromide with ethyleneoxide afforded 2-phenylethanol **52** in 50 % yield as judged from GC/MS.

However, the reaction of the Grignard reagent **53**, prepared following the standard procedure, with ethylene oxide met with difficulties, and the desired alcohol **42** was not produced. After the work-up, 50 % of starting material was recovered, which indicated that Grignard reagent **53** was not successfully prepared.

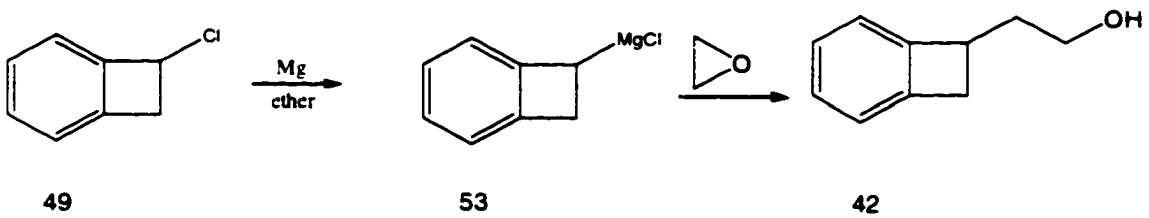

Figure 45. Attempted synthesis of alcohol **42**

Because of the experimental difficulties in our attempts to prepare the benzcyclobutene alcohol **42**, we have discontinued this route. Other routes towards the alcohol **42** were not investigated.

It is necessary to be pointed out here, that route 1 would lead to the benzcyclobutene derivative **19 a,** with the double bond at the different position than in the benzcyclobutene derivative **19**.

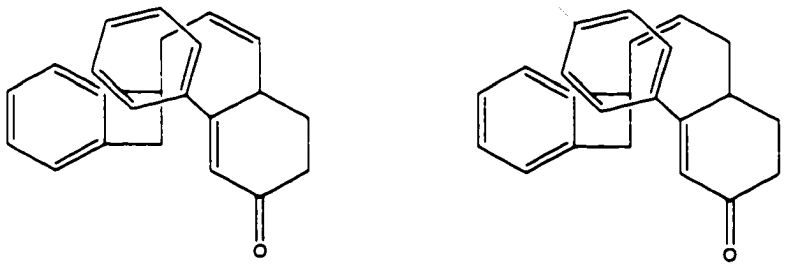

19 a 19

Figure 46. Benzcyclobutene derivatives **19 a** and **19**

It is expected that the benzcyclobutene derivative **19** would undergo the IMDA reaction at a lower temperature, due to the more stable IMDA intermediate.

3.4. ROUTE 1 TOWARDS BENZCYCLOBUTENE DERIVATIVE 19

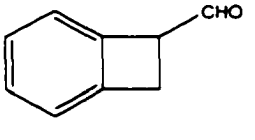

32

+

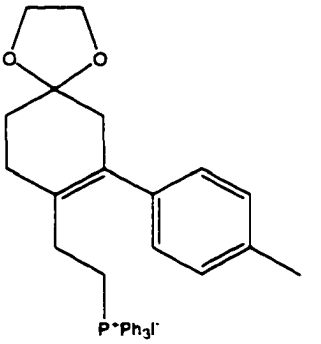

33

Route 1 involved the preparation of 1-formylbenzcyclobutene **32** and phosphonium salt **33**. Combination of these two building blocks should yield benzcyclobutene derivative **19** in cis selective Wittig reaction.

3.4.1. Synthesis of 1-formyl benzcyclobutene

The first part of the known synthesis of 1-cyanobenzcyclobutene[71], namely the synthesis of the acid **56,** shown in figure 45, was improved in terms of yields by Alva in his study of benzo-13-methylphenalene, by using α-bromo-2-chlorotoluene instead of **54**[48]. However, α-bromo-2-chlorotoluene turned out to be a strong lachrymator.

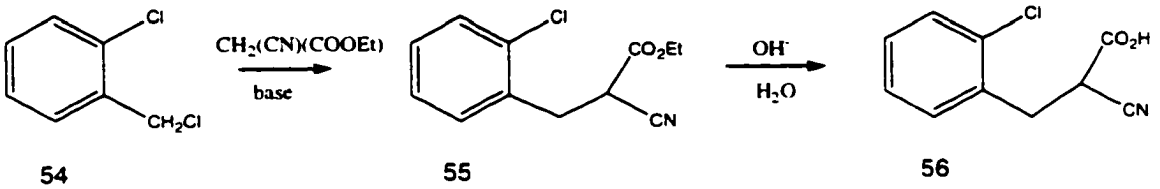

54 55 56

Figure 47. Known synthesis of carboxylic acid **56**

An alternative, very efficient method, has been reported by Jung[72] in the synthesis of analogues of podophyllotoxin.

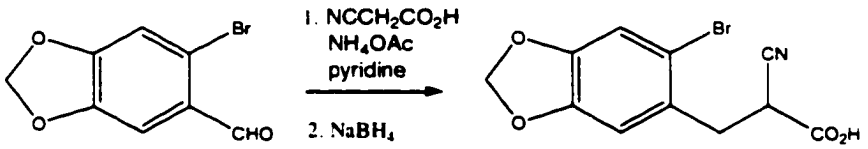

57 58

Figure 48. Jung's approach to acid **58**

They used bromopiperonal **57** as the starting material, while our synthesis started from the commercially available o-chloro benzaldehyde.

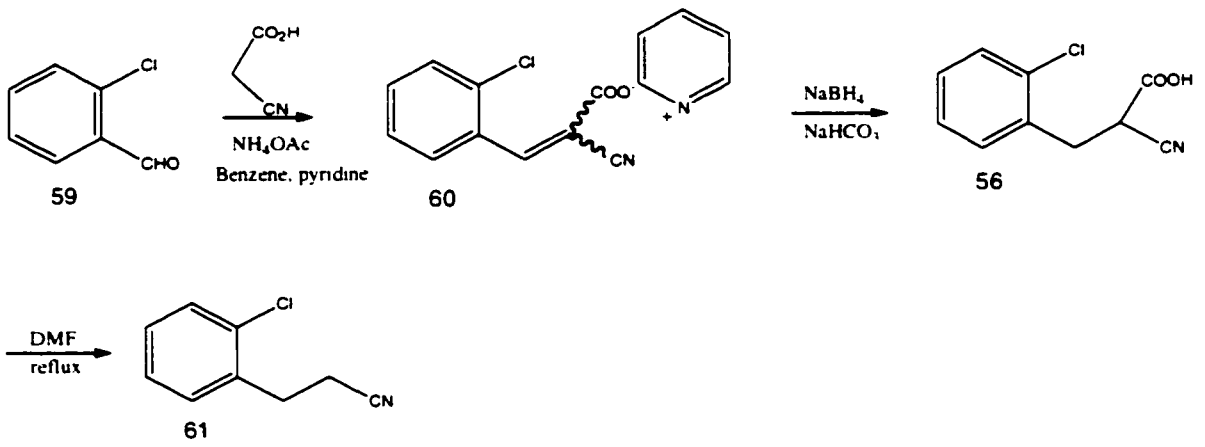

Figure 49. Synthesis of o-chlorodihydrocynnamonitrile **61**

Knoevenagel reaction between 2-chlorobenzaldehyde with cyanoacetic acid in pyridine afforded pyridine salt of cyanoacid **60**, which was, in the next step, reduced with sodium borohydride, furnishing cyanodihydrocinnamic acid **56** in 81.7 % yield. Decarboxylation of the acid **56** in refluxing DMF gave nitrile **61** in 66.4 % yield.

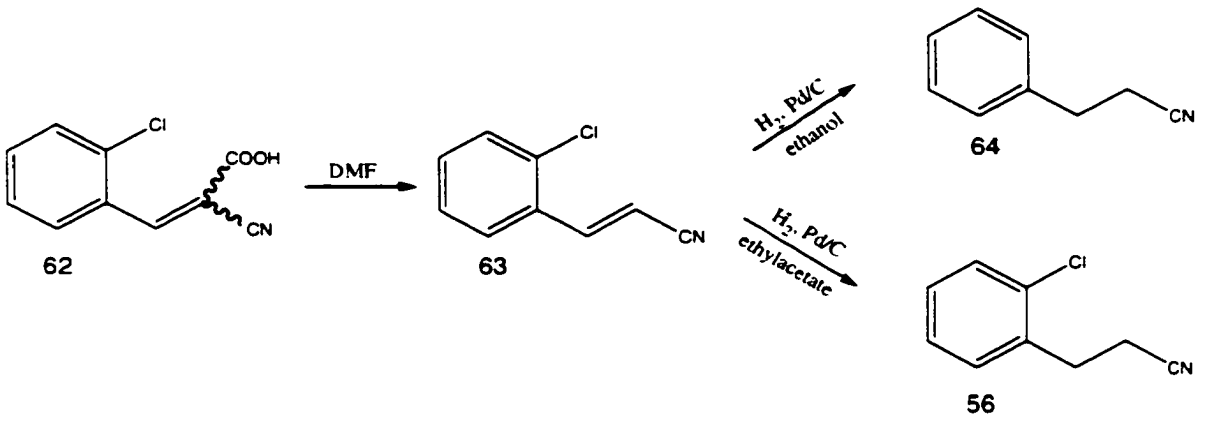

Figure 50. Hydrogenation of nitrile **63**

If the cyanocinnamic acid **62** is directly decarboxylated, than o-chlorocynnamonitrile **63** is obtained, which could be hydrogenated to give o-chlorodihydrocynnamonitrile. It is interesting to note, that the hydrogenation in ethanol with palladium on carbon gave dehalogenated product **64**. The change of the solvent to ethyl acetate afforded the right product in a very good yield, 92 %.

Intramolecular benzyne cyclization of o-chlorodihydrocynnamonitrile **56** was initially done by the use of commercially available sodium amide in liquid ammonia[73], that provided 1-cyanobenzcyclobutene **65** in 33.6 % yield. A more superior method was the that required *in situ* preparation of potassium amide from potassium hydride in liquid ammonia.

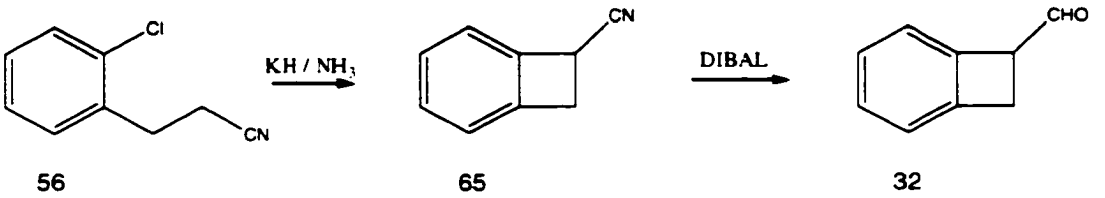

56 65 32

Figure 51. Synthesis of 1-formylbenzcyclobutene **32**

It is important to note that the outcome of the benzyne cyclization greatly depended on the temperature of the reaction. When the reaction was carried out at -78 °C, only starting material was recovered, while the reaction performed in refluxing ammonia (-33 °C) afforded the desired product **65** in 67.8 % yield. Subsequent reduction of 1-cyanobenzcyclobutene with DIBAL[74], followed by acidic work-up and continuous extraction with ether, afforded aldehyde **32** in 82 % yield.

3.4.1.Approach toward phosphonium salt 33

A retrosynthetic analysis of phosphonium salt **33** led to a scheme based on Danheiser and Stork's method for the regiospecific alkylation of cyclic β diketone enol ethers[75].

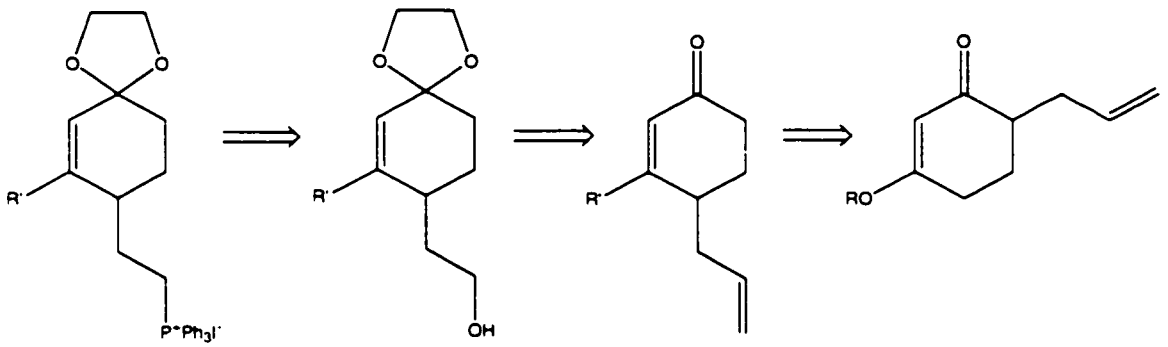

Figure 52. Retrosynthetic analysis towards phosphonium salt **33**

The importance of this methodology lies in its flexibility: it can give a variety of 3 substituted 2-cyclohexenones, R' being introduced via Grignard reaction.

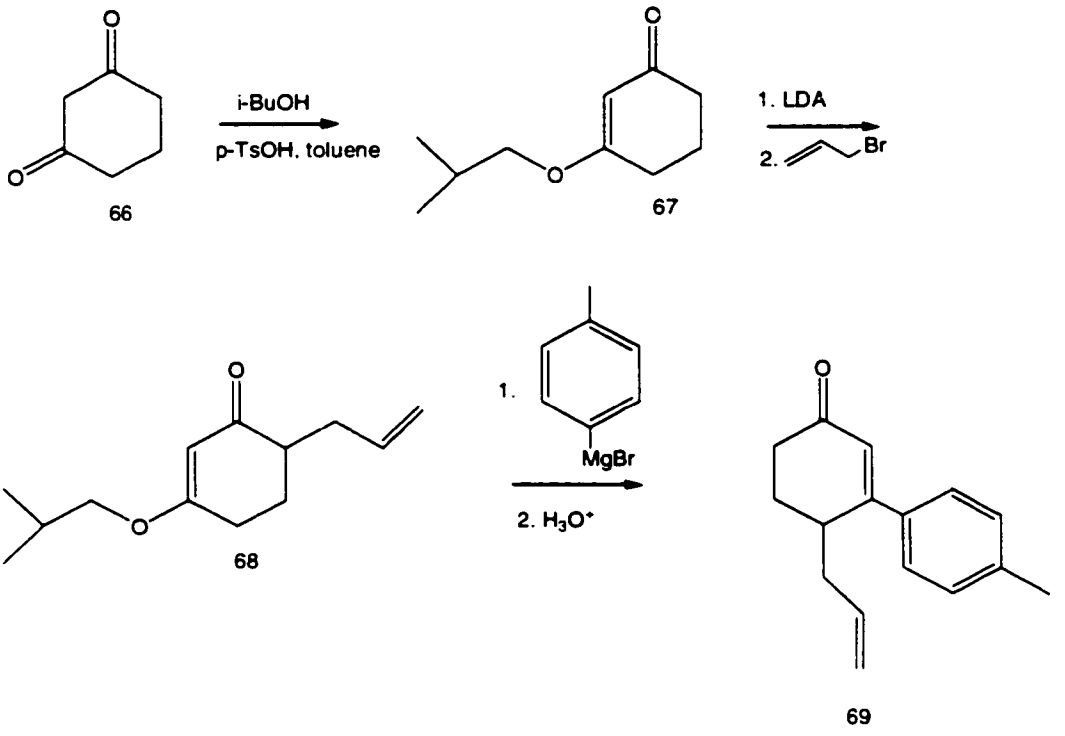

66 67 68 69

Figure 53. Synthesis of allyl tolyl ketone **69**

Reaction of 1,3 cyclohexadione with isobutyl alcohol provided 3-isobutoxy-2-cyclohexenone **67** in 91.3 % yield. Alkylation with allyl bromide following Danheiser and Stork's procedure provided the alkylated product **68** in 92 % yield after recrystalization. Subsequent Grignard reaction with p-tolylmagnesium bromide afforded allyl tolyl ketone **69** in 95 % yield.

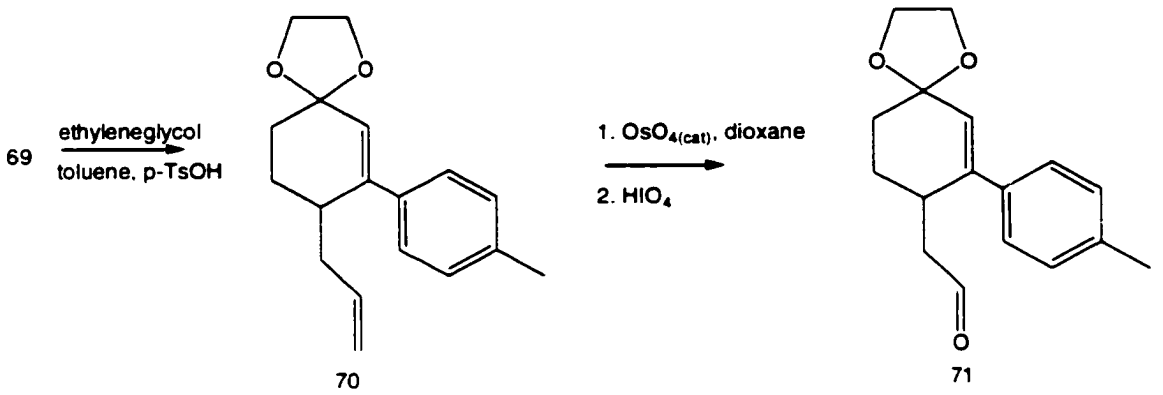

Figure 54. Preparation of protected tolyl aldehyde **71**

Protection of the ketone with ethylene glycol gave the terminal alkene **70** in 77.1 % yield. The reaction of **70** with osmium tetroxide, followed by the cleavage of the formed osmate ester with sodium periodate, provided aldehyde **71** in 73.5 % yield.

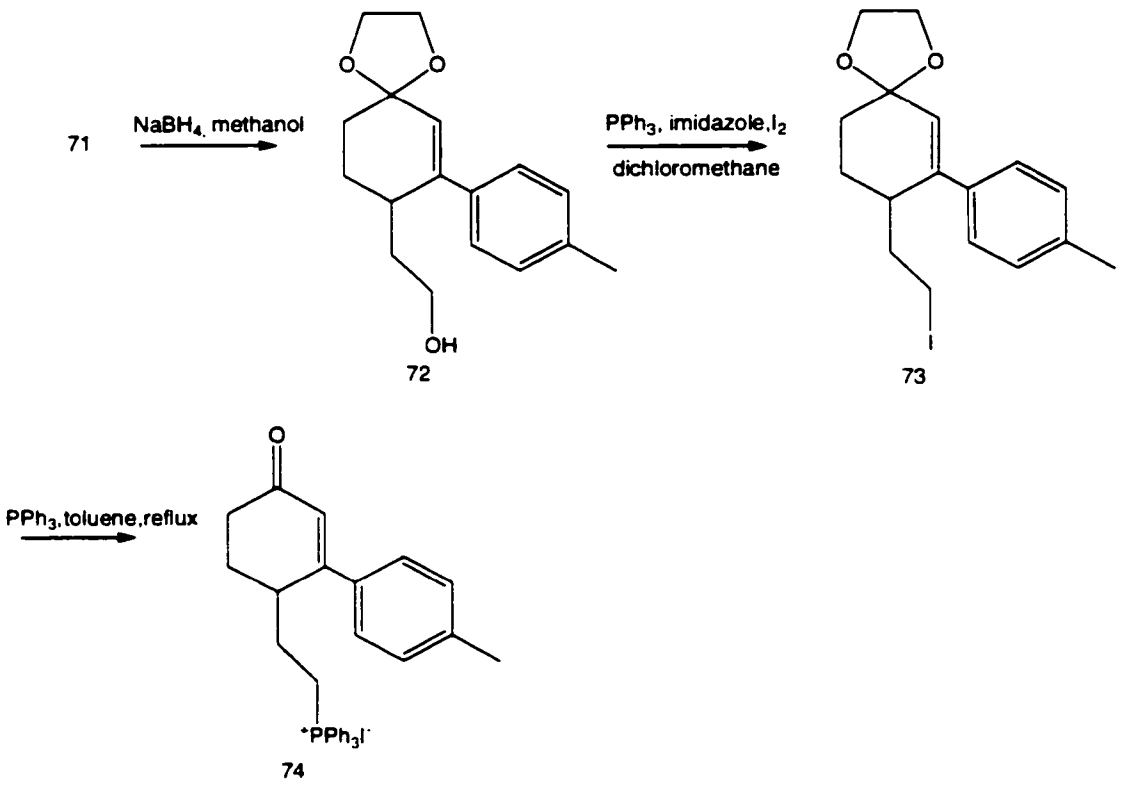

Figure 55. Formation of phosphonium salt **74**

Aldehyde **71** was reduced with sodium borohydride in methanol to give alcohol **72** in 88.6 % yield. Transformation of the primary alcohol **72** into iodide **73** was achieved with the use of triphenylphosphine, imidazole and iodine in dichloromethane in 72.3% yield[76]. The reaction of iodide **73** with triphenylphosphine in refluxing toluene did not provide the protected phosphonium salt **33** but the unprotected, keto phosphonium salt **74**.

It seems that minute amounts of hydroiodic acid, formed during the preparation of the salt, caused deprotection of the keto group[48]. To avoid the observed

deprotection we considered protecting the ketone **69** as thioketal and using diisopropylethylamine as an acid scavenger, as reported by McCarry[77]. Assuming that the thioketal would not survive the conditions used in the oxidative cleavage of the double bond (figure 54), we explored the possibilities of regiospecific alkylation of β-diketone enol ethers with an alkylating reagent that would not require such a transformation, namely ethyl bromo acetate.

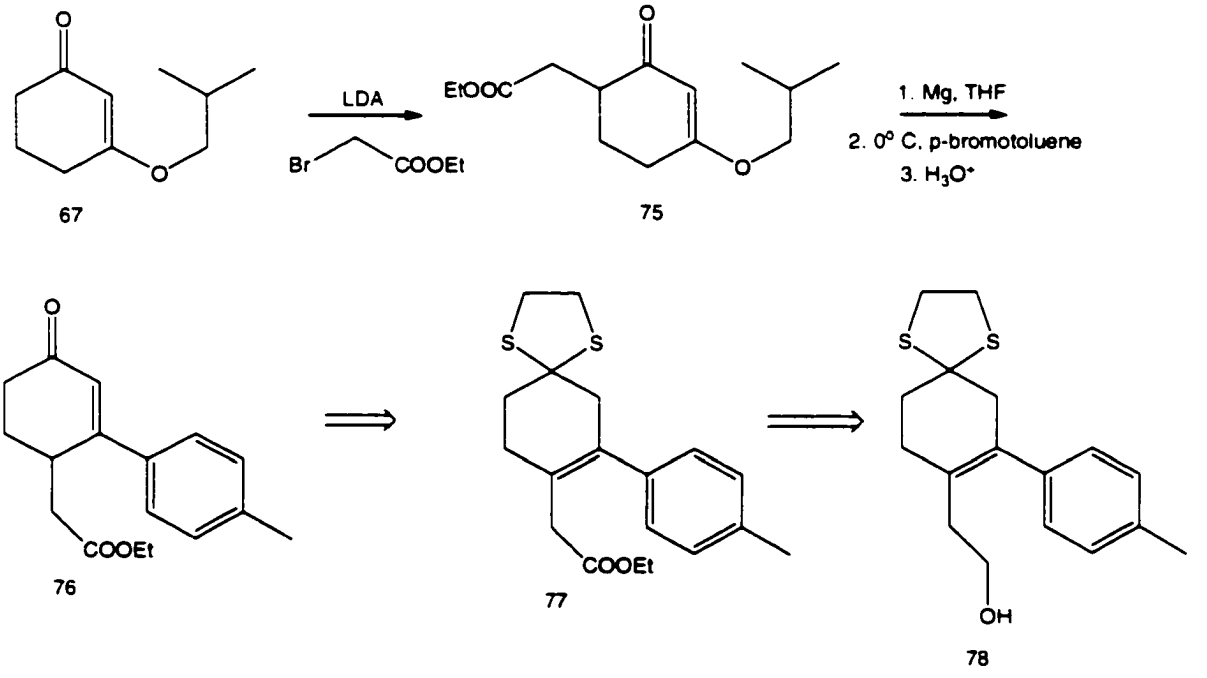

Figure 56. Proposed synthesis of alcohol **78**

The alkylation reaction with ethylbromoacetate was carried out in the same manner as the reaction with allyl bromide as an alkylating reagent. Unfortunately,

yields were significantly lower,36.2 %, compared to 92 % obtained in the synthesis of allyl tolyl ketone **69**. Subsequent Grignard reaction, done at 0° C to avoid the reaction of p-tolylmagensium bromide with the carbonyl group of the ethyl ester, gave a mixture of starting material and the product. Due to the low yields we haven't pursued this approach any further.

The obvious disadvantage of phosphonium salt **74** is that it has an unprotected keto group with a phosphonium salt functionality in the same molecule. For that reason the standard procedure for Wittig reaction that involves the preparation of the ylide first, with the subsequent addition of the carbonyl compound could not be applied for this combination of phosphonium salt and aldehyde. Instead, we have attempted, the so called *in situ* Wittig reaction, by adding lithium ethoxide to the stirred mixture of phosphonium salt and aldehyde in dimethyl formamide, but unfortunately, no Wittig product could be isolated. We therefore discontinued this route.

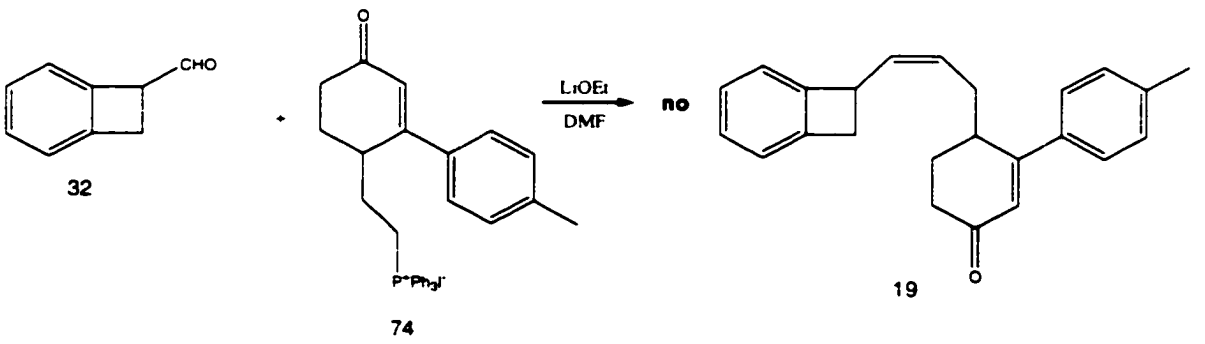

Figure 57. Attempted "*in situ*" Wittig reaction

3.5. ROUTE 2 TO BENZCYCLOBUTENE DERIVATIVE 19

In view of the problems associated with route two, and unsuccessful attempts to obtain benzcyclobutene derivative **19** via "*in situ*" Wittig reaction, we investigated the alternative Wittig reaction, using reactants with reversed functionalities, phosphonium salt **34** and aldehyde **35**.

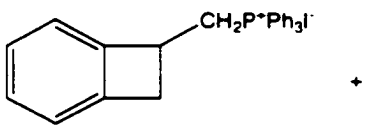

34

+

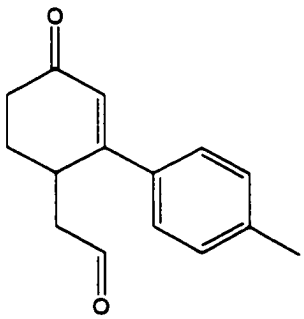

35

The advantages of route 2 include:

-crystalline phosphonium salt **34** (vs. oily phosphonium salt **74**)

-easily accessible aldehyde **35**

-protection of the keto functionality in **35** is not necessary, since the Wittig reaction with the aldehyde group is expected to proceed faster than with the conjugated keto group.

3.5.1. Synthesis of phosphonium salt 34

Route 2 required further manipulation of 1-cyano benzcyclobutene **65**, the synthesis of which was well developed for the purpose of route 2.

Benzcyclobutene phosphonium salt **34** was obtained in the following manner:

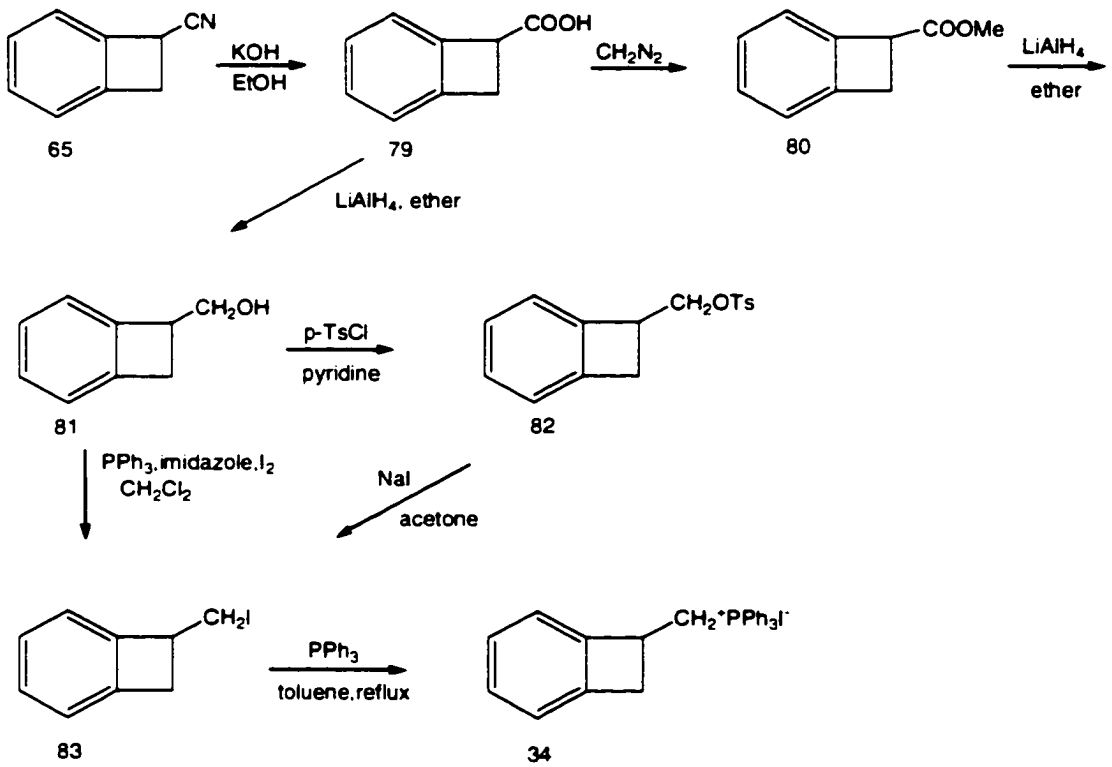

Figure 58. Formation oh phosphonium salt **34**

Carboxylic acid **79** was prepared by base hydrolysis[78] of 1-cyanobenzcyclobutene **65** in 93.3 % yield. Esterification of the acid with diazomethane[79] followed by lithium aluminum hydride reduction of the methyl

ester **80** to alcohol **81**, proved to be of no advantage over the direct reduction of acid **79** with lithium aluminum hydride. One step transformation of alcohol **81** into iodide **83** using triphenylphosphine, imidazole and iodine[76], proceeded in higher yield than the two step reaction involving formation of tosylate **82**, and its subsequent conversion into iodide **83**. Iodide **83** was reacted with triphenylphosphine in refluxing toluene to provide phosphonium salt **34** in nearly quantitative yield.

3.5.2. Synthesis of aldehyde 35

For the synthesis of aldehyde **35** we used the already described route involving regiospecific alkylation of enol ketones, followed by Grignard reaction to obtain 4-allyl-3-tolyl-2-cyclohexenone **69** (figure 51).

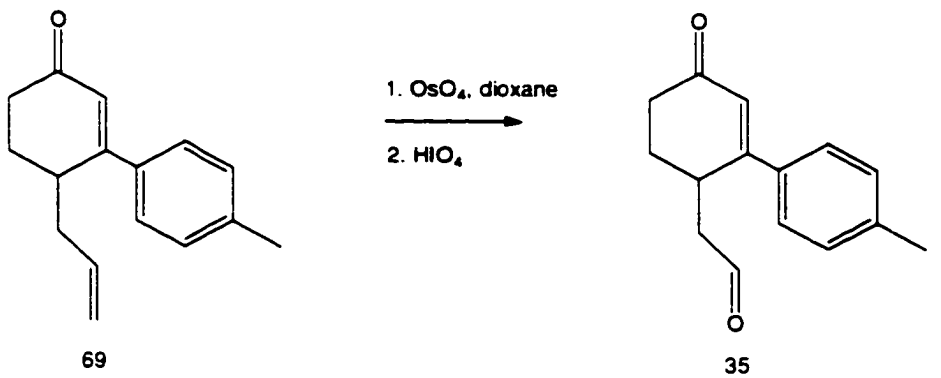

Figure 59. Formation of aldehyde 35

Yields of the subsequent transformation of allyl compound **69** into aldehyde **35** varied, depending on the scale used. For the conversion of 5g and less of the allyl compound **69** into aldehyde **35**, 77.3 % yields were obtained when sodium periodate was added in a solid form in small portions[80]. However, scaling up led to decrease in yields (62 %). The same observation has been reported by Shamma and Rodriguez[81]. We modified the procedure by adding the aqueous solution of sodium periodate, very slowly, through a precision addition funnel. This way, scales of up to 20 grams of allyl compound **69** provided aldehyde **35** in 78 % yield.

3.6. The Wittig reaction

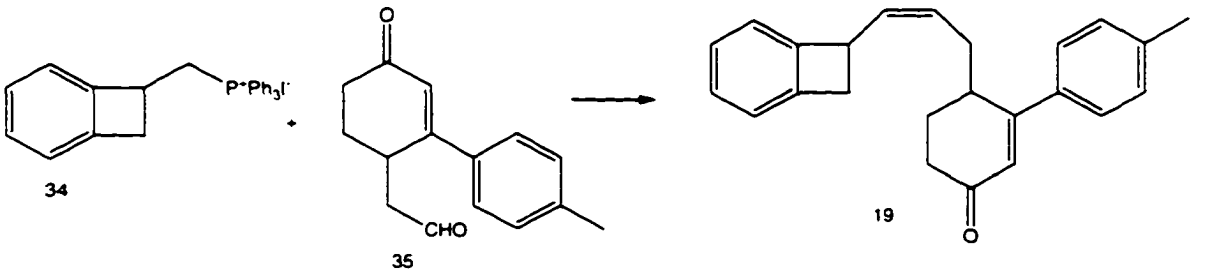

Figure 60. Preparation of the Wittig product **19**

In order to allow the proper diene-dienophile interaction in the subsequent intramolecular Diels Alder reaction we needed a cis geometric isomer of **19**. The trans isomer does not have a right arrangement of diene and dienofile to react. Although many cis selective Wittig reaction have been reported[82,83], in our case, Wittig reaction turned out to be not a trivial reaction to do. Most common bases used for the formation of a cis double bond gave poor yields of the Wittig product. The reaction of aldehyde **35** and phosphonium salt **34** with potassium tert-butoxide as a base gave Wittig product **19** in 10 % yield. With potassium hexamethyldisilyl amide as base[83], an even lower yield (6 %) was obtained. Common to both reactions was the fact that there was always a complete consumption of the aldehyde, and the formation of a very polar compound, that we have not identified.

In order to find out what is causing low yields, and investigate the problems associated with this combination pf phosphonium salt and aldehyde, we tested both phosphonium salt as well as aldehyde with different reactants.

The first reaction carried out was of phosphonium salt **34** with benzaldehyde **84** in toluene, with potassium tert-butoxide as a base. The product **85** formed in 55 % yield. We have concluded that the phosphonium salt was not the cause of problems experienced in the Wittig reaction.

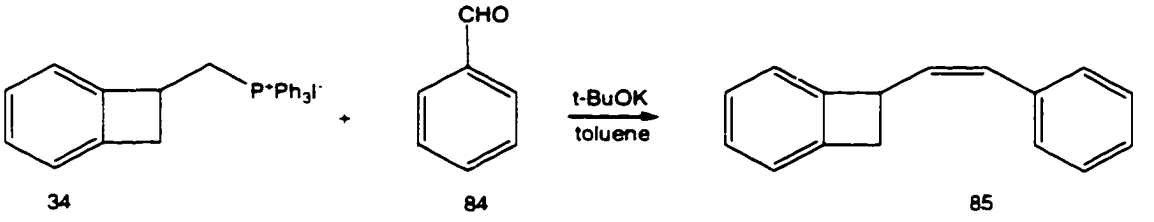

34 84 85

Figure 61. The Wittig reaction of phosphonium salt **34** with benzaldehyde **84**

We considered the possibility for the α hydrogen in aldehyde **34** to be too acidic, making an aldol condensation faster than the desired Wittig reaction. In order to avoid such a problem we investigated a method reported by Boden[84], using potassium carbonate as a base in the presence of 18-crown-6 ether (1,4,7,10,13,16 – hexaoxycyclooctadecane). A model reaction with the phenylacetaldehyde and isobutylphosphonium iodide proved to be successful. The reaction proceded in 55% yield as judged by GC/MS.

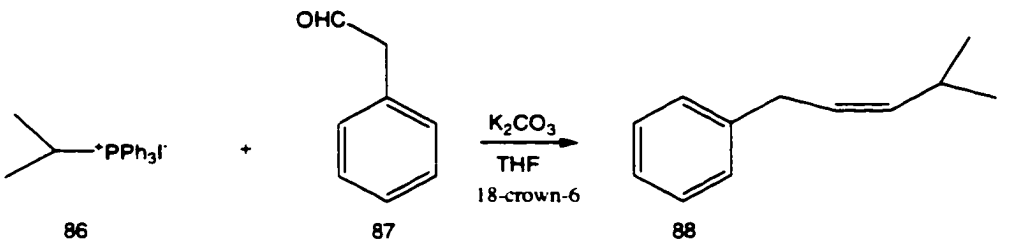

Figure 62. The Wittig reaction between phenylacetaldehyde **87** and isobutylphosphonium iodide **86**

The best conditions for this solid phase reaction were found to be as follows: addition of the aldehyde and 18 crown ether to the solution of the finely ground mixture of the dry phosphonium salt with the oven dried anhydrous potassium carbonate. After finding the best conditions,the reaction of isopropylphosphonium bromide **86** with aldehyde **34** was carried out. The reaction proceeded in 77 % yield as judged by GC/MS.

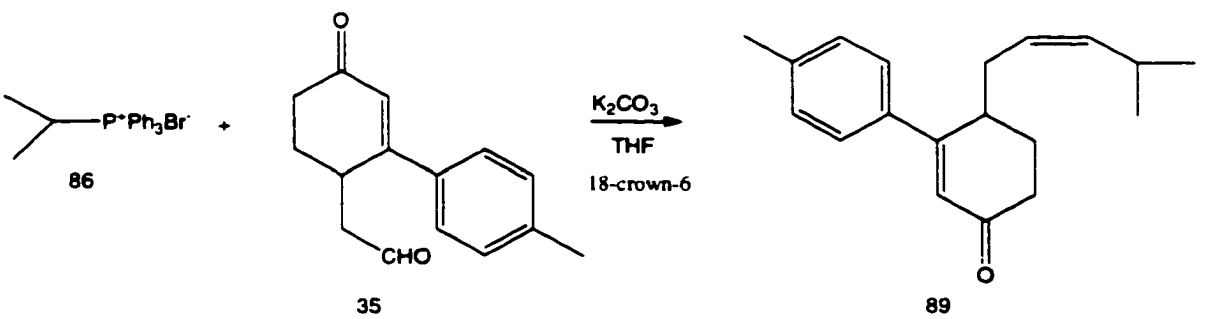

Figure 63. Heterogenous Wittig reaction

After testing both phosphonium salt **34** and aldehyde **35**, and with the careful investigation of the reaction conditions, the most promising method seemed the one that makes use of the mild base and heterogeneous conditions.

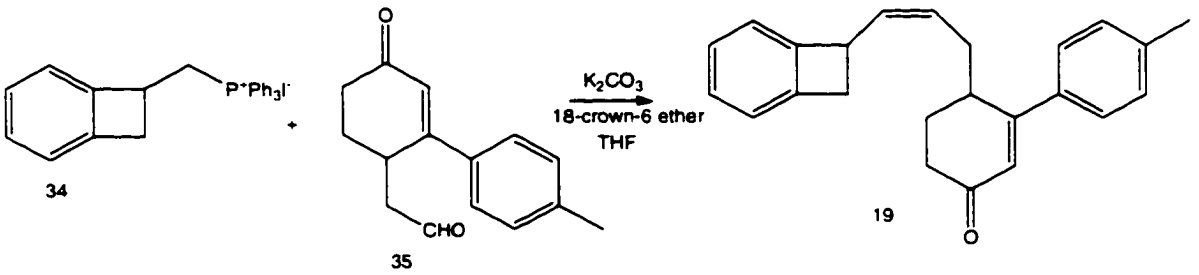

Figure 64. Formation of the Wittig adduct **19**

Phosphonium salt **34** was finely ground with the oven dried anhydrous potassium carbonate, and the fine powder suspended in dry THF. After addition of aldehyde **35** and 18- crown-6 ether, the suspension was refluxed under nitrogen. The progress of the reaction was monitored by TLC, that showed a very slow disappearance of the aldehyde. The Wittig product **19 b** was obtained in 66.8 % yield. The NMR indicated the presence of less than 10 % of the trans product, as suggested by the coupling constants.

3.6.1. Characterization of the Wittig product 19

Confirmation of the structure of Wittig product **19** came from its ^{1}H/ ^{13}C NMR and IR spectra.

Its ^{1}H NMR spectrum showed the following peaks:

- a singlet at δ2.39 ppm corresponding to the methyl group of the p-tolyl substituent;
- a singlet at δ 6.34 ppm corresponding to vinylic proton conjugated to the ketone group of the cyclohexenone moiety;
- two sets of multiplets, one at δ3.46 ppm, the other at δ 2.86 ppm, corresponding to the secondary benzylic protons of the cyclobutene moiety;
- a multiplet at δ 4.26 ppm corresponding to the tertiary benzylic proton of the cyclobutene part;
- a triplet of doublets at δ 5.70 ppm corresponding to the vinylic proton next to the cyclobutene unit;
- a multiplet at δ 5.50 ppm corresponding to the second vinylic proton of the formed double bond.

The peaks observed in ^{1}H NMR spectrum of the p-tolyl benzcyclobutene derivative **19**, are comparable to the ones observed in the ^{1}H NMR spectrum of its methyl analog obtained by Alva[48].

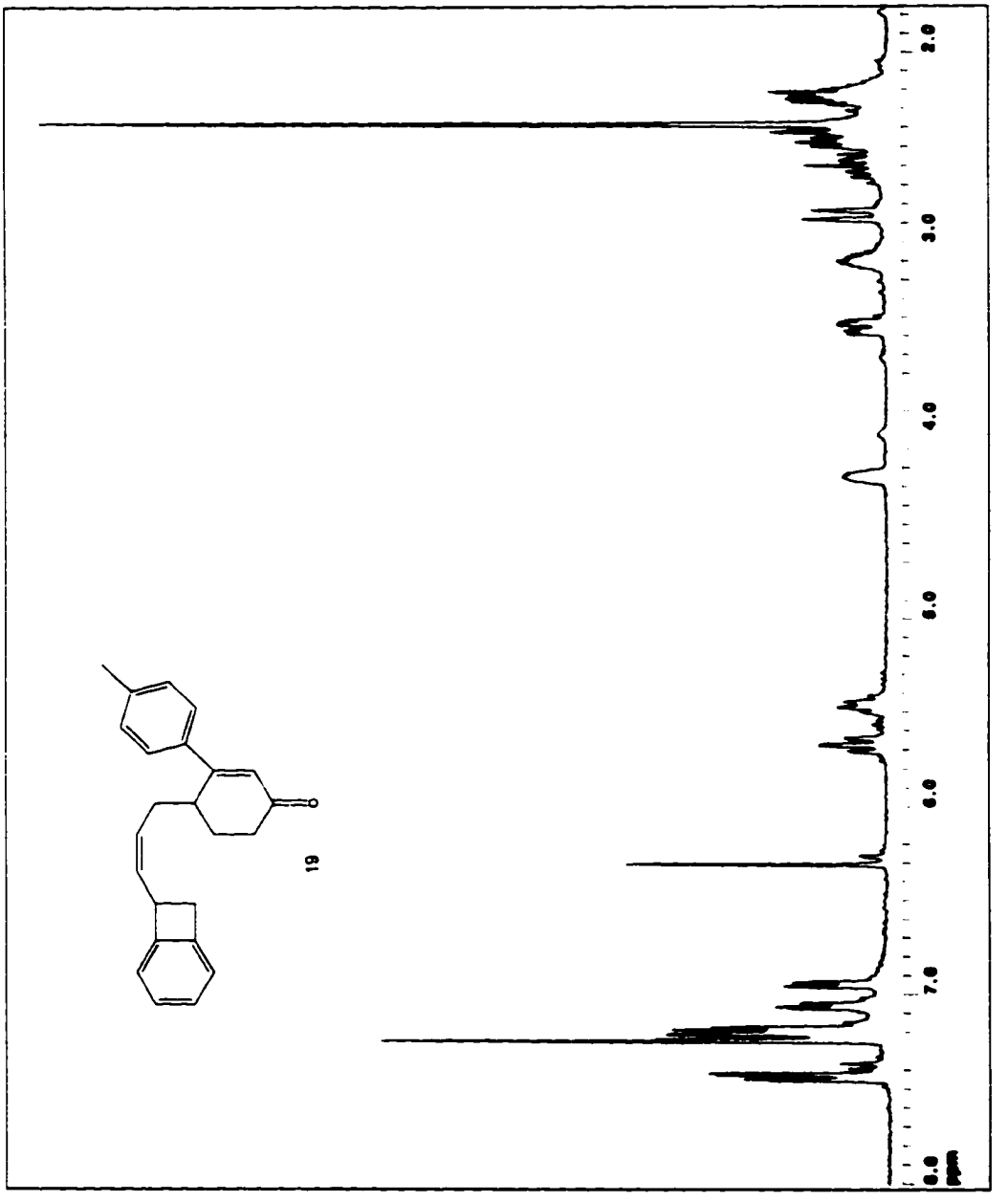

^{1}H NMR spectrum of ketone 19

3.7. The intramolecular Diels-Alder reaction

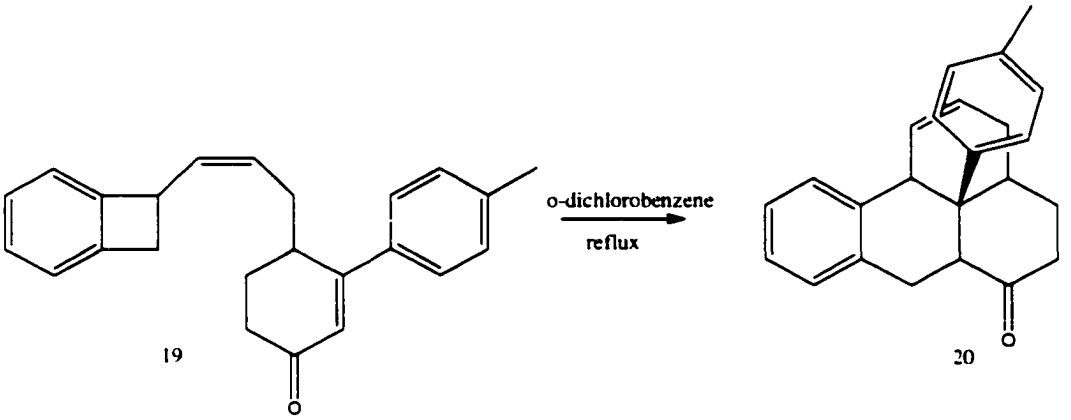

Figure 65. Intramolecular Diels-Alder reaction

Although competition between intramolecular and intermolecular Diels-Alder reaction has not been specifically investigated, we expect that the IMDA would be more kinetically favored. However, many IMDA reactions are run at high dilutions, usually 0.001 mol/L. We performed the reaction at higher concentration, 0.022 mol/ L and no product of a bimolecular Diels- Alder reaction has been observed.

Wittig product **19** was refluxed in o-dichlorobenzene for 16 hours to afford Diels-Alder product **20** in 53.3 % yield. In addition to the Diels–Alder adduct, the formation of two, more polar, isomers of ketone **20** was observed. These two isomers could not be separated from each other, but based on the investigation done by Alva in his study of benzo-13-methylphenalene, they are most likely the products of the following reactions during thermolysis[48]:

1,7 hydrogen shift

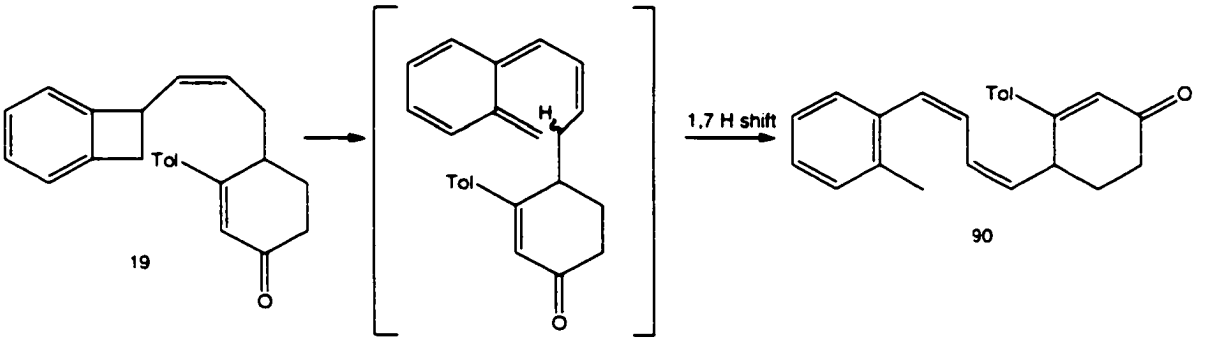

Figure 66. Formation of the isomer 90 via 1,7 hydrogen shift

Cope rearrangement

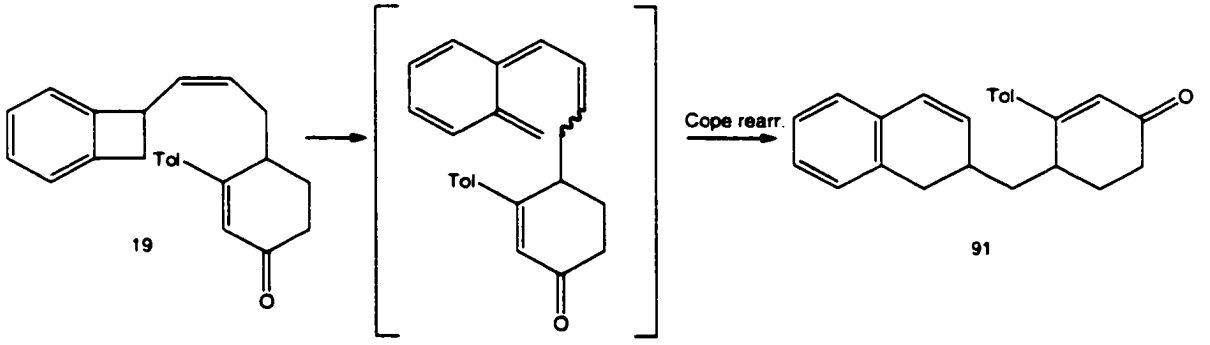

Figure 67. Formation of isomer 91 via Cope rearrangement

3.7.1. Characterization of the Diels- Alder adduct 20

The Diels Alder adduct, ketone **20**, was completely characterized based on its $^{1}H/^{13}C$ NMR and IR spectra , and its structure ultimately confirmed by X ray spectroscopy. Following features in the ^{1}H NMR spectrum of the ketone **20** indicated that the intramolecular Diels –Alder reaction has occurred:

- disappearance of the signal for vinylic proton of the cyclohexenone moiety ;
-disappearance of three sets of signals that corresponded to the secondary and tertiary benzylic positions of cyclobutene part;

-appearance of the doublet of doublets at δ 6.52 ppm (J=2 Hz; 8 Hz) and a multiplet at δ 5.67 ppm corresponding to the vinylic hydrogens;
-appearance of the doublet at δ 3.24 ppm corresponding to the equatorial proton at C(3) position with the coupling to the geminal axial proton (J=17 Hz);

-IR band corresponding to the cyclohexanone (1705 cm^{-1}).

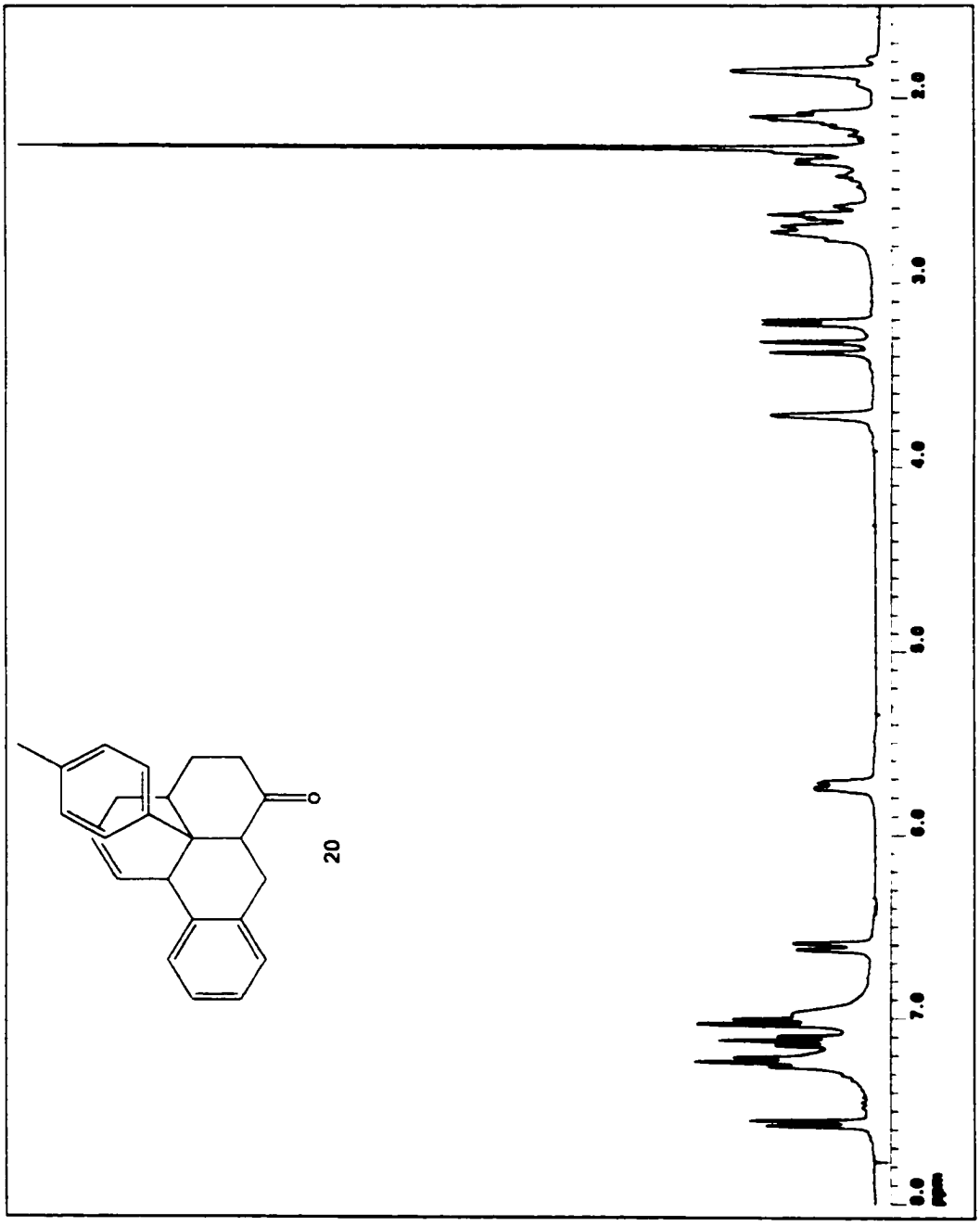

^{1}H NMR spectrum of ketone 20

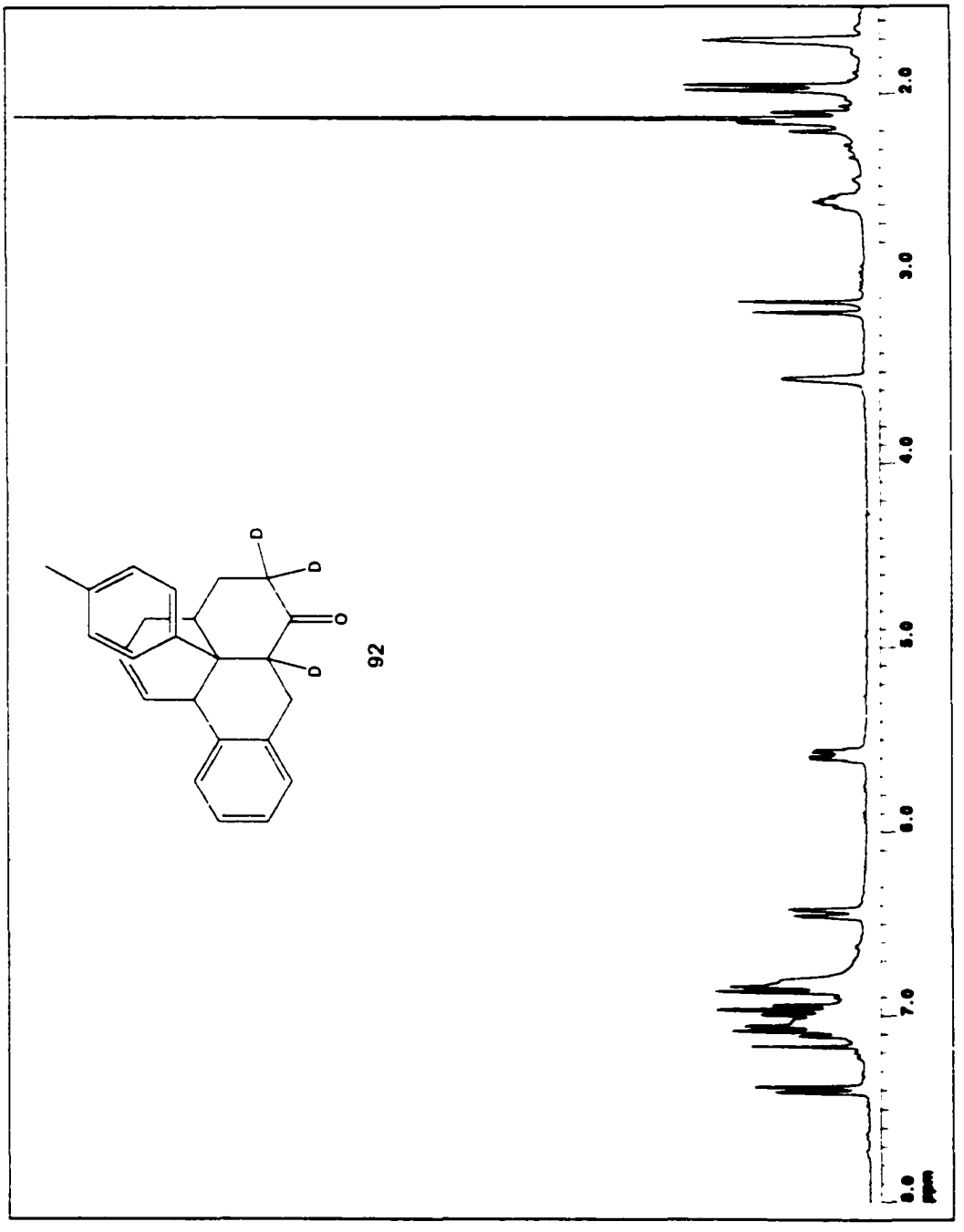

^{1}H NMR spectrum of deuterated ketone 92

Deuterium exchange experiment provided assistance for the assignment of the peaks in ^{1}H NMR spectrum. The reaction of the ketone **20** with sodium ethoxide in the mixture of ethanol-d and D_2O gave ketone **92** with deuterium at positions C(4) and C(6).

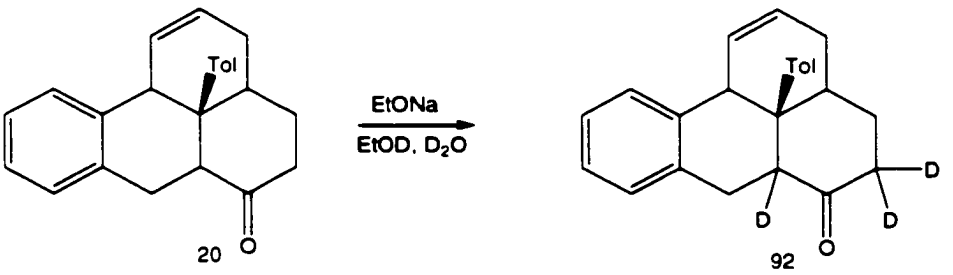

Figure 68. Deuterated ketone **92**

^{1}H NMR spectrum of deuterated ketone showed:

-disappearance of the doublet at δ 3.12 ppm integrating as one proton – corresponding to the proton at C (4) position,

-disappearance of the multiplet at δ 2.64 ppm, integrating as two protons- corresponding to the proton at the C(6) position.

-change in the splitting pattern for the proton at C(7) position.

Final assignment of the peaks was possible through the COSY spectrum of ketone **20**.

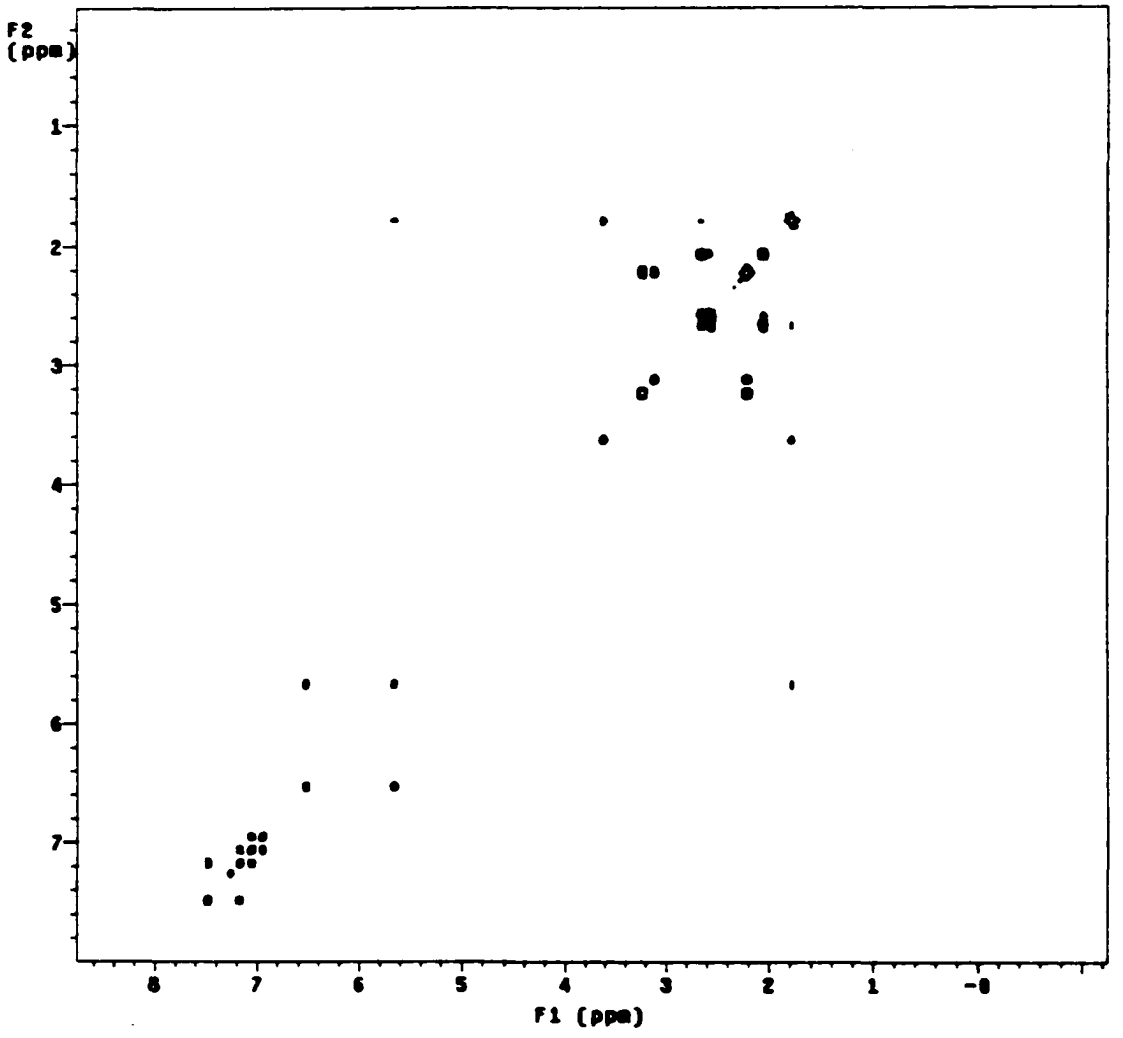

Cosy spectrum of ketone **20**

The following coupling correlations in the cosy spectrum provided further support for the assignment of the peaks in the 1H NMR spectrum of ketone **20**:

- a correlation between the doublet at δ 6.52 ppm (H_{11}) and the resonance at δ 5.67 ppm (H_{10})

- a correlation between the multiplet at δ 5.67 ppm (H_{11}) and the broad peak at δ 1.8 ppm (H_9)

-correlations of the broad peak at 1.79 ppm (H_9) with the peak at δ 3.62 ppm (H_{12}), and a multiplet at δ 2.67 ppm (H_8),

- correlations of the peak at δ 2.22 ppm (axial H_3) with the doublet at δ 3.24 ppm (equatorial H_3) and with a doublet at δ 3.13 (H_4)

- a correlation between the multiplet at δ 2.67 ppm (H_8) and the multiplet at δ 2.06 ppm (H_7).

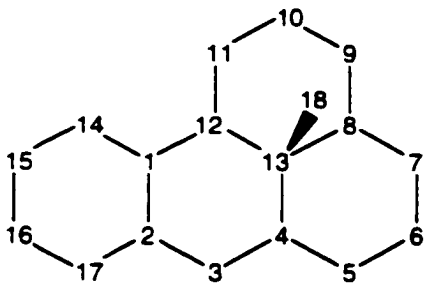

Figure 69. The numbering in the ketone **20**

The observation of the broad signals corresponding to the benzene protons of the p-tolyl group suggested the existence of dynamic processes in the molecule. A set of variable ^{1}H NMR spectra taken between 50 ° C and – 60 ° C, confirmed this assumption.

At 50 ° C, broad signals corresponding to the arene protons of the p-tolyl group sharpen to give two sets of doublets, one at δ 6.86 ppm and the other at δ 7.10 ppm. In addition, signals corresponding to C(7) protons at δ 2.06 ppm and C(9) protons at δ 1.79 ppm, show sharper peaks with better observable splitting.

At low temperature, - 60 °C following changes in the appearance and chemical shifts of the peaks are observed:

1. peaks corresponding to arene protons of the p-tolyl group show four sets of doublets (two sets of AB doublets) : one at δ 6.66 ppm, second at δ 6.73 ppm; the other two doublets are overlapping with the protons of the fused benzene ring at δ 7.53 ppm and δ 7.22 ppm.
2. peaks corresponding to C(9) protons show a clear AB system.
3. doublet of doublet corresponding to the axial C(3) proton shows an upfield shift, while a doublet corresponding to the equatorial C(3) shows a downfield shift.
4. doublet of triplets corresponding to C(6) protons shows an upfield shift

The changes observed for the peaks corresponding to the arene protons of the p-tolyl group as well as for C (9) protons, indicate the presence of the restricted rotation around central carbon-p-tolyl group bond. Although the rotation around an sp^2-sp^3 bond is expected to have a low energy barrier[85], it is possible to rationalize a high energy barrier for such a rotation in our case by the steric hindrance of the arene protons and peripheral protons [C(3), C(8) and C (9) protons].

Furthermore, the change in the chemical shifts of C(3) and C(6) at different temperatures, suggests the existence of the cyclohexanone ring-inversion barrier.

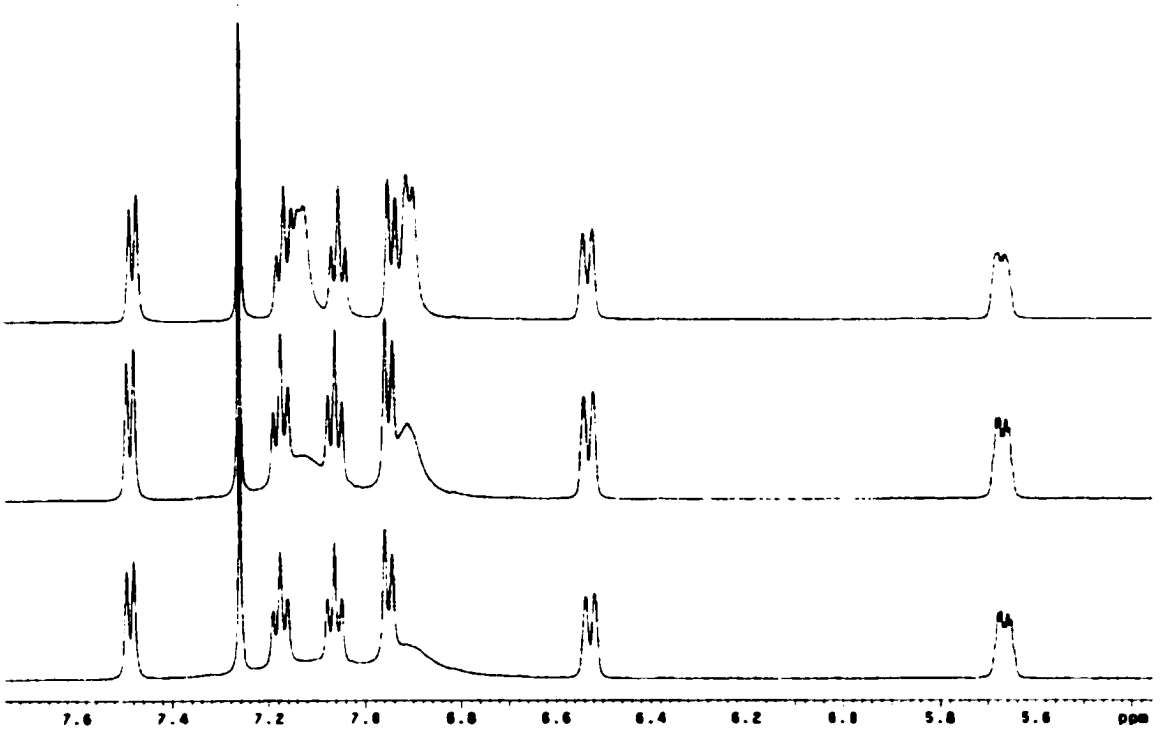

Downfiled section of the ^{1} H NMR spectrum of ketone (20)

taken at different temperatures.

From top to bottom 49.9 °C; 23 °C; 12.5 °C

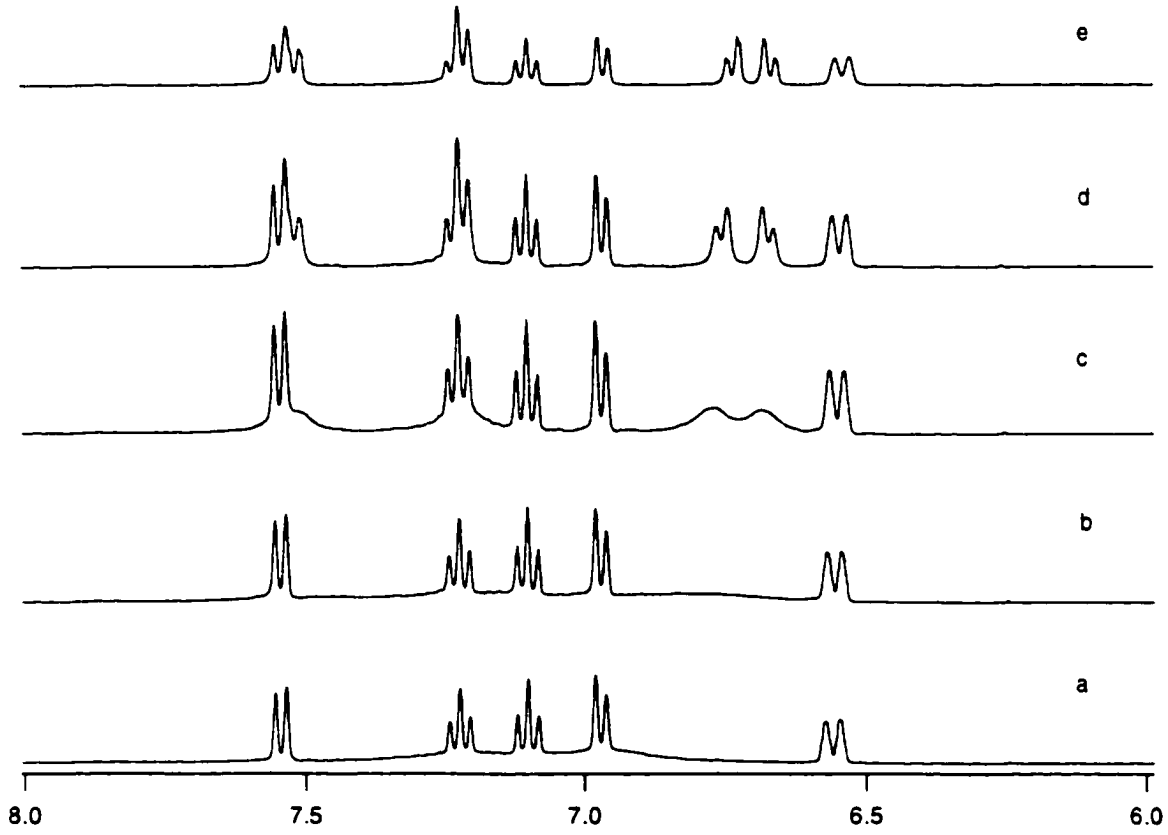

Downfield section of the ^{1}H NMR spectrum of ketone 20 at 10 °C (a), -3 °C (b), -20 °C (c), -40 °C (d), -60 °C (e).

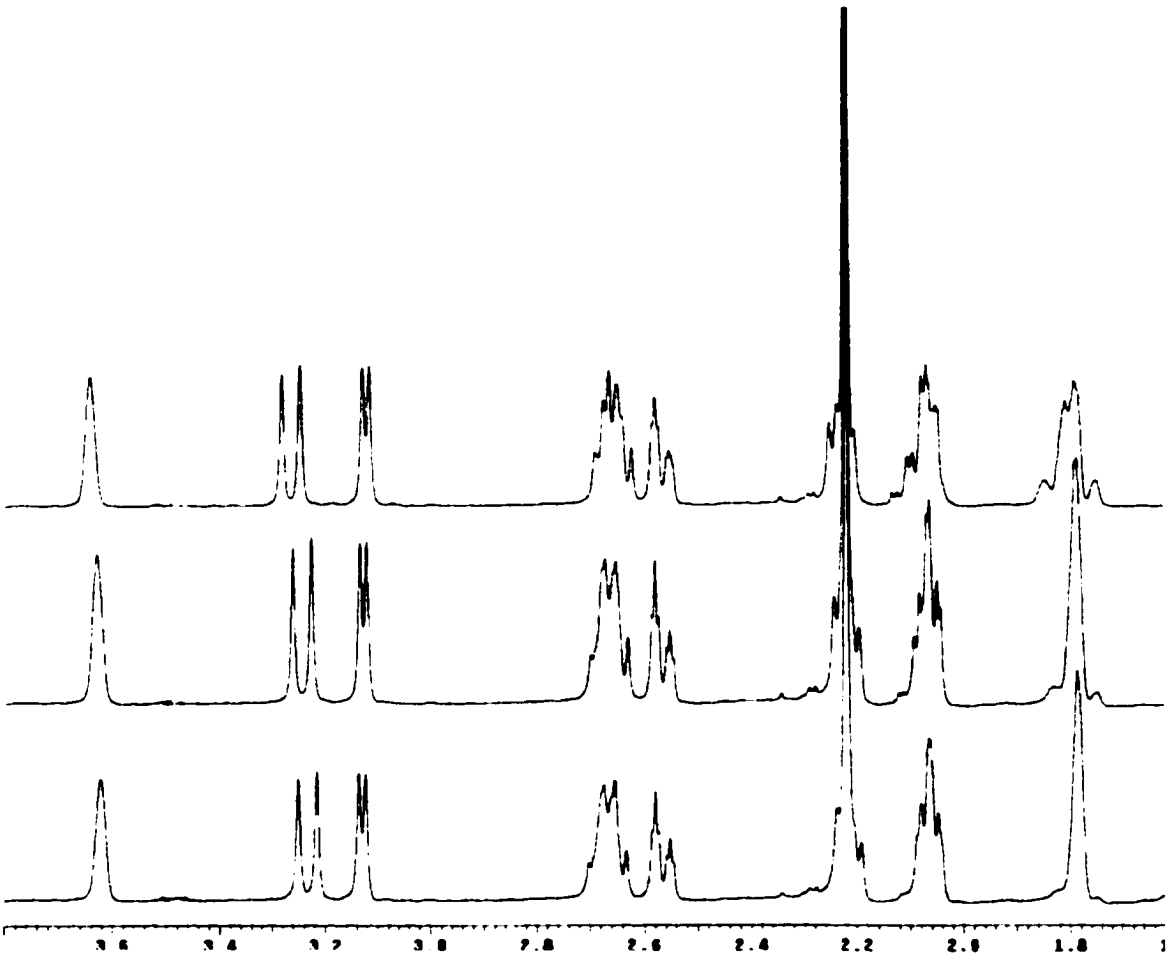

Upfield section of the ^{1}H NMR spectrum of ketone 20

taken at 50 °C, 23 °C, 12.5 °C (from top to bottom)

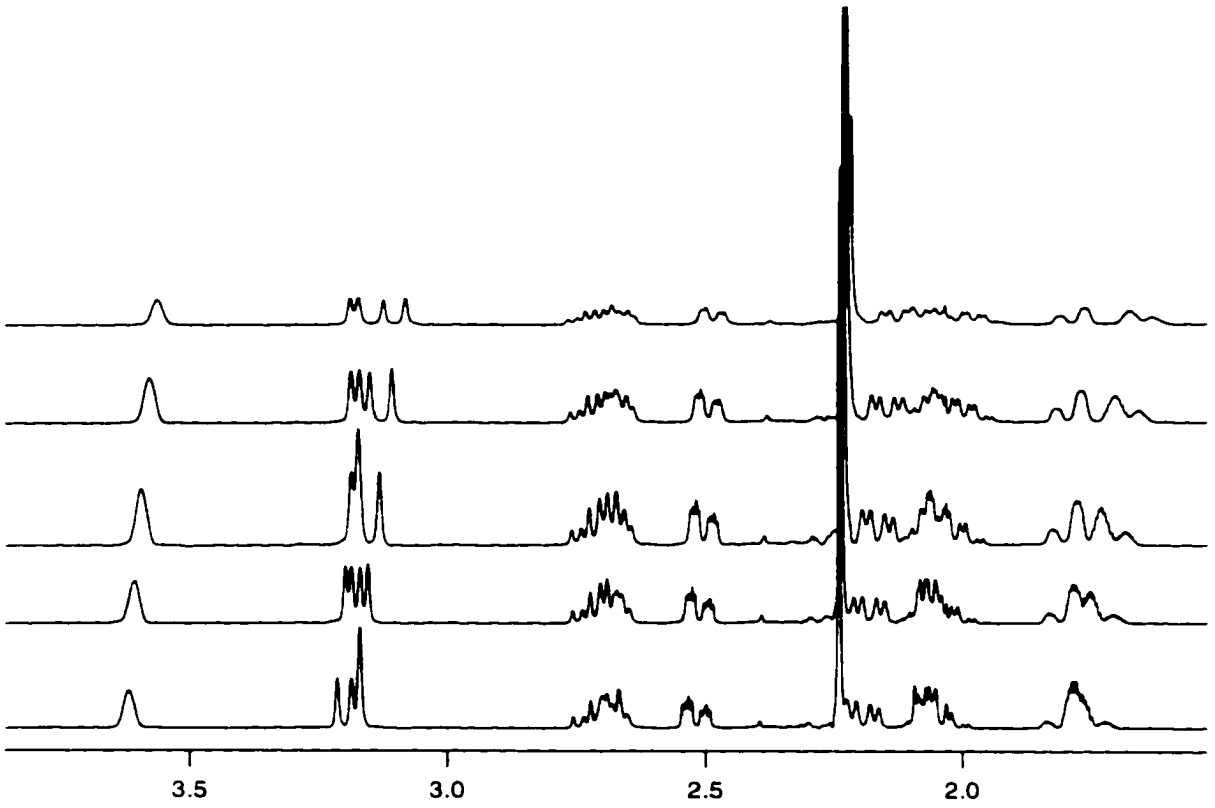

Upfield section of the ^{1}H NMR spectrum of ketone 20

taken at – 60 °C, -40 °C, -20 °C, -3 °C, 10 °C (from top to bottom)

The ultimate confirmation of the structure and the stereochemistry of the ketone **20**, came from its X-ray structure. Protons at C(8) and C(4) position are cis , while proton at C(12) is trans to the p-tolyl group. This stereochemistry indicated the stereochemistry of the transition state in the Diels-Alder reaction, shown in figure.

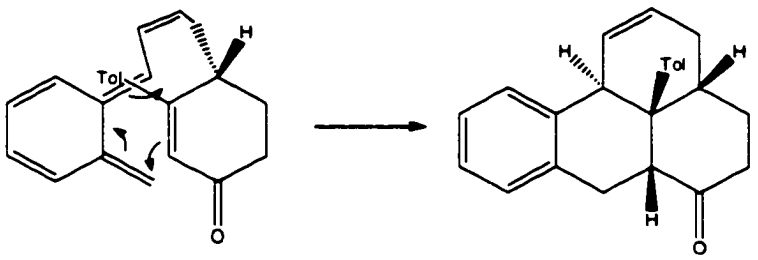

Figure 70. Transition state in the Diels – Alder reaction

The expected endo transition state accounts best for the observed stereochemistry of the protons at C(4) and C(8) and p-tolyl group. In addition, proton at C(8) was expected to point away from the reaction site, leading to its cis position to the p-tolyl group in the product.

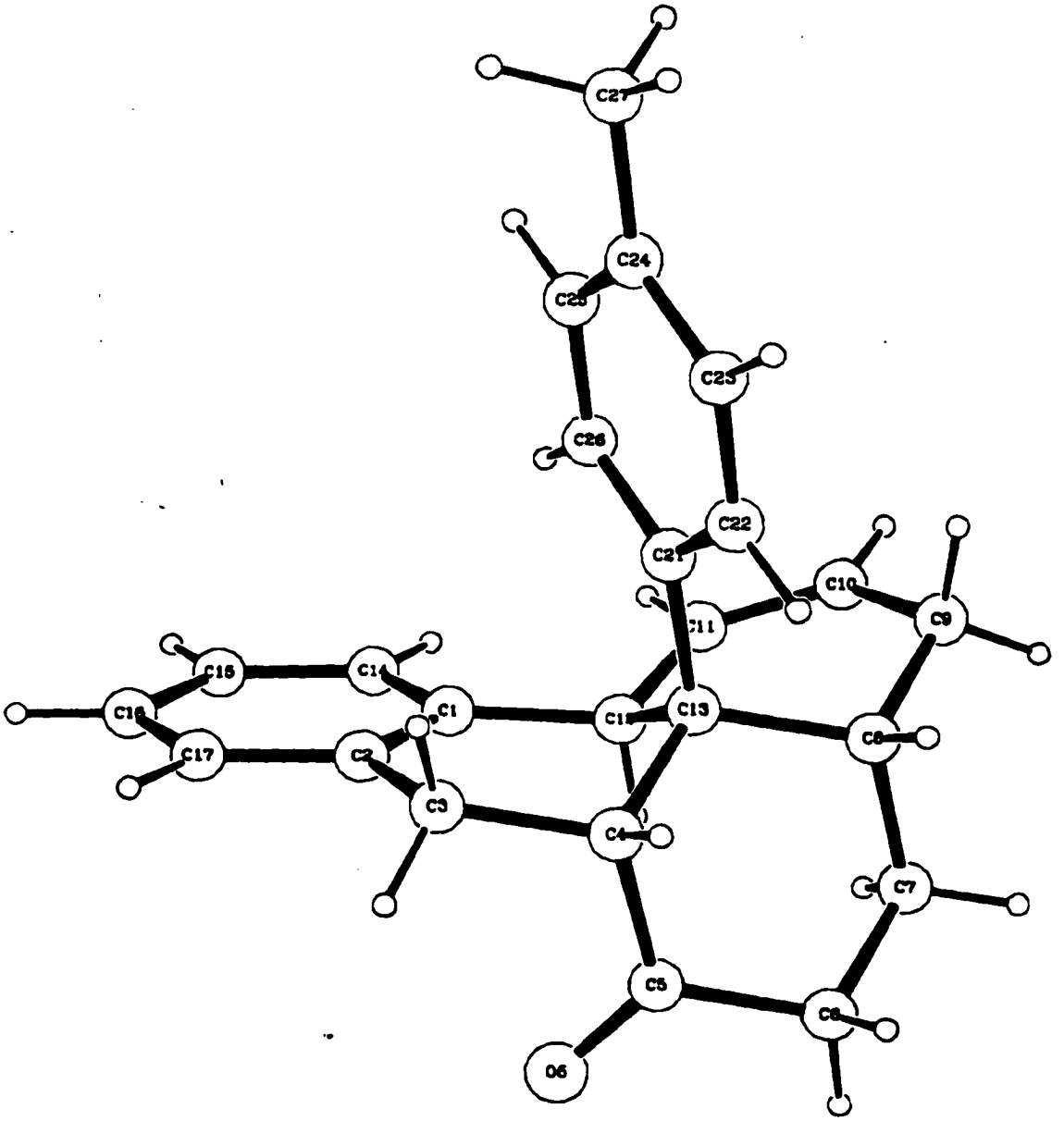

X-ray structure of the ketone 20

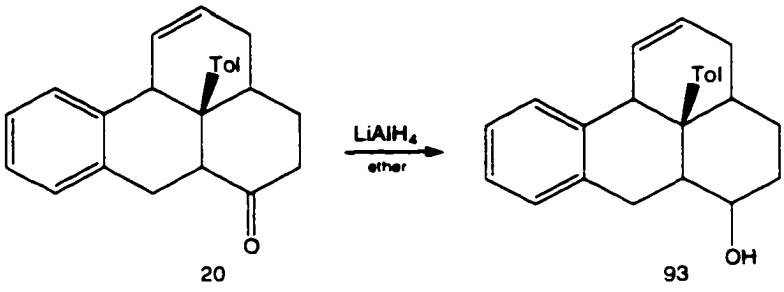

Figure 71. Reduction of ketone (20)

Reduction of ketone **20** using sodium borohydride in ethanol gave only one isomer of alcohol **93**. However, the yield was very low, 47 %, with the formation of a more polar fraction which was not characterized. Lithium aluminum hydride as a reducing reagent provided the same isomer of alcohol **93** but in a much higher yield, 86.7 %. Dehydration of alcohol **93** was carried out in two ways. One way involved the transformation of alcohol **93** into mesylate **94**, that proceeded in 81.3 % yield, and subsequent dehydromesylation[86] on alumina that gave diene **90** in 78.6 % yield.

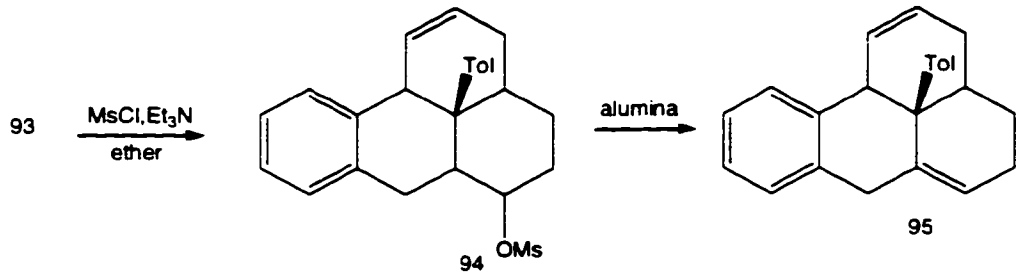

Figure 72. Mesylation-dehydromesylation route to diene **95**

The direct dehydration of alcohol **93** in refluxing HMPA[87] proceeded much faster, and provided a mixture of dienes (**95** and **96**) in higher overall yield , 78.9 %.

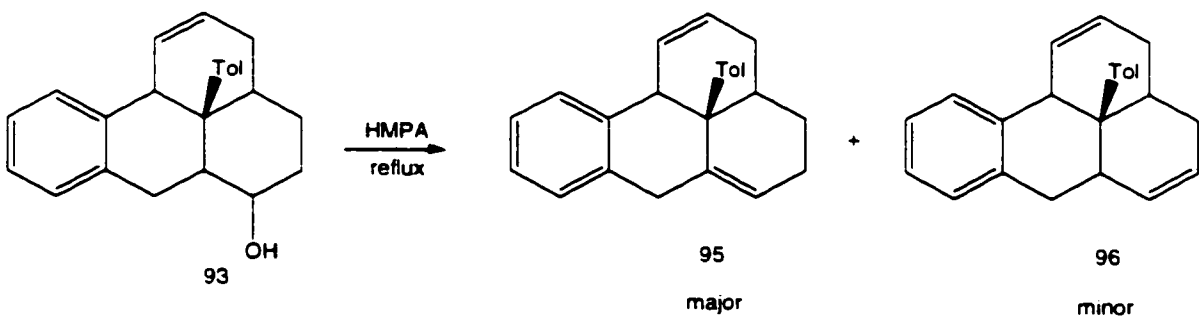

Figure 73. Dehydration of alcohol **93** with HMPA

3.8. Introduction of additional double bonds into diene 95

3.8.1. DDQ approach

Reaction of diene **95** with DDQ in benzene gave triene **97** in 41.3 % yield. Attempts to transform triene **97** into tetraene **98** by the reaction of DDQ in refluxing benzene failed, only starting material was recovered.

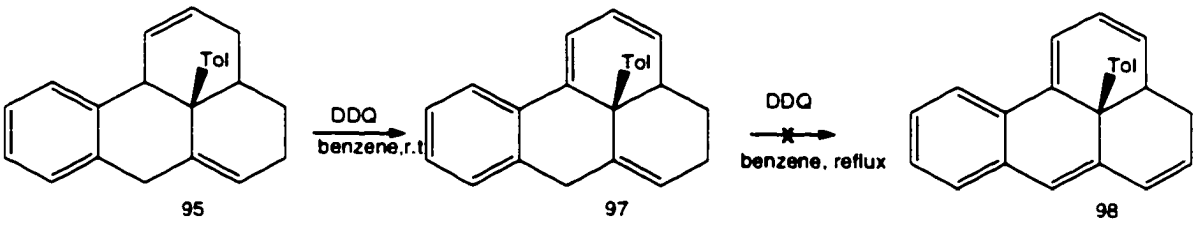

Figure 74. Formation of triene **97**

Reaction of triene **97** with DDQ in higher boiling solvent, anisole, gave the mixture of starting material and what appears to be **99**.

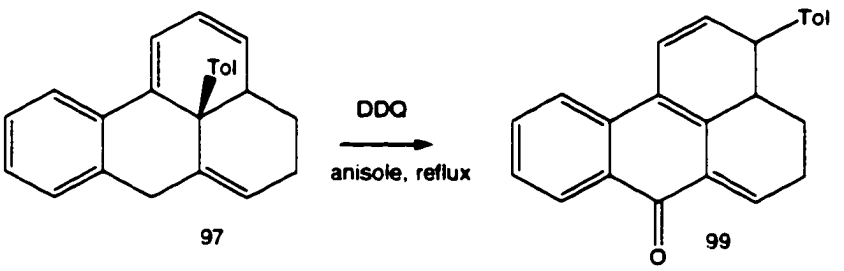

Figure 75. Formation of ketone **99**

3.8.2.Bromination-dehydrobromination approach

Since the attempts to introduce additional double bonds into triene **97** with DDQ did not succeed, we decided to investigate the bromination-dehydrobromination approach.

The reaction of diene **95** with pyridinium perbromide in the presence of pyridine gave only dibromide **100**[88].

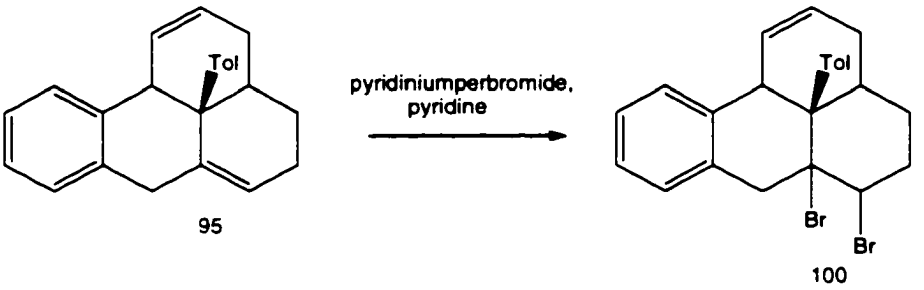

Figure 76. Formation of dibromide **100**

In contrast, bromination without the presence of pyridine[89] yielded a mixture of tetrabromides **101**.

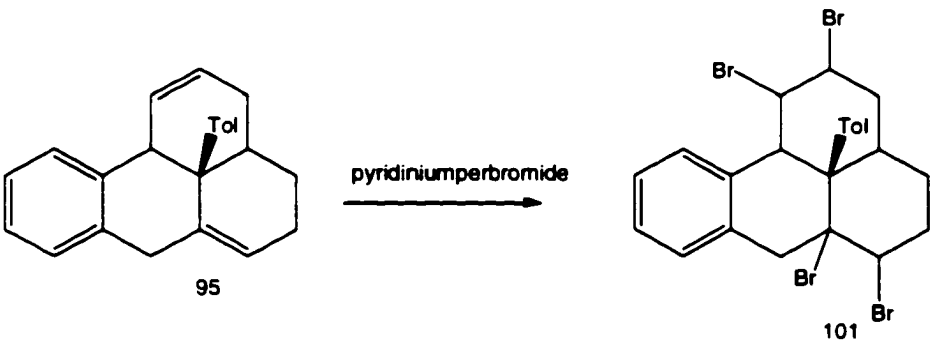

Figure 77. Formation of tetrabromides **101**

Dehydrobromination was attempted in several ways. Reaction of dibromide **100** with $LiCl/Li_2CO_3$[89] gave back diene **95**. The reaction of dibromide **100** with potassium tert-butoxide afforded a mixture of triene **102** as a minor product, and diene **95**, as a major product.

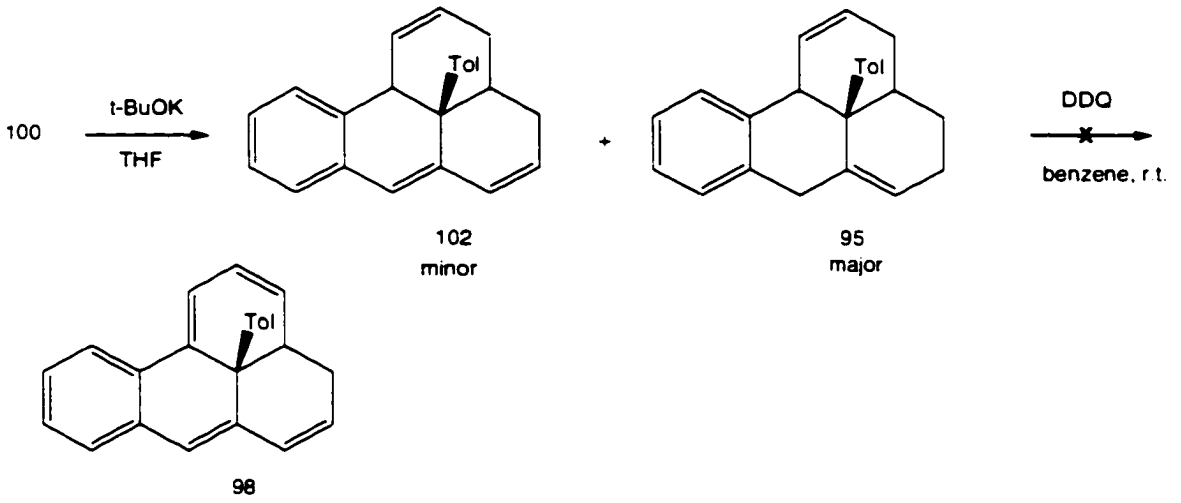

Figure 78. Dehydrobromination of dibromide **100**

Similarly, the reaction of tetrabromides **101** with $LiCl/Li_2CO_3$ gave back diene **95** , while the reflux in THF with potassium tert-butoxide afforded the mixture of triene **102**, diene **95** and tetraene **98** in the ratio of 86:10:4 as judged by GC/MS.

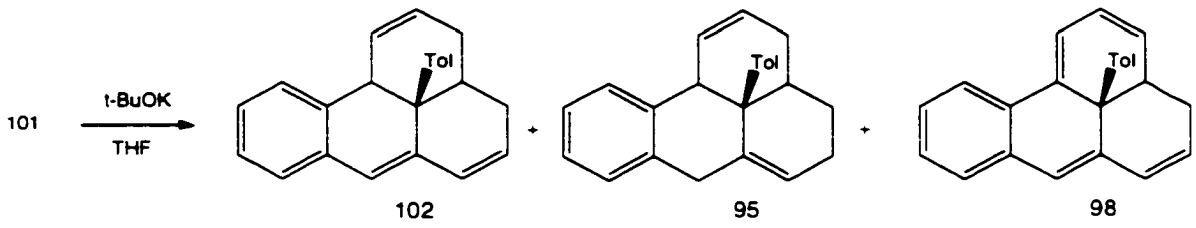

Figure 79. Dehydrobromination/debromination of tetrabromide **101**

Since the reaction of diene **95** with DDQ in benzene at room temperature furnished triene **97** (figure 79), we expected that the triene **102** would react similarly, giving tetraene **98.** Unfortunately, triene **102** did not dehydrogenate with DDQ – only starting material was recovered.

A possible speculative explanation for these unexpected results could be that the stereochemistry of the dibromide **100** and tetrabromides **101** is not suitable for E2 elimination. The complications involved with this approach, namely debromination being favored over dehydrobromination, led us to try a different pathway towards tetraene **98**.

3.8.3. Bromination- reductive bromination approach

Allylic bromination of diene **95** with NBS furnished a mixture of tetrabromides **103** in high yield.

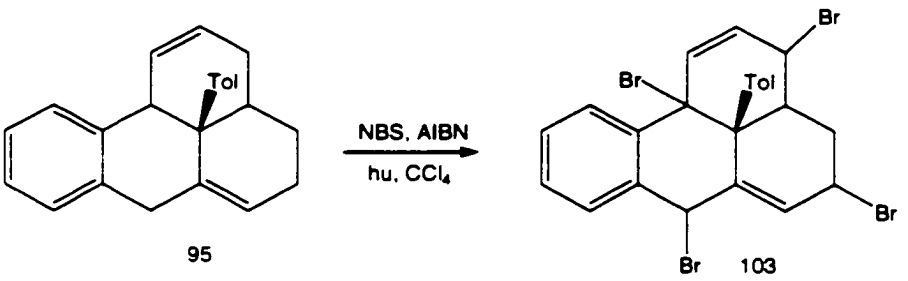

Figure 80. Formation of tetrabromides **103**

Dehydrobromination of the tetrabromides mixture **103** with potassium tert-butoxide in THF, gave a mixture of tetraene **98** and bromotetraene **104**, having a vinylic bromide.

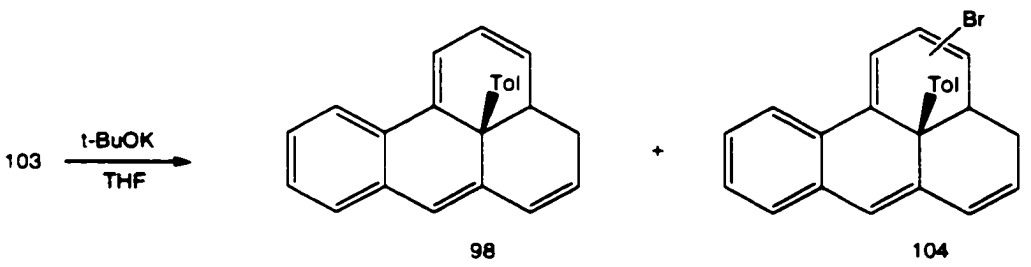

Figure 81. Dehydrobromination of tetrabromides **103**

While the vinylic bromide **104**, could be converted into tetraene **98**, by the reaction with *tert*-butyllithium, followed by the protonation, we decided to investigate the direct reductive debromination of tetrabromide **103** with ter-butyllithium as reported by Paquette[89]. Indeed, the reaction of tetrabromide **102** with tert-butyllithium provided tetraene **98** in 51 % yield. The overall yield from diene **95** to tetraene **98** was 43 %. The other product formed in the reaction accounted as t-butyltriene **105** as judged by GC/MS .

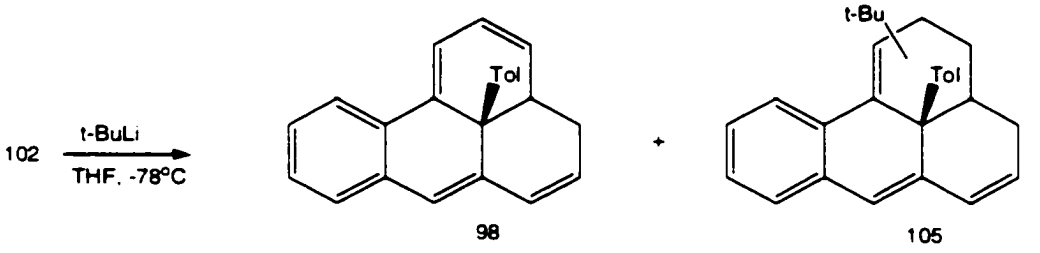

Figure 82. Reductive debromination of tetraene **102**

3.9. Introduction of the last double bond

3.9.1. The "Streitweiser approach"

In analogy to Streitweiser' approach to cyclooctatetraenes[90], we have decided to investigate (tetraene **98**) – 14 π dianion (**106**)- pentaene (**21**) sequence for the introduction of the last double bond. The other two methods considered were allylic bromination-dehydrobromination and dehydrogenation with DDQ. The mildness of the conditions and the lack of side reactions is what makes the Streitweiser's approach the most promising method for the last step.

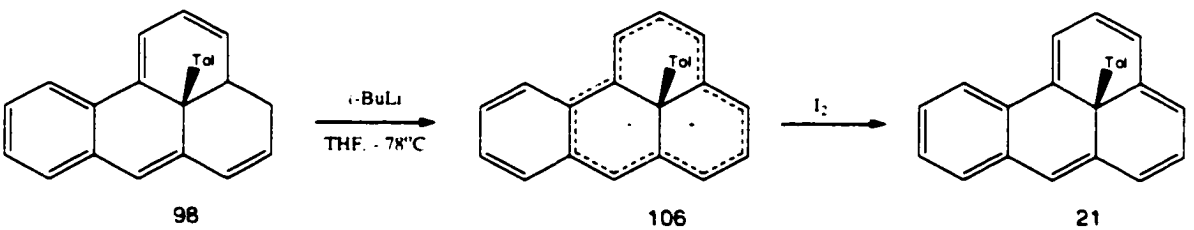

Figure 83. Introduction of the last double bond.

For the formation of dianion **106**, instead of potassium amide in the original procedure, we used t-butyl lithium. The dark green solution of dianion was stirred for 10 minutes before it was oxidized with iodine. The ^{1}H NMR of the crude mixture showed the peaks corresponding to the starting material i.e tetraene, as well as additional peaks in the alkene region. No significant changes

in chemical shifts in terms of upfield shifts expected for the exocyclic protons of the 12 π system, nor downfield shifts for the arene protons of the p-tolyl group were observed. GC/MS of the ^{1}H NMR sample provided more information on the outcome of the reaction. Besides the peak corresponding to tetraene **93**, the peak for a compound of the molecular weight of 342/344 in the ratio of 3/1 was observed. The molecular weight, as well as the fragmentation in the MS, leads to the conclusion that the compound formed was chloroderivative of tetraene.

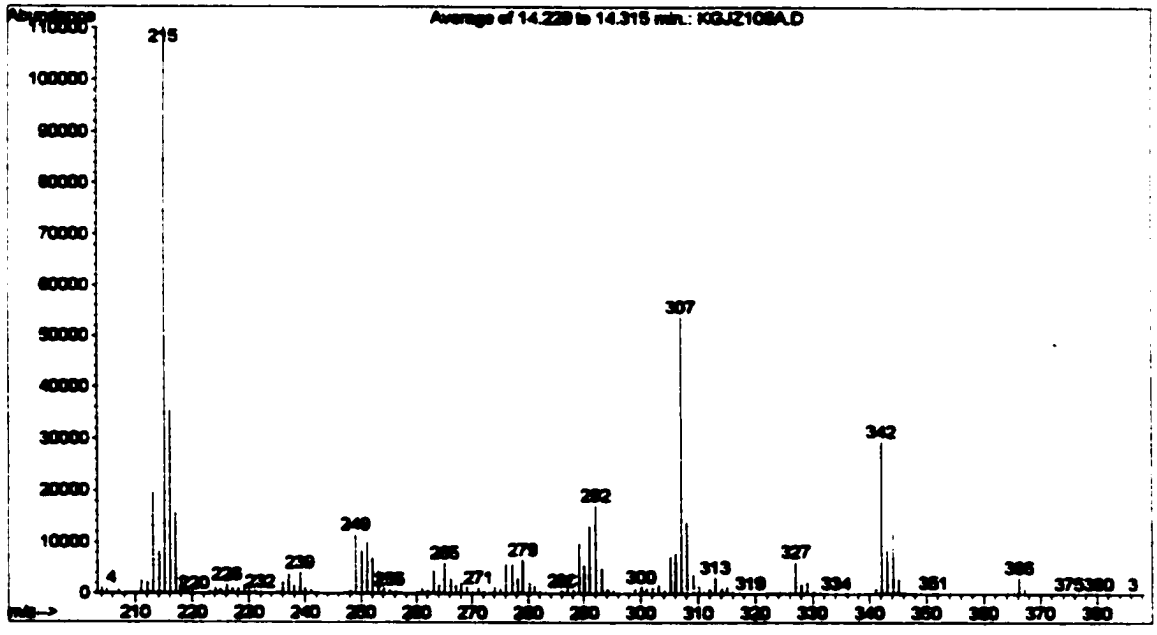

GC/MS of the chloro derivative **107**

The formation of the chloroderivative can be rationalized as the result of the addition of hydrochloric acid, present in deuterated chloroform, across one of the double bonds of benzo-13-tolylphanalene (**21**), formed in the reaction showed in figure 83. As expected, GC/MS also showed a presence of a compound of

molecular weight 343/345 which could have resulted from an addition of DCl, also present in deuterated chloroform onto pentaene **21**.

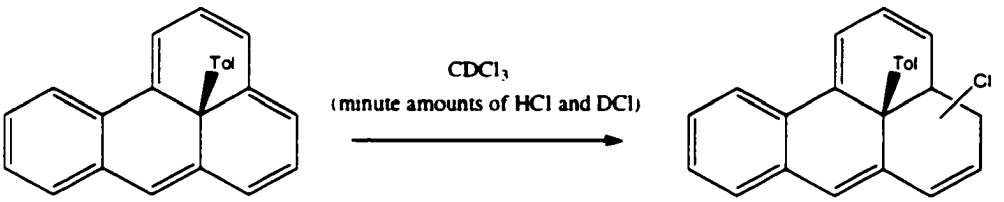

21 107

Figure 84. Formation of the chlorotetraene **107**

The modification to the Streitweiser's approach has been made in terms of the time allowed for the formation of the dianion. A dark green solution of dianion was stirred for four hours before the oxidation with iodine. Besides the peaks corresponding to tetraene **98**, the ^{1}H NMR spectrum of the crude product mixture, taken in deuterated acetonitrile, showed the peaks in the region expected for the exocyclic protons of the 12 π system[46]. The downfield shift, expected for the arene protons of the p-tolyl group was less obvious.

Yet another modification of the procedure, using a combination of n-butyl lithium and tert-butoxide as a base[91], appeared not to have improved the formation of the dianion **106**.

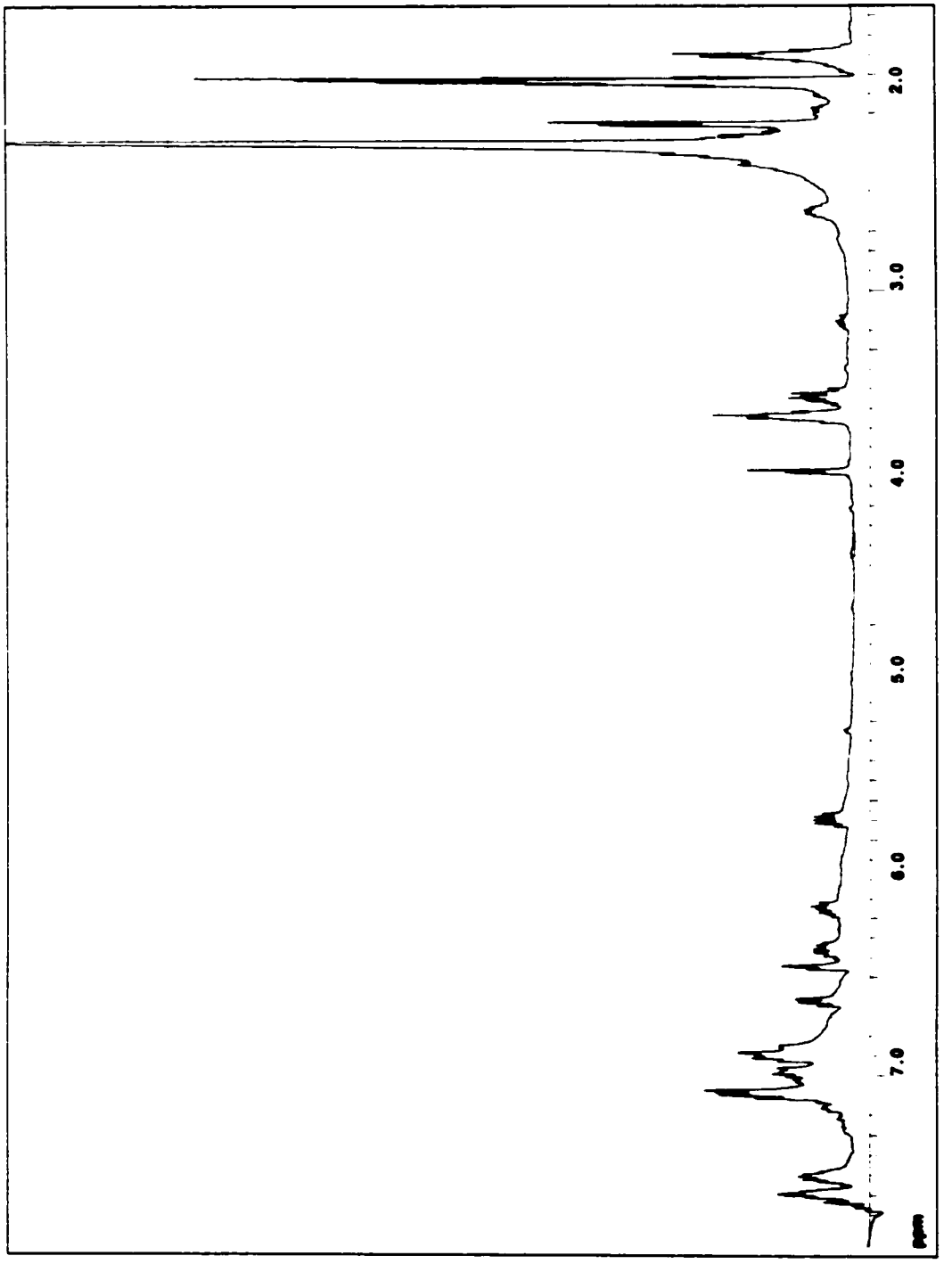

^{1}H NMR spectrum of the crude mixture

3.10. Future studies

3.10.1. The Intramolecular Friedel-Crafts Acylation Approach towards Benzo-13-substitutedphenalene.

In addition to the IMDA approach, we have looked into a possibly very fast approach toward the tetracyclic skeleton, namely Friedel Crafts acylation.

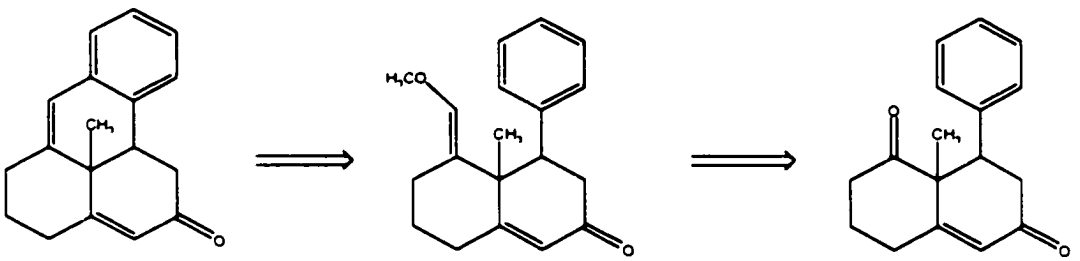

110 109 108

Figure 85. Retrosynthetic approach toward benzo-13-methylphenalene.

We have briefly investigated Robinson annulation reaction[92] between 2-methyl-1,3-cyclohexadione and benzalacetone, and found that the best yield (26.4%) is obtained with the use of potassium hydroxide in methanol for the Michael addition step, and pyrrolidine in benzene for the subsequent aldol condensation.

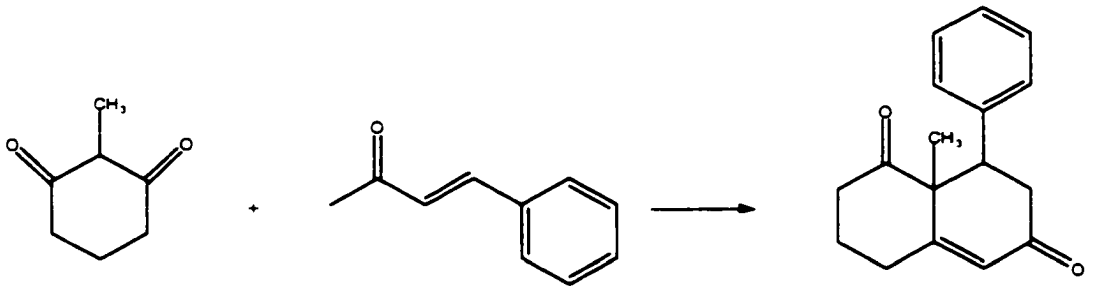

111 112 108

Figure 86. Preparation of diketone **108**

3-phenyi-1,3-cyclohexadione, needed for the synthesis of the phenyl analog of diketone **108** could be synthesized by the known method[93].

The closure of the ring could be anticipated as the result of the following reaction steps:

1. Wittig reaction of diketone with methoxymethylphosphonium salt to give **109**
2. hydrolysis of the Wittig adduct followed by the cyclodehydration of the formed aldehyde to give **110**.

3.10.2. Photochemical Generation of o-Quinodimethanes

Synthetically simpler approach toward benzo-13- substituted phenalene is based on the photochemical generation of o-quinodimethanes[94].

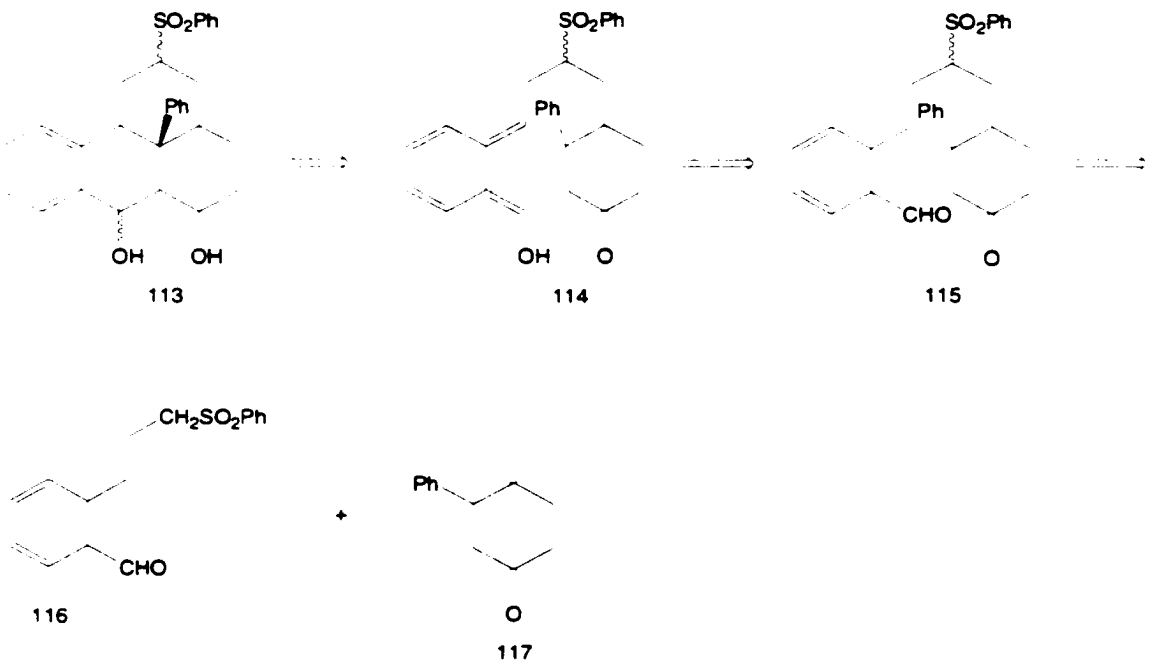

Figure 87. Retrosynthetic approach to the precursor **113** for benzo-13-phenylphenalene

What makes this approach very attractive is the accessibility of starting materials. We have already synthesized dienone **117** by treatment of alcohol **40** with 10 % hydrochloric acid in refluxing THF.

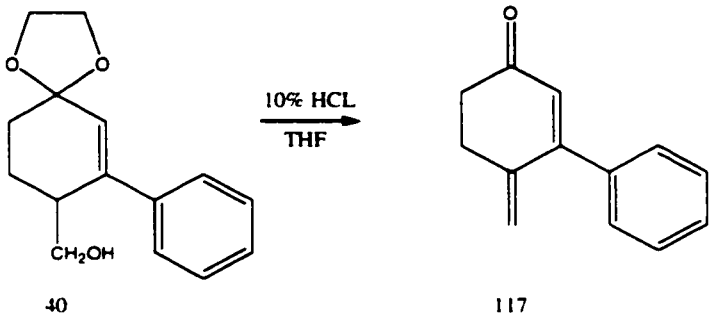

Figure 88. Preparation of dienone **117**

The methyl analog of dienone 118 was obtained by Alva[48] in his Hagemann's ester approach toward benzo-13-methylphenalene. Treatment of methyl dienone **118** with acid ($HOAc/H_2O/HCl$ (5/5/1)) gave the phenol **119**.

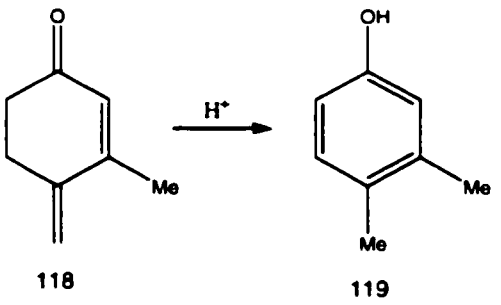

Figure 89. Formation of phenol **119**

The stability of phenyl dienone **117** was investigated by exposing it to the base (10% NaOH) as well as to the acid (10% HCl).The exposure showed that it is very stable, remaining intact even after the prolonged reflux in the acid.

The other building block, aldehyde **116** could be available in a few steps from o-phthalaldehyde **121**.

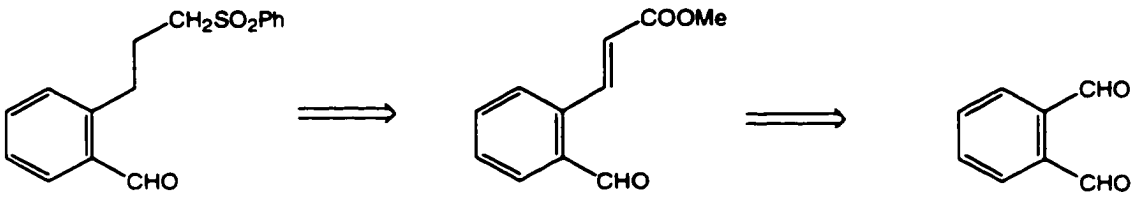

116 120 121

Figure 90. Retrosynthetic sequence toward aldehyde **116**

3.10.3. The Extension of the IMDA Methodology

3.10.3.1. 13-p-Tolylphenalene

For a further investigation of a 12 π system present in benzo-13-p-tolylphenalene it would be advantageous to synthesize its non benzannelated derivative, 13-p-tolylphenalene. Apart from the properties already present in benzo-13-p-tolylphenalene, namely, rigidity and planarity, the non benzannelated derivative would also have a highly symmetrical structure that would make the pseudo Jahn-Teller distortion minimal. In addition, comparison of chemical shifts in the ^1H NMR spectra, would give further insight into the effects of benzannelation on the paramagnetic ring current present in the system.

We propose the utilization of the developed IMDA methodology for the synthesis of 13-p-Tolylphenalene.

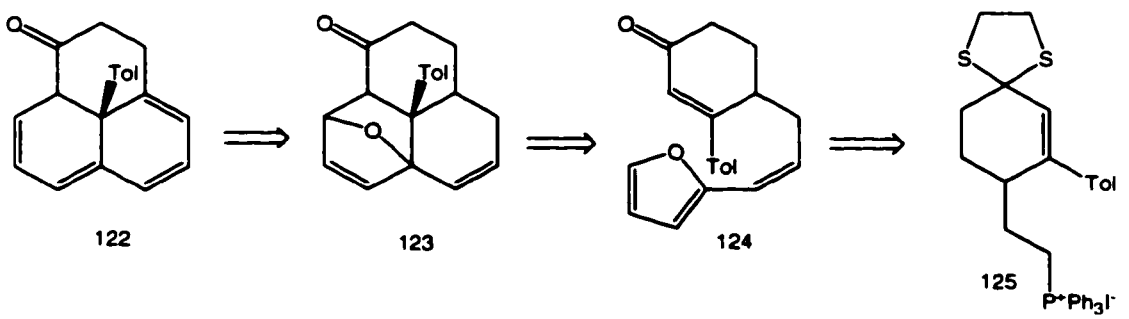

Figure 91. Retrosynthetic approach toward 13-p-Tolylphenalene

The system suitable for IMDA reaction **124** would be available via Wittig reaction of phosphonium salt **125** and furfural. The elimination of water from IMDA product would give a highly functionalized precursor for 13-p-tolylphenalene **122**. Phosphonium salt **125** can be obtained by the methods already described in figure 54.

3.10.3.2. Benzo-13-ethynylphenalene

The same synthetic methodology to the one developed for Benzo-13-p-tolylphenalene can be applied for the synthesis of Benzo-13-ethynylphenalene.

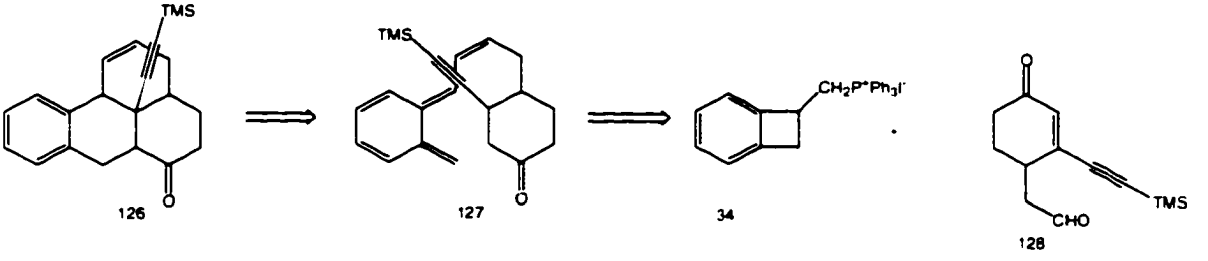

Figure 92. Proposed synthetic sequence for the synthesis of ketone **128**

Retrosynthetic analysis shows that the same 4 step sequence used for the synthesis of aldehyde **35** can be applied for the synthesis of its ethynyl analog **128**.

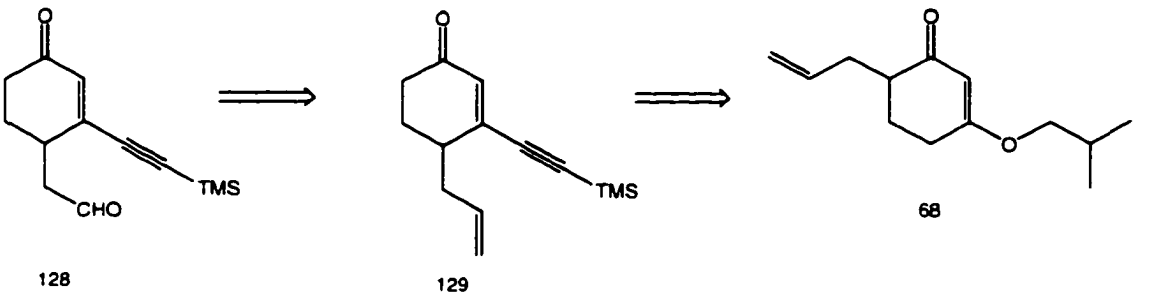

Figure 93. Retrosynthesis for aldehyde **128**

The synthesis of benzo-13-ethynylphenalene is important and fascinating for another yet reason : the possibility of oxidative coupling of the terminal acetylene that is expected to yield the topologically interesting dimer **129**, with two planar 12 π systems parallel to each other and connected by a diacetylene unit.

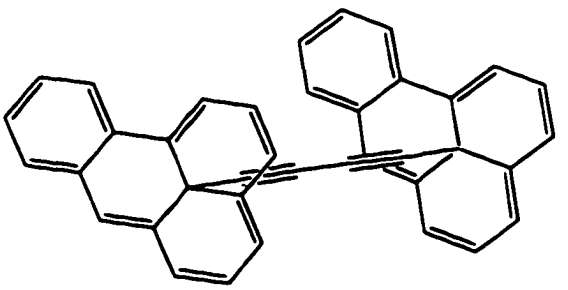

Figure 94. Dimer **129**

CHAPTER 4. EXPERIMENTAL SECTION

Spectroscopy

NMR

Proton and carbon Nuclear Magnetic Resonance spectra (^{1}H and ^{13}C NMR spectra) were recorded using a 300 MHz General Electric QE-300 and Varian Unity Plus 500 MHz nuclear magnetic resonance spectrophotometer. All samples were prepared by dissolving 10 - 100 mg in chloroform-d_3 (99.8 % D, 0.03 % V/V tetramethylsylane, Aldrich). Chemical shifts are expressed in parts per million (ppm) downfield from the TMS internal standard, δ=0 ppm, and are reported in the following order : chemical shift (multiplicity of the signal, number of protons, coupling constant). Multiplicity of the signals are described as follows : s- singlet; d- doublet; t- triplet; q-quartet; m-multiplet; b-broad. Coupling constant, J, is reported in Hertz units.

IR

Infrared spectra were recorded on a Perkin- Elmer 1310 IR spectrophotometer. Bands are reported in wave numbers (υ = 1/cm) and are described as s-sharp, m- medium, w-weak, b-broad. Solid samples were prepared as KBr pellets.

UV

Ultraviolet spectra were measured with Varian-Bio 100 spectrophotometer, between 400 and 250 nm using dichloromethane as solvent.

GC/MS

Gas Chromatography/Mass spectra were determined by either electron impact (EI) ionization or chemical ionization (CI) using methane as the carrier gas on a Hewlett-Packard 5989 A mass spectrometer. Some molecules were analyzed by direct inlet probes. GC/MS data are reported in the following manner: molecular ion, followed by selected significant fragmentations.

X-ray

X- ray intensity data were measured on an Enraf-Nonius Turbo KappaCCD diffractometer (graphite-monochromated Mo $K\alpha$ radiation, ω-ϕ scans). The structure was solved by a multiple-solution procedure[95] and was refined by full-matrix least squares. In the final refinement, the nonhydrogen atoms were refined anisotropically. The hydrogen atoms were included in the structure-factor calculations, but their parameters were not refined.

CHROMATOGRAPHY

Column chromatography.

All flash column chromatography separations were performed using grade 60 silica gel available from Aldrich Chemical Co, following Still's procedure[96].

Thin layer chromatography.

TLC analysis was performed using pre-coated plastic sheets of silica gel, thickness 0.25 mm, available from J.T. Baker. Spots were visualized by using 254 nm UV lamp. For non UV-active compounds ethanolic solution of phosphomolybdic acid as well as ceric sulfate spray was used to visualize the spots on the TLC plates.

Radial Thin-layer chromatography.

In the cases when flash chromatography did not provide compounds of desirable purity, radial chromatography was performed, usually on samples of 500 mg and less. Radial chromatography was carried out using chromatotron, model 7924T, made by Harrison research. The plates were coated with silica gel 60 PF-254, containing calcium sulfate as binder (available from VWR Scientific), following the procedure of Harrison[97]. The samples were first prepurified on a short column, and then introduced into the chromatotron. For the eluent was used the solvent that gives R_f values of about 0.25 . The separation of compounds was followed by irradiating the plate with 254 nm UV lamp. After the

separation, plates were washed with the solvent of high polarity, usually dichloromethane or ethyl acetate.

ELUENTS

Hexane and ethyl acetate were distilled prior to use. Both solvents were distilled over calcium hydride.

MELTING POINTS

Melting points were determined on a Fisher-Johns apparatus and are uncorrected

SOLVENTS AND REAGENTS

Solvents

Most of the solvents were ACS reagent grade, available from either Fisher or Aldrich Chemicals. Anhydrous diethyl ether and ethanol were used as supplied. All other solvents were dried using following drying agents:

SOLVENT	DRYING AGENT
Acetone	Potassium carbonate/ Calcium chloride
Benzene	Calcium hydride
Liquid ammonia	Potassium hydroxide(solid)
Diisopropylamine	Sodium metal
Triethylamine	Sodium metal
Dimethylformamide	Calcium hydride
Dimethylsulfoxide	Calcium hydride
1,4 Dioxane	Sodium metal
THF	Potassium metal
Methanol	Magnesium metal
Dichlormethane	Calcium hydride/phosphorous pentoxide
Piperidine	Sodium metal
Pyridine	Calcium hydride

Table 6. Solvents and corresponding drying agents.

All solvents were purified by distillation under a blanket of nitrogen, over corresponding drying agent.

Reagents

Potassium tert-butoxide was sublimed prior to use. Sodium iodide, potassium carbonate were kept in oven (125 °C) until needed.
Tosyl chloride was recrystalized from chloroform following the procedure by Pelletier. Phosphonium salts were dried either by heating at -60 °C for 2 hours at reduced pressure (0.03 mm Hg) or by removing water as an azeotrope with benzene.

MASS AND YIELDS

Masses were obtained using OHAUS balance model 300. Yields are reported in grams as well in percentage.

GENERAL REACTION CONDITIONS

Glassware used in moisture sensitive reactions was either oven dried overnight (150 ° C) or flame dried under vacuum, and flushed with nitrogen or argon prior to use. Wherever possible, reactions were followed by TLC. Usual work–up, after quenching the reaction with a suitable cold aqueous solution, involved removing water miscible solvents by rotary evaporation or distillation prior to extraction. Acid neutralization was accomplished by addition of saturated sodium bicarbonate solution, while for basic neutralization dilute (usually 10 %) hydrochloric acid was used. Organic solvents used for extraction were dried over

anhydrous magnesium or sodium sulfate. Solvents were first removed by rotary evaporation at water aspirator pressure (roughly 11 mm Hg), followed by evaporation *in vacuo* at an oil pump of roughly 0.1mm Hg. In some cases traces of solvent were removed by dissolving the compound in carbon tetrachloride, removing the solvent first by rotary evaporation and then keeping the sample on a vacuum pump (0.1 mm Hg) for at least 2 hours.

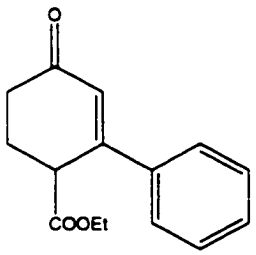

38

4-Oxo-2-phenyl-cyclohex-2-ene carboxylic acid ethyl ester (**38**)

Method 1

To the 250 ml round bottom flask containing 90 ml dry benzene, 0.1 g sodium hydride was added and stirred for 5 minutes. 19.2 g (0.1 mol, 1 eq) ethyl benzoylacetoacetate and 7.7 g (0.11 mol, 1.1 eq) methyl vinyl ketone were added to the flask, and the mixture stirred. After 4 hours of stirring, 0.5 ml distilled piperidine and 0.5 ml acetic acid were added and the mixture refluxed for 24 hours with Dean Stark equipment. After cooling to room temperature, the solvent was removed on a rotary evaporator. Column chromatography (hexane:ethyl acetate/ 2:1) did not afford pure ester **38**.

Method 2.

To the solution of 9.62 g (0.05 mol, 1 eq) of ethyl benzoylacetate and 3.52 g (0.05 mol, 1 eq) in 20 mL tert-butylalcohol were added 9.2 mL 40 % aqueous Triton B (benzyltrimethylammonium hydroxide) in one portion. Soon after, the solution became dark green. After 2 hours of stirring, the solution was poured into 50 mL of cold water. The product was extracted with ether-ethyl acetate. After washing the organic solution three times with cold water, and drying over

magnesium sulfate, solvents were removed by rotary evaporation. Crystals formed after evaporation of the solvent were separated by trituration with ether. Evaporation of the solvent from the filtrate yielded 6.5 g (0.027 mol, 53.3%).

^{1}H NMR (300 MHz, $CDCl_3$): δ 7.48 ppm (m, 2H); δ 7.40 ppm (m, 3H); δ 6.47 ppm (s, 1H); δ 4. 09 ppm (q, 2H, 7 Hz); δ 3.96 ppm (m, 1H); δ 2.35-2.7 ppm (m, 4H); δ 1.12 ppm (t, 3H, 7 Hz)

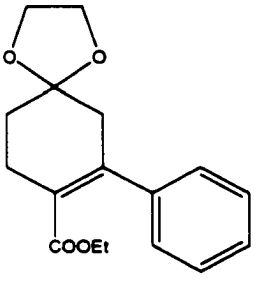

39

7-phenyl-1,4-dioxa-spiro[4,5]dec-6-ene-8-carboxylic acid ethyl ester (**39**)

The solution of 21 g (0.086 mol, 1eq) phenyl Hagemann's ester, 7.44 g (0.12 mol, 1.4 eq) ethylene glycol and 0.8 g p-toluenesulfonic acid in 250 ml benzene was placed in a round bottom flask equipped with Dean- Stark collector and condenser and refluxed until the right amount of water was collected (1.5 ml). After removal of the solvent *in vacuo*, the residue was dissolved in ether. The ether solution was washed with sodium bicarbonate and brine and dried over magnesium sulfate. Column chromatography (hexane:ethyl acetate 1:1) afforded 21.3 g of ketal **39** (85.9%).

^{1}H NMR(300 MHz, $CDCl_3$): δ 7.19 ppm (m, 3H); δ 7.05 ppm (m, 2H); δ 3.92 ppm (s,4H); δ 3.79 ppm (q, 2H, 7 Hz); δ 2.59 ppm (m, 2H); δ 2.53 ppm (s,2H); δ1.79ppm (t, 2H, 7 Hz); δ 0.75 ppm (t, 3H, 7Hz).

^{13}C NMR (75 MHz, $CDCl_3$): δ 168.84 ppm; δ 142.80 ppm; δ 142.13 ppm; δ 128.39 ppm; δ 128.25 ppm; δ 128.08 ppm; δ 127.83 ppm; δ 126.97 ppm; δ 126.71 ppm; δ 107.19 ppm; δ 64.48 ppm ; δ 60.32 ppm; δ 42.46 ppm; δ 30.61 ppm; δ 26.02 ppm; δ 13.52 ppm;

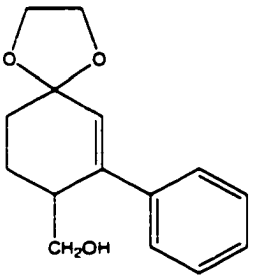

(7-Phenyl-1,4-dioxa-spiro[4,5]dec-6-en-8-yl)-methanol (**40**)

A two neck flask equipped with an addition funnel and a condenser was charged with 70 ml dry ether and immersed in an ice bath. Under nitrogen, 1.9 g (0.05 mol, 2 eq) lithium aluminum hydride was added, and mixture stirred for 5 minutes. 7.2 g (0.025 mol, 1 eq) of the protected ester 39 were dissolved in 40 ml dry ether, and dropwise added to the suspension of lithium aluminum hydride in ether. After stirring overnight, the solution was again cooled to 0°C and the reaction quenched by the careful addition of a saturated sodium sulfate.The white granular precipitate was filtered off and washed with ether. The ether

solution was dried with anhydrous magnesium sulfate. After removal of the ether on a rotary evaporator, the residue was chromatographed (hexane/ethyl acetate : 1/2) to afford 5 g (81 %) of alcohol.

^{1}H NMR(300 MHz, $CDCl_3$): δ 7.21 ppm (m,3 H); δ 7.06 (m, 2H); δ 3.90 ppm (s,4H); δ 3.86 ppm (s, 2H); δ 2.42 ppm (m, 4H); δ 2.25 (s, 1H); δ 1.78 ppm (t, 2H, 6.5 Hz)

^{13}C NMR (75 MHz, $CDCl_3$): δ 141.19 ppm; δ 133.25 ppm; δ 131.83 ppm; δ 127.81 ppm; δ 127.73 ppm; δ 126.47 ppm; δ 125.98 ppm ; δ 107.75 ppm; δ 64.15 ppm ; δ 62.57 ppm; 41.61 ppm; δ 30.75 ppm; δ 25.97 ppm.

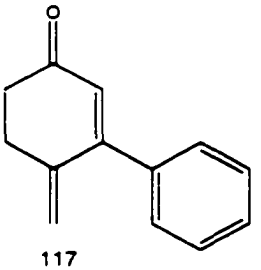

117

4-Methylene-3-phenyl-cyclohex-2-enone (**117**)

To the solution containing 2.5 g (0.01 mol) alcohol **40** in 50 ml THF, were added 50 ml 10 % hydrochloric acid and the solution was refluxed for 3 hours. After removal of most of the solvent on a rotary evaporator, the residue was diluted with ether. The organic layer was separated, washed with sodium bicarbonate

and brine and dried over magnesium sulfate. Column chromatography (hexane/ethyl acetate:4/1) afforded 1.39 g dienone (74.7%), m.p. 88-92 °C.

^{1}H NMR(300 MHz, $CDCl_3$): δ 7.39 ppm (m, 5H); δ 6.06 ppm (d, 1H, 1Hz); δ 5.53 ppm (m, 1H); δ 5,18 ppm (s, 1H); δ 2.89 ppm (t, 2H, 7 Hz); δ 2.62 ppm (t, 2H, 7 Hz)

^{13}C NMR (75 MHz, $CDCl_3$): δ 198.79 ppm; δ 158.06 ppm; δ 141.66 ppm; δ137.91 ppm; δ 129.24 ppm; δ 128.80 ppm; δ 128.19 ppm; δ 126.64 ppm; δ 126.48 ppm; δ 119.94 ppm; δ 119.84 ppm; δ 38.02 ppm; δ 32.44 ppm

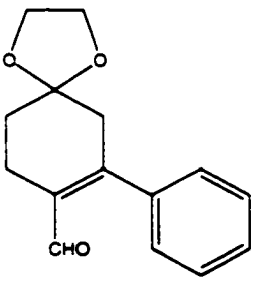

31

7-Phenyl-1,4-dioxa-spiro[4.5]dec-7-ene-8-carbaldehyde (**31**)

Alcohol was oxidized using pyridinium chloro chromate (PCC) as oxidant. PCC was prepared as follows:

To 184 ml of 6M hydrochloric acid (1.1 mol, 1.1 eq) was added rapidly, with stirring 100 gr (1 mol, 1 eq) of chromium trioxide. After 5 minutes of stirring, the homogeneous solution was cooled to 0°C and 79.1 g (1 mol, 1 eq) of pyridine

was carefully added over 10 minutes. With cooling the solution again to 0°C, yellow-orange solid formed which was collected on a sintered glass funnel and dried for one hour *in vacuo*. Yield 151 g (70 %).

Oxidation of alcohol **40**:

In a 500 ml round bottom flask fitted with a reflux condenser were suspended 3.23 g (0.015 mol, 1.5 eq) of PCC in 50 ml of dry dichloromethane. Solution of 2.5 g (0.01 mol, 1 eq) of alcohol (**40**) in 10 ml dry dichloromethane was added in one portion and the solution stirred overnight. Dry ether (50 ml) was added and the supernatant was decanted from the black gum. The insoluble residue was thoroughly washed three times with 20 ml of dry ether. The combined organic solutions were passed through Celite and the solvent removed by rotary evaporation. Column chromatography (hexane/ethyl acetate: 3/1) afforded aldehyde (**31**) in 74.7 % yield (1.83 g).

^{1}H NMR(300 MHz, $CDCl_3$): δ 9.43 ppm (s,1H); δ 7.29 (m, 3H); δ 7.18 ppm (m, 2H); δ 3.96 ppm (s, 4H); δ 2.71 ppm (s, 2H); δ 2.53 ppm (t, 2H, 7 Hz); δ 1.79 ppm (t, 2H, 7 Hz);

^{13}C NMR (75 MHz, $CDCl_3$): δ 192.62 ppm; δ 155.61 ppm; δ 137.93 ppm; δ 134.53 ppm; δ 128.59 ppm; δ 128.49 ppm; δ 128.21 ppm; δ 107.19 ppm; δ 64.60 ppm; δ 43.52 ppm; δ 30.22 ppm; δ 21.75 ppm.

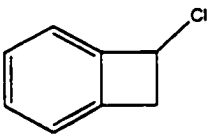

49

7-chloro-bicyclo[4.2.0]octa-1,3,5-triene (1-chlorobenzcyclobutene) (**49**)

A round bottom flask was charged with 9 g of α,α'-dichloro-o-xylene (0.05 mol). The flask was connected to the flash vacuum equipment and slowly heated in an oil bath. The pressure was 0.3 mm Hg and the temperature of the oven was kept between 750 and 770 °C. After 4 hours of heating, all of α,α'-dichloro-o-xylene had passed through the quartz tube heated by the oven. The product was taken out of the receiving flask by dissolving it in methylene chloride. After removal of the methylene chloride, the product mixture was vacuum distilled to afford 2 g (28 % yield) of **49**. The starting material was recovered from the product mixture. In addition, the product mixture contained ~ 10 % o-chloro styrene.

^{1}H NMR (300 MHz, $CDCl_3$) δ 7.43- 7.17 ppm (m, 4H); δ 5.40 ppm (dd, 1H, 1.9 Hz, 4.8 Hz); δ 3.86 ppm (dd, 1H, 4.8 Hz, 14.3 Hz); δ 3.43 ppm (d,1H, 14.3 Hz).

GC/MS: 138 (M^+); 103 (M^+-Cl)

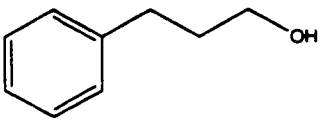

52

A flask containing 0.49 g (0.02 mol, 2eq) magnesium was flame dried. To the flask were added 20 mL dry ether followed by the dropwise addition of 1.25 g benzylchloride (0.01 mol, 1 eq) in 10 mL dry ether. After stirring for one hour, most of the magnesium had dissolved. 5 mL ethylene oxide, dried over soda lime, were introduced to the solution with cannula. The solution was stirred overnight. GC/MS of the crude sample showed the formation of the alcohol **52** in ~ 50 % yield.

GC/MS : 136 (M^+); 117 (M^+-H_3O^+)

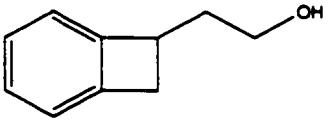

42

Attempted syntheses of 2-Bicyclo[4.2.0]octa-1,3,5-triene-7-yl-ethanol (**42**)

Method 1

All glassware was flame dried prior to use. A round bottom flask was charged with 0.49 g (0.02 mol, 2 eq) magnesium and 20 mL dry ether. A solution of 1.38 g

1-chlorobenzcyclobutene, **49** (0.01 mol, 1 eq) in 10 mL dry ether was added dropwise. The reaction started after the addition of 2 mL 1,2 dibromoethane. The solution was stirred for one and a half hours, when most of the magnesium had dissolved. 3 mL ethyleneoxide were condensed in a graduated cylinder containing 0.5 g soda lime and transferred to the flask with the Grignard reagent by cannula. After stirring the solution for 3 hours, the reaction was quenched by addition of

10 % hydrochloric acid. Ether solution was washed with saturated sodium bicarbonate and brine, and dried over magnesium sulfate. Solvent was removed by rotary evaporation. GC/MS showed no presence of alcohol **42**.

Method 2

130 mL methanol were added to a closed, cooled recirculation system, and argon bubbled through for half an hour. To that were added 0.592 g 3-buthenyl phenyl ether (4 mmol, 1 eq) and 0.04 mL concentrated sulfuric acid (0.8 mmol; 0.2 eq). The solution was irradiated with a 100 W low pressure Hg lamp(Λ= 254 nm). The temperature of the solution was kept between 10 °C and 15 °C. The reaction was monitored by GC/MS. One hour after irradiation GC/MS showed complete disappearance of the starting material, but the complex product mixture did not contain the desired alcohol **42**.

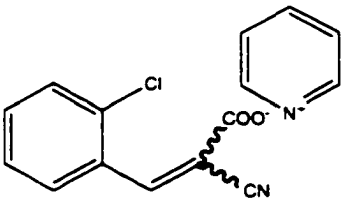

60

3-(2-chloro-phenyl)-2-cyano-acrylic acid pyridine-1-yl ester (**60**)

To the round bottom flask containing 500 mL benzene were added 70.2 g o-chlorobenzaldehyde (0.5 mol, 1 eq), 44.3 g cyanoacetic acid (0.5 mol, 1eq), 4.55 g ammonium acetate (0.06 mol, 0.12 eq) and 100 mL pyridine. The flask was equipped with a Dean-Stark collector and the mixture refluxed until 9 mL of water were collected. The pyridinium salt precipitated from the solution after cooling, and it was used in the next step without further purification.

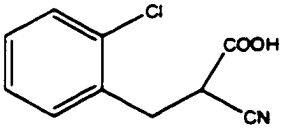

56

3-(2-Chloro-phenyl)-2-cyano-propionic acid (**56**)

The pyridine salt **60** (0.5 mol, 1 eq) was dissolved in ~ 1 L warm saturated solution of sodium bicarbonate. Excess sodium borohydride (57 g, 1.5 eq) was carefully added in small portions, and solution left refluxing overnight. After cooling, the solution was acidified until a pH of 2. The acid was filtered off and air

dried. It was used in the next step without further purification. Yield 81.7 % (85.6 g).

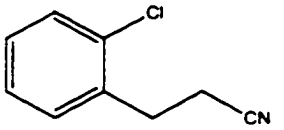

61

3-(2-Chloro-phenyl)-propionitrile (**61**)

Method 1

The acid **56** was dissolved in 250 ml of dry dimethylformamide and refluxed for 2 days. 2-chlorohydrocinnamonitrile was purified by vacuum distillation (b.p 65-67 ° C, at 0.01 mm Hg). Yield 66.4 % (44.7 g, 0.268 mol).

Method 2

Approximately 200 mg of palladium on carbon was added under nitrogen to the stirred solution of 10.5 g of o-chlorocynnamonitrile **63** (0.064mol) in 300 ml ethyl acetate. Absorption of the hydrogen was followed by the volume of the absorbed hydrogen. Theoretical amount of hydrogen, 1.43 L, was absorbed in the course of several days. Product was collected by vacuum distillation, b.p. 102-104°C at 0.3 mm Hg. Yield was 92 %, 9.62 g.

^{1}H NMR (300 MHz, $CDCl_3$): δ 7.41-7.22 ppm (m, 4H); δ 3.10 ppm (t, 2H, 7.3 Hz); δ 2.69 ppm (t, 2H, 7.3 Hz).

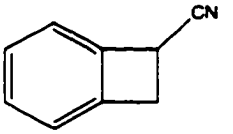

65

Bicyclo[4.2.0]octa-1,3,5-triene-7-carbonitrile (1-cyanobenzcyclobutene) (**65**)

Method 1

To a flask containing 600 ml liquid ammonia 65.5 g 30 % wt. potassium hydride in mineral oil (0.49 mol; 3.5 eq) were added and the mixture stirred until most of the hydride had reacted. 23.24 g of o-chlorodihydrocynnamonitrile (**61**) (0.14 mol; 1eq) in 50 ml THF was added dropwise over 15 minutes. The mixture was stirred for 2 hours,maintaining the temperature at boiling ammonia (-35 °C), and then quenched by careful addition of excess solid ammonium chloride (about 25 g). Ammonia was left to evaporate overnight. 100 ml water were added and the product extracted with methylene chloride. The dichloromethane extracts were washed with 10 % hydrochloric acid and brine solution and dried with magnesium sulfate. After removing the dichloromethane on the rotary evaporator, the product was collected by vacuum distillation, b.p. 90°C-92°C. Yield was 12.33 g (0.095 mol, 67.8%).

Method 2

To a flask containing 300 ml liquid ammonia, 19.5 g (0.5 mol, 5 eq) commercial sodium amide were added. The solution of 16.5 g (0.1 mol, 1 eq) o-chlorodihydrocinnamonitrile (**61**) in 15 mL THF was added over the course of 15 minutes.The mixture was stirred for 3 hours, and the reaction quenched with the addition of solid ammonium nitrate. After overnight stirring, the residue was dissolved in water and product extracted with dichloromethane. The organic layer was washed with 10 % hydrochloric acid and brine. After drying over anhydrous magnesium sulfate, the solvent was removed on a rotary evaporator, and the product isolated by vacuum distillation. Yield 4.33 g (33.6 %).

^{1}H NMR(300 MHz, $CDCl_3$): δ 7.25ppm (m, 4H); δ 4.25 ppm (dd, 1H, 3Hz, 6Hz); δ 3.68 ppm (dd, 1H, 6 Hz, 14 Hz); q 3.55 ppm (dd, 1H, 3Hz, 14 Hz).

^{13}C NMR (75 Mz, $CDCl_3$) δ 142.5 ppm; δ 138.4 ppm; δ 128.8 ppm; δ 127.6 ppm; δ 122.8 ppm; δ 121.8 ppm; δ 119.1 ppm; δ 35.8 ppm; δ 28.4 ppm.

GC/MS: 165 (M^+); 125 (M^+-CH_2CN)

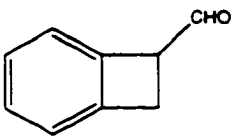

32

Bicyclo[4.2.0]octa-1,3,5,-triene-7-carbaldehyde (**32**)

To a 500 mL flask equipped with a nitrogen inlet, condenser and a rubber septum was added a solution containing 4.68 g (3.6 mmol, 1 eq) nitrile **69** in 200 mL dichloromethane. At 0 °C, 36 mL 1.0 M solution DIBAL in toluene were injected. The solution was refluxed for 2 hours. After cooling the solution in an ice bath, ~ 80 mL 10 % sulfuric acid were added dropwise. The mixture of organic and aqueous layers was transferred to a continuous extraction apparatus. The solution was saturated with sodium chloride and extracted with ether overnight. The organic layer was washed with saturated sodium bicarbonate and brine. Vacuum distillation (b.p. 44 °C , 0.01 mm Hg) afforded 3.98 g (83.7 %).

^{1}H NMR (300 MHz, $CDCl_3$): δ 9.76 ppm (d, 1H, 4Hz); δ 7.3 (m, 4H); δ 4.25 ppm (ddd, 1H, 4 Hz, 3.5 Hz); δ 3.44 (d, 2H, 3.5 Hz).

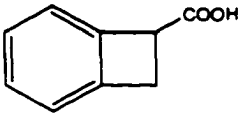

79

Bicyclo[4.2.0]octa-1,3,5-triene-7-carboxylic acid (**79**)

11.2 g potassium hydroxide (0.2 mol ;2 eq) was dissolved in the needed amount of ethanol to obtain a saturated solution (~ 75 ml), and added to 12.9 g 1-cyanobenzcyclobutene **65** (0.1 mol; 1eq). The solution was stirred for 24 hours and refluxed for another 3 hours. The resulting suspension was poured into 500 ml cold water and extracted with ether. Ether layer was discarded. Water layer was acidified with 6M hydrochloric acid and again extracted with ether. The organic layer was dried over magnesium sulfate. After evaporation of the solvent, the residue was dissolved in a minimum amount of warm petroleum ether, and the solution decanted from an insoluble oily residue. Evaporation of petroleum ether gave oil that solidified with standing, m.p. 73-75 °C. Yield 13.82 g (0.093 mol, 93.3 %)

^{1}H NMR (300 MHz, $CDCl_3$): δ 7.2 ppm (m, 4H); δ 4.35 (t, 1H, 4Hz); δ 3.5 ppm (d, 2H, 4Hz).

^{13}C NMR (75 MHz,$CDCl_3$): δ 178.74 ppm; δ 143.86 ppm; δ 141.92 ppm; δ 128.20 ppm; δ 127.29 ppm; δ 122.74 ppm; δ 122.40 ppm; δ 45.68 ppm; δ 33.89 ppm.

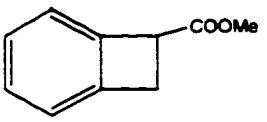

80

Bicyclo[4.2.0]octa-1,3,5-triene-7-carboxylic acid methyl ester (**80**)

In a 500 ml round bottom flask, immersed in an ice-salt mixture, are placed 120 ml dry ether, 16 ml diethylene glycol monoethyl ether and 21 ml 30 % sodium hydroxide. The mixture was cooled to -3 °C , and 6.4 g of N,N'- dimethyl-N,N'-dinitrosoterephthalamide (70% in mineral oil) were added in one portion. The mixture was stirred for 30 minutes, the ice bath replaced by a wter bath and ether distilled until distillate is almost colorless. The ether solution of diazomethane was immediately poured into ice cold ether solution of 2 g benzcyclobutene-1-carboxylic acid. The mixture was stirred for half an hour. Glacial acetic acid was added dropwise until the yellow color of diazomethane disappeared. Ether was washed with a saturated solution of sodium bicarbonate and water and dried over magnesium sulfate.The solvent was removed by rotary evaporation to give 2 g (91.3 %) of the pale yellow ester (**81**).

^{1}H NMR (300 MHz,$CDCl_3$): δ 7.23-7.08 ppm (m, 4H); δ 4.31 ppm (t, 1H, 4Hz); δ 3.73 ppm (s, 3H); δ 3.47 ppm (d, 2H, 4 Hz).

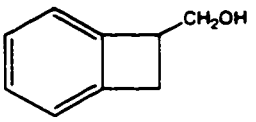

81

Bicyclo[4.2.0]octa-1,3,5-triene-7-yl methanol (**81**)

Under nitrogen, a solution of 13.9 g benzcyclobutene-1-carboxylic acid (0.094 mol; 1 eq) in 100 ml dry ether was added dropwise to a stirred suspension of 7.12 g lithium aluminum hydride (0.188 mol; 2 eq) in 200 ml dry ether. The mixture was stirred overnight. Excess lithium aluminum hydride was destroyed by careful, dropwise addition of saturated sodium sulfate. After the formation of the thick, white precipitate, the solution was filtered, and the precipitate washed with ether.The ether solution was dried over magnesium sulfate. Evaporation of the solvent afforded 11.28 g (89.66%) of alcohol **81**.

^{1}H NMR(300 MHz, $CDCl_3$): δ 7.3 ppm (m, 4H); δ 3.95 ppm (d, 2H, 7Hz); δ 3.8 ppm (m, 1H) δ 3.64 ppm (dd, 1H, 5Hz, 14 Hz) δ 3.05 ppm (dd, 1H, 2Hz, 14 Hz) δ 2.67 ppm (s, 1H).

^{13}C NMR (75 MHz, $CDCl_3$) δ 145.97 ppm; δ 144.12 ppm; δ 127.50 ppm; δ 126.66 ppm; δ 122.92 ppm; δ 122.07 ppm; δ 65.22 ppm; δ 45.25 ppm; δ 33.10 ppm.

GC/MS: M^+ at 134; 133 ($M-H^+$); 103 ($M-CH_3O$)

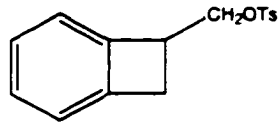

82

Toluene-4-sulfonic acid bicycle[4.2.0]octa-1,3,5-triene-7-yl methyl ester (**82**)

1-Hydroxymethylbenzcyclobutene (1.2 g, 9 mmol, 1 eq) was dissolved in 10 mL dry pyridine and cooled to 0° C in an ice bath. A solution of tosyl chloride (2g, 10 mmol, 1.1 eq) in 10 ml dry pyridine, was added dropwise to the stirred solution of alcohol **81** in pyridine. After 2 hours of stirring , the mixture was poured into 36 mL ice cold 10 % hydrochloric acid and 50 mL ether. The ether layer was washed with sodium bicarbonate and brine and dried over anhydrous magnesium sulfate. The solvent was removed by rotary evaporation. The residue crystallized on standing in the refrigerator, m.p. 73-76 °C .Yield 1.3 g, 64.4 %.

^{1}H NMR (300 MHz, $CDCl_3$) δ 7.79 ppm (d, 2H, 8 Hz); δ 7.77 ppm (d, 2H, 8 Hz); δ 7.2 ppm (m, 2 H); δ 7.03 ppm (m, 2H); δ 4.26 ppm (m, 2H); δ 3.77 (m, 1H); δ 3.3 ppm (dd, 1H, 5 Hz, 14Hz); δ 2.82 ppm (dd, 1H, 14Hz); δ 2.44 ppm (s, 3H).

^{13}C NMR (75 MHz, $CDCl_3$) δ 144.6 ppm; δ 143.9 ppm; δ 143.3 ppm; δ 132.9 ppm; δ 129.7 ppm; δ 128.0 ppm; δ127.7 ppm; δ 126.9 ppm; δ 123.0 ppm; δ 122.3 ppm; δ 72.4 ppm; δ 41.5 ppm; δ 33.5 ppm; δ 21.6 ppm.

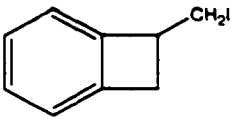

83

7-Iodomethyl-bicyclo[4.2.0]octa-1,3,5-triene (**83**)

Method 1

1.3 g Tosylate **82** (5.8 mmol, 1 eq) were dissolved in 20 mL reagent grade acetone (distilled over calcium chloride). To that solution were added 0.04 mL diisopropylethylamine and a solution of 1.74 g sodium iodide in 20 mL acetone. The solution was stirred for 3 hours at room temperature. Acetone was removed by rotary evaporation and the organic residue dissolved in ether. Ether was washed with sodium thiosulfate, saturated sodium bicarbonate and brine and dried over anhydrous magnesium sulfate. After removal of the solvent, the residue was purified by column chromatography (hexane/ethyl acetate: 4/1) to provide 1.2 g iodide (**83**) (84.4 %).

Method2

To a cold solution of 20.98 g dry triphenyl phosphine (0.08 mol;1.1 eq) and 10.89g imidazole (0.16 mol; 2.2 eq) in 170 ml dichloromethane, 20.32 g of iodine (0.08 mol; 1.1 eq) were added. After 30 minutes of stirring, the solution of 9.76 g alcohol **81** (0.073 mol; 1 eq) in 30 ml dichloromethane was added . The reaction was quenched after 2 hours of stirring by the addition of ether. A precipitate, formed after the addition of ether, was filtered off and washed with ether. Organic extracts were washed with 10 % sodium thiosulfate and brine and dried with

anhydrous magnesium sulfate. The solvent was evaporated on a rotary evaporator. Column chromatography (hexane/ethyl acetate : 3/1) gave 14.15 g of iodide **83** (83%).

^{1}H NMR(300 MHz, $CDCl_3$): δ 7.2 ppm (m, 4H); δ3.87 ppm (m, 1H); δ 3.5 ppm (m, 1H) δ 3.38 ppm (m, 2H) δ 2.82 ppm (dd, 1H, 2Hz, 5Hz).

^{13}C NMR (75 MHz, $CDCl_3$) δ 147.11 ppm; δ 142.10 ppm; δ 127.97 ppm; δ 126.56 ppm; δ 122.82 ppm; δ 121.34 ppm; δ 45.54 ppm; δ 38.31 ppm; δ 9.67 ppm.

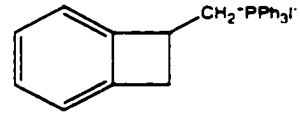

34

Phosphonium salt (**34**)

The solution of 14 g of iodide **83** (0.06; 1 eq) and 17.3 g of triphenylphosphine (0.066 mol; 1.1 eq) in 120 ml toluene was refluxed for three days. The first crop of phosphonium salt was filtered off, washed with toluene and filtrate returned to reflux until all of the iodide has reacted. The yield was 28 g (92.2 %). After recrystalization from dichloromethane/ethyl acetate, melting point was determined to be 198-201°C.

^{1}H NMR (300 MHz, $CDCl_3$) δ 7.65 ppm (m, 15 H); δ 6.95 ppm (t, 1H, 8 Hz); δ 6.83 ppm (t, 1H, 8Hz); δ 6.74 ppm (d, 1H, 8 Hz); δ 6.53 ppm (d, 1H, 8 Hz); δ 4.27 ppm (m, 1H); δ 3.73 ppm (m, 2H); δ 3.03 ppm (dd, 1H, 5 Hz, 14 Hz); δ 2.66 (d, 1H, 14 Hz).

^{13}C NMR (75 MHz, $CDCl_3$): δ 144.82 ppm; δ 144.65 ppm; δ 141.92 ppm; δ 134.81 ppm; δ 133.36 ppm; δ 133.24 ppm; δ 130.23 ppm; δ 130.06 ppm; δ 127.85 ppm; δ 126.69 ppm; δ 122.75 ppm; δ 122.32 ppm; δ 117.87 ppm; δ 116.75 ppm; δ 37.33 ppm; δ 37.23 ppm; δ 35.71 ppm; δ 35.64 ppm; δ 27.78 pm; δ 27.14 ppm.

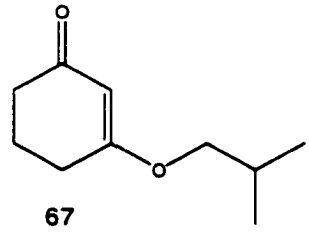

67

3-Isobutoxy-cyclohex-2-enone (**67**)

To a 500 ml round bottom flask equipped with Dean-Stark arm were added 60 g 1,3 cyclohexanedione (0.53 mol) , 90 ml isobutyl alcohol , 1.5 g p-toluenesulfonic acid and 300 ml of benzene. The mixture was refluxed until the right amount of water was collected. The product was purified by vacuum distillation, b.p. 84°C . Yield 81.3 g (91.3%).

^{1}H NMR (300 MHz, $CDCl_3$): δ 5.04 ppm (s, 1H); δ 3.31 ppm (d, 2H, 7Hz); δ 2.13 ppm (t, 2H, 6 Hz); δ 2.03 ppm (t, 2H, 6Hz); δ 1.69 ppm (m, 3H); δ 0.69 ppm (d, 6H, 5 Hz).

^{13}C NMR (75 MHz, $CDCl_3$): δ 198.39 ppm; δ 177.10 ppm; δ 101.86 ppm; δ 73.91 ppm; δ 36.09 ppm; δ 28.34 ppm; δ 27.08 ppm; δ 20.65 ppm; δ 18.42 ppm.

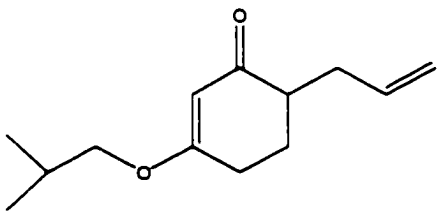

68

6-allyl-3-isobutoxy-cyclohex-2-enone (**68**)

Lithium diisopropyl amide was prepared *in situ*, under nitrogen, by adding 58.8 ml 2.5 M n-buthyllithium (0.147 mol;1eq) to the solution of 14.85 ml diisopropylamine(0.147 mol;1 eq) in 50 ml THF, at -20 °C. After 15 minutes of stirring, the reaction was cooled to -78 °C and the solution of 24.63 g of isobutoxycyclohexanone (0.147;1eq) in 50 ml THF added dropwise in the course of 1 hour. The mixture was stirred for 45 minutes, after which time the solution of 17.79 g freshly distilled allyl bromide (0.147 mol;1 eq) in 50 ml THF was added

over 20 minutes. The mixture was left stirring overnight. 5 mL water were added, the solvent removed on a rotary evaporator, and the product extracted with ether. The ether was washed with 10 % hydrochloric acid, saturated sodium bicarbonate and brine solution, and dried over anhydrous magnesium sulfate. Evaporation of the ether under reduced pressure gave a crystalline product that was recrystalized from ether-acetone at dry ice temperatures, m.p.36-38 °C. Yield 25.96 g (92%).

^{1}H NMR (300 MHz, $CDCl_3$): δ 5.78 ppm (m, 1H); δ 5.32 ppm (s, 1 H); δ 5.05 ppm (m, 1H); δ 3.58 ppm (d, 2H, 6.6 Hz); δ 2.65 ppm (m, 1H); δ 2.41 ppm (m, 2H); δ 2.3-2.0 ppm (m, 4H); δ 1.71 ppm (m, 1H); δ 0.97 ppm (d, 6H, 6.6 Hz).

^{13}C NMR (75 MHz, $CDCl_3$): δ 200.10 ppm; δ 176.88 ppm; δ 136.21 ppm; δ 116.38 ppm; δ 102.08 ppm; δ 74.59 ppm; δ 44.60 ppm; δ 33.99 ppm; δ 28.01 ppm; δ 27.65 ppm; δ 25.76 ppm; δ 19.02 ppm.

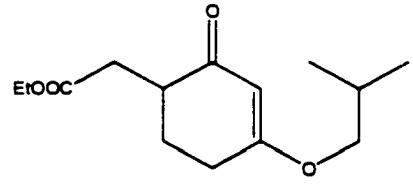

75

(4-Isobutoxy-2-oxo-cyclohex-3-enyl)-acetic acid ethyl ester (**75**)

To a flask equipped with nitrogen inlet, dropping funnel and magnetic stirrer and containing 1.5 g diisopropyl amine (0.015 mol,1.5 eq) in 25 mL THF

were added 8 mL 2.5 M n-butyllithium (0.02 mol, 2 eq) at -20 ° C , and the solution stirred for 15 minutes. After cooling the mixture to – 78 °C, the solution containing 1.68 g isobutoxycyclohexanone (0.01 mol, 1 eq) in 5 mL THF was added dropwise over the course of 10 minutes. After stirring for 45 minutes, the solution of 1.1 mL ethyl bromoacetate in 5 mL THF was added over the course of 5 minutes. The mixture was left stirring overnight. 3 mL water were added and most of the solvent removed by rotary evaporation. Th residue was dissolved in diethyl ether. The ether was washed with 10 % hydrochloric acid and brine, and dried over magnesium sulfate. Evaporation of the solvent afforded 0.92 g (36.2 %) of alkylated product **75**.

^{1}H NMR(300 MHz, $CDCl_3$): δ 5.35 ppm (s, 1H); δ 4.16 ppm (q, 2H, 7 Hz); δ 3.60 ppm (dd, 2H; 2.6 Hz, 6.6 Hz); δ 2.93 (dd, 1H , 5 Hz, 16.5 Hz); δ 2.74 ppm (m, 1H); δ 2.58 ppm (m,1H); δ 2.42 ppm (m, 1H); δ 2.26 ppm (dd, 1H, 8 Hz, 16.5 Hz); δ 2.09 ppm (m, 2H); δ 1.81 ppm (m, 1H); δ 1.27 ppm (t, 3H, 7 Hz); δ 0.97 ppm (d, 6H, 6.6 Hz).

GC/MS: 254 (M^+); 209 (M^+ - C_2H_5O)

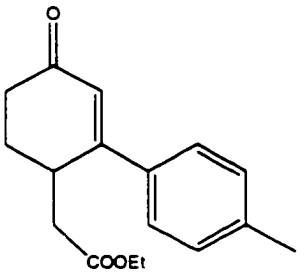

76

(4-Oxo-2-p-tolyl-cyclohex-2-enyl)-acetic acid ethyl ester (**76**)

All the glassware was flame dried prior to use. Round bottom flask was charged with 0.11g magnesium (4.3 mmol, 1.2 eq) in 10 mL THF. A solution containing 0.73 g (4.3 mmol, 1.2 eq) p-Bromotoluene in 10 mL THF was added dropwise until the magnesium started to dissolve. The rate of addition was then adjusted in such a manner so that magnesium dissolves slowly. After all of the magnesium had dissolved, the mixture was cooled in an ice bath to 0°C, and the solution of 0.92 g of **75** (3.6 mmol, 1 eq) in 5 mL THF added dropwise. After two hours of stirring, the mixture was poured into 50 mL 10 % hydrochloric acid and stirring continued for additional one hour. The mixture was transferred to a separatory funnel and 100 mL ether added. The aqueous layer was separated and organic layer washed with saturated sodium bicarbonate and brine. After drying over anhydrous magnesium sulfate, the solvent was removed by rotary evaporation to afford the mixture of unreacted starting material **75** and the product **76**.

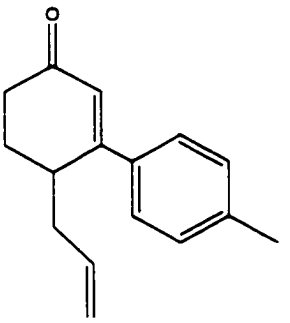

69

4-Allyl-3- p-tolyl-cyclohex-2-enone (**69**)

A flask equipped with a droping funnel, magnetic stirrer, nitrogen inlet and a condenser, and containing 1.2 g of magnesium (0.0495 mol, 1.5 eq) was flame dried before 25 ml THF were added. The solution of 8.46 g p-bromotoluene in 25 ml of THF was added dropwise until magnesium started dissolving. After that, addition was adjusted so that the mixture boils gently. When most of the magnesium had dissolved, the solution of 6.95 g of 6-allyl-3-isobutoxy-cyclohex-2-enone (**69**) in 25 mL THF was added dropwise. The solution was stirred for 2 hours, poured into 100 ml 10 % hydrochloric acid, and stirred for another hour. THF was removed on the rotary evaporator and 200 ml ether added to the residue. Ether was washed with saturated sodium bicarbonate solution, brine and dried over anhydrous magnesium sulfate. Removal of ether under reduced pressure afforded the product **69** in 95 % yield. No further purification has been done before proceeding to the next step.

^{1}H NMR(300 MHz, $CDCl_3$): δ 7.4 ppm (d, 2H, 8.4 Hz); δ 7.22 ppm (d, 2H, 8.4 Hz); δ 6.28 ppm (s, 1H); δ 5.75 ppm (m, 1H); δ 5.09 ppm (d, 1H, 1.5 Hz); δ 5.04 ppm (s, 1H) ; δ 2.05 ppm (m, 1H); δ 2.1 – 2.5 ppm (m, 6H); δ 2.37 ppm (s,3H).

^{13}C NMR (75 MHz, $CDCl_3$): δ 198.74 ppm; δ 162.98 ppm; δ 139.75 ppm; δ 135.75 ppm; δ 135.61 ppm; δ 134.67 ppm; δ 129.17 ppm; δ 126.14 ppm; δ 124.57 ppm ; δ 124.47 ppm; δ 116.65 ppm; δ 35.74 ppm; δ 35.51 ppm; δ 32.46 ppm; δ 25.02 ppm; δ 21.02 ppm.

GC/MS: 226 (M^+); 198 (M^+- C_2H_4)

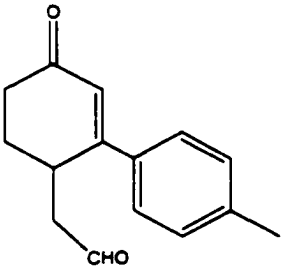

35

(4-Oxo-2-p-tolyl-cyclohex-2-enyl)-acetaldehyde (**35**)

6.78 g (0.03 mol;1eq) of 4-allyl-3-tollyl-2-cyclohexenone **69** were dissolved in the mixture of 150 ml freshly distilled dioxane and 50 ml water. After the addition of 6.15 ml 2.5 wt.% osmium tetroxide in t-butyl alcohol (0.006 mol; 0.2 eq), mixture was stirred until the solution turned black (5-10 minutes). Sodium periodate, (12.84 g, 0.06 mol; 2 eq) was added in small portions, so that the temperature of

the solution stayed between 26 and 28°C. Half an hour after the last portion was added, stirring was stopped and the white precipitate filtered off. The solution was diluted with 300 ml ether, and washed with 30% sodium thiosulfate until the washings were free of precipitate and color. Organic layer was dried with anhydrous magnesium sulfate. Column chromatography (hexane/ethyl acetate: 2/1) gave the aldehyde in 62 % yield. Note that with the modification in the procedure, by adding aqueous solution of sodium periodate over the course of 10 hours, the yield was significantly improved -78 %.

^{1}H NMR (300 MHz, $CDCl_3$): δ 9.68 ppm (s, 1H); δ 7.34 ppm (d, 2H, 8 Hz); δ 7.17 ppm (d, 2H, 8 Hz); δ 6.27 ppm (s, 1H); δ 3.66 ppm (m, 1 H); δ 2.71 ppm (dd, 1H, 9.9 Hz, 18 Hz); δ 2.49-2.39 ppm (m, 4 H); δ 2.33 ppm (s, 3H); δ 2.27-2.23 ppm (m, 2 H); δ 2.02 ppm (m, 1H).

^{13}C NMR (75 MHz, $CDCl_3$): δ 199.50 ppm; δ 198.25 ppm; δ 161.59 ppm; δ 140.19 ppm; δ 133.83 ppm; δ 129.35 ppm; δ 126.18 ppm; δ 125.29 ppm; δ 44.82 ppm; δ 32.48 ppm; δ 29.78 ppm; δ 25.99 ppm; δ 21.02 ppm.

GC/MS: 228 (M^+); 186 (M^+-C_2H_2O)

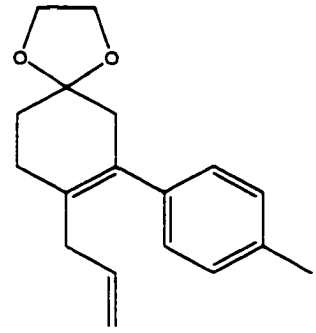

70

8-Allyl-7-p-tolyl-1,4-dioxa-spiro[4.5]dec-7-ene (**70**)

A round bottom flask was equipped with Dean Stark arm and charged with 7.9 g allyl ketone **69** (0.035 mol, 1 eq), 6.2 g distilled ethylene glycol (0.1 mol, 2.8 eq) , 50 mg p-toluene sulfonic acid and 100 ml benzene. The solution was refluxed until required amount of water was collected (0.6 ml). After removal of benzene, organic residue was dissolved in ether, washed with saturated sodium bicarbonate followed by brine and dried over magnesium sulfate. After the solvent was removed under reduced pressure, protected allyl compound **70** was purified by column chromatography (hexane/ ethyl acetate: 4/1) to afford 7.29 g (0.027 mol, 77.1%).

^{1}H NMR (300 MHz, $CDCl_3$) δ 7.10 ppm (d, 2 H, 8 Hz); δ 7.05 ppm (d, 2H, 8 Hz); δ 5.70 ppm (m, 1 H); δ 5.10 ppm (d, 1H, 1.5 Hz); δ 5.08 ppm (m, 1H); δ 3.99 ppm (s, 4H); δ 2.67 ppm (d, 2H, 6Hz); δ 2.50 ppm (s, 2H); δ 2.32 ppm (m, 4H); δ 1.83 ppm (t, 2H, 6 Hz).

^{13}C NMR (75 MHz, $CDCl_3$): δ 139.36 ppm; δ 136.55 ppm; δ 135.46 ppm; δ 131.22 ppm; δ 129.60 ppm; δ 128.42 ppm; δ 127.64 ppm; δ 115. 08 ppm; δ 107.82 ppm; δ 64.07 ppm; δ 41.86 ppm; δ 37.89 ppm; δ 31.09 ppm; δ 27.77 ppm; δ 20.89 ppm.

GC/MS: 270 (M^+); 169 (M^+-101)

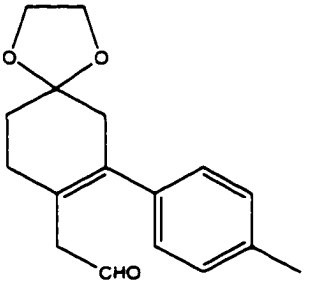

71

(7-p-tolyl-1,4-dioxa-spiro[4.5]dec-7-en-8-yl)-acetaldehyde (**71**)

To the solution of 2.7 g protected allyl compound **70** (10 mmol, 1 eq) in 50 mL freshly distilled dioxane and 15 mL water, 2.05 mL 2.5 wt% osmium tetroxide in tert-butanol (0.2 mmol, 0.02 eq) were added and the mixture stirred for 10 minutes during which time the mixture became dark brown. Maintaining the temperature of the solution at 26-28 °C, 4.28 g (20 mmol, 2 eq) of sodium periodate were added in small portions over period of one hour. Soon after the last portion of sodium periodate was added, solution became pale yellow. Stirring was continued for another hour, after which time, precipitate was filtered off and washed with ether. The solution was diluted with 300 ml ether, and ether layer

washed with 10 % sodium sulfide heptahydrate until washings were free of any color or precipitation. After subsequent washing three times with brine, ether was dried with magnesium sulfate and afterwards removed *in vacuo*. Column chromatography (hexane/ethyl acetate: 3/1) afforded pure aldehyde **71** in 73.5 % yield (2 g).

^{1}H NMR (300 MHz, $CDCl_3$): δ 9.46 ppm (t, 1H, 1.8 Hz); δ 7.03 ppm (d, 2H, 7.7 Hz); δ 6.91 ppm (d, 2H, 7.7 Hz); δ 3.90 ppm (s, 4H); δ 2.95 ppm (s, 2H); δ 2.46 ppm (broad, 2 H); δ 2.24 ppm (m,6H); δ 1.78 ppm (t, 2H, 6.6 Hz);

^{13}C NMR (75 MHz, $CDCl_3$) δ 199.93 ppm ; δ 138.74 ppm ; δ 136.74 ppm ; δ 135.71 ppm; δ 128.99 ppm ; δ 127.76 ppm ; δ 123. 81 ppm; δ 107.63 ppm; δ 82.02 ppm ; δ 64.55 ppm; δ 48.88 ppm; δ 42.18 ppm; δ 31.09 ppm; δ 29.34 ppm; δ 21.10 ppm.

GC/MS: 272 (M^+)

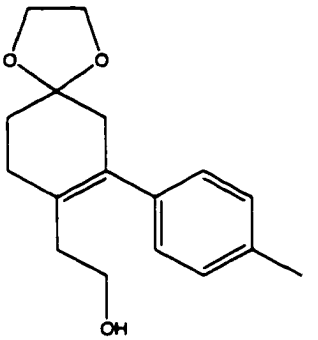

72

2-(7-p-Tolyl-1,4-dioxa-spiro[4.5]dec-7-en-8-yl)-ethanol (**72**)

2g (0.0073 mol, 1 eq) of aldehyde **71** were dissolved in 10 ml methanol. To that was added a slurry of 0.82 g (0021 mol, 3 eq) sodium borohydride in 5 ml methanol. The solution was stirred for 2 hours before it was quenched with water. Alcohol **72** was extracted three times with 20 mL methylene chloride and dried with anhydrous sodium sulfate. Evaporation of solvent by rotary evaporation provided 1.76g alcohol **72** (88.6 % yield).

^{1}H NMR (300 MHz, $CDCl_3$): δ 7. 08 ppm (d, 2H, 8 Hz); δ 6.99 ppm (d, 2H, 8 Hz); δ 3.92 ppm (s, 4H); δ 3.54 ppm (t, 2H, 7 Hz); δ 2.43 ppm (s, 2H); δ 2.29 ppm (m, 5 H); δ 2.19 ppm (broad t, 3 H, 7 Hz); δ 1.81 ppm (t, 2H, 7 Hz).

^{13}C NMR(75 MHz, $CDCl_3$): δ 139.53 ppm; δ 135.76 ppm; δ 132.99 ppm; δ 128.78 ppm; δ 128.43 ppm; δ 128.02 ppm; δ 107.95 ppm; δ 64.26 ppm; δ 60.95 ppm; δ 42.30 ppm; δ 36.84 ppm; δ 31.19 ppm; δ 28.30 ppm; δ 21.07 ppm.

GC/MS: 274 (M^+); 244 (M^+-CH_2O)

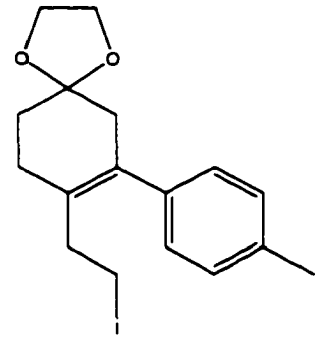

73

8-(2-Iodo-ethyl)-7-p-tolyl-1,4-dioxa-spiro[4.5]dec-7-ene (**73**)

Triphenylphosphine (1.86g, 0.0071 mol, 1.1 eq) and imidazole (0.97 g, 0.014 mol, 2.2 eq) were dissolved in 20 mL dichloromethane. The solution was cooled in an ice bath before 1.8g iodine (0.071 mol, 1.1 eq) were added. After stirring for 30 minutes, to the mixture was added a solution of 1.76 g (0.0065 mol, 1 eq) alcohol **72** in 10 mL dichloromethane. The mixture was stirred for 1.5 hours after which time 60 mL ether was added. The precipitate was filtered off and washed with ether. The filtrate was washed with 10 % sodium thiosulfate, 10 % hydrochloric acid, and brine and dried over anhydrous magnesium sulfate. After the evaporation of the solvent on a rotary evaporator, residue was purified by column chromatography (hexane/ethyl acetate: 3/1,) to afford iodide **73** in 72.3 % yield (1.78 g).

^{1} H NMR (300 MHz, $CDCl_3$): δ 7.16 ppm (d, 2H, 8 Hz); δ 7.04 ppm (d, 2H, 8Hz); δ 4.00 ppm (s, 4H); δ 3.12 ppm (t, 2H, 8Hz); δ 2.54 (t, 2H, 8 Hz); δ 2.47 ppm (s, 2H); δ 2.38 ppm (m, 2 H); δ 2.36 ppm (s, 3H); δ 1.87 ppm (t, 2H, 7 Hz).

^{13}C NMR (75 MHz, $CDCl_3$) δ 139.02 ppm; δ 135.98 ppm; δ 133.17 ppm; δ 130.80 ppm; δ 128.86 ppm; δ 127.66 ppm; δ 107.62 ppm; δ 64.30 ppm; δ 42.34 ppm; δ 37.71 ppm; δ 31.16 ppm; δ 27.51 ppm; δ 21.14 ppm; δ 3.83 ppm.

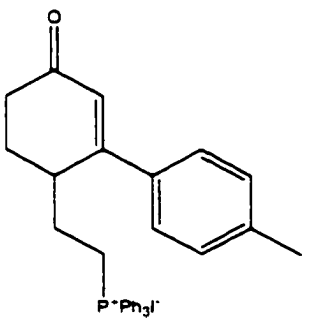

74

Method 1.

1.7 g iodide **73** (0.0044 mol, 1 eq) and 1.31 g triphenylphosphine (0.005 mol, 1.1 eq) were dissolved in 50 mL DMF. The solution was gently refluxed overnight. After cooling the solution to room temperature, 200 mL ether was added to precipitate phosphonium salt. Removal of the solvent, afforded phosphonium salt **74** as a viscous liquid in 48.6 % yield (1.3 g).

Method 2.

1.2 g (0.003 mol, 1 eq) iodide **73** were dissolved in 50 mL toluene. To the solution were added 0.84 g triphenylphosphine (0.0037 mol, 1.2 eq). After reflux for 48 hours, toluene was decanted, phosphonium salt **74** in the form of viscous liquid washed with toluene twice. Toluene was completely removed on a vacuum pump. Yield was 51 % (0.95 g).

^{1}H NMR (300 MHz, $CDCl_3$): δ 7.71-7.18 ppm (m, 15 H); δ 6.10 ppm (s, 1H); δ 3.98 (m, 3H); δ 3.65 (m, 3H); δ 2.28 ppm (m, 5H); δ 1.69 ppm (m, 2H).

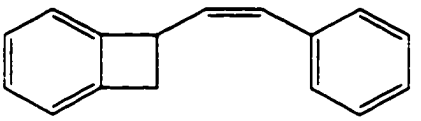

85

7-Styryl-bicyclo[4.2.0]octa-1,3,5-triene (**85**)

Phosphonium salt was dried on a vacuum pump (0.02 mm Hg) at 50 °C for one hour prior to use. To a flask containing suspension of 260 mg phosphonium salt **34** (0.5 mmol, 1.1 eq) in 5 mL dry toluene, at -10 °C were added 60 mg freshly sublimed potassium tert-butoxide (0.5 mmol, 1 eq). The mixture was stirred for one hour before the solution of 50 mg benzaldehyde (0.47 mmol, 1 eq) in 5 mL dry toluene was added. The solution was stirred for 3 hours, after which time it was quenched with water. Most of the solvent was removed on a rotary evaporator and residue diluted with ether. Ether solution was washed with 10 %

hydrochloric acid and brine and dried with anhydrous magnesium sulfate. Ether was removed *in vacuo*. Column chromatography (hexane/ethyl acetate : 8:1) yielded 35 mg Wittig product **85**(52.2 %).

^{1}H NMR (300 MHz,$CDCl_3$) : δ 7.41-7.05 ppm (m,8H); δ 6.52 ppm (d, 1H); δ 5.90 ppm (t, 1H); δ 4.62 ppm (m, 1 H); δ 3.56 ppm (dd, 1H); δ 3.03 ppm (dd, 1H).

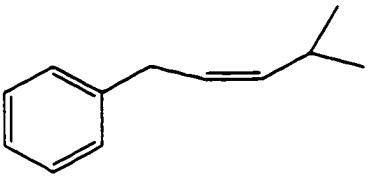

88

(4-Methyl-pent-2-enyl)-benzene (**88**)

Isobutylphoshphoniumiodide (2.67 g, 6 mmol, 1.2 eq) was ground with 0.82 g anhydrous, oven dried potassium carbonate (6 mmol, 1.2 eq) and transferred to a 100 mL round bottom flask. 50 mL dry THF was added, followed by the addition of 0.5 mL phenylacetaldehyde (5 mmol, 1 eq) and 15 mg 18 crown ether. The mixture was refluxed overnight. GC/MS showed Wittig product **88** in ~ 65 % yield.

GC/MS: 160(M^+); 104 (M^+-C_4H_8)

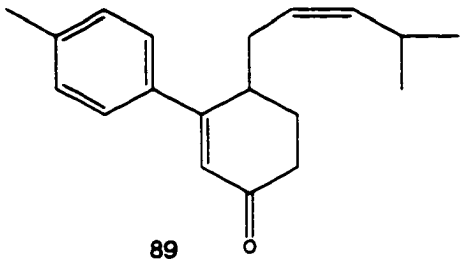

89

4-(4-Methyl-pent-2-enyl)-3-p-tolyl-cyclohex-2-enone (**89**)

Isobutylphosphoniumiodide (0.446 g, 1 mmol, 1.2 eq) was ground with anhydrous, oven dried potassium carbonate (0.138 g, 1 mmol, 1.2 eq) and basic alumina and transferred to a round bottom flask. 10 mL THF were added to the flask followed by the solution of 190 mg aldehyde **35** (0.83 mmol, 1 eq) in 2 mL THF and 3 mg crown ether. After reflux overnight, the mixture was cooled to room temperature, precipitate filtered off. GC/MS of the crude product showed Wittig product in ~77 % yield.

GC/MS: 244(M^+).

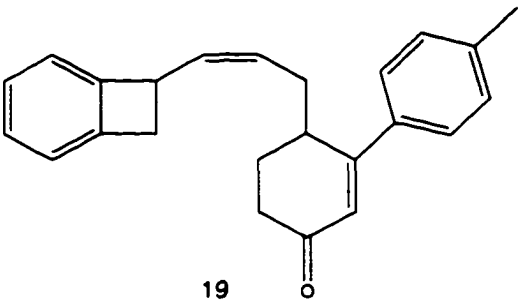

19

4-(3-Bicyclo[4.2.0]octa-1,3,5-trien-7-yl—allyl)-3-p-tolyl-cyclohex-2-enone (**19**)

Phosphonium salt **34**, 18.2 g (0.036; 1.2 eq) and 4.97 g oven dried anhydrous potassium carbonate (0.036 mol; 1.2 eq) were ground together before added to 500 ml flask containing 180 ml THF. To that was added 7 g aldehyde **35** (0.03 mol; 1 eq) in 25 ml THF and 90 mg 18-crown ether. After the reflux of 43 hours, mixture was filtered, solid washed with ether and solvent evaporated *in vacuo*. Column chromatography (hexane/ethyl acetate : 3/1,) afforded 6.65 g (66.8%) of the cis/trans mixture in the ratio of 11/1 as judged by the ^{1}H NMR.

^{1}H NMR (300 MHz, $CDCl_3$): δ 7.44 ppm (d, 1 H, 2Hz); δ 7.41 ppm (d, 1H, 2 Hz); δ 7.18 ppm (m, 4H); δ 7.05 ppm (d, 1H, 2 Hz); δ 6.93 ppm (d, 1H, 2Hz); δ 6.30 ppm (s, 1H); δ 5.66 ppm (td, 1H, 8 Hz, 1 Hz); δ 5.49 ppm (m, 1H); δ 4.22 ppm (dd, 1 H, 3 Hz, 6 Hz); δ 3.44 ppm (m, 1H); δ 3.06 ppm (m, 1H); δ 2. 85 ppm (d, 1H, 14 Hz); δ 2.58 ppm (m,1H) ; δ 2.46 (m, 3H); δ 2.37 ppm (s, 3H); δ 2.23 ppm (m, 2H).

^{13} C NMR (75 MHz, $CDCl_3$): δ 199.06 ppm; δ 163.31 ppm; δ 148.04 ppm; δ 143.64 ppm; δ 140.07 ppm; δ 134.89 ppm; δ 133.32 ppm; δ 129.42 ppm; δ

129.33 ppm; δ 127.44 ppm; δ 127.36 ppm; δ 127.28 ppm; δ 126.88 ppm; δ 126.37 ppm; δ 124.81 ppm; δ 122.74 ppm; δ 121.73 ppm; δ 40.62 ppm; δ 37.64 ppm; δ 37.58 ppm; δ 36.46 ppm; δ 36.42 ppm; δ 32.92 ppm; δ 29.76 ppm; δ 25.42 ppm; δ 21.25 ppm.

IR (neat,cm-1): 3063 (w), 3023 (w), 3008 (w), 2923 (s), 1714 (m),1665 (s,b), 1599 (s)' 1512 (m), 1453(s), 740 (s), 665 (w).

GC/MS: 328 (M^+)

Attempted Wittig syntheses

Method 1.

Phosphonium salt **74** (1.13 g, 1.8 mmol, 1.2 eq) and aldehyde **32** (0.19 g, 1.5 mmol, 1 eq) were dissolved in 10 mL freshly distilled DMF. To the stirred solution was dropwise added a solution of lithium ethoxide prepared *in situ* from 0.016 g Li (2.2 mmol, 1.4 eq) in 2 mL absolute ethanol. Red solution was stirred for 4 hours. Reaction was quenched with the addition of water. Product was extracted with ether and ether solution washed with 10 % hydrochloric acid and brine and dried over anhydrous magnesium sulfate. Product mixture did not contain the desired Wittig product **19**.

Method 2.

400 mg phosphonium salt **34** (0.8 mmol, 1.1 eq) were suspended in 10 ml THF, and solution cooled to – 40 °C. At that temperature, 90 mg freshly sublimed potassium tert-butoxide (0.8 mmol, 1.1 eq) were added and the mixture stirred for one hour. A solution of 164 mg aldehyde **35** (0.72 mmol, 1 eq) in 5 mL THF was dropwise added to the orange solution of the ylide, and mixture slowly warmed to room temperature. After 2 hours thin layer chromatography showed complete disappearance of aldehyde **35**. Water was added, and most of the solvent removed by rotary evaporation. The residue was dissolved in ether, and ether washed with 10 % hydrochloric acid and brine. After drying over magnesium sulfate, solvent was removed and residue purified by column chromatography (hexane/ ethyl acetate :3/1). The yield was very low ,10 % (23 mg).

Method 3

To the mixture of 1.86 g phosphonium salt **34** (3 mmol, 1.4 eq) in 10 mL dry toluene was added at room temperature 6 mL 0.5 M potassium bis (trimethylsilyl) amide in toluene. After stirring for 15 minutes, mixture was cooled to – 78 °C . The solution of 0.46 g aldehyde **35** in 3 mL toluene was added dropwise to the ylide mixture. The solution was slowly warmed to room temperature, and 5 mL water added to quench the reaction. Usual work –up, followed by column chromatography (hexane/ethylacetate : 3/1) afforded only 6 % (60 mg) of the Wittig product .

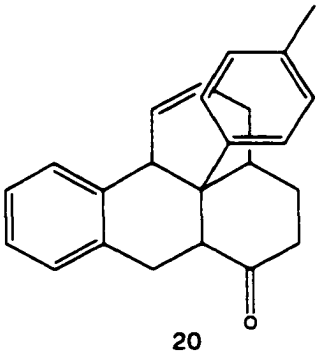

20

11c-p-Tolyl-3,3a,4,5,6a,7,11b,11c-octahydro-benzo[de]anthracen-6-one (**20**)

1L flask was charged with 6 g (0.018 mol) of ketone and 800 ml o-dichlorobenzene. After 19 hours of reflux, o-dichlorobenzene was removed by vacuum distillation and the residue purified by column chromatography (hexane/ethyl acetate : 3/1) to afford 3.2 g (53.3%) white crystals, m.p. 135-137 °C.

^{1}H NMR (300 MHz, $CDCl_3$): δ 7.47 ppm (d, 1 H, 7.7Hz); δ 7.16 ppm (m, 3H); δ 7.05 ppm (t, 1H, 7.7 Hz); δ 6.92 ppm (m, 3 H); δ 6.52 ppm (dd, 1H, 2.2 Hz, 10.25 Hz); δ 5.67 ppm (m, 1H); δ 3.62 ppm (s, 1H); δ 3.24 ppm (d, 1H, 17.2 Hz); δ 3.12 ppm (d, 1H, 6 Hz); δ 2.64 ppm (m, 4 H); δ 2.21 ppm (m, 4 H); δ 2.06 ppm (m, 2H); δ 1.79 ppm (broad s, 2H).

^{13} C NMR (75 MHz, $CDCl_3$): δ 209.38 ppm; δ 139.16 ppm; δ 135.77 ppm; δ 134.91 ppm; δ 134.04 ppm; δ 128.94 ppm; δ 127.90 ppm; δ 126.96 ppm; δ 126. 34 ppm; δ 125.48 ppm; δ 125.29 ppm; δ 123.94 ppm; δ 122.87 ppm; δ 53. 95

ppm; δ 47.90 ppm; δ 40.81 ppm; δ 40.12 ppm; δ 35.65 ppm; δ 29.36 ppm; δ 29.03 ppm; δ 25.16 ppm; δ 20.70 ppm.

IR (KBr,cm^{-1}) : 3029 (w), 2926 (w), 2983 (m), 2827 (w), 2812 (w), 1705 (s,b), 1516 (w), 1492 (m),1450 (m), 1426(m), 1416 (m), 728 (s), 718 (s), 675 (m).

UV : 345 nm (max)

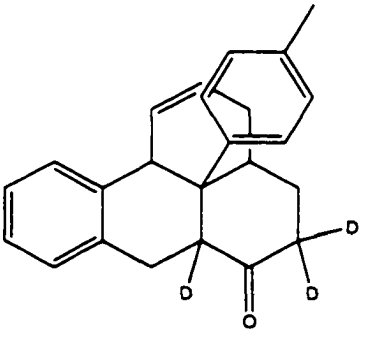

92

Ketone 20 D_3 (**92**)

To a flask containing 15 mL deuterated ethanol, sliver of sodium (~ 70 mg) was added. After complete dissolution of sodium, 20 mL D_2O were added. 50 mg ketone **20** were added to the solution, and mixture heated to dissolve ketone (a few milliliters deuterated benzene were added to help the dissolution). After overnight stirring, deuterated ketone **92** was extracted with ether. Ether was removed on a rotary evaporator.

^1H NMR (300 MHz, $CDCl_3$): δ 7.39 ppm (d, 1H, 7.7 Hz); δ 7.06 ppm (m, 4H); δ 6.87 ppm (m, 3H); δ 6.44 ppm (dd, 1H, 1.8 Hz, 10.25 Hz); δ 5.57 ppm (m, 1H); δ

3.54 ppm (s, 1H); δ 3.15 ppm (d, 1H, 17.2 Hz); δ 2.57 ppm (m, 1H); δ 2.14 ppm (m, 4H); δ 1.97 ppm (d, 2 H, 8.4 Hz); δ 1.70 ppm (broad, 2H,).

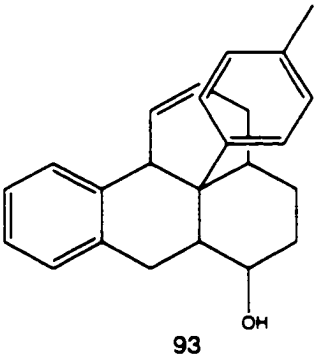

93

11c-p-Tolyl-3,3a,4,5,6,6a,7,11b,11c-octahydro-benzo[de]anthracen-6-ol (**93**)

Method 1

Ketone **20** (1.64g, 0.005 mol, 1 eq) was dissolved in the mixture of 50 ml THF and 50 ml absolute ethanol. Excess sodium borohydride (0.57 g, 0.015 mol, 3 eq) was added to the solution as a slurry in 5 ml ethanol. The solution was stirred for 2 hours.The reaction was quenched with the addition of 10 % hydrochloric acid. The alcohol **93** was extracted with ether and ether solution dried with anhydrous magnesium sulfate. After removal of ether by rotary evaporation, residue was purified by column chromatography (hexane:ethyl acetate/ 3:1) to provide 780 mg (47.3 % yield) of alcohol **93**.

Method 2

A two neck flask, equipped with addition funnel and nitrogen inlet, was charged with 20 mL dry ether and cooled in an ice bath. Under nitrogen, 106 mg (2.8 mmol, 2 eq) lithium aluminum hydride were added, followed by a dropwise addition of the solution containing 470 mg (1.4 mmol, 1 eq) ketone **20** in 10 mL ether. The mixture was stirred for 1.5 hours. After careful addition of saturated sodium sulfate, ether layer was drawn off and white precipitate washed twice with 10 ml ether. Ether solution was dried over anhydrous magnesium sulfate. After removal of the solvent under reduced pressure, residue was subjected to column chromatography (hexane:ethyl acetate/ 3:1) to afford 410 mg alcohol **93** (86.7 % yield).

^{1}H NMR (300 MHz, $CDCl_3$): δ 7.61 ppm (d, 1H, 7.7 Hz); δ 7.24 ppm (t, 1H, 7.3 Hz); δ 7.13 ppm (broad, 2H); δ 7.07 ppm (t, 1H, 7.3 Hz); δ 6.93 ppm (m, 3H); δ 6.60 (d, 1H, 10.25 Hz); δ 5.60 ppm (m, 1H); δ 4.92 (broad, 1H); δ 4.23 ppm (d, 1H, 3 Hz); δ 2.70 ppm (dd, 1H, 7.7 Hz, 17.9 Hz); δ 2.55 ppm (d, 1H, 17.9 Hz); δ 2.24 ppm (m, 4H); δ 2.08 ppm (m, 2H); δ 1.93 ppm (m, 4H)

^{13}C NMR (75 MHz, $CDCl_3$): δ 141.49 ppm; δ 139.667 ppm; δ 134.87 ppm; δ 134.48 ppm; δ 128.73 ppm; δ 127.77 ppm; δ 127.39ppm; δ 125.83 ppm; δ 125.57 ppm; δ 125.31 ppm; δ 124.76 ppm; δ 123.33 ppm; δ 72. 47 ppm; δ 44.90 ppm; δ 44.69 ppm; δ 42.35 ppm; δ 35.89 ppm; δ 33.41 ppm; δ 31.06 ppm; δ 30.39 ppm; δ 24.57 ppm; δ 20.83 ppm.

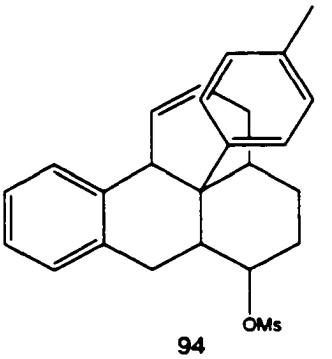

94

Methane sulfonic acid 11c-p-tolyl-3,3a,4,5,6,6a,7,11b,11c-octahydro-benzo[de]anthracen-6-yl ester (**94**)

Alcohol **93** (100 mg, 0.3 mmol, 1 eq) was dissolved in 5 ml dry ether. At 0° C, to the solution was dropwise added freshly distilled triethylamine (0.209 ml, 1.5 mmol, 5 eq) followed by a slow addition of mesyl chloride (0.07 ml, 0.9 mmol, 3 eq). After 4 hours of stirring at room temperature, solution was diluted with 20 ml of ether. Ether solution was washed with saturated sodium bicarbonate and brine and dried with anhydrous magnesium sulfate. The final residue (100 mg, 81.3 % yield) was used without further purification (m.p. 75-77 °C)

^{1}H NMR (300 MHz, $CDCl_3$): δ 7.57 ppm (d, 1H, 7 Hz); δ 7.20 ppm (t, 1H, 6 Hz); δ 7.04 ppm (m, 3H); δ 6.91 ppm (m, 3H); δ 6.55 ppm (dd, 1H, 2Hz, 6 Hz); δ 5.85 ppm (m, 1H); δ 5. 28 (d, 1H, 3Hz); δ 4.41 ppm (broad s,1H); δ 2.62 ppm (broad s, 2 H); δ 2.36 ppm (m, 4H); δ 2.23 ppm (s, 4H); δ 2.03 ppm (m, 2H); δ 1.85- 1.61 ppm (m, 2H)

^{13}C NMR (75 MHz, $CDCl_3$): δ 140.32 ppm; δ 138.46 ppm; δ 135.05 ppm; δ 134.88 ppm; δ 128.64 ppm; δ 125.72 ppm; δ 125.58 ppm; δ 125.47 ppm; δ 124.88 ppm; δ 123.15 ppm; δ 81.14 ppm; δ 44.28 ppm; δ 44.23 ppm; δ 41.19 ppm; δ 37.59 ppm; δ 34.86 ppm; δ 32.14 ppm; δ 30.51 ppm; δ 30.26 ppm; δ 24.59 ppm; δ 20.91 ppm.

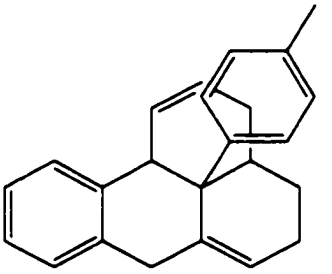

95

11c-p-Tolyl-3,3a,4,5,7,11b,11c-hexahydro-benzo[de]anthracene (**95**)

Method 1

Mesylate **94** (100 mg, 0.24 mmol) was treated with 1 g of neutral alumina, activity I. To that was added minimum amount of methylene chloride (3 ml). The suspension was stirred for 2 days. The alumina was filtered off and washed thoroughly with methylene chloride. The solvent was removed under reduced pressure and residue purified by column chromatography (hexane/ethyl acetate :4/1) to provide 60 mg diene **95** (78.6 % yield)

Method 2.

Alcohol **93** (410 mg, 1.2 mmol) was dissolved in 12.5 g HMPA and the solution gently refluxed for 2 hours. After cooling to room temperature, the solution was diluted with water and diene extracted with ether. Ether solution was washed with 10 % hydrochloric acid and brine and dried over anhydrous magnesium sulfate. The solvent was removed by rotary evaporation. Column chromatography (hexane/ethyl acetate : 4/1) afforded 306 mg diene **95** (78.9 %) yield.

^{1}H NMR (300 MHz, $CDCl_3$): δ 7.52 ppm (d, 1 H, 7.7 Hz); δ 7.1 ppm (m, 4 H); δ 6.86 ppm (m, 3H); δ 6.57 (d, 1H, 10.25 Hz); δ 5.87 ppm (m, 1H); δ 5.69 ppm (d, 1 H, 6.2 Hz); δ 4.18 ppm (s, 1 H); δ 3.34 (d, 1H, 17.9 Hz);δ 3.24 ppm (d,1H,17.7); δ 2.38 ppm (m, 1H); δ 2.25 (m, 2 H); δ 2.22 ppm (s, 3H); δ 2.08 (m, 1H); δ 1.87 ppm (m, 2 H); δ 1.67 ppm (m, 1H);

^{13}C NMR (75 MHz, $CDCl_3$): δ 141.88 ppm; δ 140.96 ppm; δ 138.72 ppm; δ 135.97 ppm; δ 134.44 ppm; δ 128.53 ppm; δ 128.48 ppm; δ 127.80 ppm; δ 127.64 ppm; δ 127.53 ppm; δ 125.42 ppm; δ 125.34 ppm; δ 123.69 ppm; δ 123.66 ppm; δ 119.57 ppm; δ 47.49 ppm; δ 42.78 ppm; δ 41.69 ppm; δ 37.64 ppm; δ 29.78 ppm; δ 27.58 ppm; δ 25.99 ppm; δ 20.95 ppm.

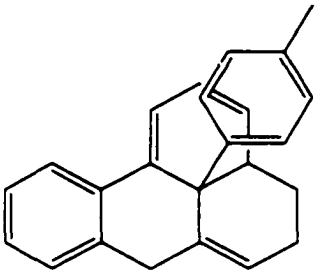

97

11c-p-Tolyl-3a,5,7,11c-tetrahydro-4H-benzo[de]anthracene (**97**)

To the solution of 50 mg diene **95** (0.16 mmol, 1 eq) in 15 ml benzene, 73.6 mg DDQ were added. The orange solution was stirred overnight at room temperature. The reaction was quenched by the addition of sodium sulfite and ether. Ether layer was washed two times with 10 mL saturated sodium sulfite solution and brine and dried over anhydrous magnesium sulfate. After filtration of the drying agent, the solvent was removed by rotary evaporation. Column chromatography (hexane/ethyl acetate: 6/1) had to be done twice to afford 10 mg pure triene **97** (yield 20.1 %).

^{1}H NMR (300 MHz, $CDCl_3$): δ 7.85 ppm (dd, 1H, 7 Hz, 0.7 Hz); δ 7.23 – 6.88 ppm (m, 8 H); δ 6.06 ppm (dd, 1H, 5.8 Hz, 9.2 Hz); δ 5.98 ppm (m, 1 H); δ 5.67 ppm (dd, 1H, 5.8 Hz, 9.15 Hz); δ 3.20 ppm (dd, 1H, 1 Hz; 17.6 Hz); δ 3.07 ppm (d, 1H, 17.6 Hz); δ 2.62 ppm (m, 1H); δ 2.16 ppm (s, 3H); δ 2.10 ppm (m, 1H); δ 1.96 (m, 1H); δ 1.65 ppm (m, 1H).

GC/MS: 310 (M^+); 295 (M^+-CH_3);

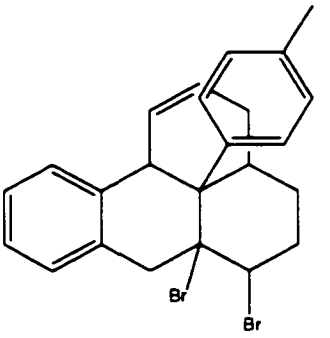

100

6,6a-Dibromo-11c-p-tolyl-3a,4,5,6,6a,7,11b,11c-octahydro-3H-benzo[de]anthracene (**100**)

To the solution of 40 mg diene **95** (0.13 mmol, 1 eq) in 8 mL dichloromethane were added 98 mg pyridinium perbromide (0.3 mmol, 2.4 eq) and 0.05 mL pyridine.The mixture was stirred for 1.5 hours. To the mixture were added 15 mL 10 % solution sodium thiosulfate. The solution was transferred to the separatory funnel and diluted with 20 mL of ether. Ether layer was washed with 10 % hydrochloric acid, saturated sodium bicarbonate and brine, and dried over anhydrous magnesium sulfate. Evaporation of the solvent by rotary evaporation afforded 57.8 mg dibromide **100** as white powder (95.5 %). Dibromide(**100**) was used in the next step without further purification.

^{1}H NMR (300 MHz, $CDCl_3$): δ 7. 49 ppm (d, 1 H, 7.7 Hz); δ 7.30 ppm (m, 3 H); δ 7.19 ppm (t, 1H, 7.7 Hz); δ 7.01 ppm (d, 1H, 7 Hz); δ 6.88 ppm (m, 2 H); δ 6.28 ppm (dd, 1 H, 2 Hz, 10.25 Hz); δ 5.46 ppm (m, 1H); δ 5.26 ppm (m, 1H); δ 5.02 ppm (broad s, 1H); δ 3.65 ppm (d, 1 H, 17.2 HZ); δ 4.5 ppm (d, 1H, 17.2 Hz); δ 3.14 ppm (m, 1H); δ 2.28 ppm (m, 2 H); δ 2.24 ppm (s, 3H); δ 1.88 ppm (m, 2H).

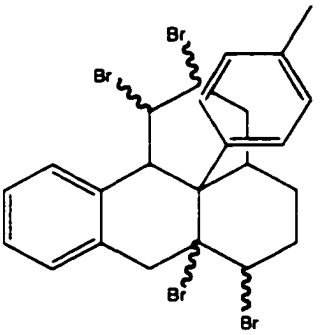

101

1,2,6,6a-Tetrabromo-11c-p-tolyl-2,3,3a,4,5,6,6a,7,11b,11c-decahydro-1H-benzo[de]anthracene (**101**)

To the solution of 50 mg diene **95** (0.16 mmol, 1 eq) in 10 mL dichloromethane were added 123 mg pyridinium perbromide (0.37 mmol, 2.4 eq) and solution stirred overnight. After addition of 10 mL 10 % sodiumthiosulfate, solution was transferred to a separatory funnel and diluted with ether. Ether layer was washed with 10 % hydrochloric acid, saturated sodium bicarbonate solution and brine and dried with anhydrous magnesium sulfate. Evaporation of ether provided 98.6 mg of the mixture of tetrabromides **101** (97.4 % yield) as white powder. The mixture was used in the next step without further purification.

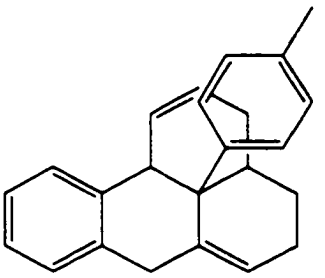

95

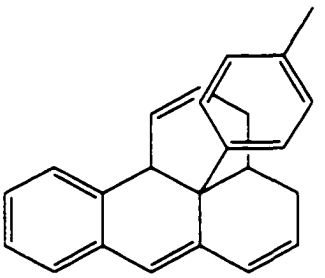

102

Dibromide **100** (57.8 mg, 0.12 mmol, 1 eq) was dissolved in 5 mL dry THF. Under nitrogen, 110.7 mg freshly sublimed potassium tert-butoxide were added and the mixture stirred for 1.5 hours. 2 mL water were added and the solvent evaporated *in vacuo*. Residue was dissolved in ether, and washed with 10 % hydrochloric acid and brine. After drying over anhydrous magnesium sulfate and filtration of the drying agent, solvent was removed by rotary evaporation. Column chromatography (hexane/ethylacetate : 5/1) gave 15 mg mixture of diene **95** and triene **102**.

GC/MS (triene 102):

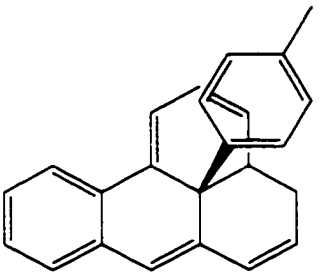

98

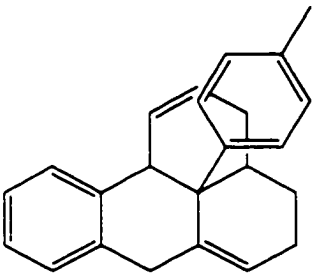

95

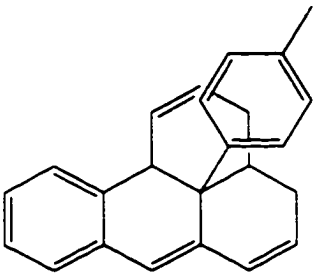

102

110 mg mixture of tetrabromides **101** (0.17 mmol, 1 eq) were dissolved in 10 mL THF. To the stirred solution, under nitrogen were added 157 mg (1.4 mmol, 8 eq) freshly sublimed potassium tert-butoxide, and stirring continued for 2 hours. To the dark brown solution were added 2 mL water and solvent evaporated on a rotary evaporator. Residue was dissolved in ether, and ether washed with 10 % hydrochloric acid and brine. After drying over anhydrous magnesium sulfate, solvent was removed and residue purified by column chromatography (hexane/ethyl acetate: 18/1). Purification yielded 50 mg of the mixture of triene **102** , tetraene **98** and diene **95** in the ratio of 86:10:4, as judged by GC/MS.

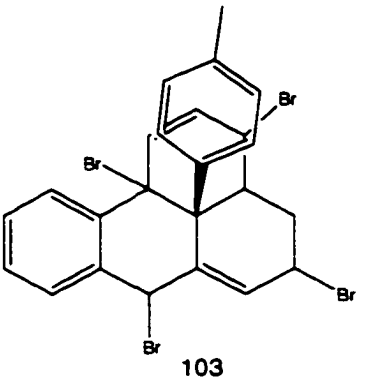

103

3,5,7,11b-Tetrabromo-11c-p-tolyl-3a,4,5,7,11b,11c-hexahydro-3H-benzo[de]anthracene (**103**)

Diene **95** (120 mg, 0.38 mmol, 1 eq) was dissolved in 8 mL freshly distilled carbon tetrachloride. To the stirred solution, under argon were added 285 mg N-bromosuccinamide (1.6 mmol, 4.2 eq) and 13 mg AIBN (0.076 mmol, 0.2 eq). The solution was irradiated with a sun lamp, and gently refluxed for 3 hours. After cooling to room temperature, suspension was filtered through a short celite column using carbon tetrachloride as eluent. Removal of the solvent by rotary evaporation afforded 237 mg crude tetrabromide **103** (98.2 % yield), that was used in the next step without further purification.

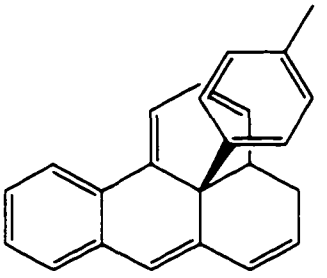

98

11c-p-Tolyl-3a,11c-dihydro-4H-benzo[de]anthracene (**98**)

254 mg tetrabromide **103** (0.4 mmol; 1 eq) were dissolved in 5 mL THF and cooled to -78 °C. Under argon, 1.2 ml tert-butyllithium (1.7 M solution in pentane, 2 mmol, 5 eq) were added dropwise. The solution immediately turned dark brown. After 10 min, at -78 °C, to the solution were added 0.1 mL methanol. After warming to room temperature, the solution was transferred to a separatory funnel and washed two times with 3 mL brine. 20 mL ether was added and solution washed with 10 % hydrochloric acid and brine. After drying with anhydrous magnesium sulfate, solvent was evaporated and residue purified by column chromatography (hexane/ethyl acetate 30/1) to afford 60.4 mg tetraene **98** (49 % yield).

^{1}H NMR (300 MHz, $CDCl_3$): δ 7.55 ppm (dd, 1 H, 2.2 Hz, 8.4 Hz); δ 7.25 – 6.84 ppm (m, 8 Hz); δ 6.59 ppm (d, 1H, 5.5 Hz); δ 6.41 ppm (s, 1H); δ 6.33 ppm (m, 1H); δ 6.14 ppm (m, 1H); δ 5.65 ppm (dd, 1H, 4.8 Hz, 9.5 Hz); δ 2.76 ppm (m, 1H); δ 2.33 ppm (m, 1 H); δ 2.22 ppm (s, 3H); δ 1.94 ppm (m, 1H).

GC/MS: 308 (M^+); 293 ($M^+ - CH_3$);

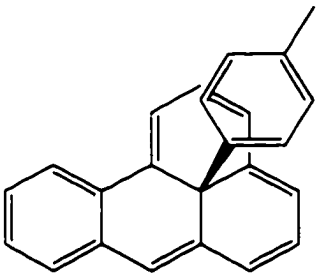

21

11c-p-Tolyl-11cH-benzo[de]anthracene (**21**)

To a flame dried flask, under nitrogen was added a solution of 41 mg tetraene **98** (0.13 mmol, 1 eq) in 5 mL THF. Solution was cooled to -78 °C and 0.17 mL 1.7 M solution of *tert*- butyl lithium in pentane (0.28 eq, 2.1 eq) injected. Color of the solution changed to dark green. The solution was stirred at – 40 °C for four hours. A solution containing ~ 80 mg freshly sublimed iodine in 2 mL THF was added and solution warmed up. The solution was transferred to a separatory funnel, diluted with ether and washed with 10 % sodium thiosulfite and brine. After drying with anhydrous magnesium sulfate, ether was evaporated by rotary evaporation.

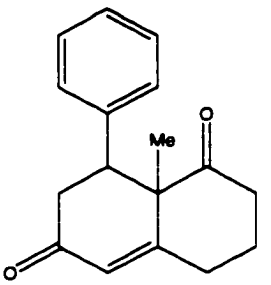

108

8a-Methyl-8-phenyl-3,4,8,8a-tetrahydro-2H,7-naphthalene-1,6-dione (**108**)

To the flask were added 1.26 g 2-methyl-1,3-cyclohexadione (10 mmol, 1 eq), 2.19 g benzalacetone (15 mmol, 1.5 eq), 14 mg potassium hydroxide (0.25 mmol, 0.025 eq) and 10 mL methanol. The solution was refluxed for 3 hours. 20 mL benzene added and methanol removed in the Dean Stark arm. Pyrrolidine (0.06 mL) added and the solution refluxed overnight. After removing benzene on the rotary evaporator, residue was diluted with ether. Ether was washed with 10 % hydrochloric acid, saturated sodium bicarbonate and brine and dried over anhydrous magnesium sulfate. Column chromatography (hexane/ethyl acetate : 2:1) afforded 0.64 g (26.4 %) product.

^{1}H NMR (300 MHz, $CDCl_3$) : δ 7.21 – 7.08 ppm (m, 5 H); δ 6.08 ppm (s, 1H); δ 3.73 ppm (dd, 1H, 1.5 Hz, 6.6 Hz); δ 3.07 ppm (dd, 1H, 6.6 Hz, 18 Hz); δ 2.67 ppm (m, 4H); δ 2.41 ppm (m, 1H); δ 2.01 ppm (m, 2H); δ 1.64 ppm (s, 3H).

^{13}C NMR (75 MHz, $CDCl_3$): δ 210.89 ppm; δ 196.75 ppm; δ 164.76 ppm; δ 141.89 ppm; δ 128.60 ppm; δ 128.36 ppm; δ 126.79 ppm; δ 125.90 ppm; δ 54.52 ppm; δ 47.98 ppm; δ 40.90 ppm; δ 38.59 ppm; δ 31.87 ppm; δ 27.32 ppm; δ 20.14 ppm.

GC/MS: 254 (M^+); 236 ($M^+ - H_2O$); 198 ($M^+-C_4H_8$).

APPENDIX A.

SELECTED SPECTRAL DATA

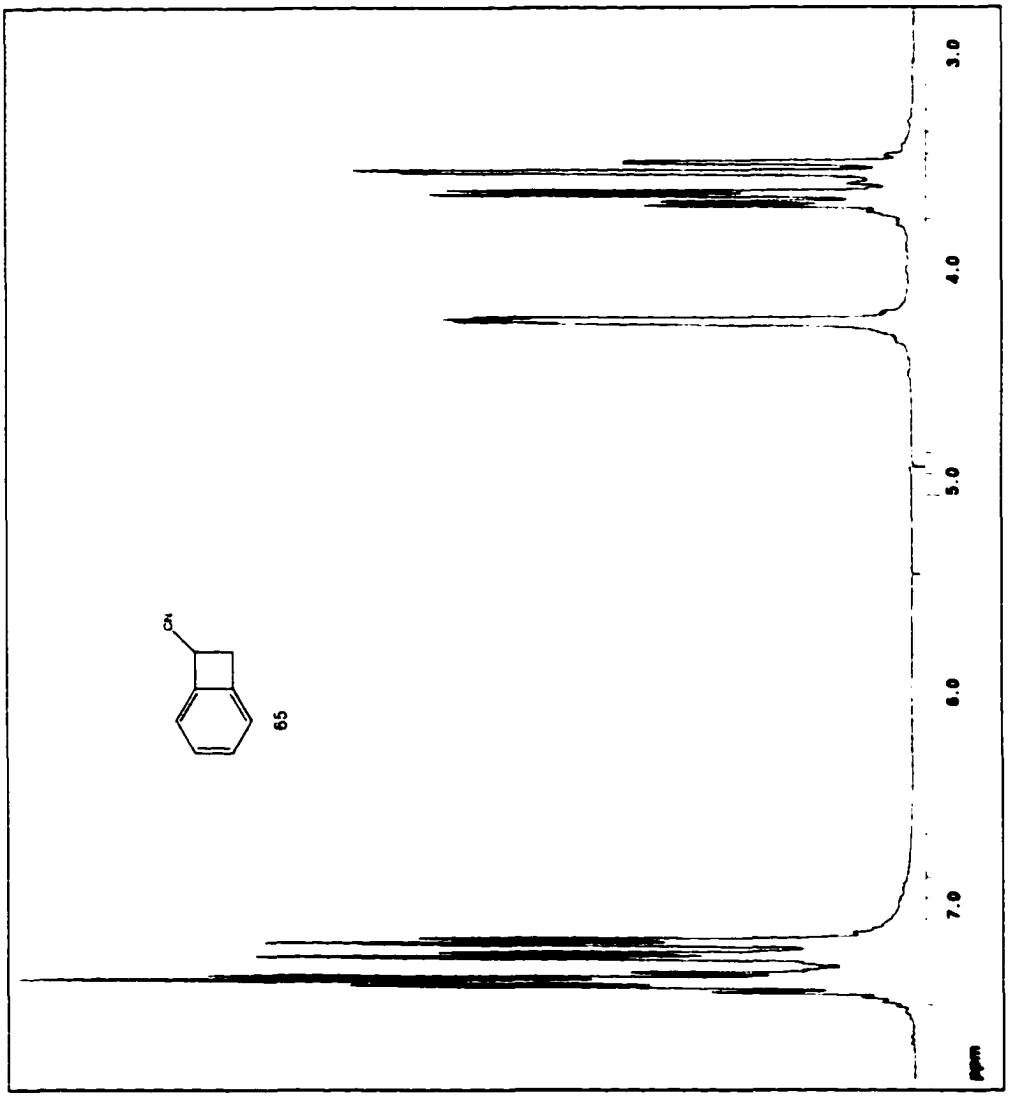

^{1}H NMR spectrum of nitrile 65

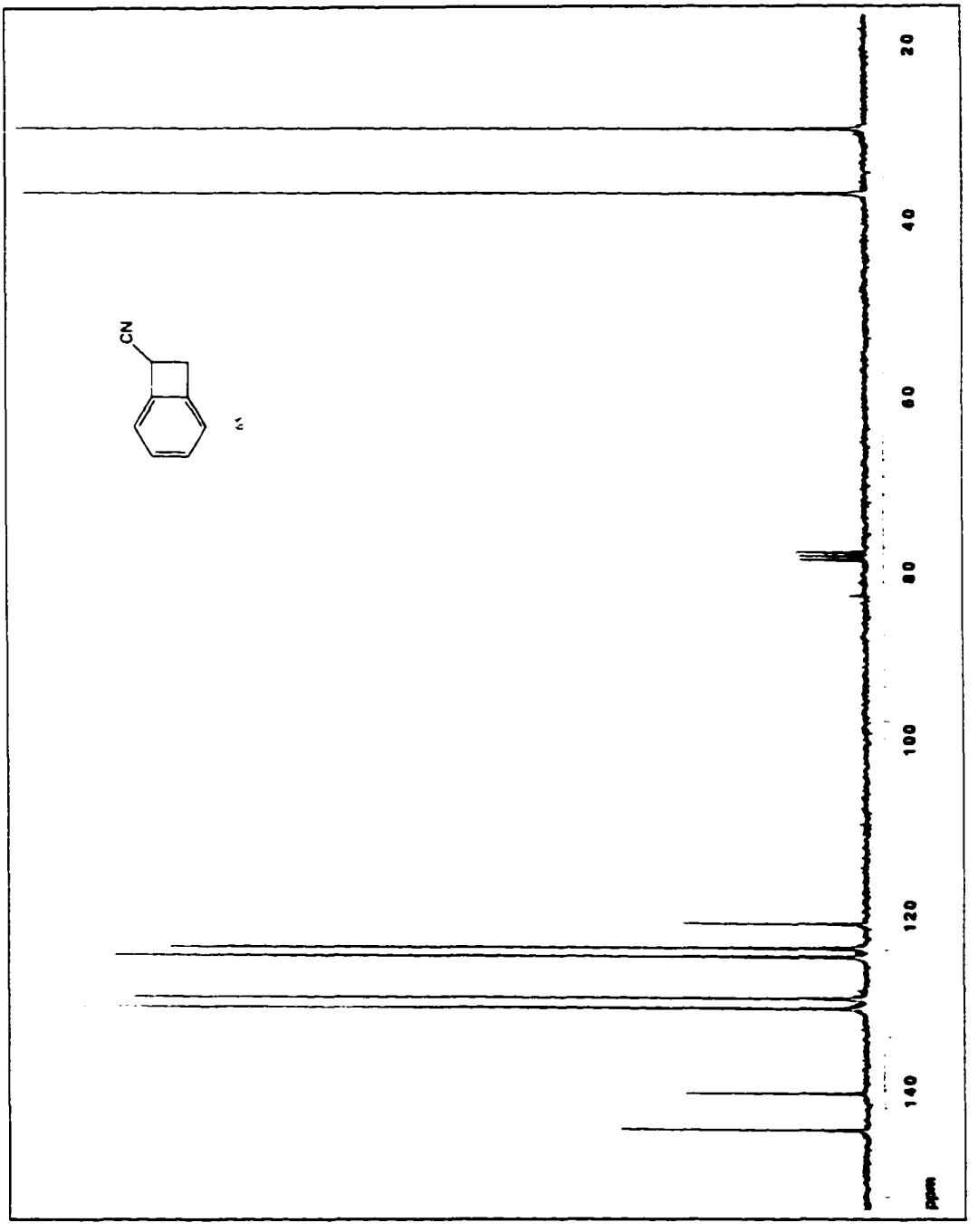

^{13}C NMR spectrum of nitrile 65

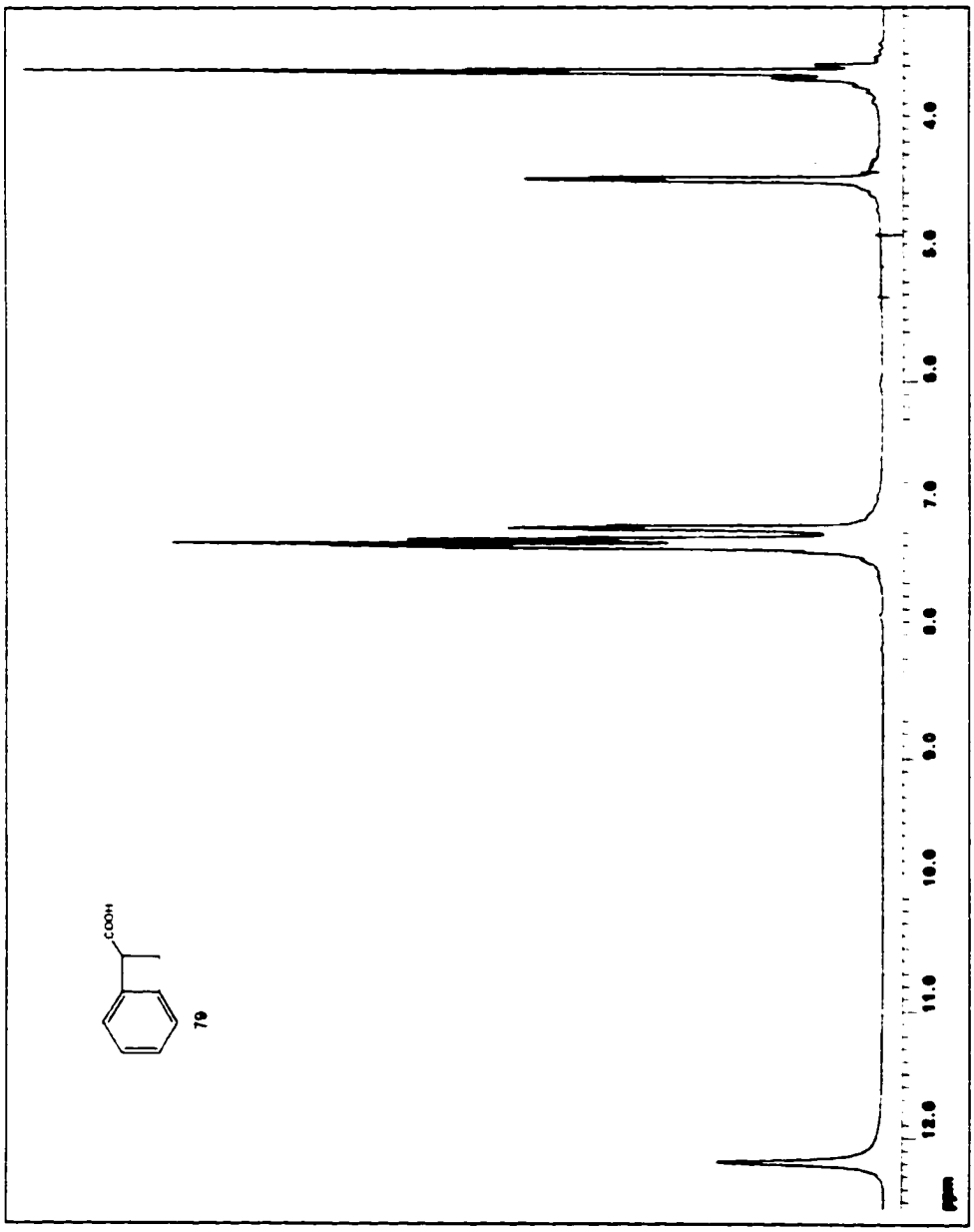

^{13}H NMR spectrum of acid 79

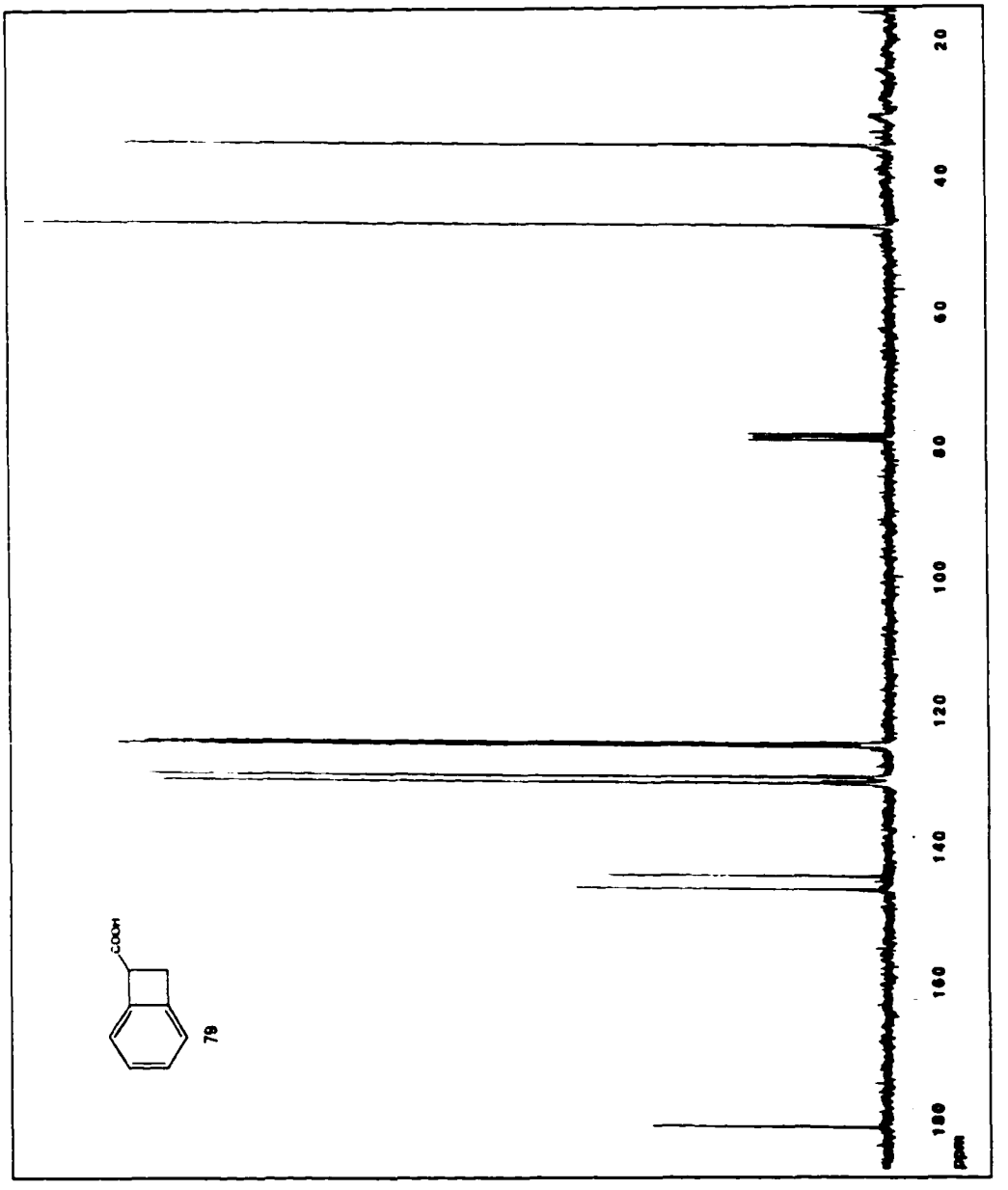

^{13} C NMR spectrum of acid **79**

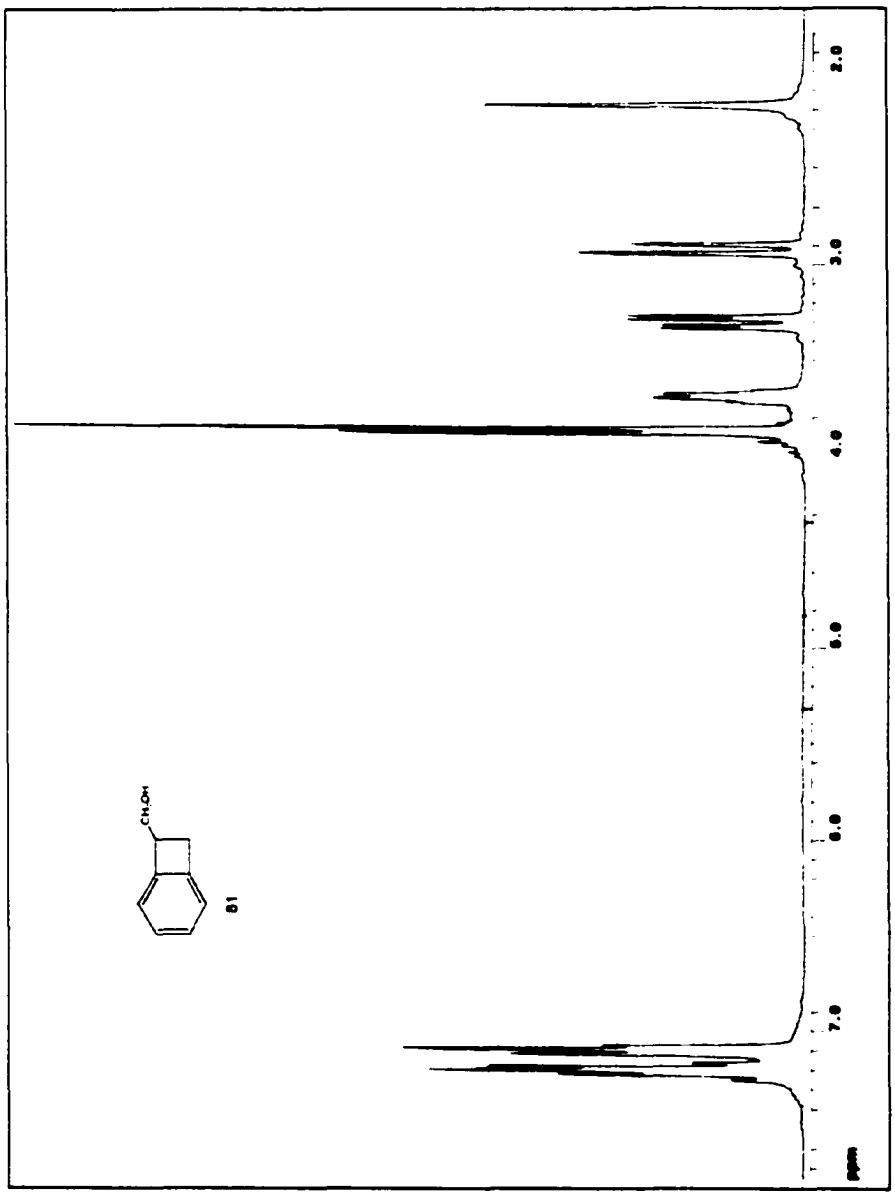

^{1}H NMR spectrum of alcohol 81

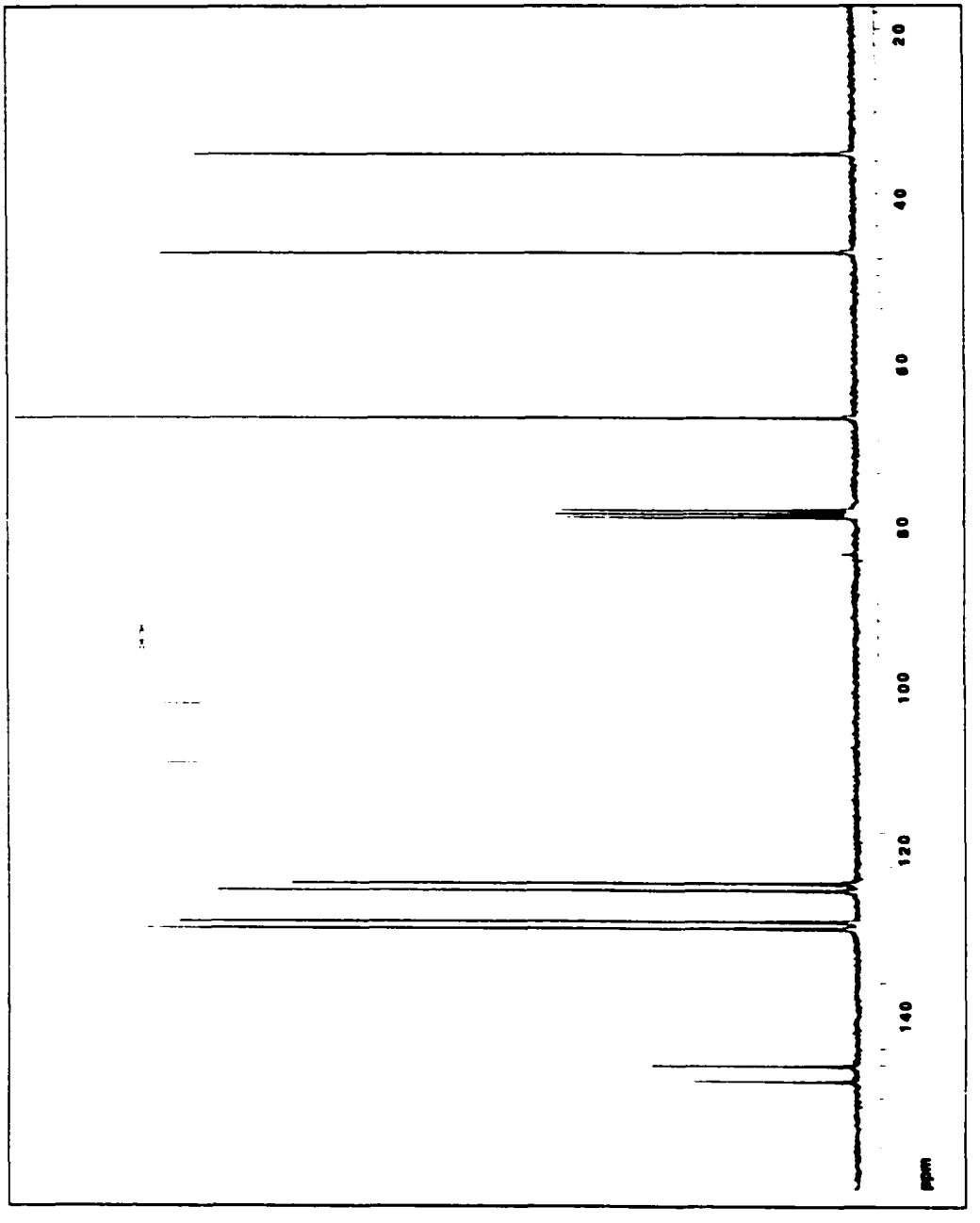

^{13}C NMR spectrum of alcohol **81**

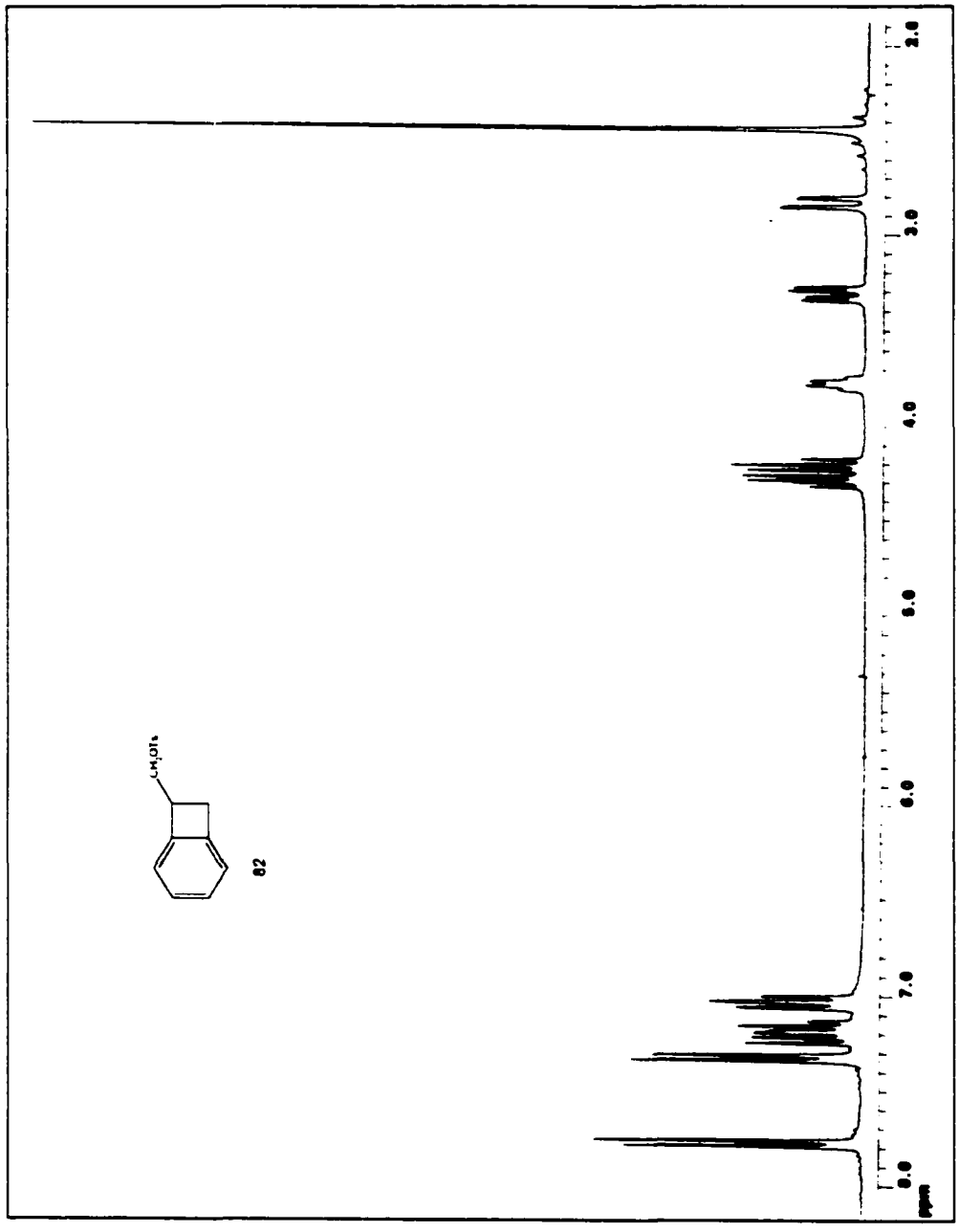

^{1}H NMR spectrum of tosylate 82

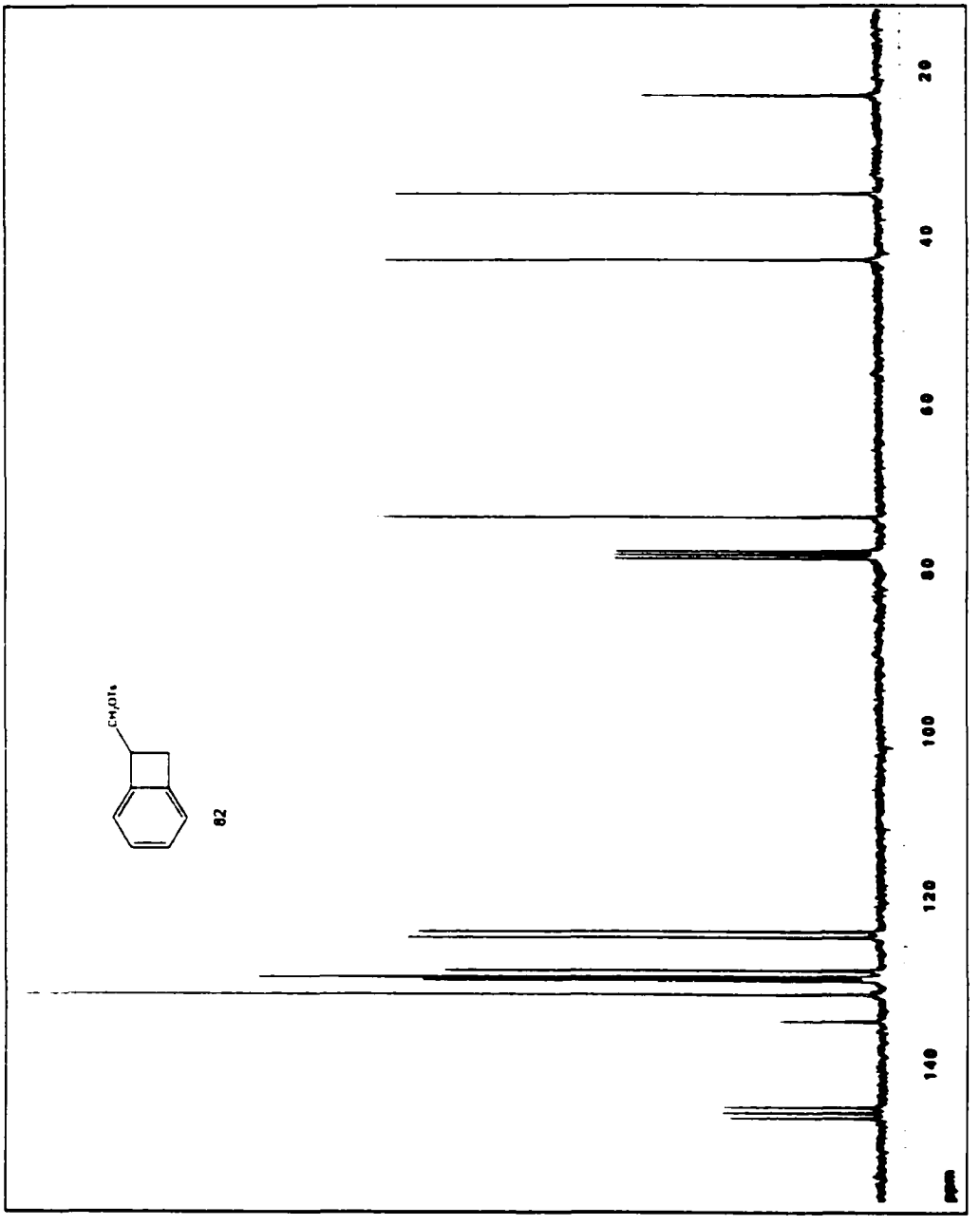

^{13}C NMR spectrum of tosylate 82

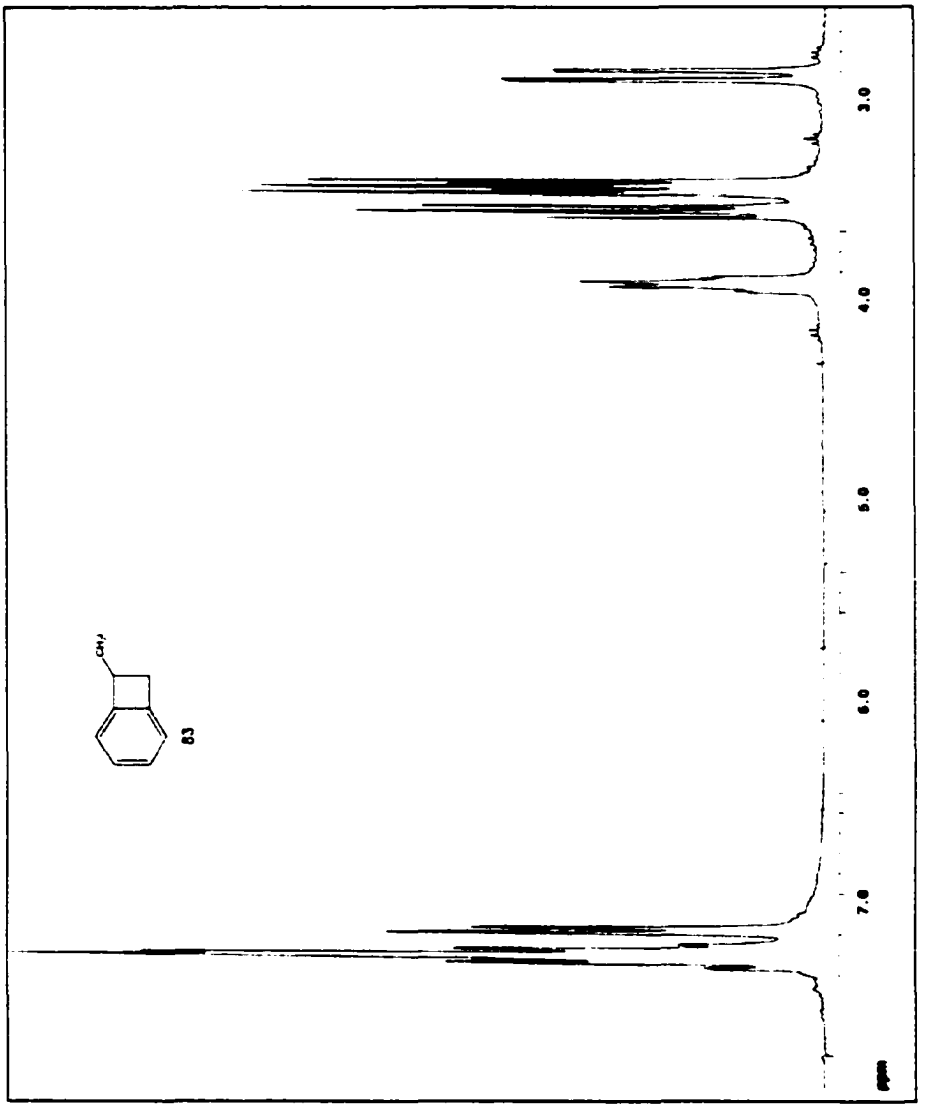

^{1}H NMR spectrum of iodide 83

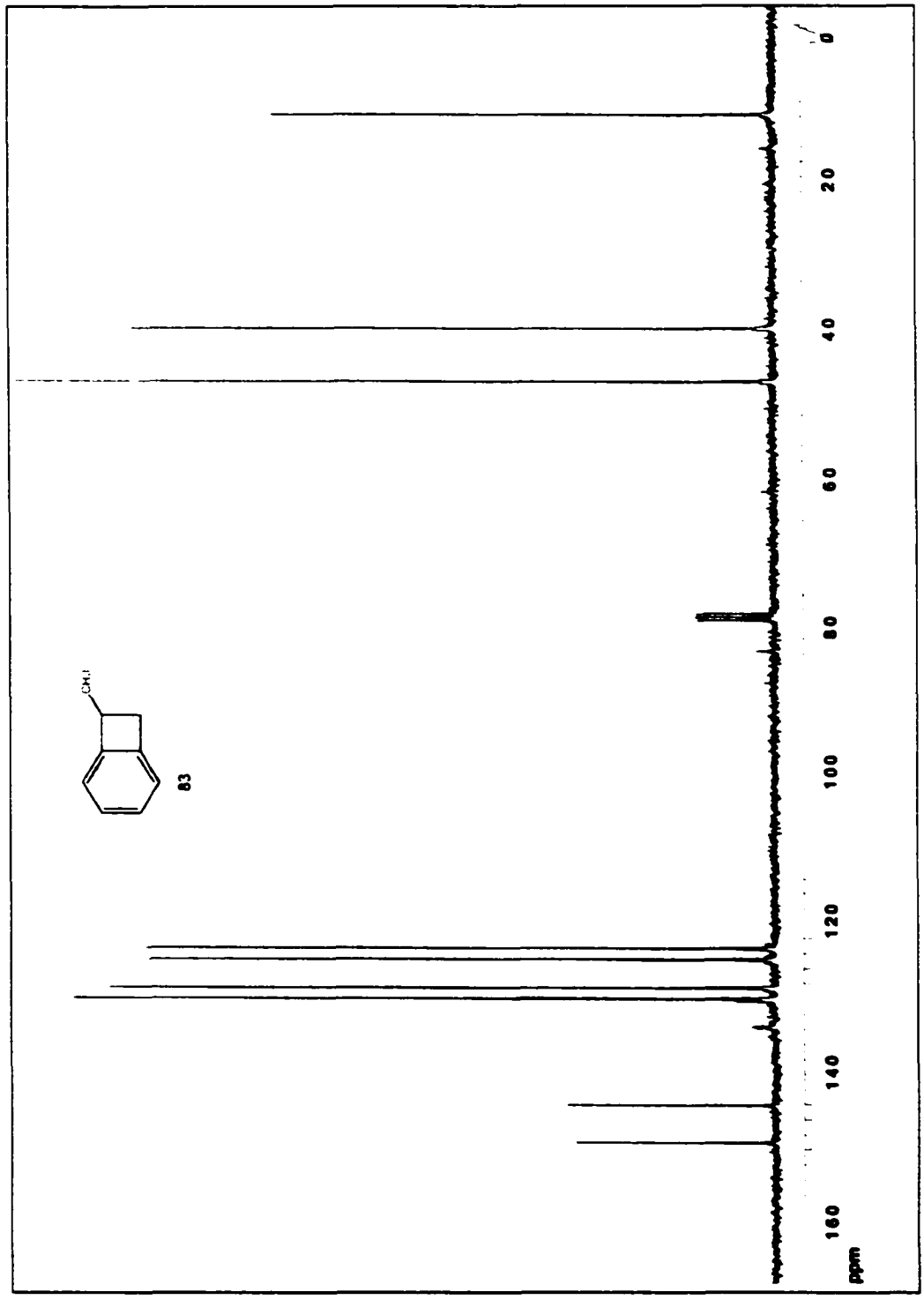

^{13}C NMR spectrum of iodide 83

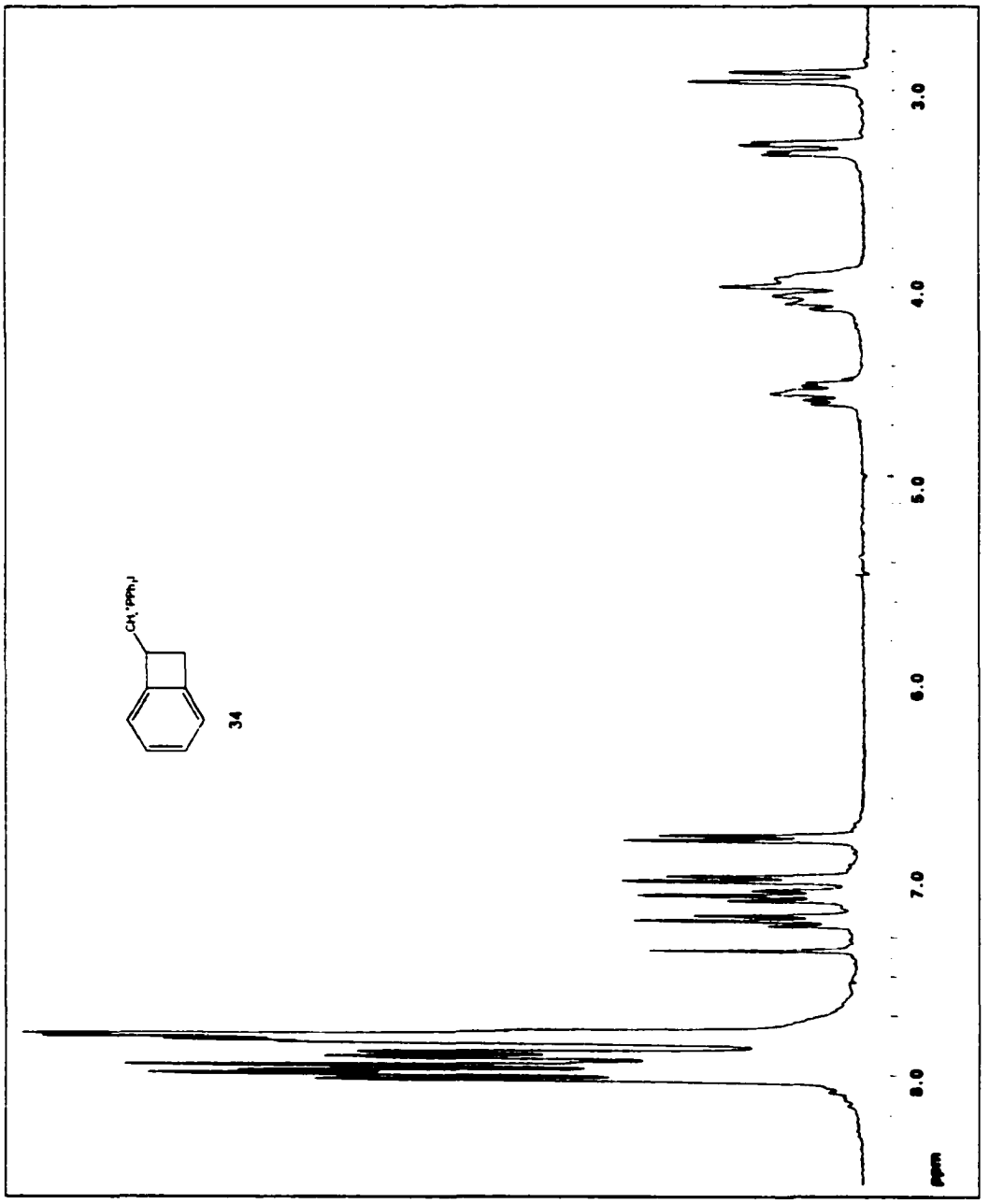

^{1}H NMR spectrum of phosphonium salt 34

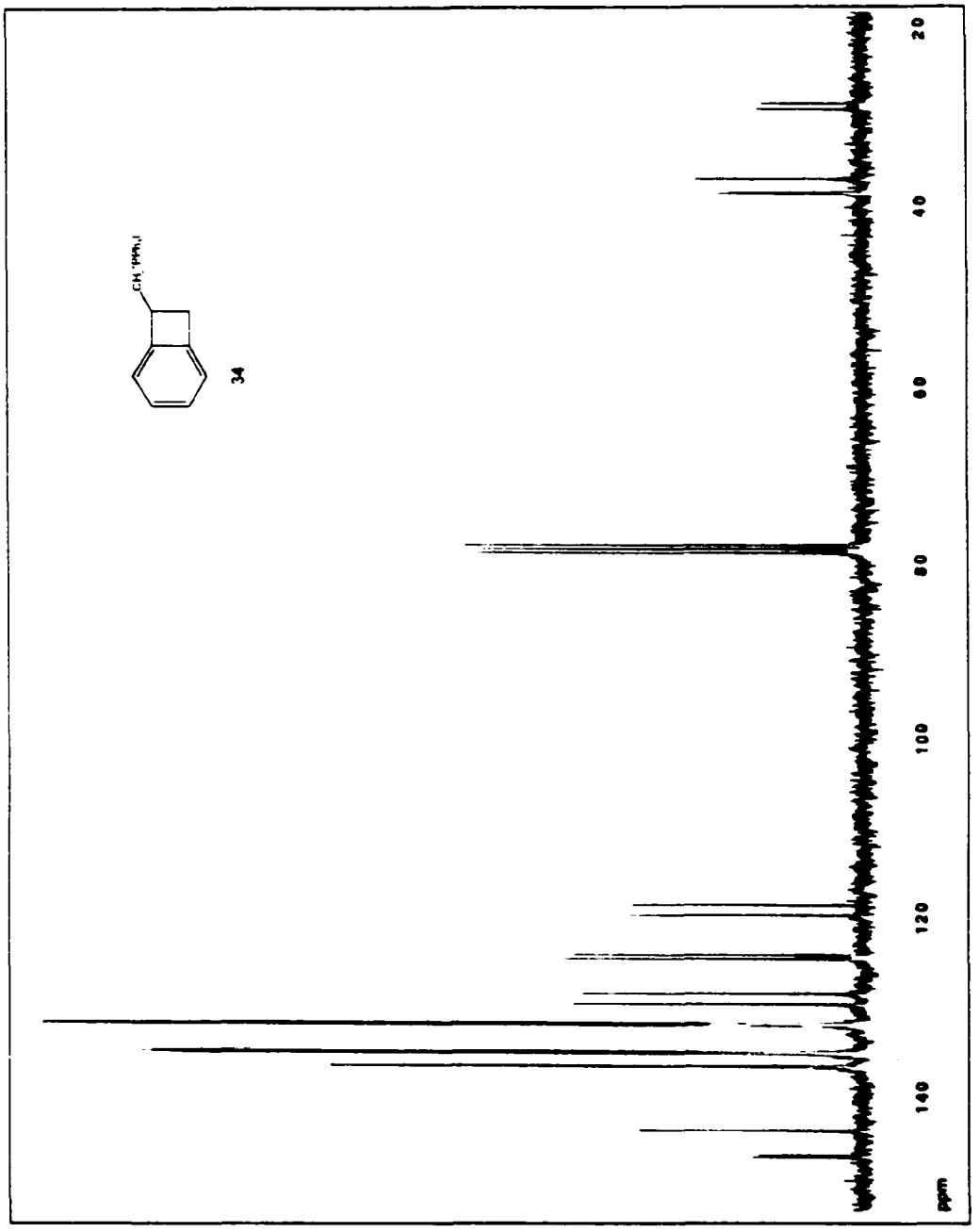

^{13}C NMR spectrum of phosphonium salt 34

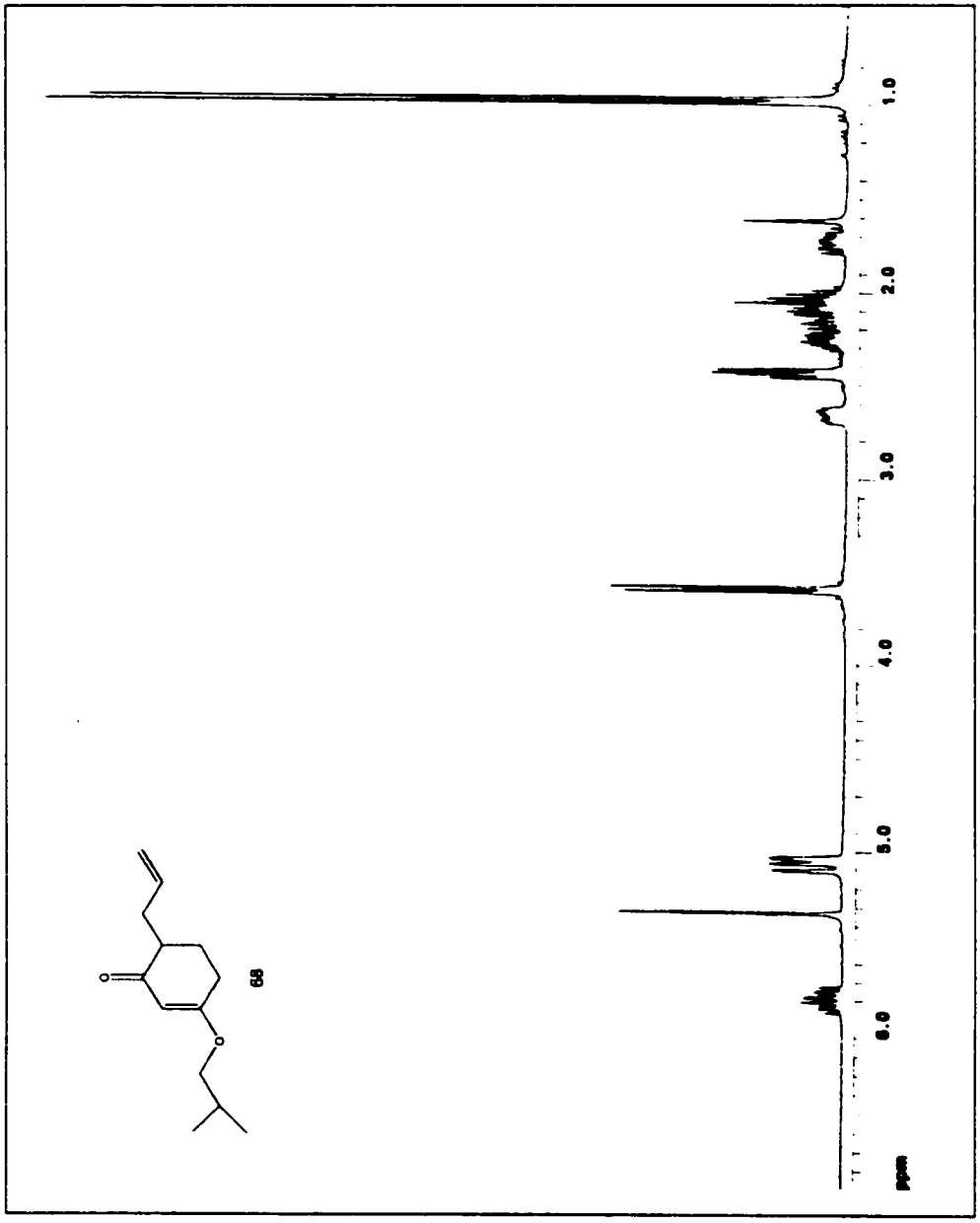

^{1}H NMR spectrum of ketone 68

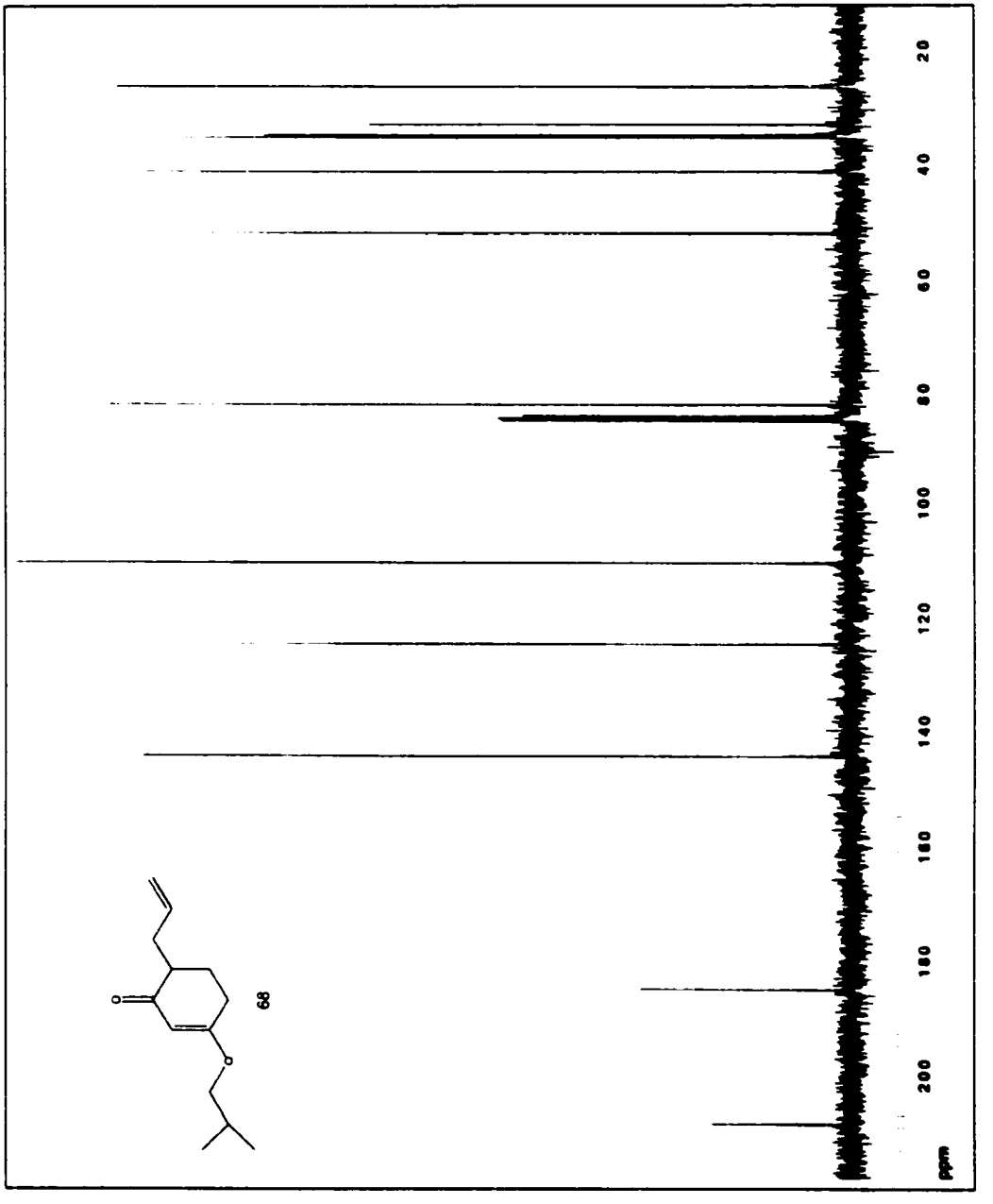

^{13}C NMR spectrum of ketone **68**

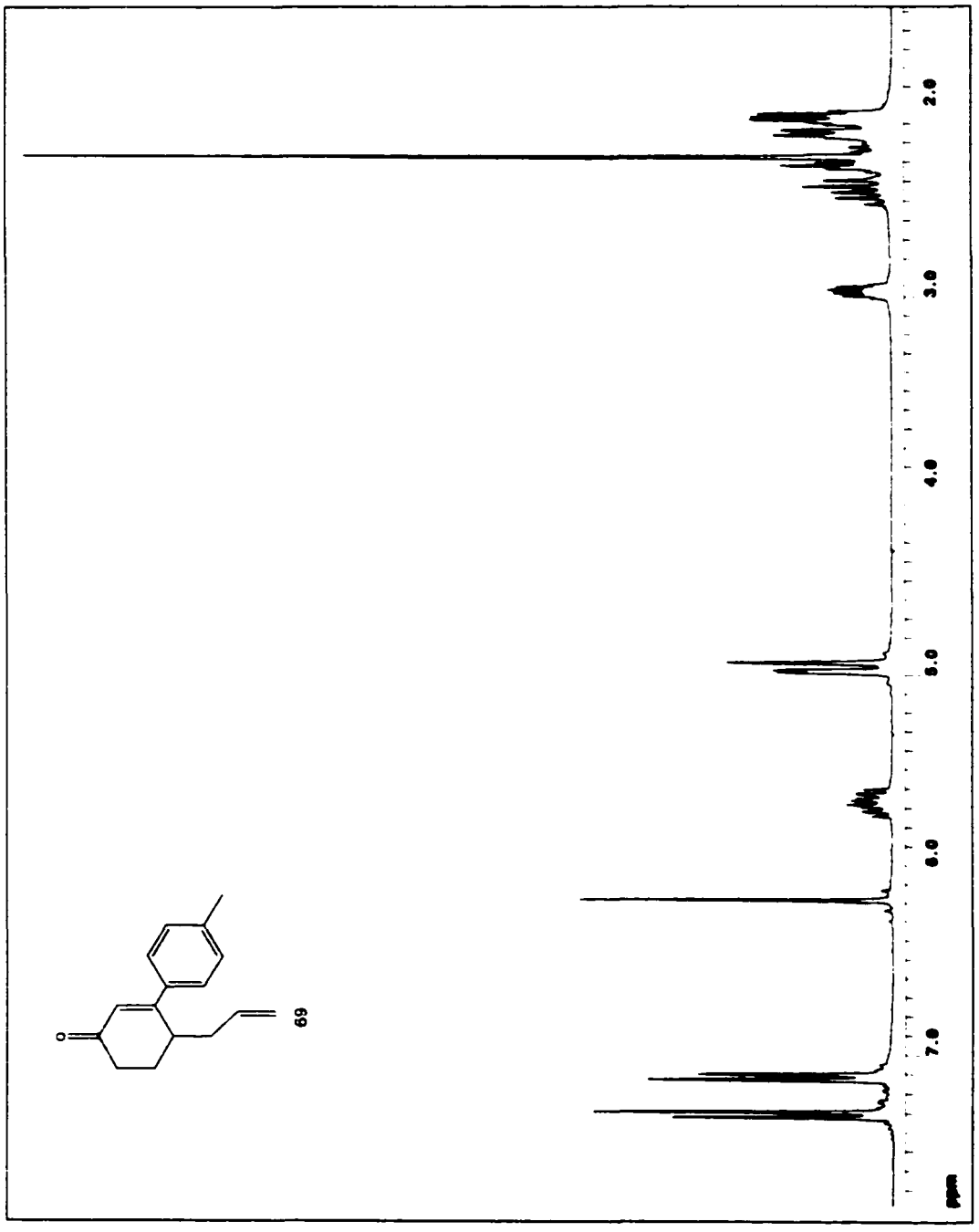

^{1}H NMR spectrum of ketone 69

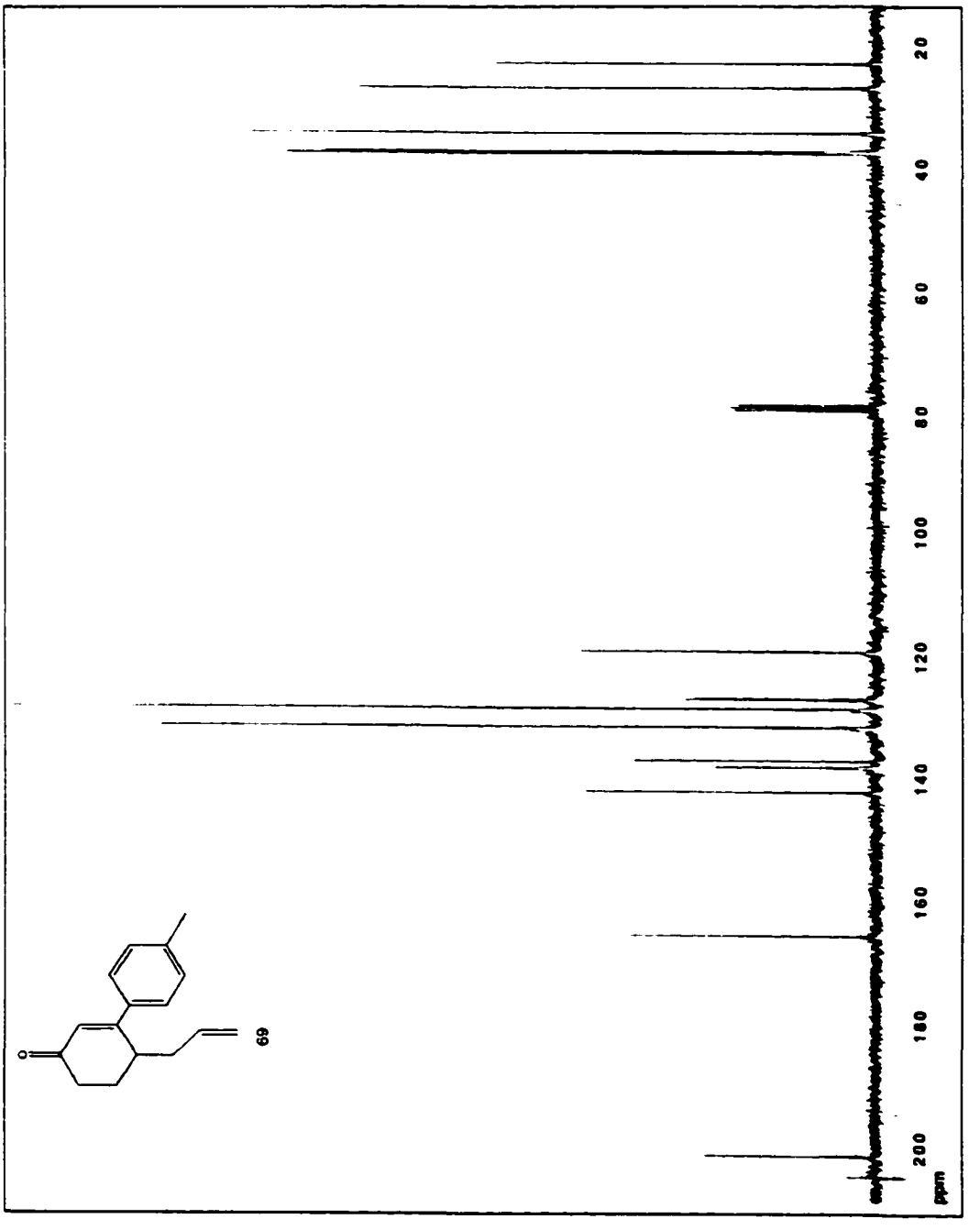

^{13}C NMR spectrum of ketone **69**

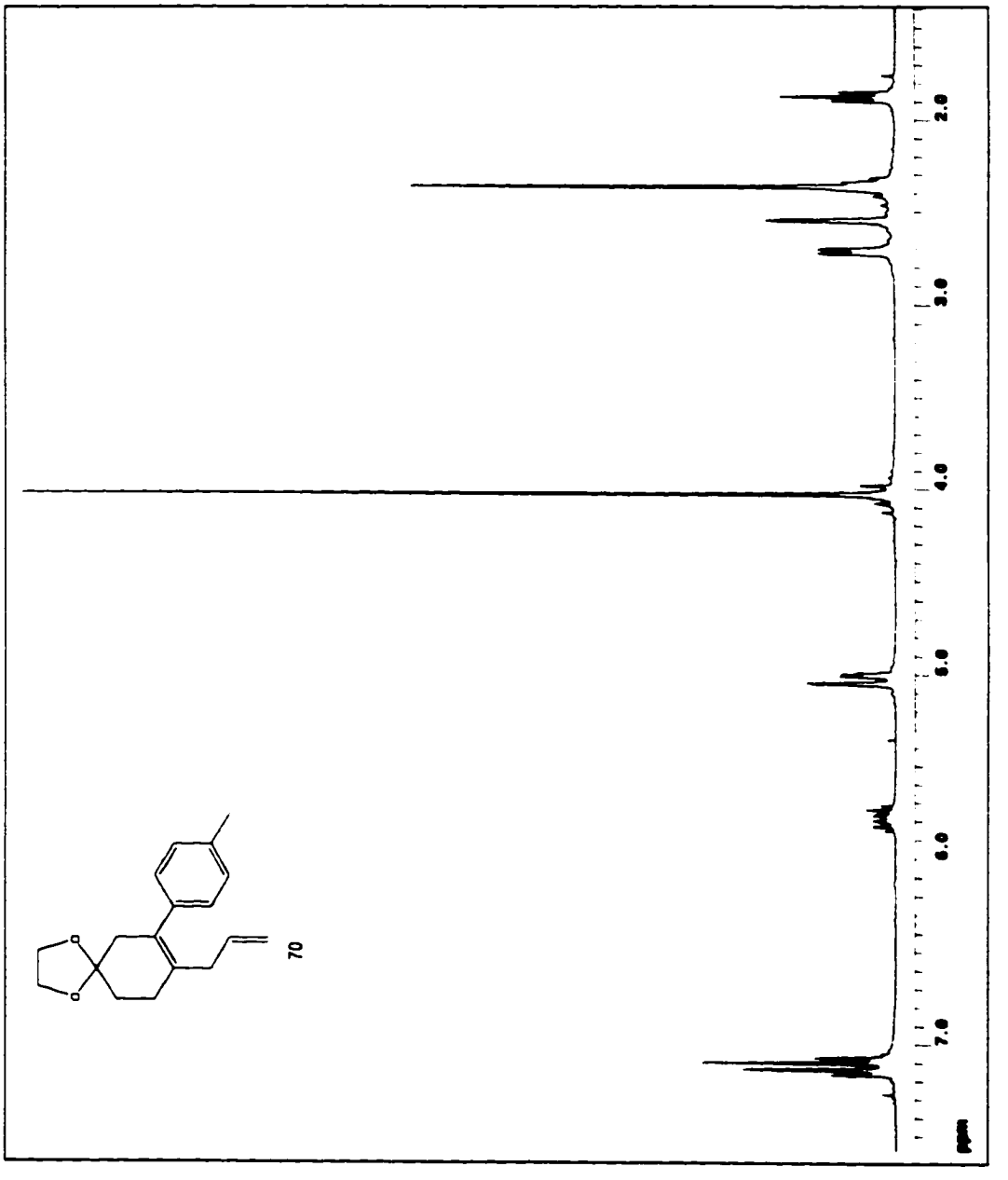

^{1}H NMR spectrum of ketal **70**

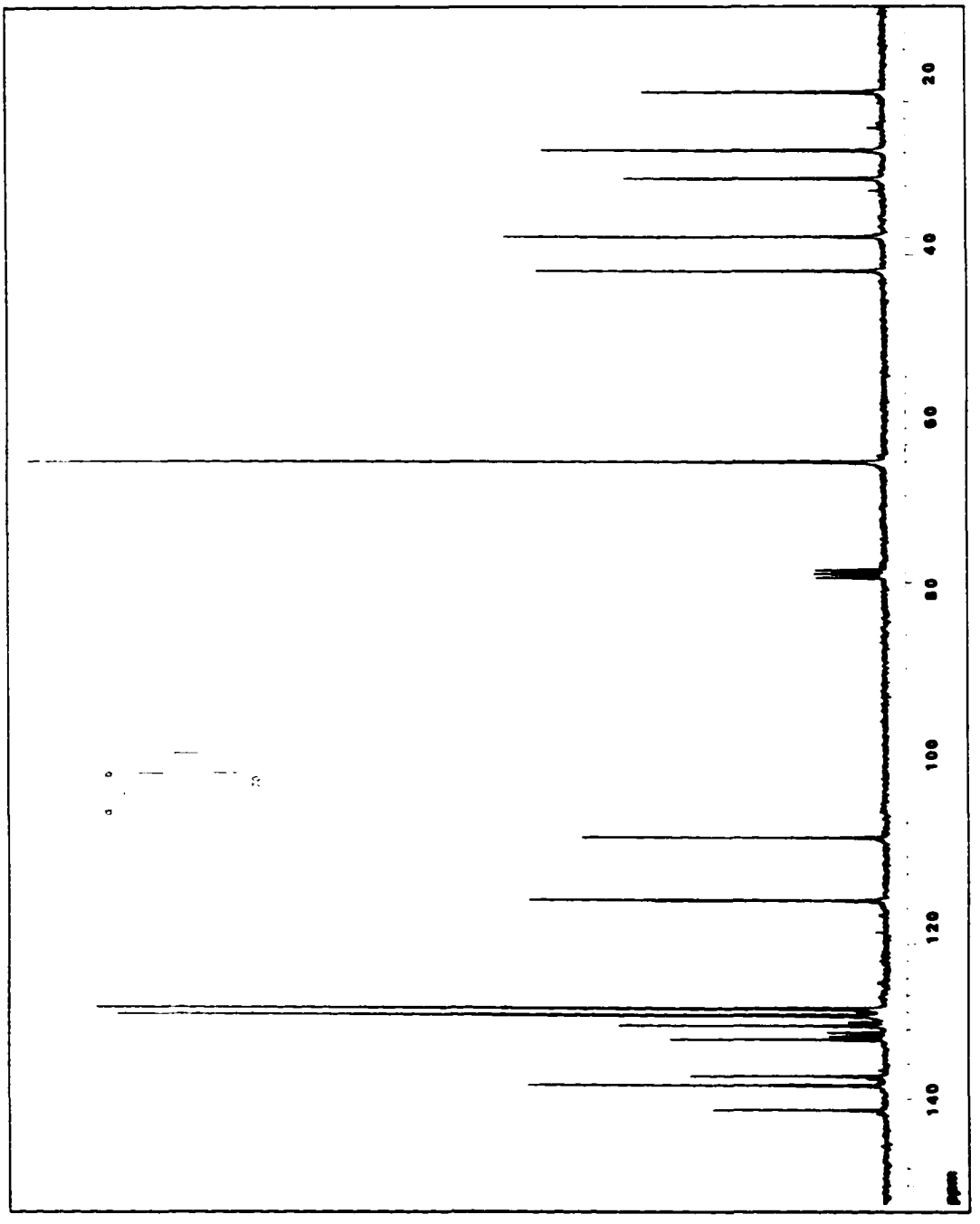

^{13}C NMR spectrum of ketal 70

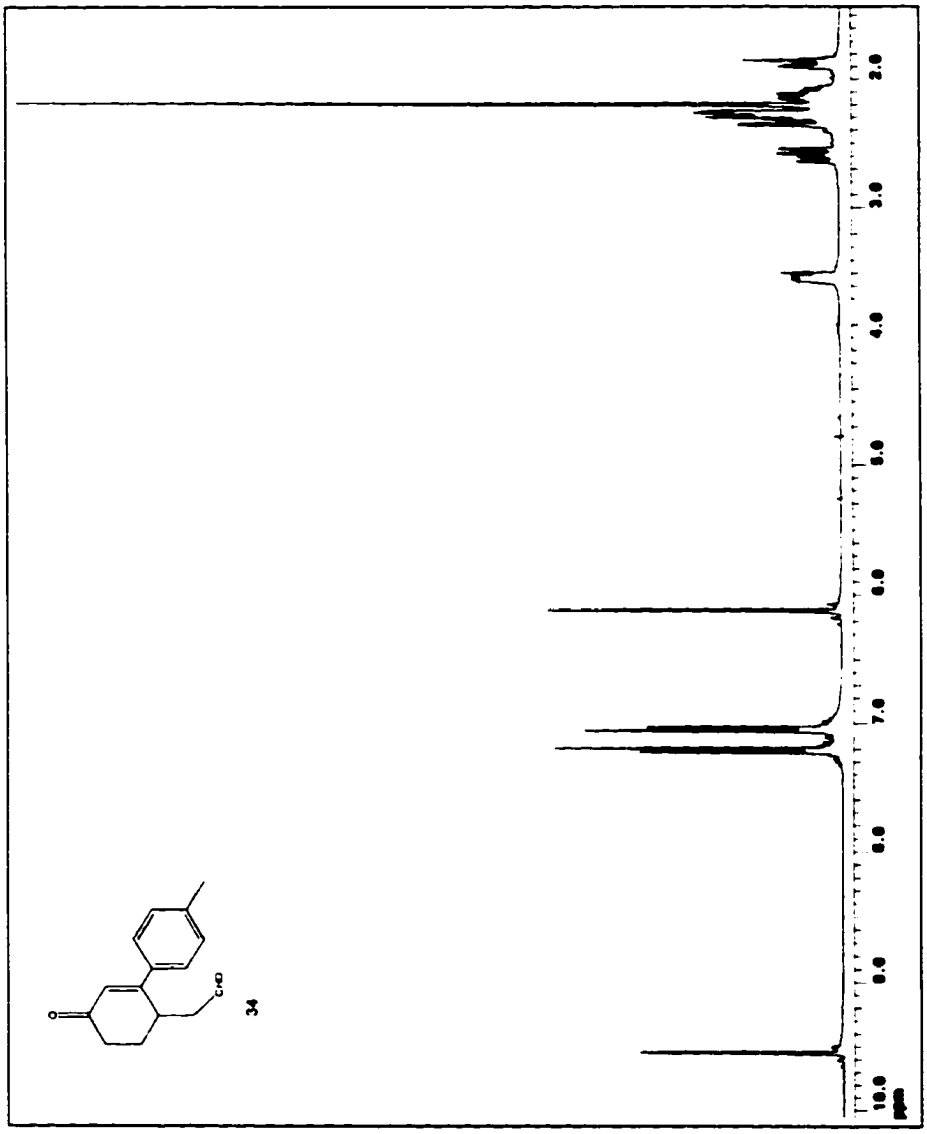

^{1}H NMR spectrum of aldehyde 35

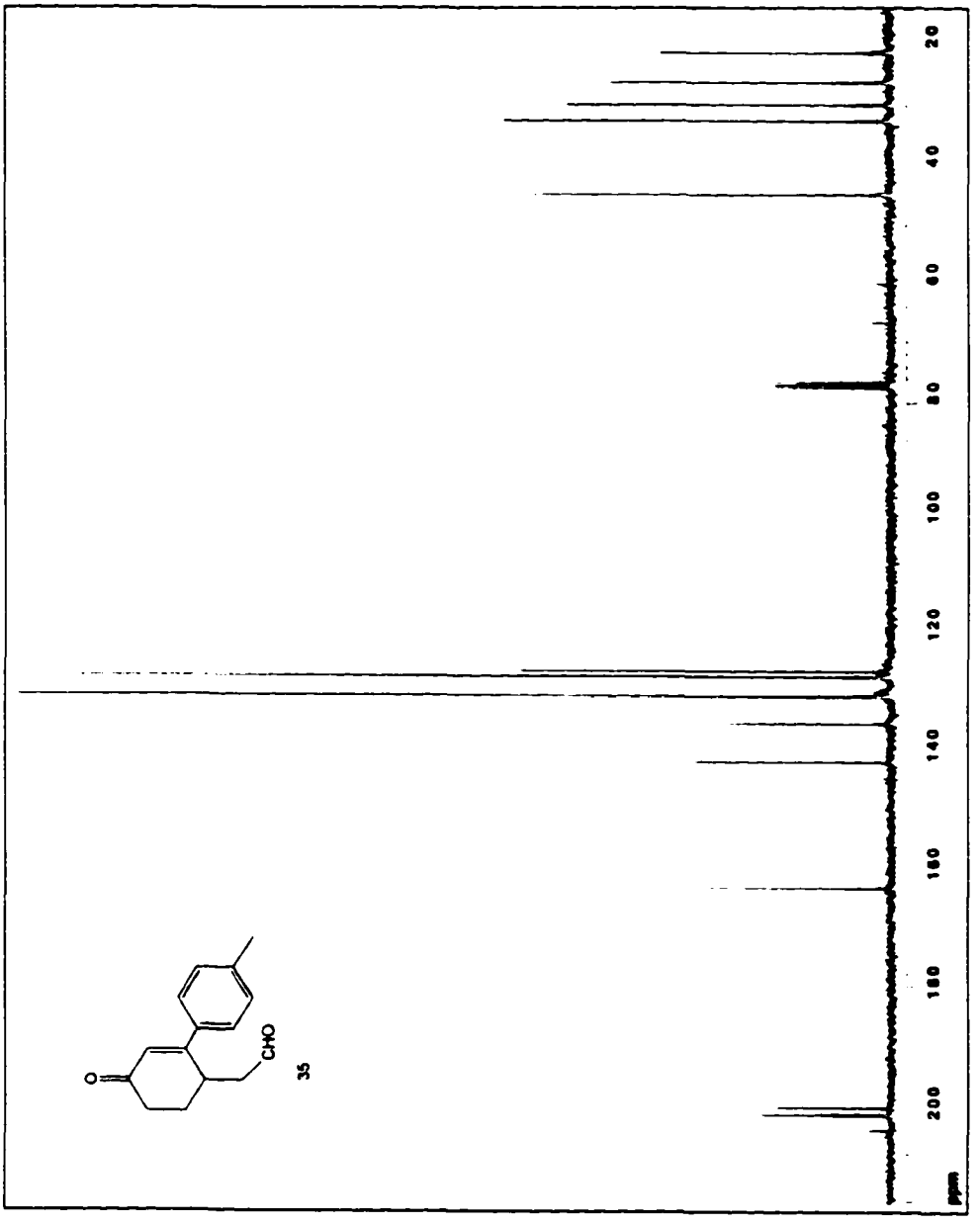

^{13}C NMR spectrum of aldehyde 35

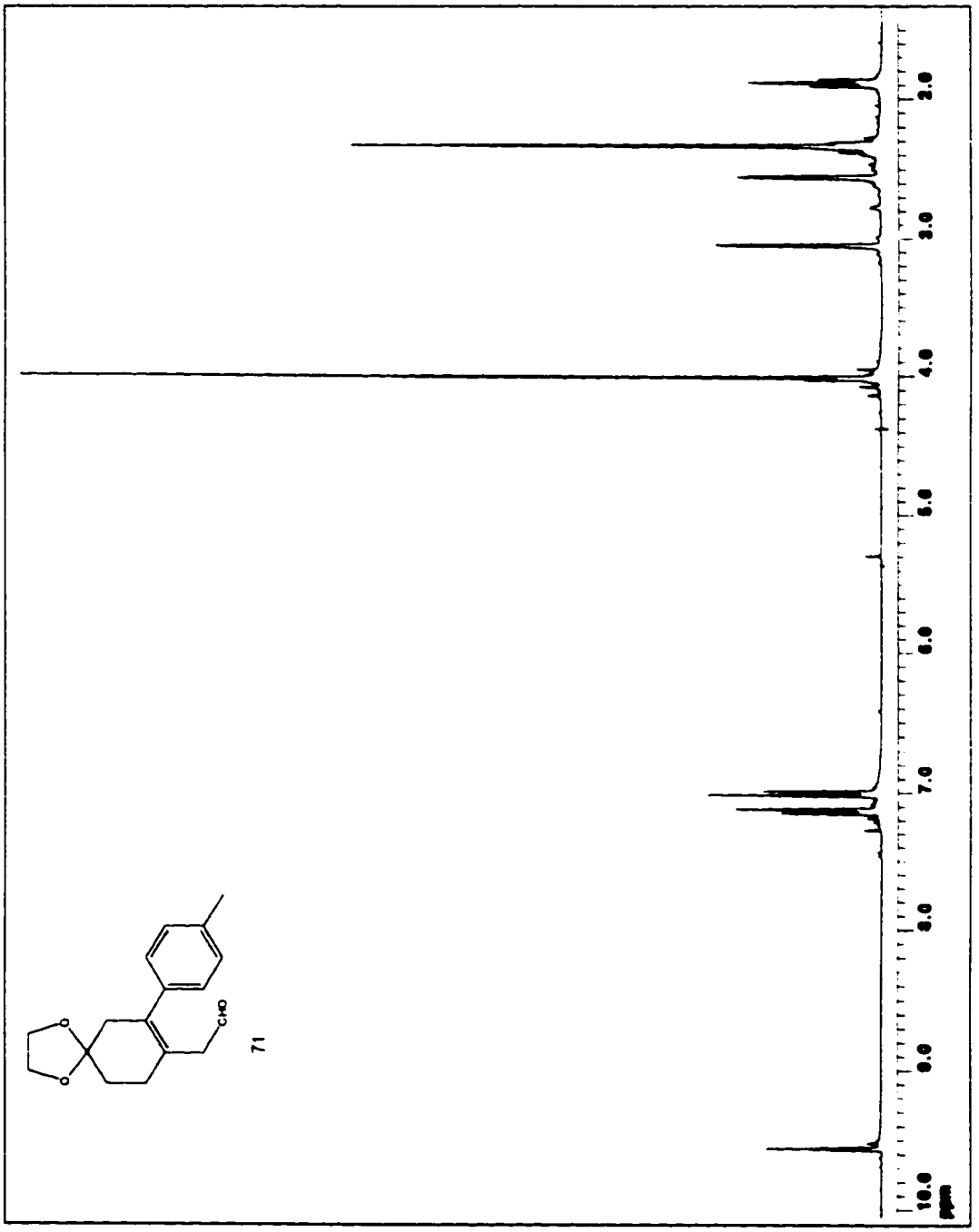

^{1}H NMR spectrum of aldehyde 71

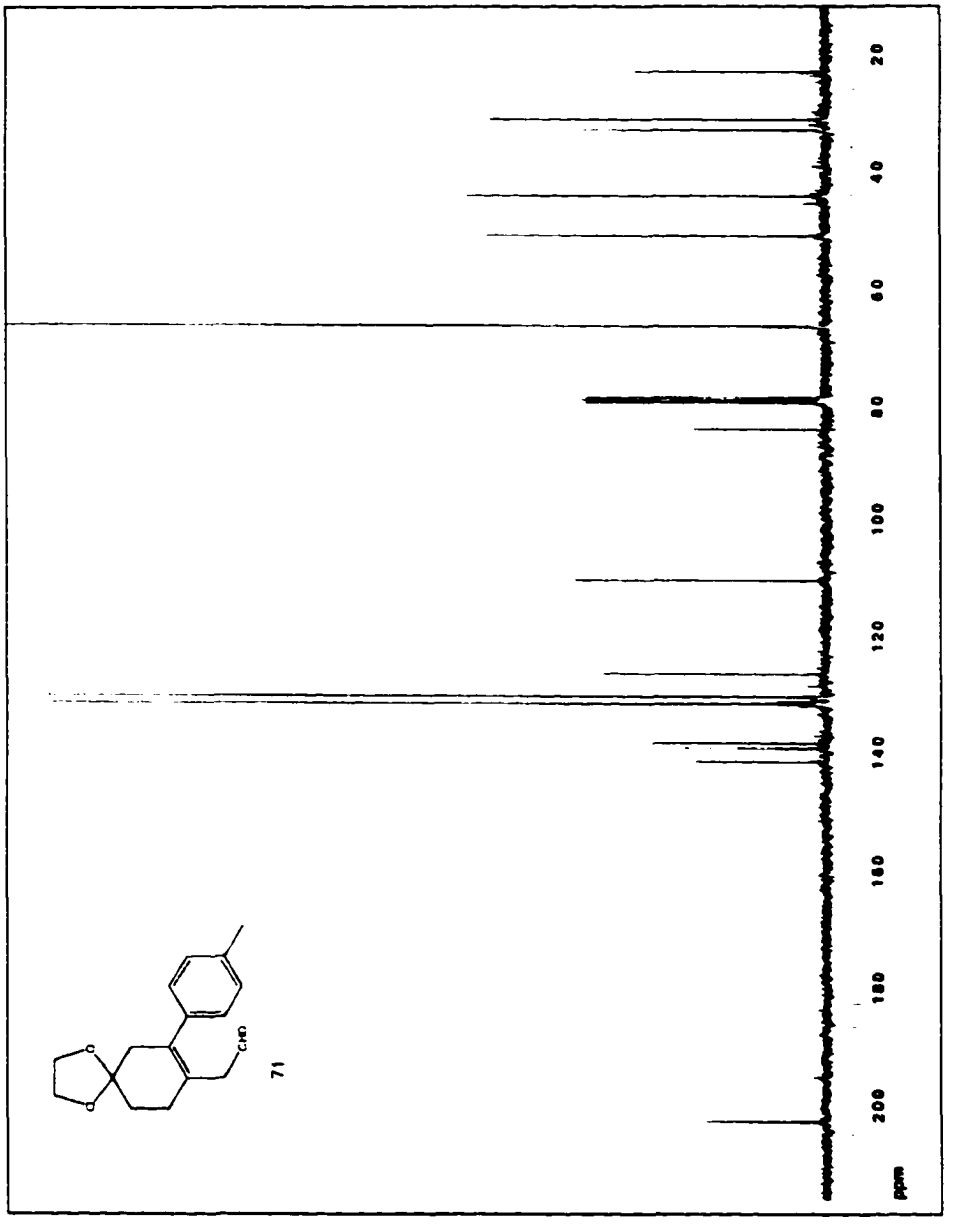

^{13}C NMR spectrum of aldehyde 71

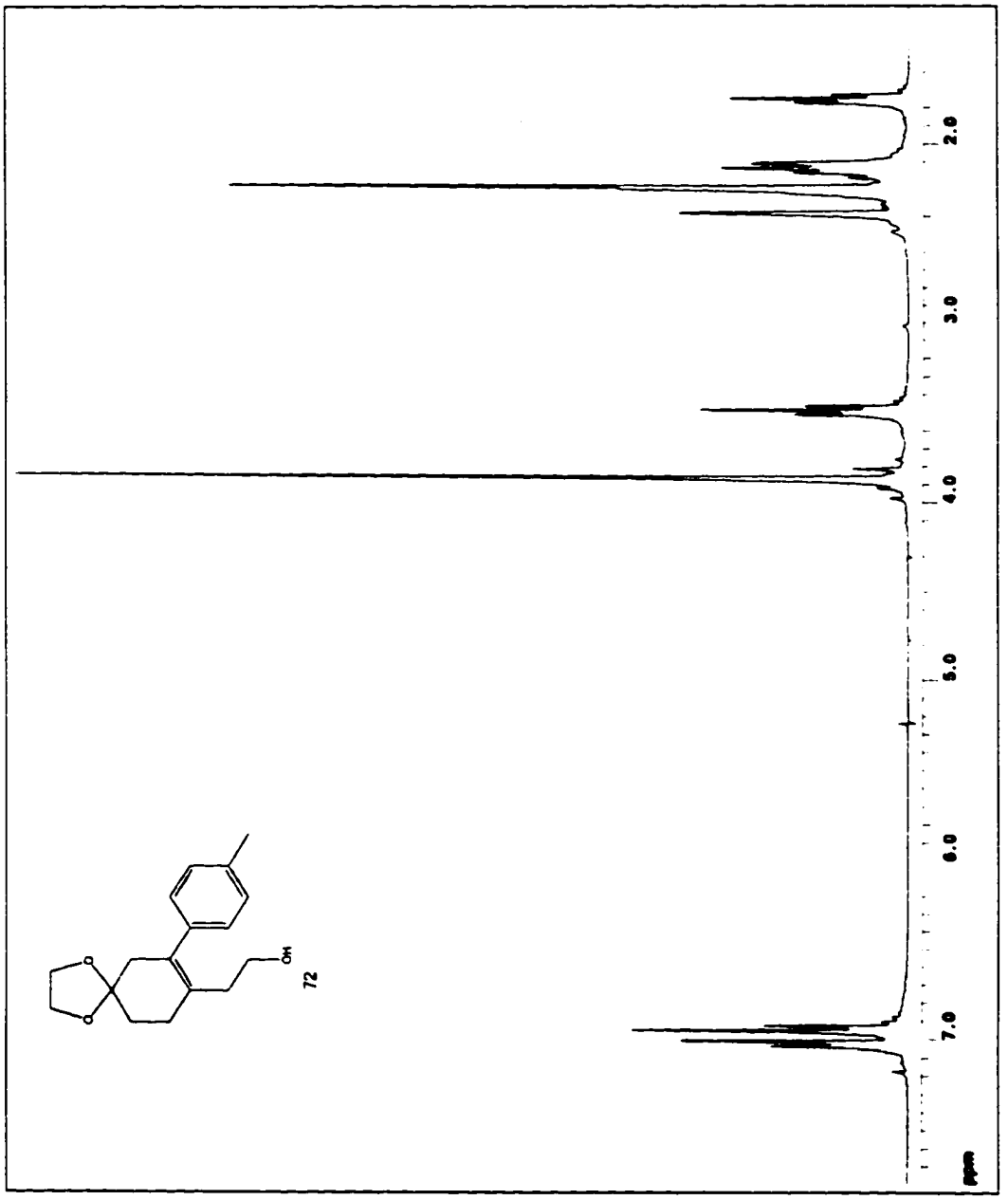

^{1}H NMR spectrum of alcohol **72**

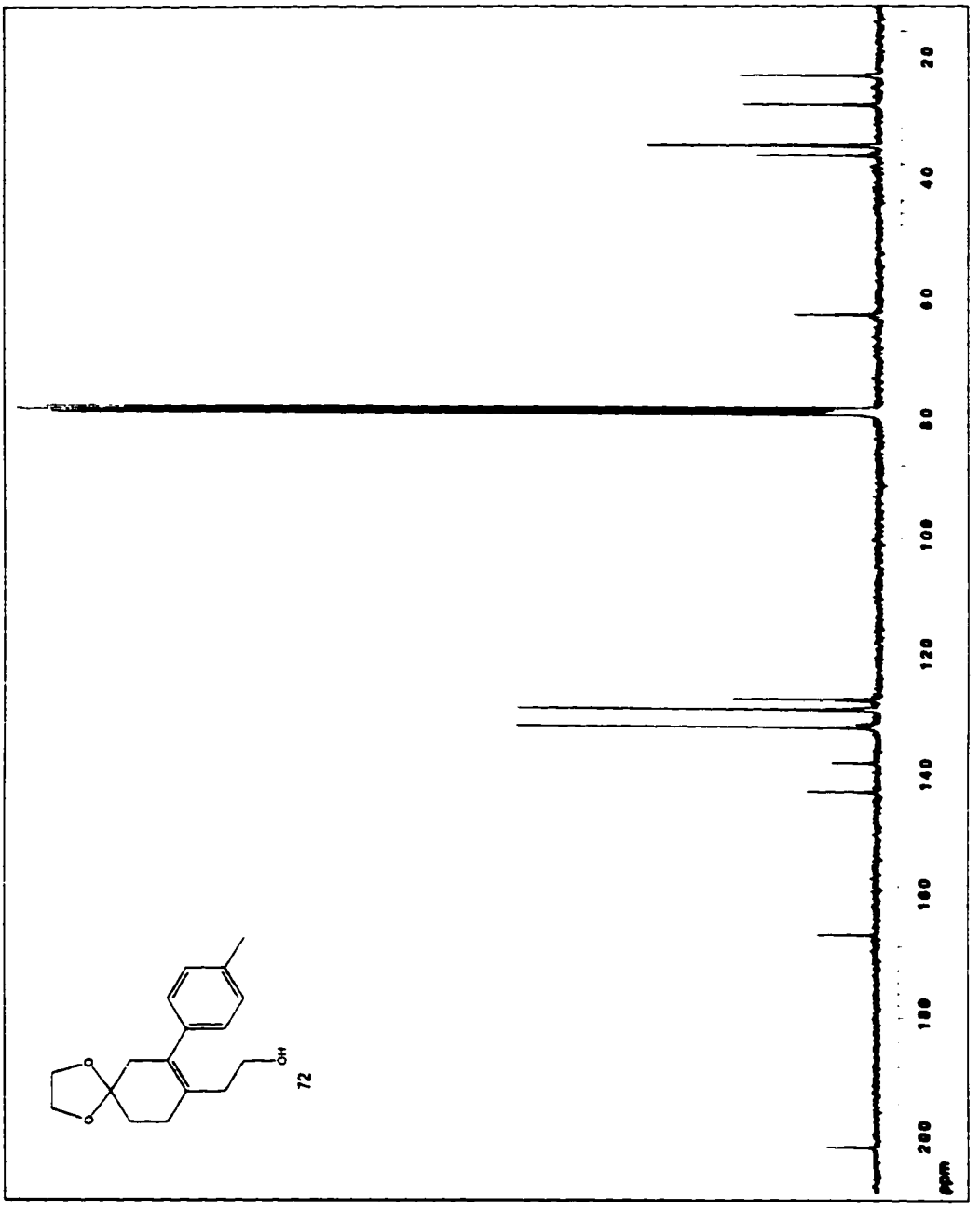

^{13}C NMR spectrum of alcohol **72**

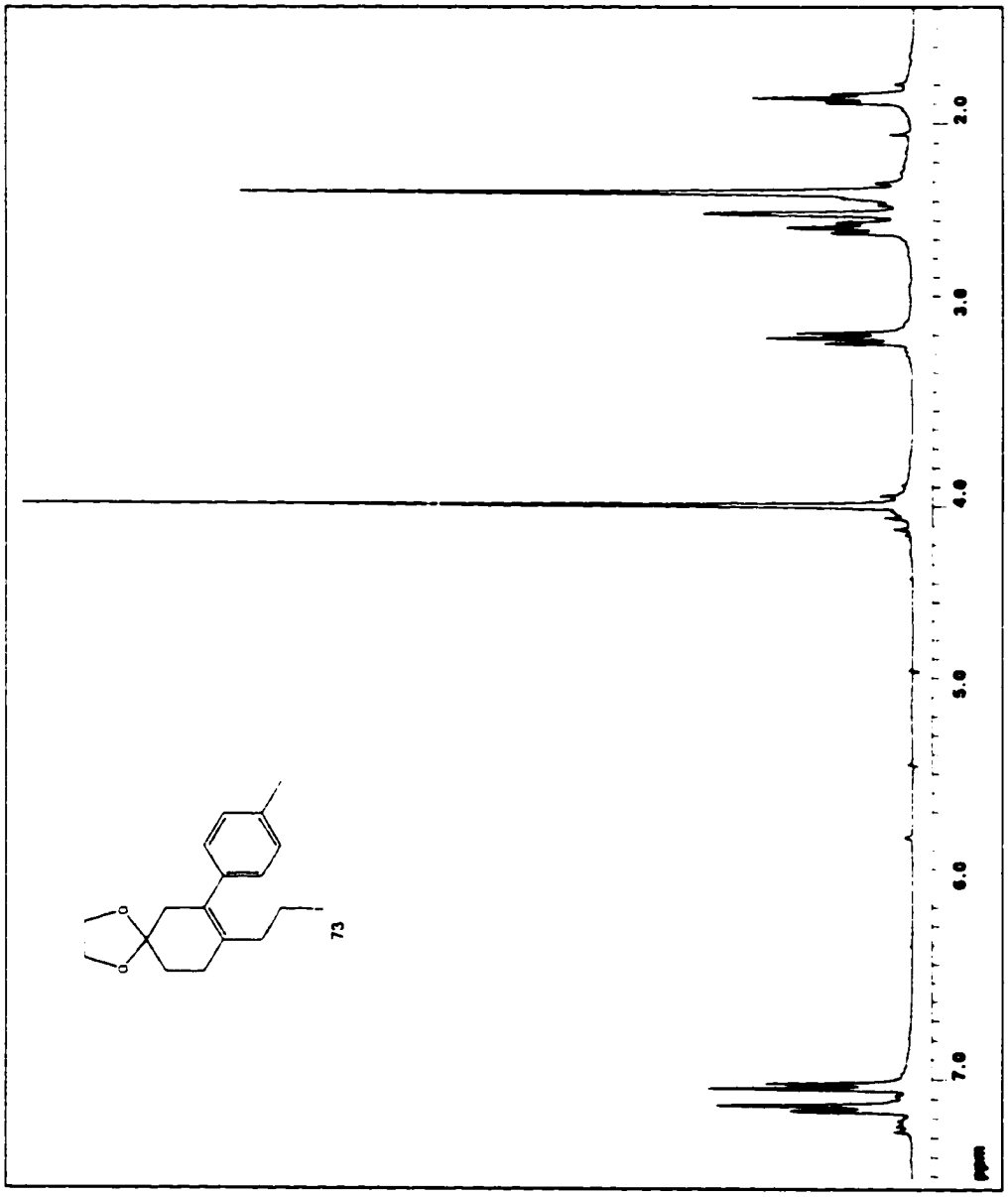

^{1}H NMR spectrum of iodide **73**

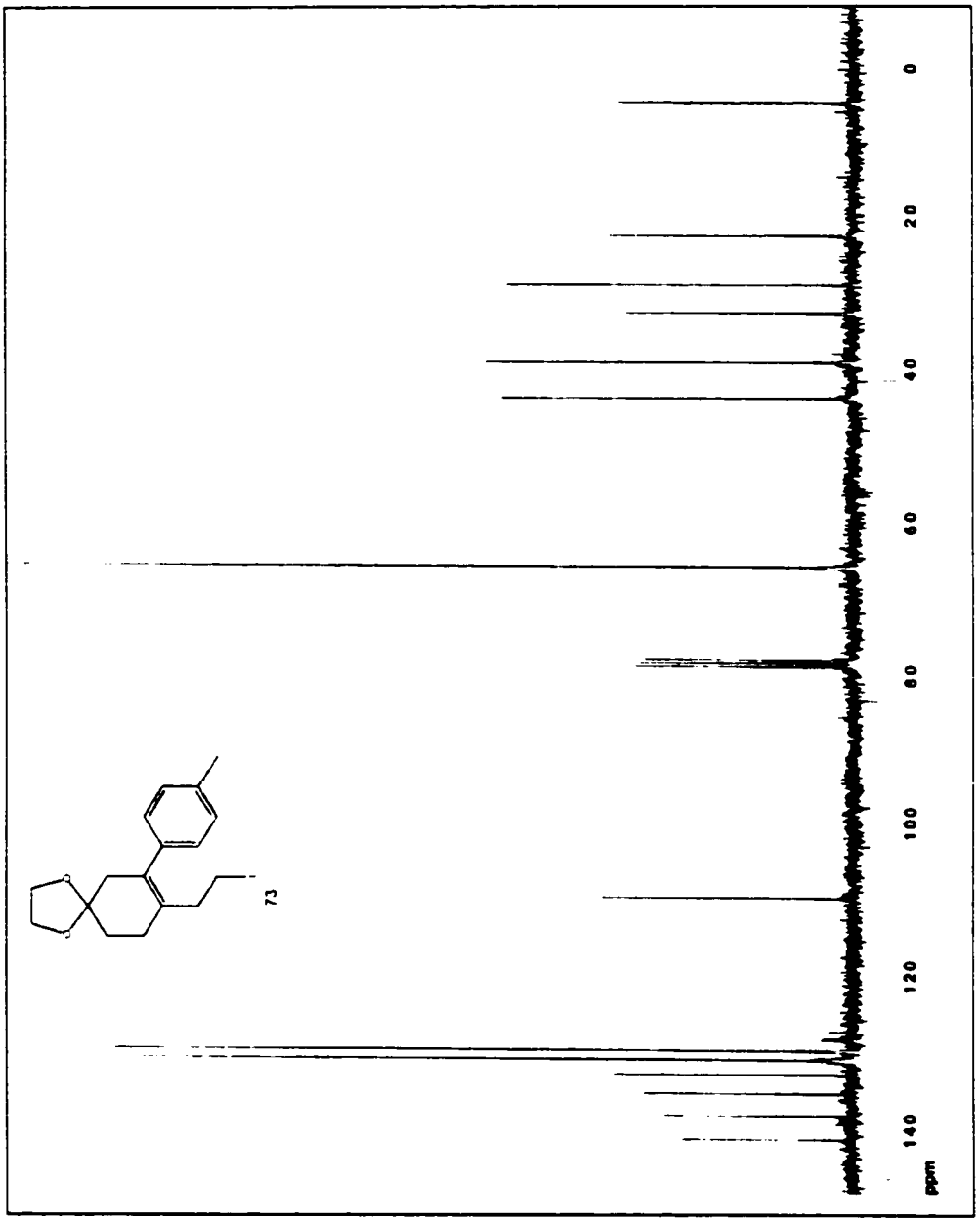

^{13}C NMR spectrum of iodide 73

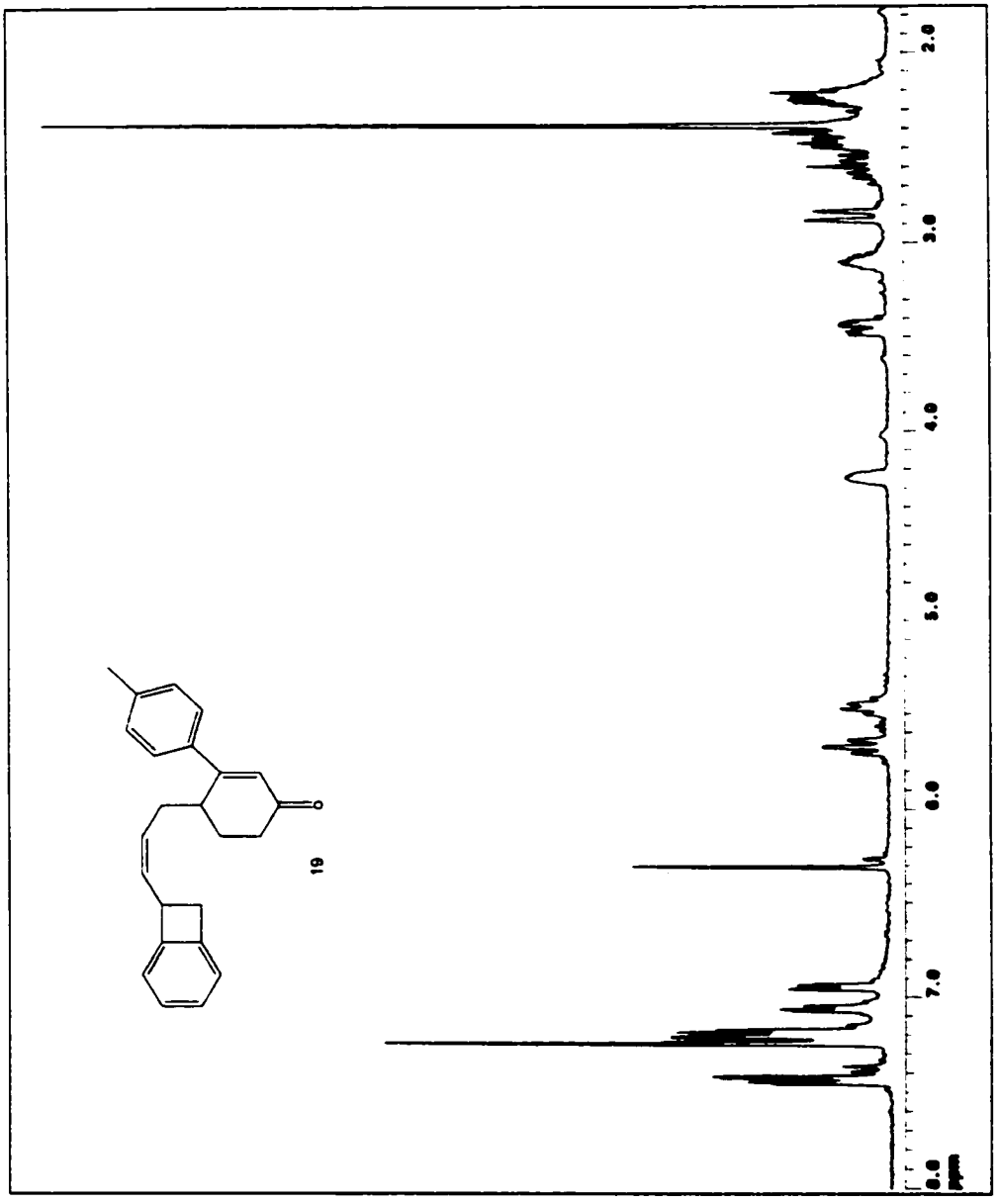

^{1}H NMR spectrum of the Wittig product 19

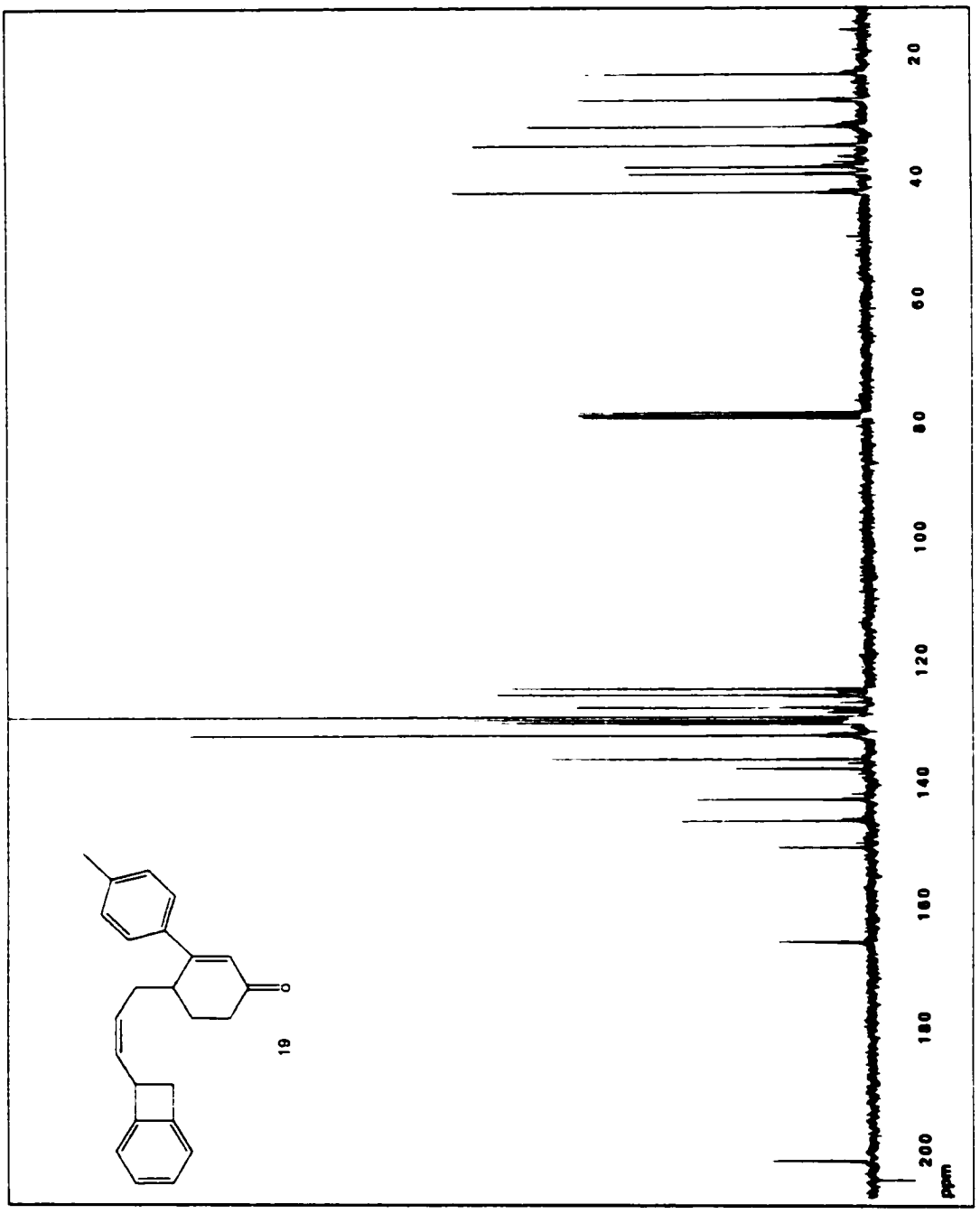

^{13}C NMR spectrum of the Wittig product **19**

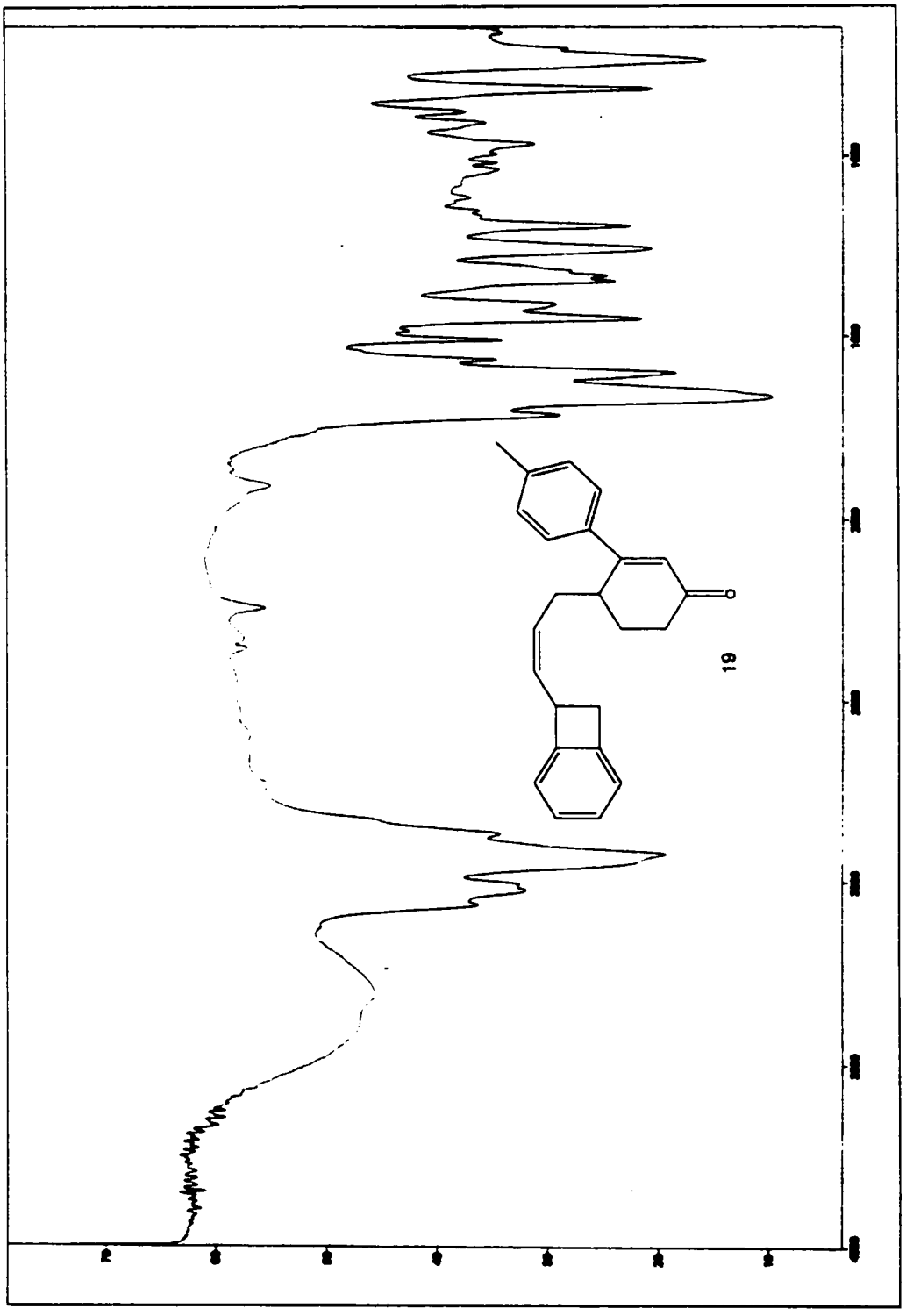

IR spectrum of the Wittig product 19

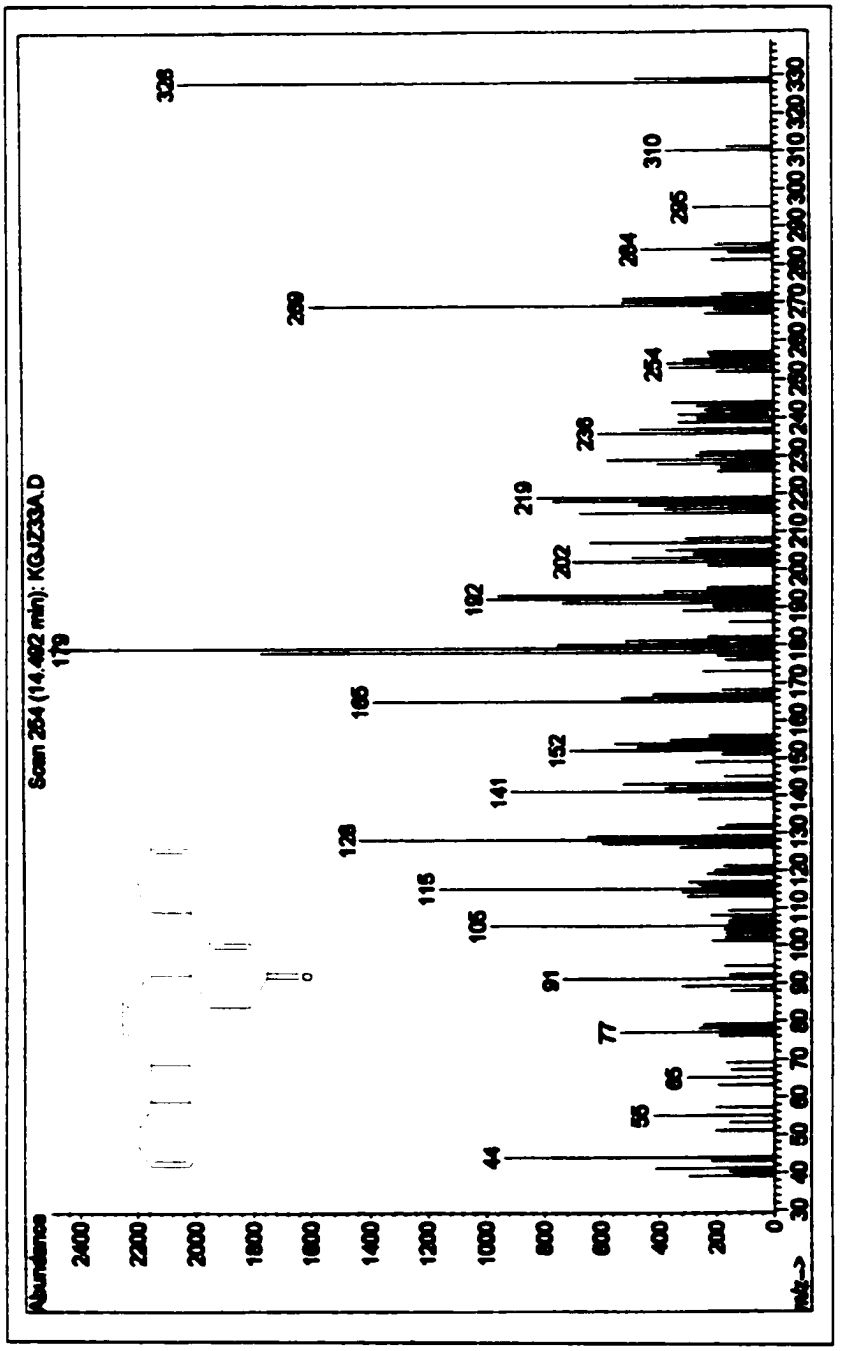

Mass spectrum of the Wittig product 19

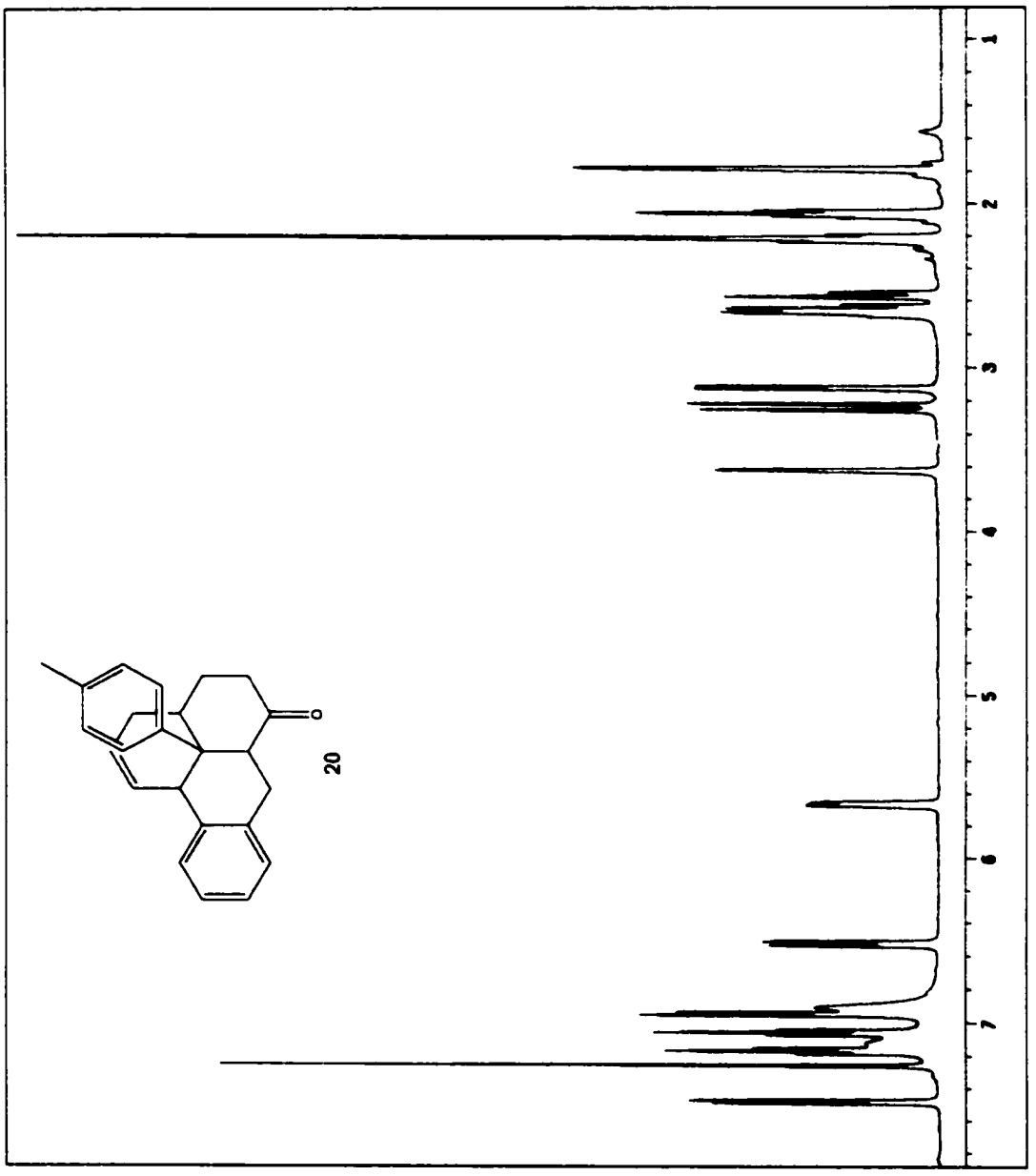

^{1}H NMR spectrum of the IMDA adduct 20

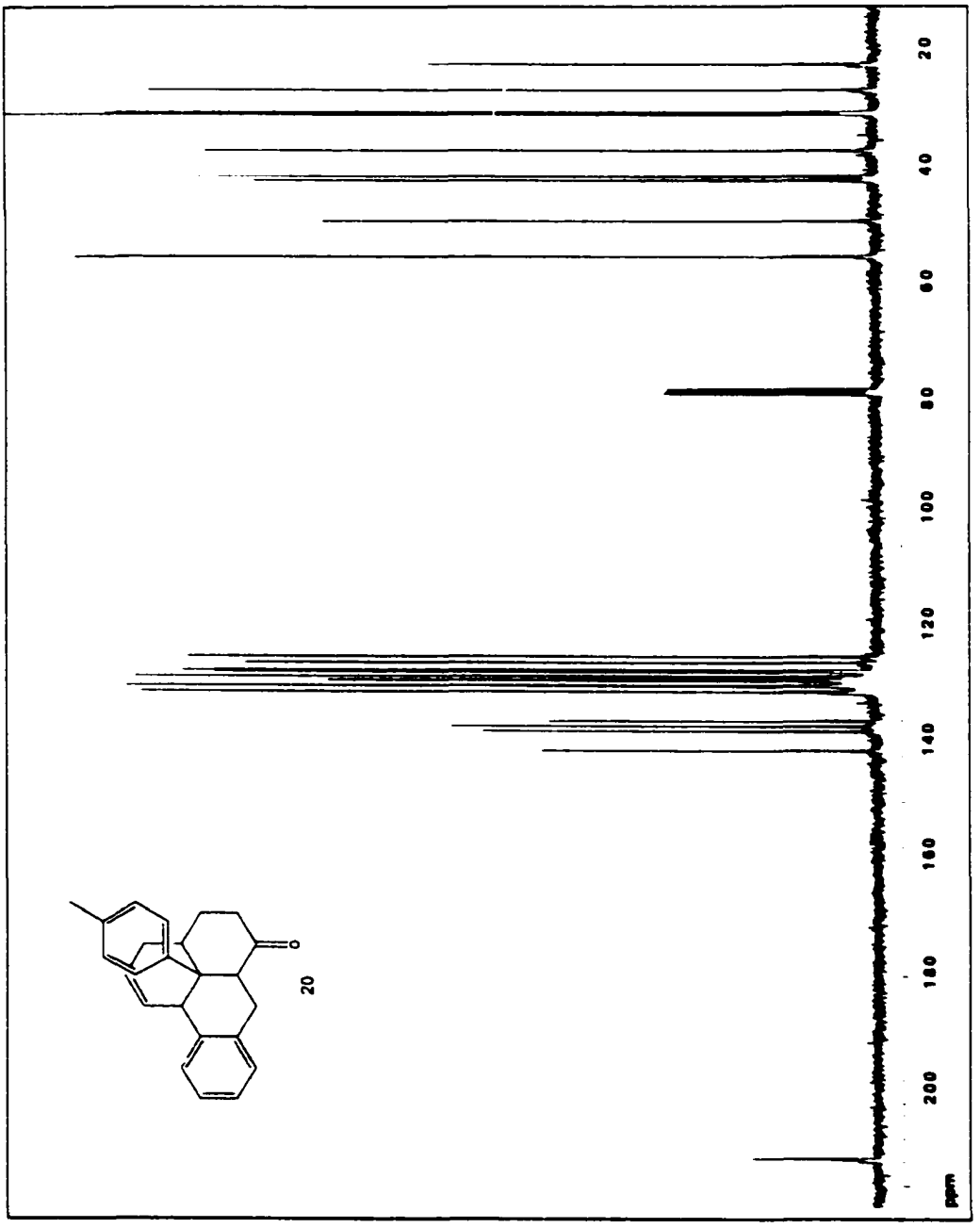

^{13}C NMR spectrum of the IMDA adduct 20

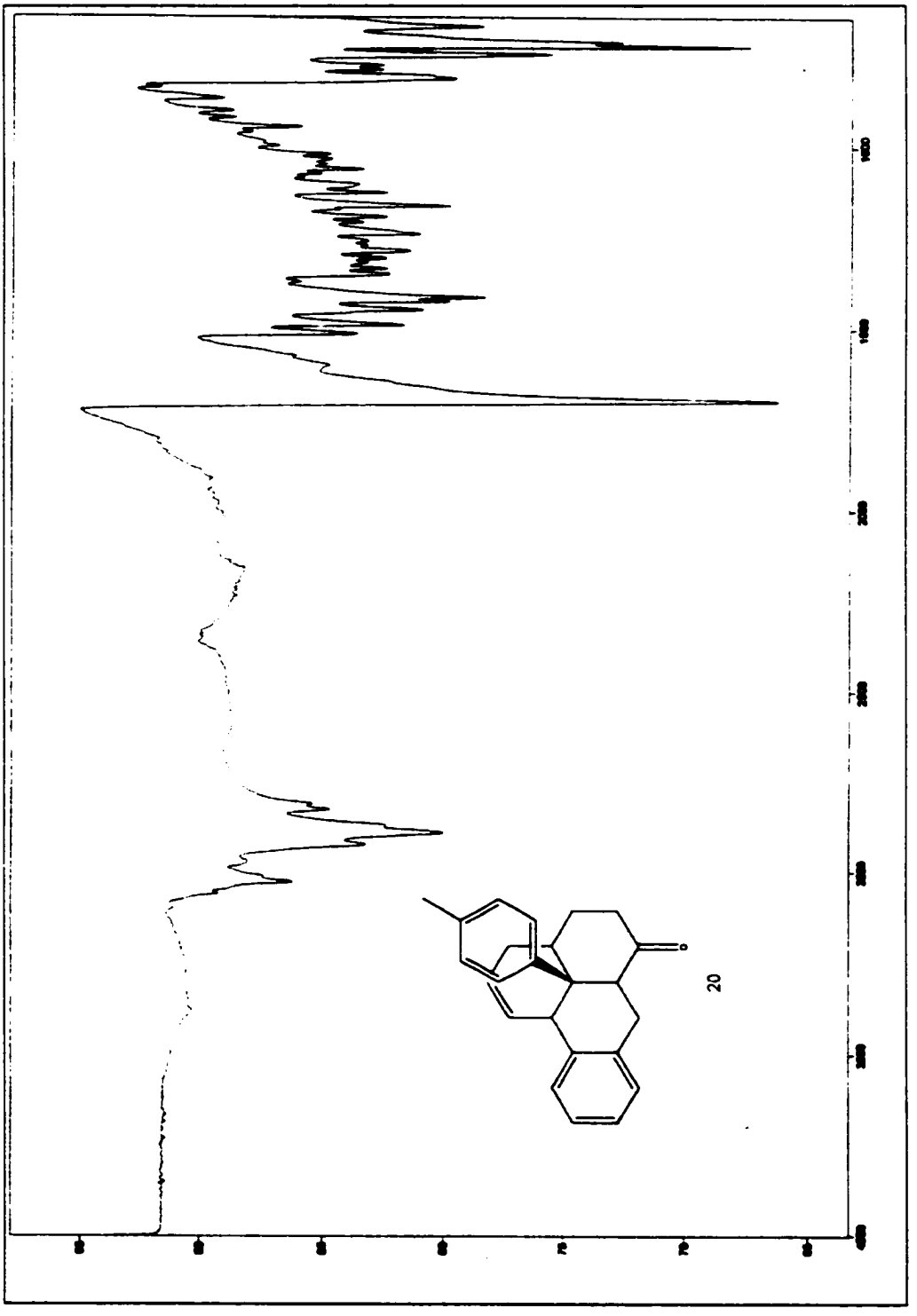

IR spectrum of the IMDA adduct 20

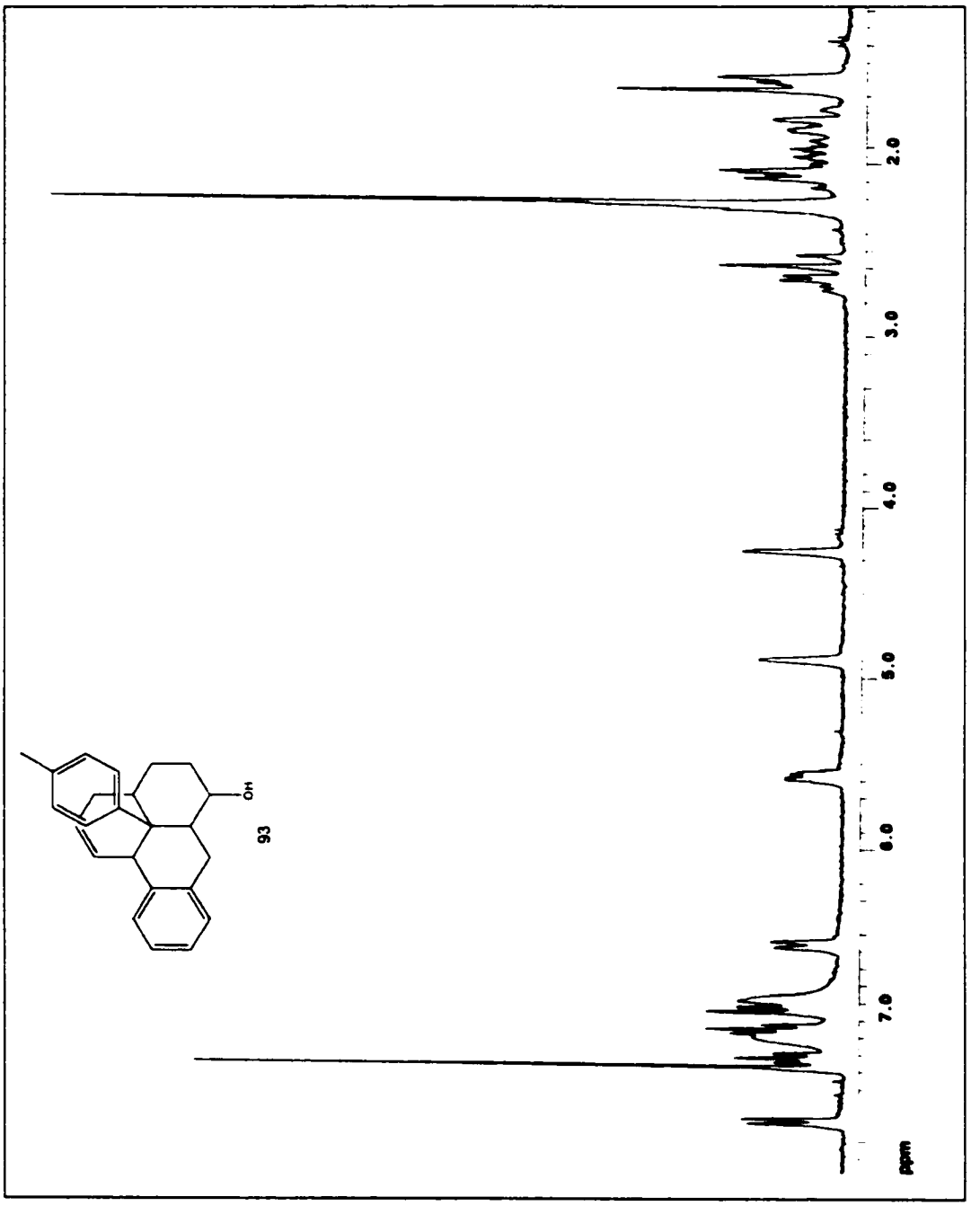

^{1}H NMR spectrum of alcohol 93

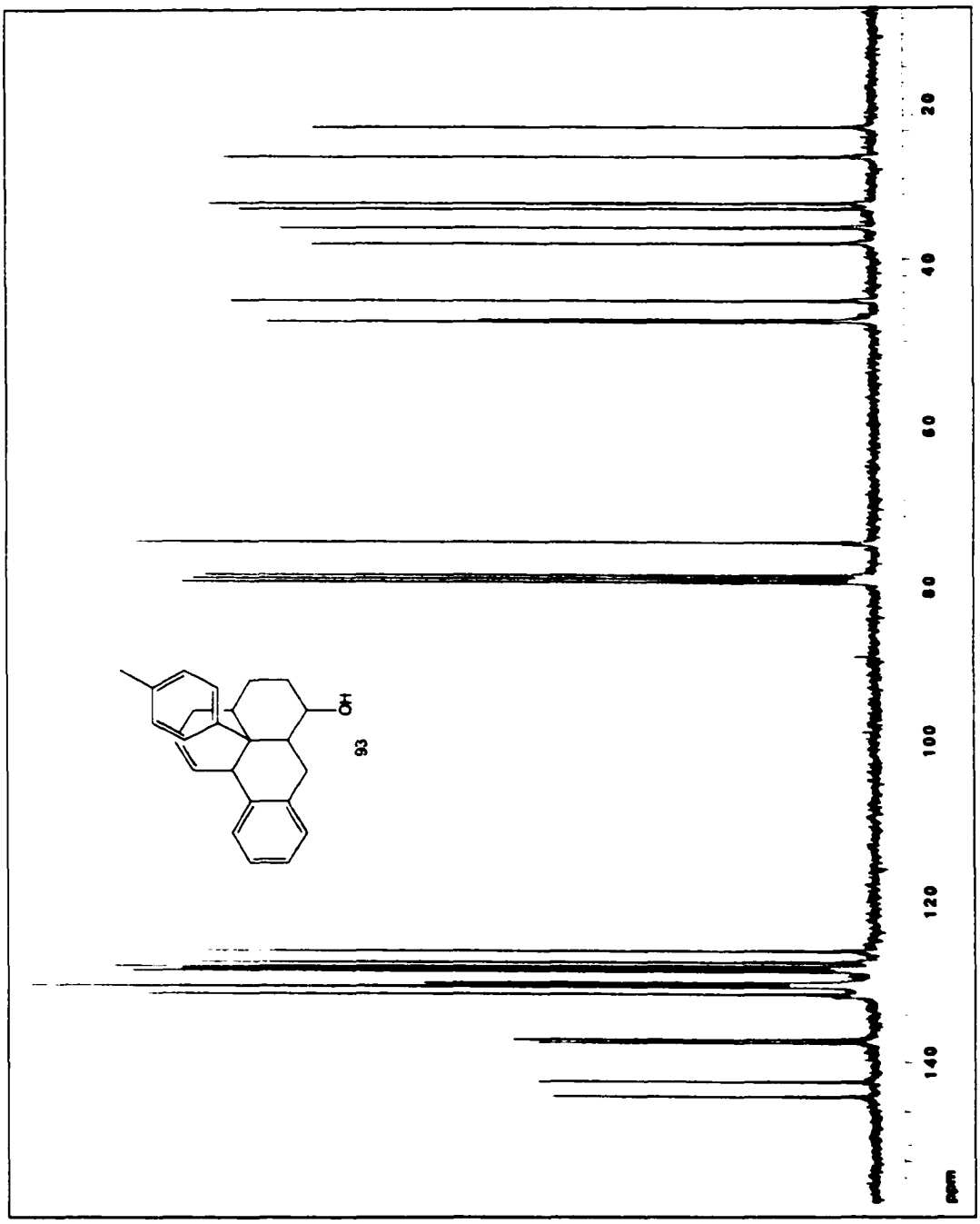

^{13}C NMR spectrum of alcohol 93

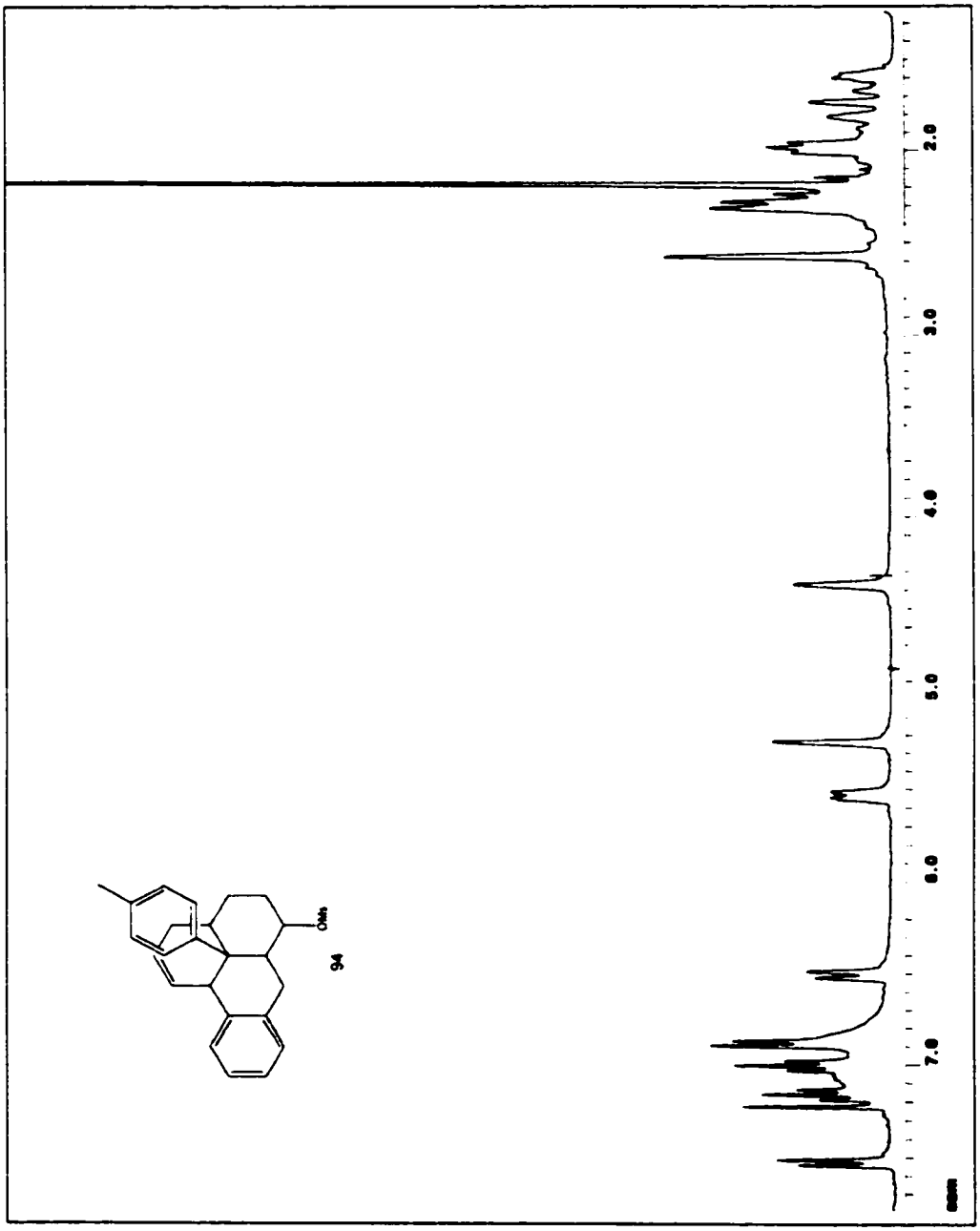

^{1}H NMR spectrum of mesylate 94

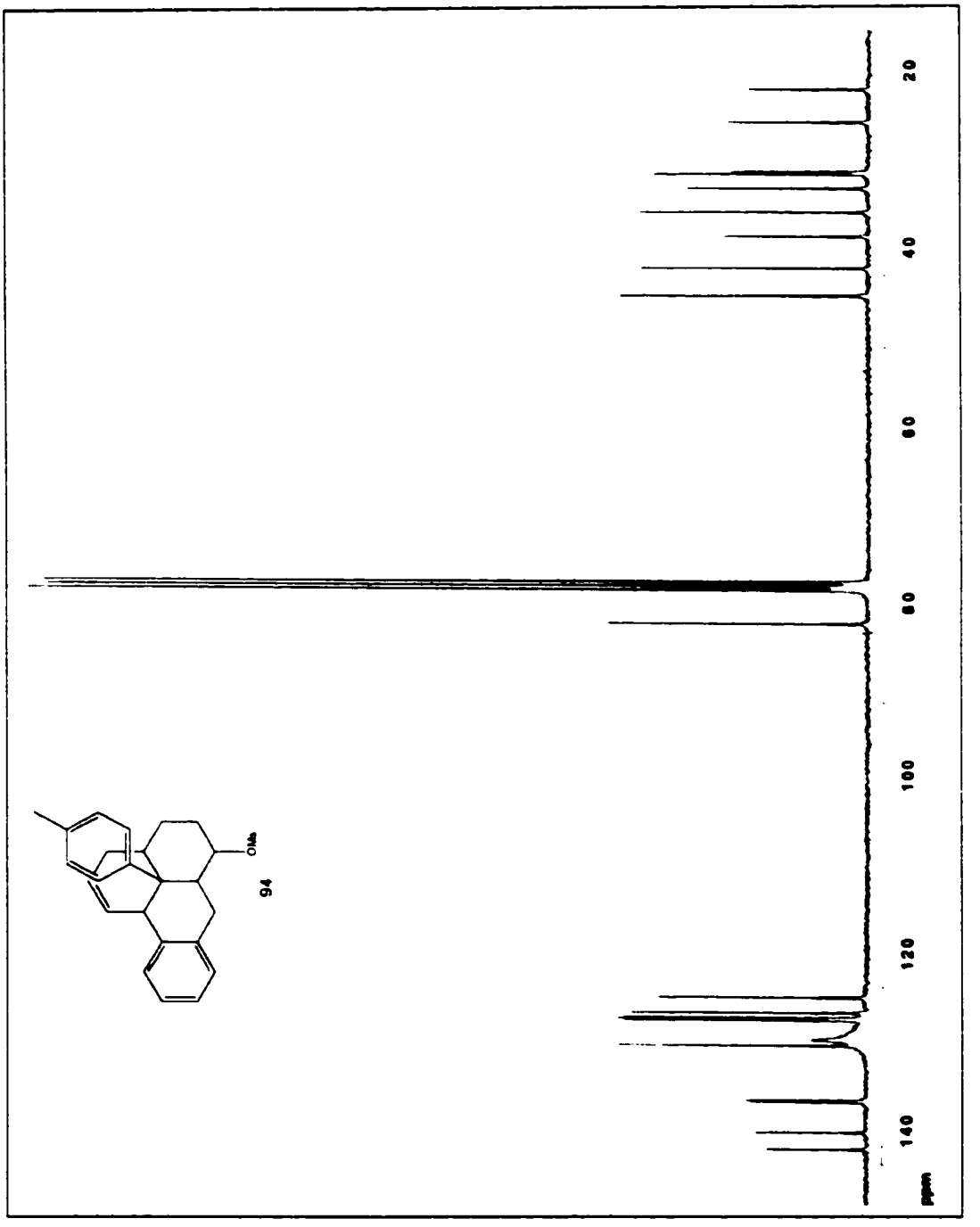

^{13}C NMR spectrum of mesylate 94

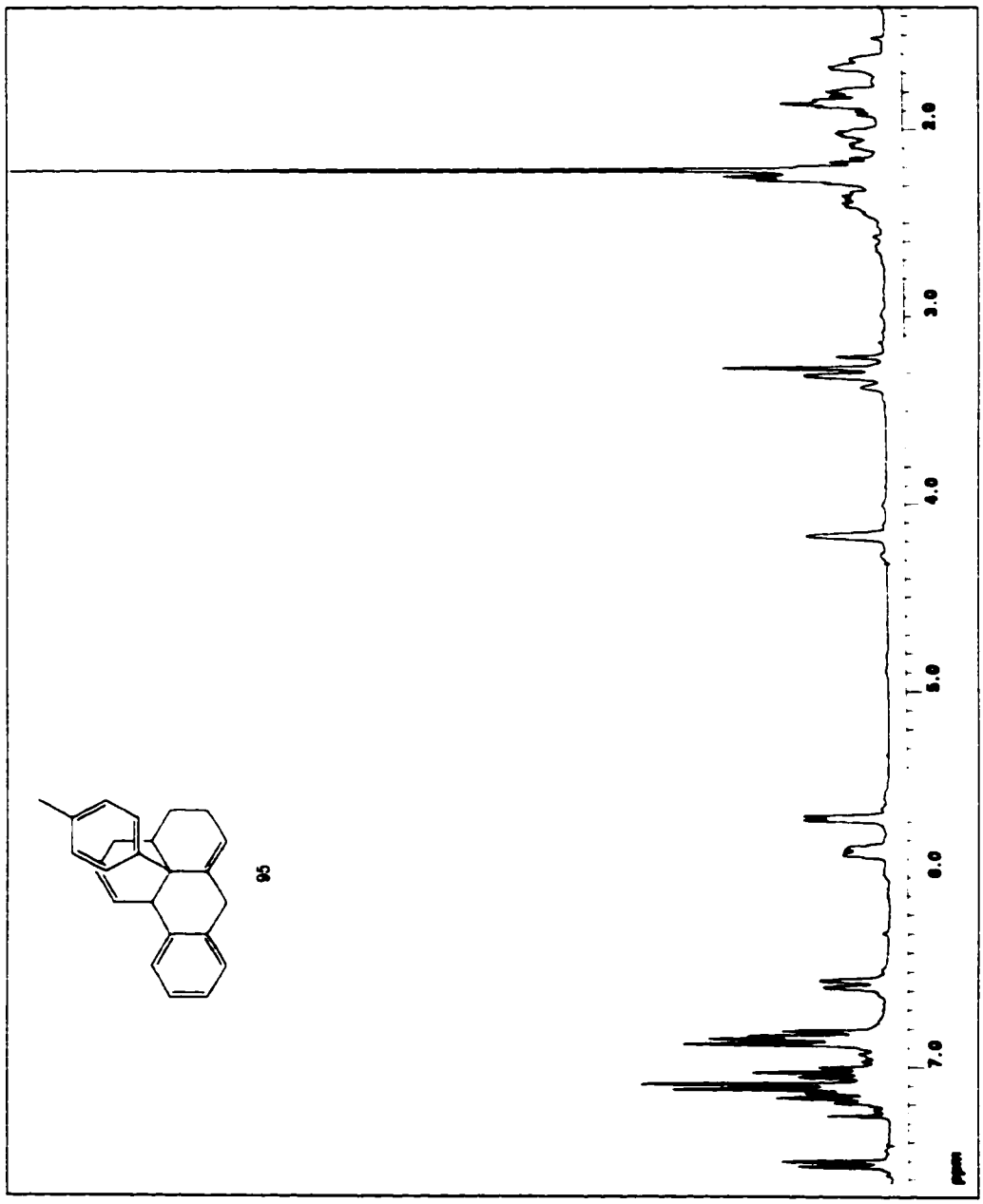

^{1}H NMR spectrum of diene 95

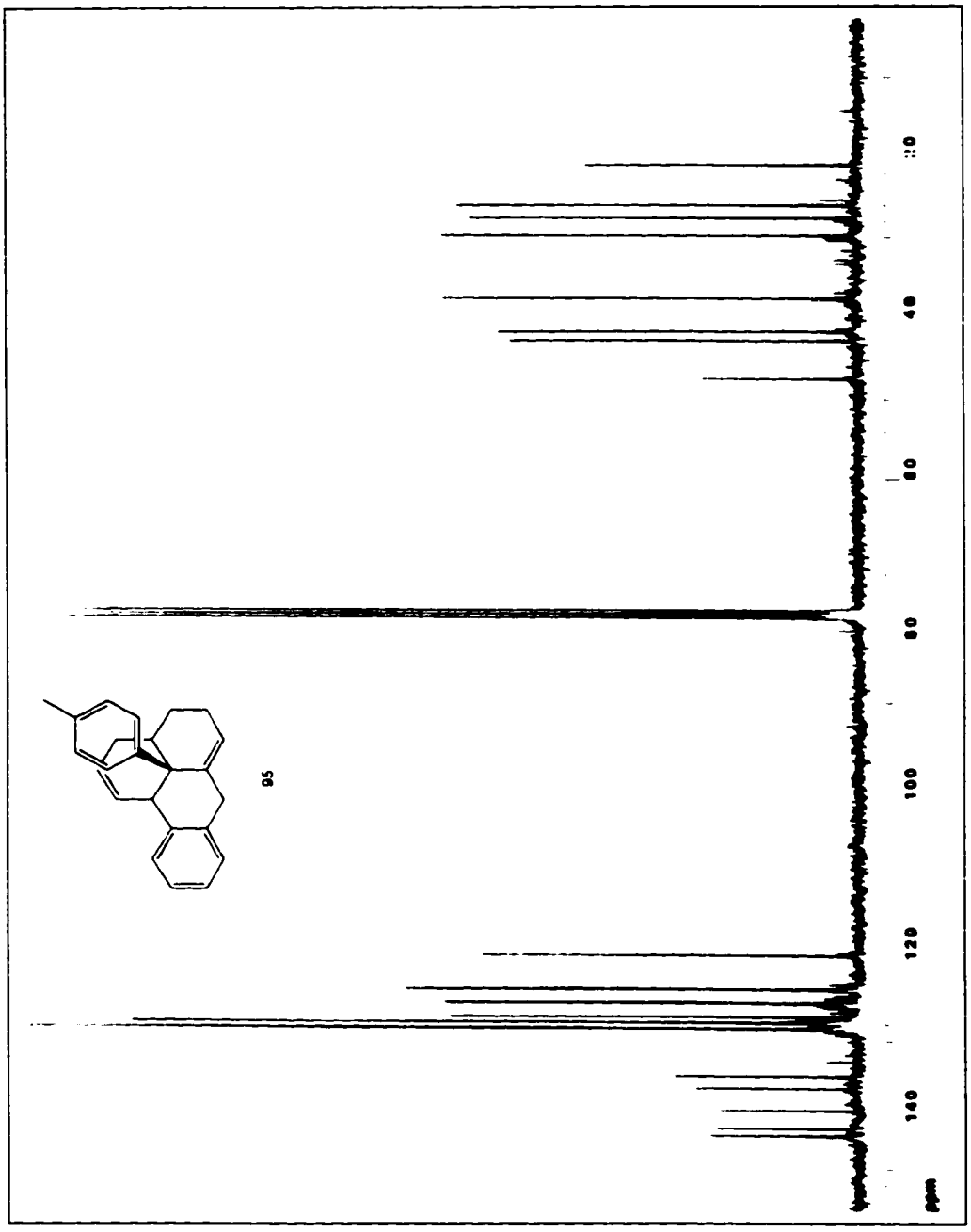

^{13}C NMR spectrum of diene **95**

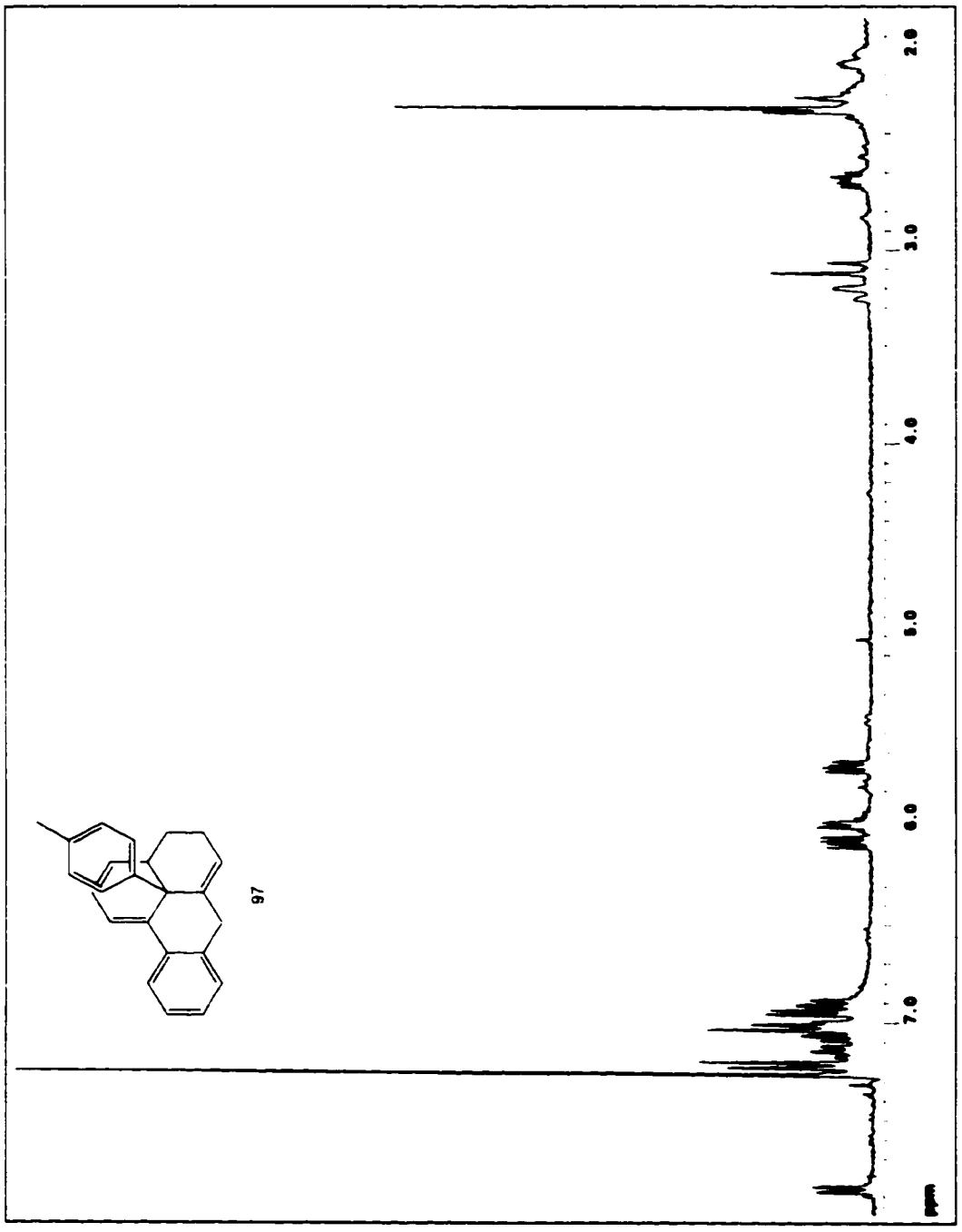

^{1}H NMR spectrum of triene **97**

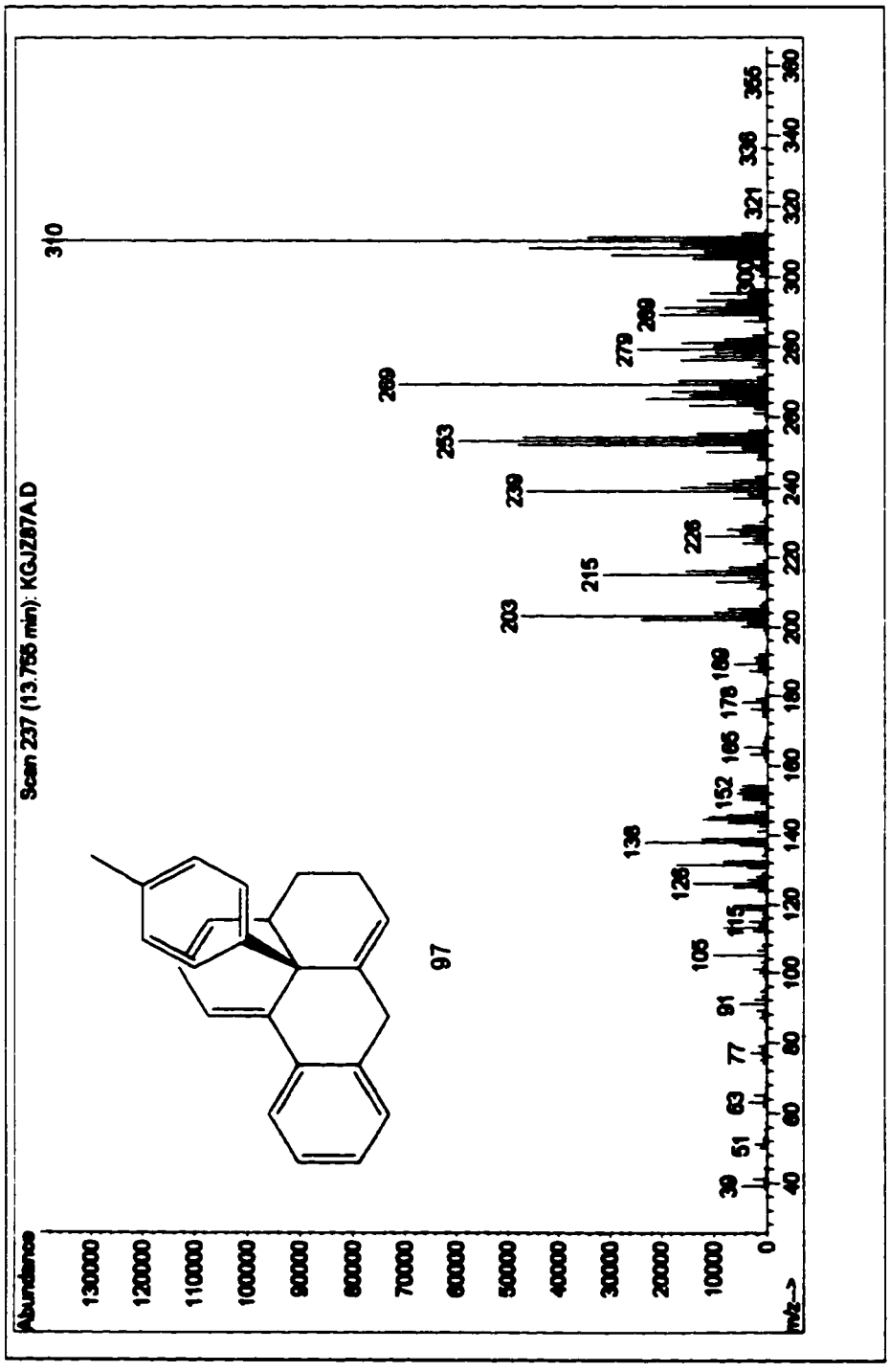

Mass spectrum of triene 97

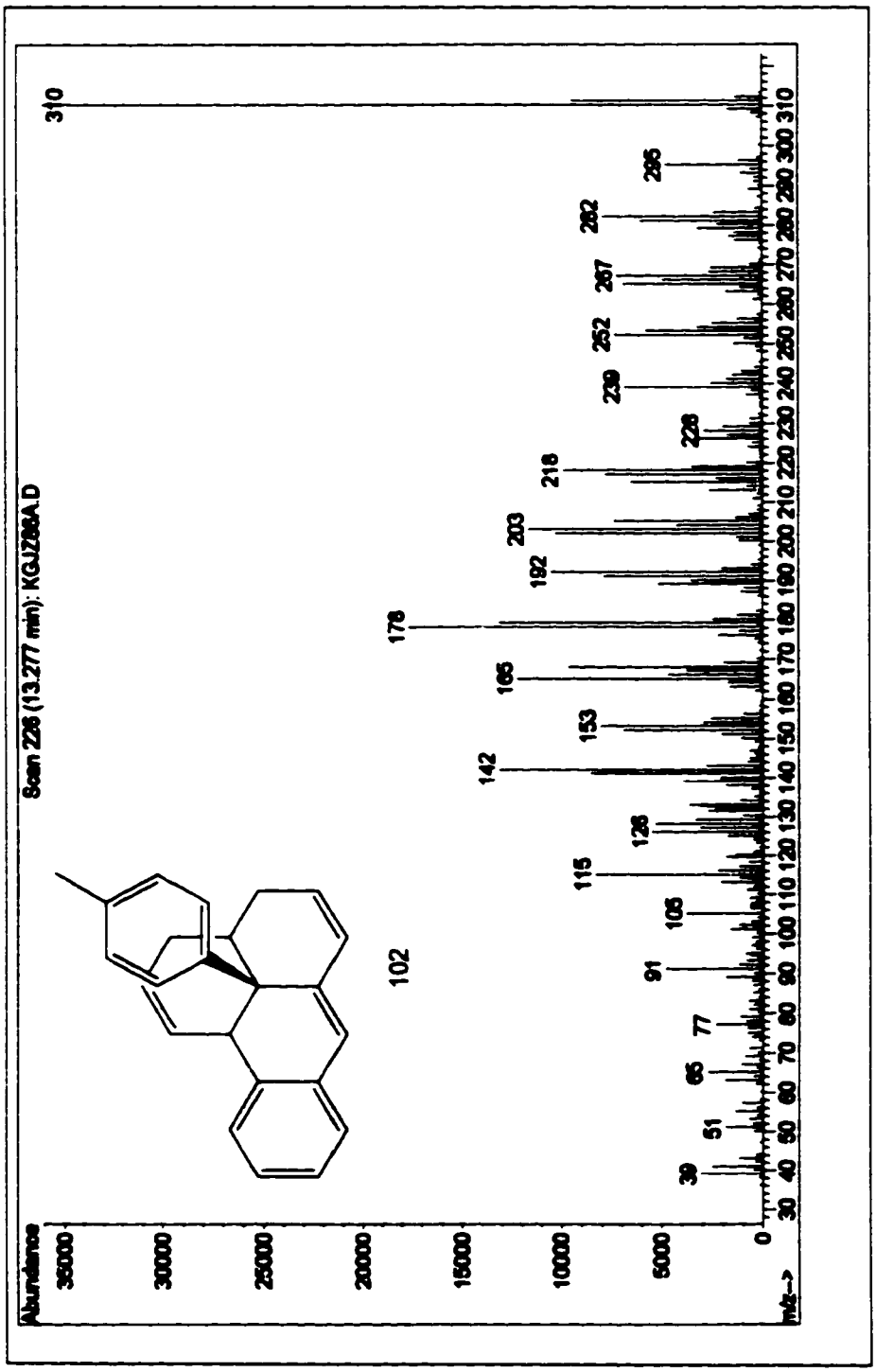

Mass spectrum of triene 102

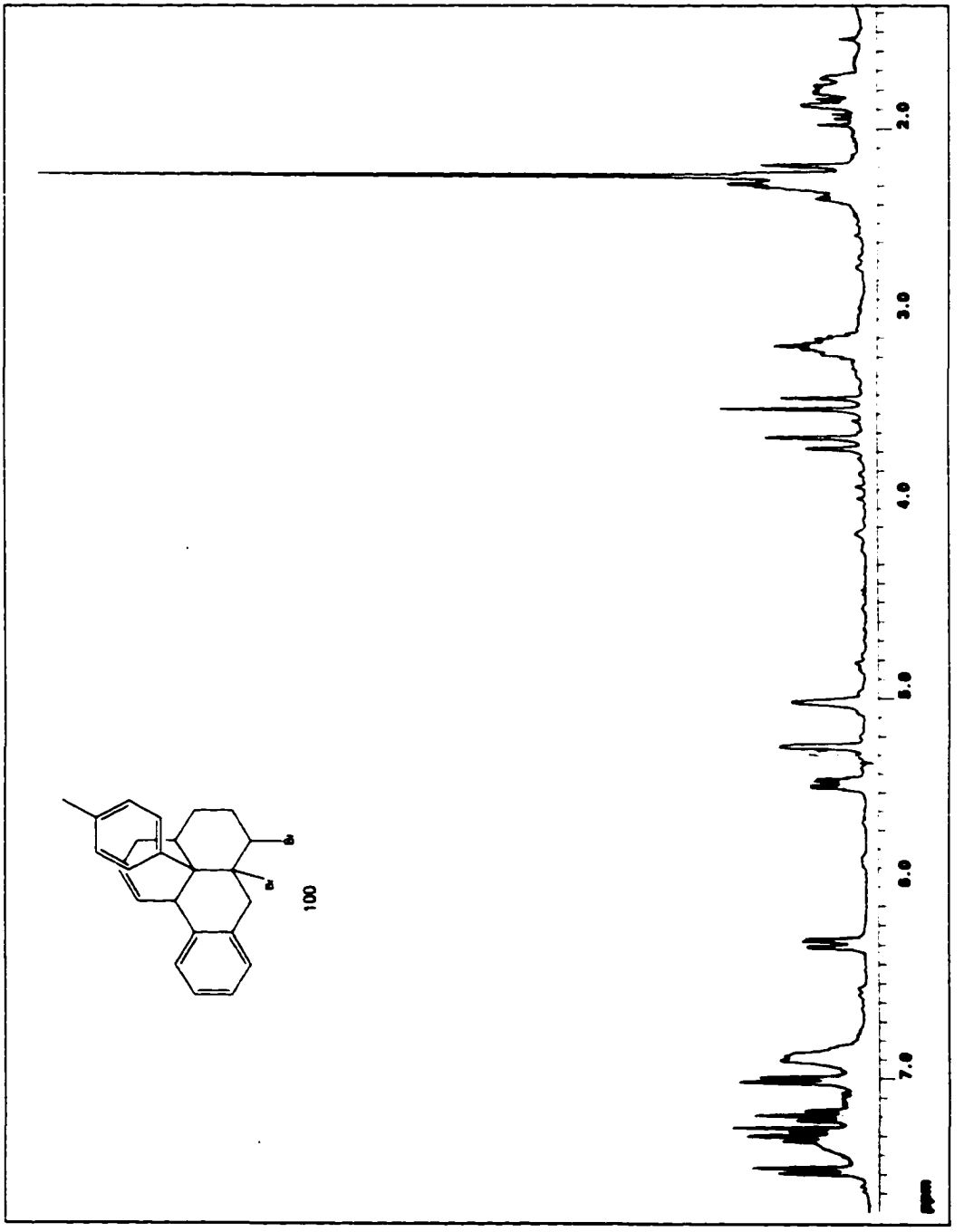

^{1}H NMR spectrum of dibromide **100**

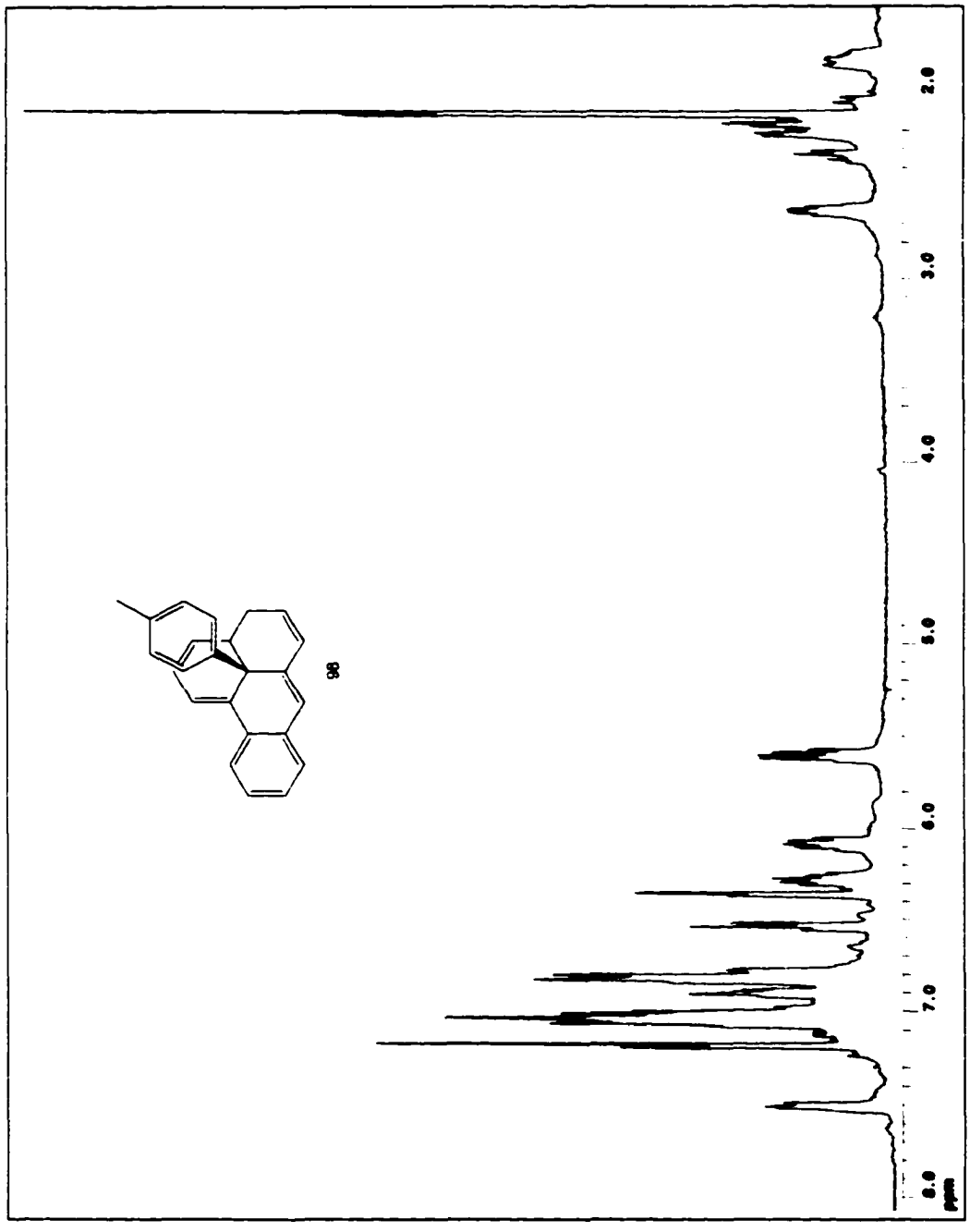

^{1}H NMR spectrum of tetraene 98

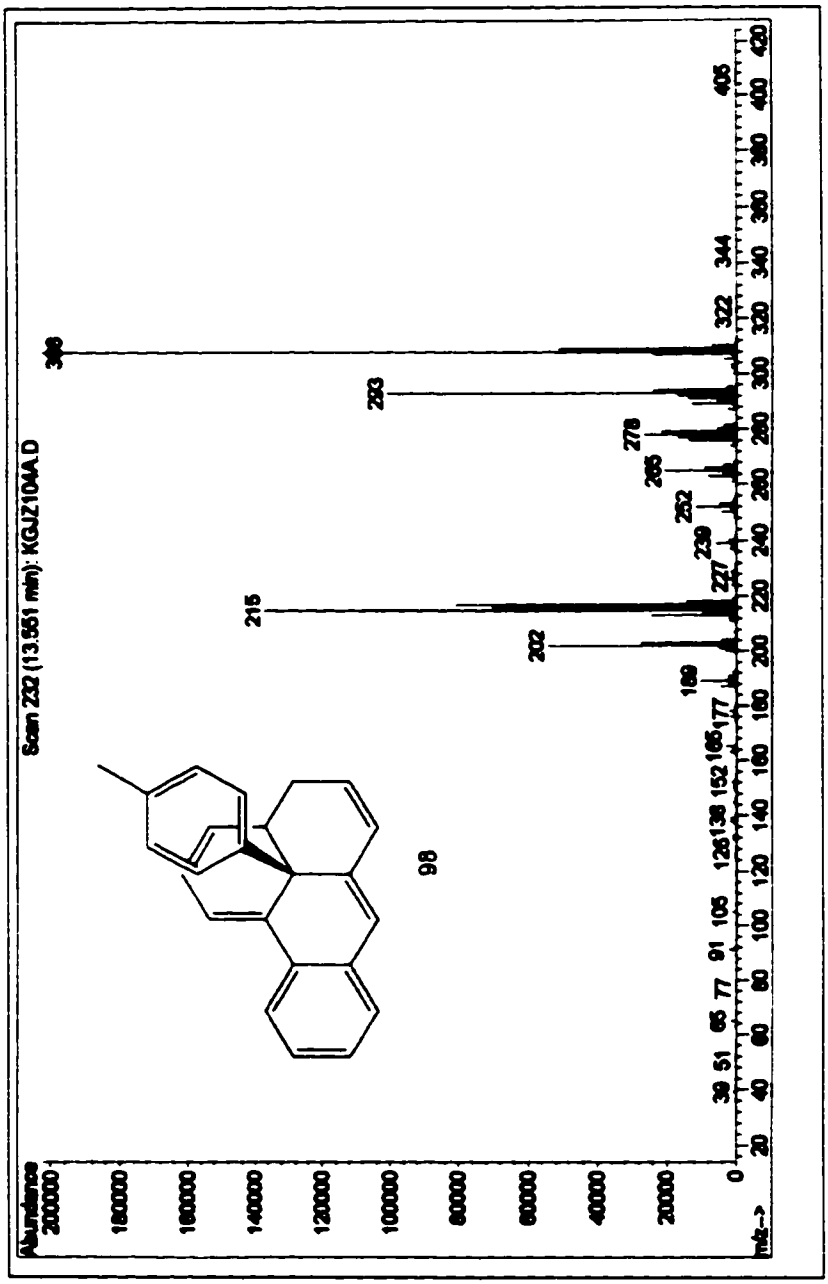

Mass spectrum of tetraene 98

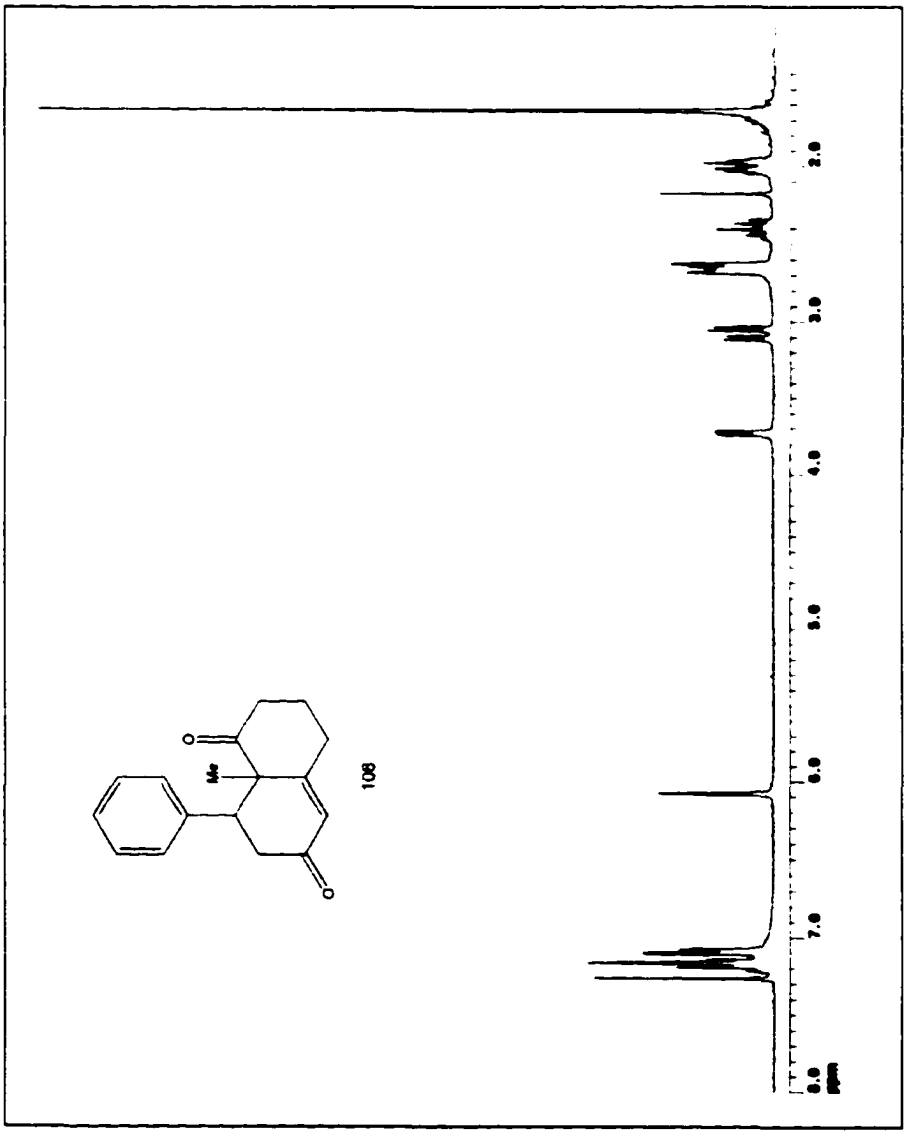

^{1}H NMR spectrum of diketone 108

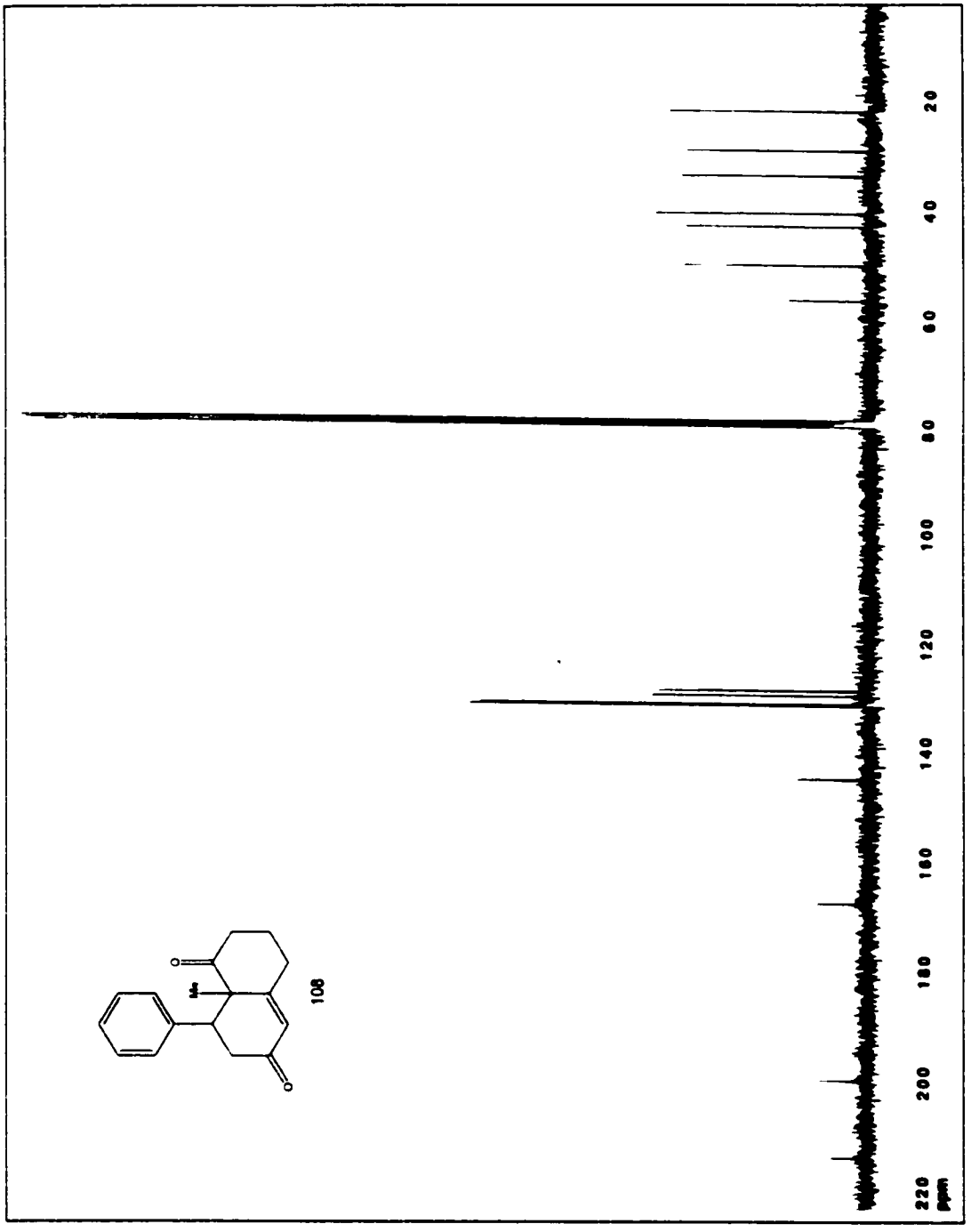

^{13}C NMR spectrum of diketone **108**

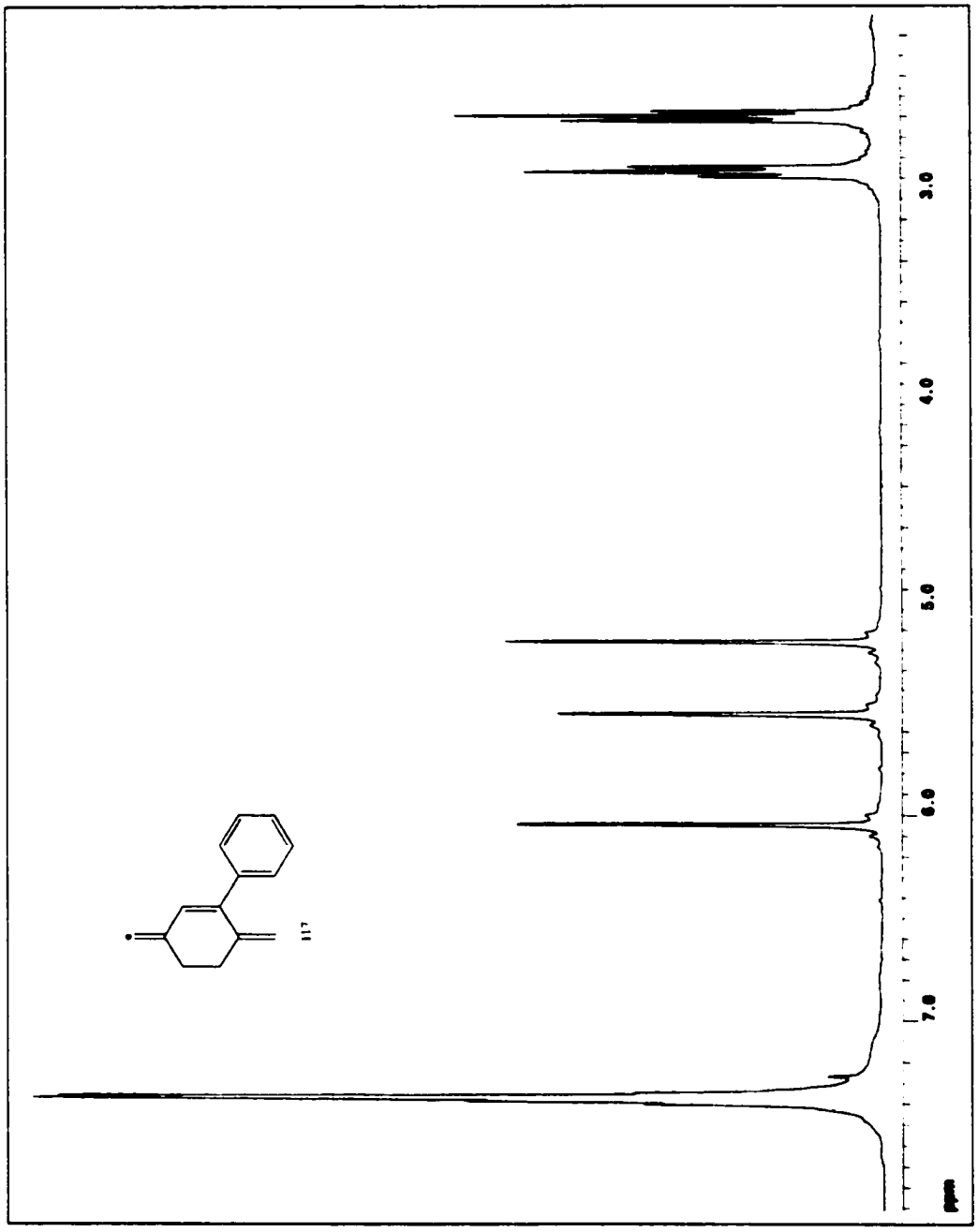

^{1}H NMR spectrum of dienone 117

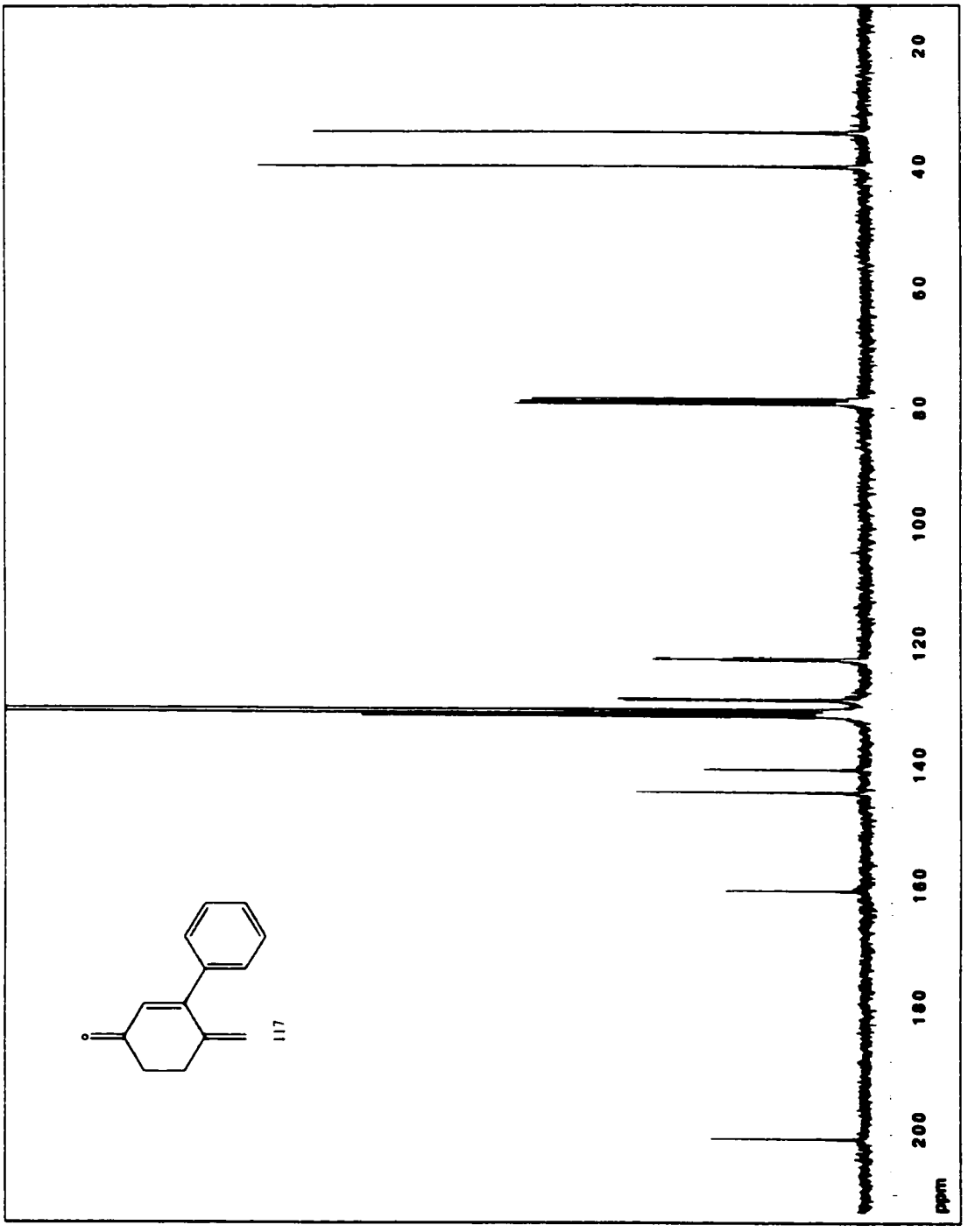

^{13}C NMR spectrum of dienone 117

APPENDIX B.

X-RAY DATA

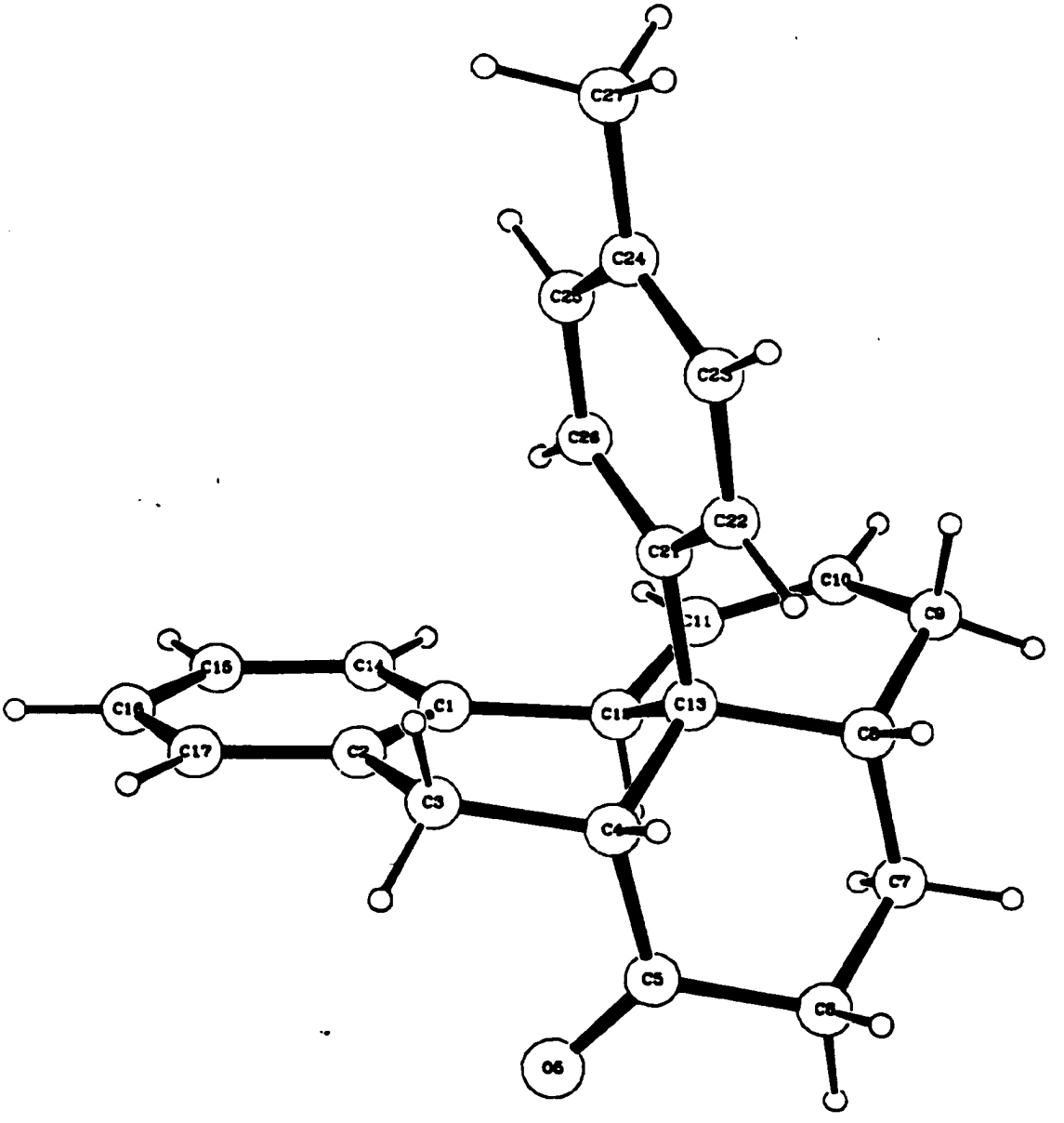

X-ray structure of ketone 20

Table I . X-ray Data for 290-DA at 295 K

Formula	$C_{24}H_{24}O$
Formula weight	328.458
Crystal size (mm)	0.24 x 0.40 x 0.40
Crystal system	monoclinic
Space group	$P2_1/n$
a (Å)	8.2970(2)
b (Å)	7.9540(2)
c (Å)	27.0730(6)
β (°)	90.879(1)
V (Å^3)	1786.51(7)
Z	8
d_{calc} (g cm^{-3})	1.221
μ(Mo $K\alpha$) (cm^{-1})	0.7243
Absorption correction	none
Maximum θ (°)	30
Unique reflections	4488
Observed reflections	2782
[$I > 3.0\sigma(I)$]	
Number of variables	227
R	0.0470

R_w	0.0512
$(\Delta\rho)_{max}$ (e Å^{-3})	0.18
$(\Delta\rho)_{min}$ (e Å^{-3})	–0.12

Table II. Final Atomic Parameters for 290-DA

Atom	x	y	z	B(Å^2)
O5	0.1405(1)	0.2261(1)	0.24292(4)	4.96(3)
C1	0.2755(2)	0.0413(2)	0.12591(5)	3.02(3)
C2	0.1729(2)	0.1807(2)	0.12151(5)	3.27(3)
C3	0.2073(2)	0.3438(2)	0.14774(6)	3.65(3)
C4	0.3384(2)	0.3349(2)	0.18758(5)	3.05(3)
C5	0.2801(2)	0.2660(2)	0.23646(5)	3.47(3)
C6	0.4061(2)	0.2516(2)	0.27649(6)	3.98(3)
C7	0.5539(2)	0.1542(2)	0.25913(6)	3.78(3)
C8	0.6171(2)	0.2209(2)	0.21048(5)	3.20(3)
C9	0.7593(2)	0.1161(2)	0.19229(6)	4.09(3)
C10	0.7071(2)	-0.0388(2)	0.16589(6)	4.15(3)
C11	0.5576(2)	-0.0694(2)	0.15125(6)	3.82(3)
C12	0.4208(2)	0.0490(2)	0.16094(5)	2.88(3)
C13	0.4843(2)	0.2291(1)	0.16968(5)	2.71(3)
C14	0.2347(2)	-0.1051(2)	0.10029(6)	4.19(4)
C15	0.0969(2)	-0.1128(2)	0.07097(7)	5.44(4)
C16	-0.0026(2)	0.0248(2)	0.06642(7)	5.37(4)
C17	0.0354(2)	0.1700(2)	0.09132(6)	4.21(3)
C21	0.5543(2)	0.3099(2)	0.12307(5)	2.90(3)
C22	0.6171(2)	0.4721(2)	0.12594(6)	4.02(3)
C23	0.6852(2)	0.5492(2)	0.08525(6)	4.43(4)
C24	0.6928(2)	0.4695(2)	0.04003(6)	3.82(3)
C25	0.6306(2)	0.3089(2)	0.03716(6)	3.86(3)

C26	0.5629(2)	0.2301(2)	0.07773(5)	3.27(3)
C27	0.7650(2)	0.5554(2)	-0.00407(6)	5.43(4)
H3A	0.106	0.382	0.164	4.4
H3B	0.241	0.428	0.123	4.4
H4	0.373	0.454	0.194	3.7
H6A	0.359	0.192	0.305	4.8
H6B	0.440	0.367	0.287	4.8
H7A	0.524	0.033	0.255	4.5
H7B	0.641	0.164	0.285	4.5
H8	0.655	0.338	0.217	3.8
H9A	0.828	0.083	0.221	4.9
H9B	0.824	0.186	0.169	4.9
H10	0.791	-0.126	0.159	5.0
H11	0.534	-0.176	0.133	4.6
H12	0.373	0.006	0.192	3.5
H14	0.306	-0.206	0.103	5.0
H15	0.070	-0.219	0.053	6.5
H16	-0.102	0.019	0.045	6.4
H17	-0.037	0.270	0.088	5.1
H22	0.613	0.534	0.158	4.8
H23	0.730	0.665	0.089	5.3
H25	0.634	0.247	0.005	4.6
H26	0.520	0.113	0.074	3.9
H27A	0.760	0.478	-0.033	6.5
H27B	0.703	0.660	-0.012	6.5
H27C	0.880	0.585	0.003	6.5

Table II (Cont'd). Final Atomic Parameters for 290-DA

Atom	x	y	z	B(Å^2)
H27BA	0.803	0.670	0.006	6.5
H27BB	0.858	0.488	-0.016	6.5
H27BC	0.682	0.565	-0.031	6.5

The parameters of the hydrogen atoms were not refined.

Standard deviations are in parentheses.

Anisotropically refined atoms are given in the form of the isotropic equivalent displacement parameter defined as:

(4/3) * [a2*B(1,1) + b2*B(2,2) + c2*B(3,3) + ab(cos gamma)*B(1,2) + ac(cos beta)*B(1,3) + bc(cos alpha)*B(2,3)]

Table IV. Bond Distances (Å) for 290-DA

Atom 1	Atom 2	Distance	Atom 1	Atom 2	Distance
O5	C5	1.216(2)	C10	C11	1.320(2)
C1	C2	1.401(2)	C11	C12	1.500(2)
C1	C12	1.524(2)	C12	C13	1.544(2)
C1	C14	1.395(2)	C13	C21	1.538(2)
C2	C3	1.504(2)	C14	C15	1.383(2)
C2	C17	1.396(2)	C15	C16	1.376(2)
C3	C4	1.522(2)	C16	C17	1.371(2)
C4	C5	1.518(2)	C21	C22	1.393(2)
C4	C13	1.557(2)	C21	C26	1.385(2)
C5	C6	1.499(2)	C22	C23	1.389(2)
C6	C7	1.530(2)	C23	C24	1.381(2)
C7	C8	1.520(2)	C24	C25	1.380(2)
C8	C9	1.532(2)	C24	C27	1.508(2)
C8	C13	1.549(2)	C25	C26	1.390(2)
C9	C10	1.485(2)			

Standard deviations are in parentheses.

Table V. Bond Angles (°) for 290-DA

Atom 1	Atom 2	Atom 3	Angle	Atom 1	Atom 2	Atom 3	Angle
C2	C1	C12	119.7(1)	C1	C12	C13	113.4(1)
C2	C1	C14	118.4(1)	C11	C12	C13	110.6(1)
C12	C1	C14	121.8(1)	C4	C13	C8	110.4(1)
C1	C2	C3	122.1(1)	C4	C13	C12	106.5(1)
C1	C2	C17	119.4(1)	C4	C13	C21	109.6(1)
C3	C2	C17	118.5(1)	C8	C13	C12	107.9(1)
C2	C3	C4	115.0(1)	C8	C13	C21	109.2(1)
C3	C4	C5	113.6(1)	C12	C13	C21	113.2(1)
C3	C4	C13	110.8(1)	C1	C14	C15	121.0(1)
C5	C4	C13	109.6(1)	C14	C15	C16	120.4(2)
O5	C5	C4	122.4(1)	C15	C16	C17	119.5(2)
O5	C5	C6	122.1(1)	C2	C17	C16	121.3(1)

C4	C5	C6	115.5(1)	C13	C21	C22
			119.1(1)			
C5	C6	C7	111.7(1)	C13	C21	C26
			124.1(1)			
C6	C7	C8	112.2(1)	C22	C21	C26
			116.7(1)			
C7	C8	C9	111.5(1)	C21	C22	C23
			121.4(1)			
C7	C8	C13	112.4(1)	C22	C23	C24
			121.7(1)			
C9	C8	C13	109.7(1)	C23	C24	C25
			116.9(1)			
C8	C9	C10	112.7(1)	C23	C24	C27
			121.2(1)			
C9	C10	C11	124.3(1)	C25	C24	C27
			121.9(1)			
C10	C11	C12	122.8(1)	C24	C25	C26
			121.9(1)			
C1	C12	C11	117.4(1)	C21	C26	C25
			121.4(1)			

Standard deviations are in parentheses.

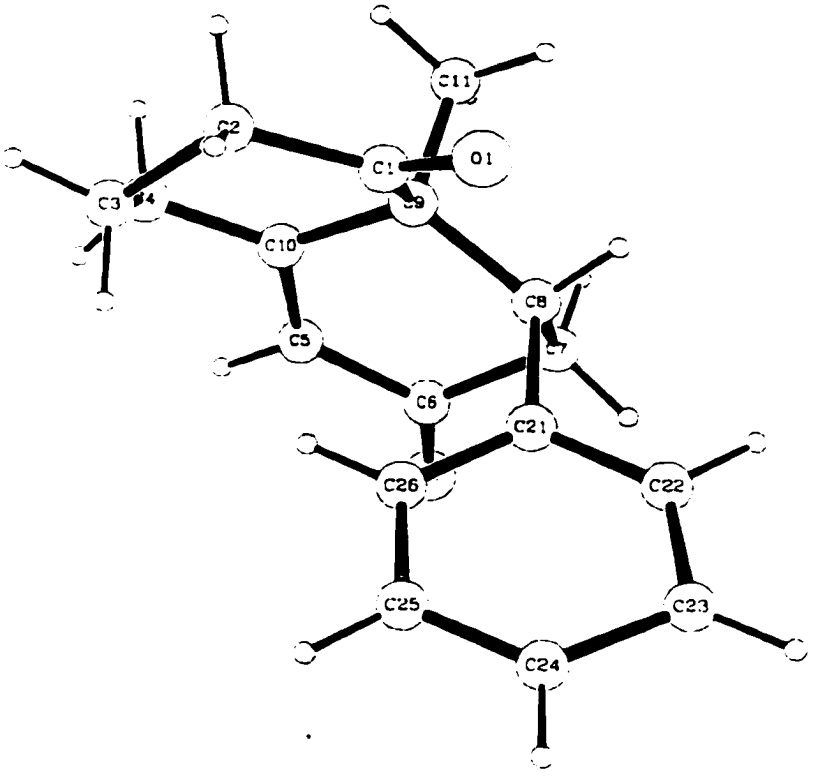

X-ray structure of diketone 108

Table I . X-ray Data for RA-1 at 295 K

Formula	$C_{17}H_{18}O_2$
Formula weight	254.332
Crystal size (mm)	0.24 x 0.32 x 0.64
Crystal system	orthorhombic
Space group	$Pna2_1$
a (Å)	14.878(1)
b (Å)	7.700(2)
c (Å)	23.576(4)
V (Å^3)	2700.8(8)
Z	8
d_{calc} (g cm^{-3})	1.251
μ(Cu $K\alpha$) (cm^{-1})	6.008
Absorption correction	none
Maximum θ (°)	65
Unique reflections	2353
Observed reflections	1759
[$I > 3.0\sigma(I)$]	
Number of variables	343
R	0.0469
R_w	0.0553

$(\Delta\rho)_{max}$ (e Å^{-3})	0.22
$(\Delta\rho)_{min}$ (e Å^{-3})	–0.16

Table II. Final Atomic Parameters for RA-1

Atom	x	y	z	B(Å^2)
O1	0.5768(2)	-0.3474(5)	0.191	4.74(8)
O6	0.3047(2)	0.2401(5)	0.2494(2)	6.1(1)
C1	0.4945(3)	-0.3530(6)	0.1908(2)	3.17(9)
C2	0.4456(4)	-0.4885(6)	0.1567(2)	4.6(1)
C3	0.3520(3)	-0.4341(7)	0.1374(2)	4.1(1)
C4	0.2973(3)	-0.3549(6)	0.1867(2)	3.6(1)
C5	0.3032(3)	-0.0490(6)	0.2189(2)	2.81(8)
C6	0.3447(3)	0.1010(6)	0.2449(2)	3.35(9)
C7	0.4370(3)	0.0756(6)	0.2698(2)	3.7(1)
C8	0.4945(3)	-0.0554(6)	0.2361(2)	3.01(9)
C9	0.4436(3)	-0.2280(6)	0.2317(2)	2.90(9)
C10	0.3439(3)	-0.2044(6)	0.2118(2)	2.63(8)
C11	0.4417(3)	-0.3251(7)	0.2879(2)	3.8(1)
C21	0.5258(3)	0.0257(5)	0.1810(2)	2.78(8)
C22	0.6007(3)	0.1330(6)	0.1828(2)	3.6(1)
C23	0.6359(3)	0.2116(7)	0.1354(2)	4.3(1)
C24	0.5934(3)	0.1837(7)	0.0825(2)	4.3(1)
C25	0.5182(3)	0.0784(6)	0.0794(2)	3.6(1)
C26	0.4849(3)	0.0010(6)	0.1292(2)	3.27(9)
O1'	0.3263(2)	0.8547(5)	0.4392(2)	4.93(8)
O6'	0.0618(2)	0.2551(4)	0.3803(2)	4.67(8)
C1'	0.2449(3)	0.8543(6)	0.4400(2)	3.36(9)
C2'	0.1936(3)	0.9848(7)	0.4732(2)	4.6(1)
C3'	0.1002(3)	0.9279(7)	0.4915(2)	4.4(1)

C4'	0.0492(3)	0.8537(6)	0.4422(2)	3.6(1)
C5'	0.0549(3)	0.5466(6)	0.4104(2)	3.27(9)
C6'	0.0989(3)	0.3960(6)	0.3838(2)	3.7(1)
C7'	0.1913(3)	0.4206(7)	0.3605(2)	3.9(1)
C8'	0.2458(3)	0.5566(6)	0.3945(2)	3.17(9)
C9'	0.1927(3)	0.7307(5)	0.4018(2)	2.59(8)
C10'	0.0975(3)	0.6986(6)	0.4180(2)	2.83(8)
C11'	0.1929(3)	0.8280(7)	0.3424(2)	4.2(1)
C21'	0.2782(3)	0.4742(5)	0.4506(2)	2.87(8)
C22'	0.3548(3)	0.3678(6)	0.4498(2)	3.8(1)
C23'	0.3849(3)	0.2892(7)	0.4989(2)	4.5(1)
C24'	0.3442(3)	0.3144(7)	0.5492(2)	4.2(1)
C25'	0.2692(3)	0.4189(6)	0.5512(2)	3.9(1)
C26'	0.2356(3)	0.4966(7)	0.5030(2)	3.46(9)
H2A	0.440	-0.595	0.180	5.5
H2B	0.482	-0.515	0.122	5.5
H3A	0.320	-0.538	0.123	4.9
H3B	0.358	-0.346	0.106	4.9
H4A	0.289	-0.446	0.217	4.3
H4B	0.238	-0.317	0.172	4.3
H5	0.240	-0.037	0.205	3.4
H7A	0.430	0.032	0.310	4.4
H7B	0.469	0.190	0.270	4.4
H8A	0.552	-0.085	0.256	3.6

Table II (cont.). Final Atomic Parameters for RA-1

Atom	x	y	z	B(Å^2)
H11A	0.505	-0.342	0.302	4.6
H11B	0.407	-0.257	0.316	4.6
H11C	0.412	-0.441	0.282	4.6
H22	0.630	0.154	0.220	4.3
H23	0.691	0.287	0.138	5.1
H24	0.618	0.240	0.047	5.2
H25	0.488	0.058	0.042	4.3
H26	0.430	-0.074	0.127	3.9
H2A'	0.187	1.092	0.449	5.5
H2B'	0.229	1.013	0.508	5.5
H3A'	0.067	1.030	0.507	5.2
H3B'	0.106	0.837	0.522	5.2
H4A'	0.043	0.945	0.412	4.3
H4B'	-0.012	0.817	0.455	4.3
H5'	-0.009	0.535	0.423	3.9
H7A'	0.186	0.460	0.320	4.7
H7B'	0.224	0.307	0.362	4.7
H8'	0.300	0.591	0.372	3.8
H11A'	0.256	0.851	0.330	5.1
H11B'	0.163	0.753	0.313	5.1
H11C'	0.160	0.940	0.346	5.1
H22'	0.388	0.349	0.413	4.5
H23'	0.438	0.211	0.497	5.4

H24'	0.368	0.259	0.584	5.1
H25'	0.239	0.439	0.588	4.6
H26'	0.180	0.570	0.505	4.2

The parameters of the hydrogen atoms were not refined.

Standard deviations are in parentheses.

Anisotropically refined atoms are given in the form of the isotropic equivalent displacement parameter defined as:

(4/3) * [a2*B(1,1) + b2*B(2,2) + c2*B(3,3) + ab(cos gamma)*B(1,2) + ac(cos beta)*B(1,3) + bc(cos alpha)*B(2,3)]

Table V. Bond Distances (Å) for RA-1

Atom 1	Atom 2	Distance	Atom 1	Atom 2	Distance
O1	C1	1.226(5)	O1'	C1'	1.210(5)
O6	C6	1.229(6)	O6'	C6'	1.221(6)
C1	C2	1.505(7)	C1'	C2'	1.485(7)
C1	C9	1.559(6)	C1'	C9'	1.524(6)
C2	C3	1.523(7)	C2'	C3'	1.519(7)
C3	C4	1.545(7)	C3'	C4'	1.502(7)
C4	C10	1.474(6)	C4'	C10'	1.506(6)
C5	C6	1.446(6)	C5'	C6'	1.471(6)
C5	C10	1.351(6)	C5'	C10'	1.343(6)
C6	C7	1.507(6)	C6'	C7'	1.493(7)
C7	C8	1.543(6)	C7'	C8'	1.549(7)
C8	C9	1.533(6)	C8'	C9'	1.566(6)
C8	C21	1.514(6)	C8'	C21'	1.544(6)
C9	C10	1.567(5)	C9'	C10'	1.486(5)
C9	C11	1.521(7)	C9'	C11'	1.588(6)
C21	C22	1.387(6)	C21'	C22'	1.404(6)
C21	C26	1.379(6)	C21'	C26'	1.398(6)
C22	C23	1.375(7)	C22'	C23'	1.381(7)
C23	C24	1.415(7)	C23'	C24'	1.344(7)
C24	C25	1.383(7)	C24'	C25'	1.376(7)
C25	C26	1.406(6)	C25'	C26'	1.379(7)

Standard deviations are in parentheses.

Table VI. Bond Angles (°) for RA-1

Atom 1	Atom 2	Atom 3	Angle	Atom 1	Atom 2	Atom 3	Angle
O1	C1	C2	120.7(4)	O1'	C1'	C2'	121.4(4)
O1	C1	C9	117.4(4)	O1'	C1'	C9'	120.1(4)
C2	C1	C9	121.6(4)	C2'	C1'	C9'	118.1(4)
C1	C2	C3	114.2(4)	C1'	C2'	C3'	115.2(4)
C2	C3	C4	111.4(4)	C2'	C3'	C4'	110.6(4)
C3	C4	C10	111.4(4)	C3'	C4'	C10'	110.7(4)
C6	C5	C10	124.7(4)	C6'	C5'	C10'	122.2(4)
O6	C6	C5	121.7(4)	O6'	C6'	C5'	121.9(4)
O6	C6	C7	121.4(4)	O6'	C6'	C7'	120.3(4)
C5	C6	C7	116.7(4)	C5'	C6'	C7'	117.8(4)
C6	C7	C8	113.0(4)	C6'	C7'	C8'	112.1(4)
C7	C8	C9	109.2(3)	C7'	C8'	C9'	111.8(3)
C7	C8	C21	110.0(4)	C7'	C8'	C21'	109.2(4)
C9	C8	C21	116.8(3)	C9'	C8'	C21'	114.5(3)
C1	C9	C8	109.7(3)	C1'	C9'	C8'	110.0(3)
C1	C9	C10	110.2(3)	C1'	C9'	C10'	116.0(3)
C1	C9	C11	104.2(4)	C1'	C9'	C11'	103.0(3)
C8	C9	C10	112.8(4)	C8'	C9'	C10'	111.5(3)
C8	C9	C11	112.1(4)	C8'	C9'	C11'	107.8(3)
C10	C9	C11	107.4(3)	C10'	C9'	C11'	107.9(3)
C4	C10	C5	122.4(4)	C4'	C10'	C5'	121.0(4)
C4	C10	C9	118.3(4)	C4'	C10'	C9'	114.8(4)
C5	C10	C9	119.3(4)	C5'	C10'	C9'	124.1(4)

C8	C21	C22	117.9(4)	C8'	C21'	C22'	118.8(4)
C8	C21	C26	124.6(4)	C8'	C21'	C26'	124.3(4)
C22	C21	C26	117.5(4)	C22'	C21'	C26'	116.8(4)
C21	C22	C23	123.0(4)	C21'	C22'	C23'	120.5(4)
C22	C23	C24	118.6(4)	C22'	C23'	C24	122.0(5)
C23	C24	C25	119.8(4)	C23'	C24'	C25'	118.7(5)
C24	C25	C26	119.3(4)	C24'	C25'	C26'	121.3(4)
C21	C26	C25	121.7(4)	C21'	C26'	C25'	120.7(4)

Standard deviations are in parentheses.

REFERENCES

1. M. Faraday, *Philos.Trans. R. Soc. London*, **I**, 440 (1825)

2. T.M. Krygowski, M.K. Cyrañski, Z. Czarnocki, G. Häfelinger, A.R. Katritzky, *Tetrahedron*, **56**, 1783 (2000)

3. A. Kekule, *Bull. Soc. Chim. Fr*, **3**, 98 (1865)

4. E. Erlenmeyer, *Liebigs Ann. Chem.* **137**, 327 (1866)

5. J.W. Armit, R. Robinson, *J. Chem. Soc.*, **127**, 1604, (1925)

6. W. Hückel, *Z Phys.* **70**,204 (1931); **72**,310 (1931); **76**,628 (1932); *Z. Electrochem.* **9**,752 (1937)

7. T.M.Krygowski, M.K. Cyrański, *Chem.Rev.* **101**,1385 (2001)

8. R.C. Haddon, V.R. Haddon, L.J. Jackman, *Nuclear Magnetic Resonance of Annulenes. Topics in Current Chemistry*; Springer, Berlin, 1971; *Vol 16*,2

9. P. v. R. Schleyer, H. Jiao, *Pure Appl. Chem*, **68**,209 (1996) ; A.R. Katritzky, M. Karelson, S. Slid, T.M. Krygowski, K. Jug, *J. Org. Chem.* **63**,5228 (1998)

10. Breslow, R., *Chem. Eng. News*, 43,90 (June 28, 1965); R. Breslow, *Acc. Chem. Res.* **6**, 393 (1973)

11. P.J. Garrat, *Aromaticity*, Wiley, New York, 1986

12. A. Streitweiser, *Molecular Orbital Theory for Organic Chemists*, Wiley, New York,1961

13. Z. Pauling, J. Sherman, *J. Chem. Phys* **1**,606 (1933)

14. M.J.S Dewar, A.J. Harget, N.Trinajstic, *J. Am. Chem. Soc.* **91**,6321 (1969); Dewar, M.J.S.; M. Gleicher, *J. Am. Chem. Soc.* **87**,692 (1965)

15. B.A. Hess, L.J. Schaad, *J. Am. Chem. Soc.* **93**, 305 (1971)

16. I. Gutman, M. Milun, N. Trinajstic, *J. Am. Chem. Soc*, **99**,1692 (1977)

17. M. Randic, *J. Am. Chem. Soc.* **99**, 444 (1977)

18. P.George, M. Trachtman, C. W. Bock, A.M. Brett, *Theor. Chim. Acta*, **38**,121 (1975); P. George, C.W. Bock, M. Trachtman, *Tetrahedron Lett.* **26**,5667 (1985)

19. V.I. Minkin, M.N. Glukhovtsev, B. Ya Simkin, *Aromaticity and Antiaromaticity. Electronic and Stuctural Aspects*; Wiley, New York, 1994

20. J. E Rice, T. J. Lee, R.B. Remington, W.D. Allen, D.A. Clabo, H.F. Schaefer, *J. Am. Chem. Soc.*, **109**, 2902 (1987)

21. L. Salem, *The Molecular Orbital Theory of Conjugated Systems* Benjamin, New York, 1966

22. A. Julg, Francois, *Theor. Chim. Acta* **7**,249 (1967)

23. J. Kruszewski, T.M. Krygowski *Tetrahedron Lett.* 3839 (1972); T.M. Krygowski, M. K. Cyrañski, *Tetrahedron* **52**,1713 (1996); T.M. Krygowski, *J. Chem. Inf. Comput. Sci* **33**,70 (1993)

24. T.M. Krygowski, R. Anulewicz, J. Krusztewski, *Acta Crystallogr.* **B** **39**,732,(1983)

25. L.Pauling, *J. Chem. Phys.*, **4**, 673 (1936); F. London, *J. Phys. Radium*, **8**, 397 (1937)

26. J.A. Pople, *J. Phys.*, **24**, 1111 (1956)

27. L.M. Jackman, F. Sondheimer, Y. Amiel, D.A. Ben-Efraim, Y. Gaori, R.Wolowsky, A.A. Bothner-By, *J. Am. Chem. Soc.*, **84**, 4307 (1962)

28. C.S. Wannere, P. v. R. Schleyer, *Org. Lett.*, **5**, 605 (2003)

29. A.T. Balaban, M. Banciu, V. Ciorba, *Annulenes, Benzo-, Hetero-, Homo-Derivatives, and their Valence Isomers* ; CRC Press, Boca Raton, Fl, 1987, Vol. I

30. G. Schröder, J.F.M. Oth, *Tetrahedron Lett.*, 4083 (1966); G. Schröder, W. Martin, J.F.M. Oth, *Angew. Chem. Int. Ed. Engl.*, **6**, 4966 (1967)

31. B. A. Hess, I.J. Schaad, M. Nakagawa, *J. Org. Chem.* **42**,1669,(1977)

32. A. Verbrugger, *Bull. Soc. Chim. Belg.* **91**,862 (1982)

33. D. Cremer, H. Günther *Liebigs Ann. Chem.* **87**,763 (1972)

34. R.H. Mitchell Isr. J. Chem. 20,294 (1980)

35. P.v.R. Schleyer, C. Maerker, A. Dransfeld, H. Jiao, N.J.R.v. H. Hommes, *J. Am. Chem. Soc.* **118**,6317 (1996)

36. P.v.R. Schleyer, M. Manoharan, Z-X. Wang, B. Kiran, H. Jiao, R. Puchta, N.J.R.v.E. Hommes, *Org. Lett.*, **3**, 2465 (2001)

37. A.R. Katritzky, K. Jug, D. C. Oniciu, *Chem. Rev.* **101**, 1421 (2001)

38. P.v.R. Schleyer, P.K. Freeman, H. Jiao, B. Goldfuss, *Angew. Chem. Int. Engl.*, **34**, 337 (1995)

39. M.K. Cyrañski, T.M. Krygowski, A.R. Katritzky, P.v.R. Schleyer, *J.Org.Chem.*, **67**, 1333 (2002)

40. F. Sondheimer, R. Wolovsky, *J. Am. Chem. Soc.*, **84**,260 (1962)

41. E. Vogel, H. Königshofen, K. Müllen, J.F.M. Oth, *Angew. Chem. Int. Ed. Engl.*, **13**,281 (1974)

42. E. Vogel, M. Mann, Y. Sakata, K. Müllen, J.F.M. Oth, *Angew. Chem. Int. Ed. Engl.*, **13**, 283 (1974)

43. D. Farquhar, D. Leaver, *Chem. Comm.*, **24** (1969)

44. J.P. Snyder, *Nonbenzenoid Aromatics*, Vol. II, Academic press, 137 (1971)

45. V. Boekelheide, C. E. Larrabee, *J. Am. Chem.Soc.*, **88**,3950, (1950)

46. K. Hafner, V. Kuhn, *Angew. Chem. Int. Ed. Engl.*, **25**, 632 (1986)

47. W. Huang, PhD Thesis, 1990

48. C.W. Alva, PhD Thesis, 1990

49. D. Levinson, PhD Thesis, 1995

50. a) R.H. Mitchell, *Chem. Rev.* **101**, 1301 (2001) ; b) R.H. Mitchell, R.V. Williams, R. Mahadevan, Y-H Lai, T.W. Dingle, *J. Am. Chem. Soc.*, **104**, 2571 (1982)

51. S. Hsu, PhD Thesis,2000

52. L.T. Scott, M.A. Kirms, *J. Am. Chem. Soc.*, **105**, 1372 (1983)

53. H. Gunther, M.E. Gunther, D. Mondeshka, H. Schmickler, F. Sondheimer, N. Darby, T.M. Cresp, *Chem. Ber.* **112**, 71 (1979)

54. AMPAC, A general Molecular Orbital Package, version 6.0

55. K. Exner, P. v R. Schleyer, *J. Phys. Chem.* A **105**, 3407 (2001)

56. X.L. Huang, J.J. Dannenberg, *J.Org. Chem*, **56**, 6367 (1991)

57. K.C. Nicolaou, S.C. Snyder, T. Montagon, G. Vassilikogiannakis, *Angew. Chem. Int. Ed.*, **41**, 1668 (2002)

58. W. Opplozer, K.Keller, *J. Am. Chem. Soc.*, **93**, 3836 (1971); R.L. Funk, K.P.C. Vollhard, *J. Am. Chem. Soc.*, **102**, 5253 (1980)

59. H. Nemoto, M. Nagai, M. Moizumi, K. Kohzuki, K. Fukumoto, T. Kametani, *J. Chem. Soc. Perkin Trans. 1*, 1639 (1989)

60. T. Kametani, H. Nemoto, H. Ishikawa, K. Shiroyama, H. Matsumoto, K. Fukumoto, *J. Am. Chem. Soc.*, **99**, 3461 (1976)

61. G.H. Douglas, J.M.H. Grares, D. Hartley, G.A. Hughes, B.J. McLoughlin, J. Siddall, H. Smith, *J. Chem. Soc.*, , 5072 (1963)

62. H.H. Wasserman, J. Solodar, *J. Am. Chem. Soc.*, **87** (17), 4002 (1965)

63. J. G. Allen, M. F. Hetenmann, S.J. Danishefsky, *J. Am. Chem. Soc.*, **122**, 571 (2000)

64. T. Kametani, M. Tsubuki, Y. Shiratori, Y. Kato, H. Nemoto, M. Ihara, K. Fukumoto, *J. Org. Chem.* , **42**, 2672 (1977)

65. E. Baggiollini, H.P. Hamlow, K. Schaffner, *J. Am. Chem. Soc.*, **92**, 4906 (1970)

66. Walker G., *J. Org. Chem.*, **77**,3664 (1955)

67. J-P. Bégué. D. Bonnet-Delpon, A. Dogbeavou, *Synthetic Communications*, **22** (4), 573 (1992)

68. C. Verrat, N. Hofmann, JP Pete, *Synlett,* **8**,1166 (2000)

69. P. Schiess , M. Heitzmann , S. Rutschmann ,R. Staheli , *Tet Letters,* **46**, 4569 (1978)

70. M. Karpf, *Angew. Chem. Int. Ed. Engl.* **25**, 414 (1986)

71. J.A. Skorz, F.E. Kaminski, *Organic Syntheses*, **48**, 54

72. M.E. Jung, P.Y-S. Lam, M. M. Mansuri, L.M. Speltz, *J.Org. Chem.* **50**, 1087 (1985)

73. J. F. Bunnet, J.A. Skorz, *J.Org. Chem.*, **27**, 3836 (1962)

74. D.F. Taber, K. Raman, M.D. Gaul, *J.Org. Chem.* **53**, 28 (1987)

75. G. Stork, R.L. Danheiser, *J. Org. Chem.* **38**, 1775 (1973)

76. P. J. Garegg, B. Samuelsson, *J. Chem. Soc. Perkin I* , 2866 (1980)

77. B.E. McCarry, Thesis Dissertation, Stanford University, 56 (1972)

78. M.P. Cava, M. J. Mitchell, *J. Org. Chem.* , **27**,631 (1962)

79. J.A. Moore, D.E Reed, *Organic syntheses*, 351

80. R. Pappo, D.S. Allen, R.U. Lemieux, W.S. Johnson, *J. Org. Chem.* **21**, 478 (1956)

81. M. Shamma, H.R. Rodriguez, *Tetrahedron*, **24**, 6583 (1968)

82. M. Schlosser, G. Müller, K.F. Christmann, Angew. Chem. Int. Ed. Engl., 5, 667 (1966)

83. C. Sreekumar, K.P.Darst, W.C. Still, *J. Org. Chem.*, **45**, (1980)

84. R. M. Boden, Synthesis, 784 (1975)

85. M. Oki, *"Applications of Dynamic NMR Spectroscopy to Organic Chemistry"*, VCH, 1985.

86. G.H. Posner, *Angew. Chem. Int. Ed. Engl.* **17**, 487 (1978)

87. R.S.Monson, D. N. Priest, *J. Org. Chem.* , **36**, 3826 (1971)

88. M.Ohkita, T. Tsuji, M. Suzuki, M. Murakami, S. Nishida, *J. Org. Chem.* , **55**, 1506, (1990)

89. J. Dressel, K. L. Chasey, L.A. Paquette, *J. Am. Chem. Soc.*, **110**, 5479 (1988)

90. M. H. Lyttle, A. Streitweiser, M.J. Miller, *J. Org. Chem.*, **54**, 2331 (1989)

91. Schlosser, Hartmann, *Angew. Chem.*, **85**, 544 (1973)

92. M.E. Jung, *Tetrahedron*, **32**, 3, (1976); F. Eiden, P. Gmeiner, H. Lotter, *Liebigs. Ann. Chem.*, 125, (1988); M. Kikuchi, A. Yoshikoshi, *Bull. Chem. Soc. Jpn.*, **54**, 3420, (1981)

93. H. Born, R. Pappo, J. Szmuszkovicz, 1779 (1953)

94. G. Quinkert, W. D. Weber, U. Schwartz, G. Durner, *Angew. Chem.* **92**, 1060 (1980)

95. P.Main, S. Fiske, S. Hull, L. Lessinger, G. Germain, J.P. Declercq, M. Woolfson (1982) MULTAN 11/82. University of York, England, and University of Louvain, Belgium.

96. W.C. Still, M. Kahn, A. Mitra, *J. Org. Chem.* , **43**, 2923 (1978)

97. Instruction Manual for Chromatotron Model 8924, Harrison Research, CA (1988)